

Comparison of epicyclic gear train configurations between Turboprops and GTFs

Marta Lechuga Romero

Master thesis submitted under the supervision of
Prof. Patrick Hendrick

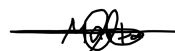
Academic year
Year 2020-2021

In order to be awarded the Master's programme in
Electromechanical Engineering with major in Aeronautics

Exemplaire à apposer sur le mémoire ou travail de fin
d'études,
au verso de la première page de couverture.

Fait en deux exemplaires, Bruxelles, le 28 mai 2021

Signature



Réservé au secrétariat : Mémoire réussi* OUI
NON

**CONSULTATION DU MEMOIRE/TRAVAIL DE FIN
D'ETUDES**

Je soussigné

NOM :

Lechuga Romero
.....
.....

PRENOM :

Marta
.....
.....

TITRE du travail :

Comparison of epyclic gear train configurationsbetween
.....
turboprops and geared turbofans
.....
.....

AUTORISE*

REFUSE*

la consultation du présent mémoire/travail de fin
d'études par les utilisateurs des bibliothèques de
l'Université libre de Bruxelles.

Si la consultation est autorisée, le soussigné concède
par la présente à l'Université libre de Bruxelles, pour
toute la durée légale de protection de l'œuvre, une
licence gratuite et non exclusive de reproduction et de
communication au public de son œuvre précisée ci-
dessus, sur supports graphiques ou électroniques, afin
d'en permettre la consultation par les utilisateurs des
bibliothèques de l'ULB et d'autres institutions dans les
limites du prêt inter-bibliothèques.

* Biffer la mention inutile

* Biffer la mention inutile

Contents

1	Abstract	1
2	Evolution of the engines	2
2.1	Turbojet	3
2.2	Propeller	5
2.3	Turbofan	6
3	Thrust-specific-fuel-consumption and its influence in engines' evolution	8
3.1	The concept of TSFC	8
3.2	Technological evolution to improve TSFC	10
4	Geared turbofan	15
5	Types of gearboxes and gears in gas turbine engines	16
5.1	The concept of the gearbox	16
5.2	State-of-art gearboxes	20
5.2.1	Gearboxes for turboprops	22
5.2.2	Gearboxes for turbofans	27
6	Gearbox design with KissSoft	32
6.1	Steps	32
7	Design procedure	35
7.1	Input parameters	35
7.1.1	Basic data	35
7.1.2	Material	37
7.1.3	Manufacturing	43
7.1.4	Reference Profile	48
7.1.5	Tolerances & Gear quality	49
7.1.6	Lubrication	50
7.1.7	Rating & factors	58
7.1.8	Gear ratio, the safety factors and the input speed	61
7.2	Rough Sizing	62
7.3	Fine Sizing	63
7.4	Modifications	65
7.5	Results	68
7.6	3D Graphics	74
8	Conclusion	76
A	Overall efficiency in jet engines	77
B	Turbojet, Turboprop and Turbofan	79
B.1	State-of-the-art turbojets	79
B.2	State-of-the-art turboprops	80
B.3	State-of-the-art turbofans	81
C	Compressor Surge	83
D	Velocity components in turbomachines	84
E	Evolution of fan technology	85
F	NASA's technology vs GE in the propfan design	86
G	Type of gears	87
H	Tilting moment and uneven load distribution in bearings in Helical Planetary GB	91

I Main design parameters in Gears	93
J Profile shifted gears	95
K DIN 3967-1978	96
L ISO Tolerances for Shafts according to ISO 286-2	97
M Aircraft 's systems interaction	98
N Bearing chamber in jet engines	102
O Lubricants Characteristics	103
P Rough sizing solutions	105
Q KissSoft results	106
List of Symbols	182
List of Figures	185
List of Tables	187
References	188

1 Abstract

Since the first effective propellers powered by piston engines, throughout impressive supersonic aircraft and up to modern airliners, a lot has changed in the aviation. The aircraft is now a balance between hundreds of different specifications. Some of them being improved at the cost of others. An aircraft engine is designed to produce thrust, however, it must be adapted to the different requirements related with take-off, climb, cruise and maneuvering, differing the relative importance from civil to military applications. The evolution of these engines, can be considered as an answer to the population's and industry's needs, but also the oil price has ruled the progress and technological advance.

As travelling started to become more feasible, airliners needed bigger, faster and longer distance planes. Piston driven engines came up short, and this led to the appearance of turbojets, which allowed to fly faster and higher. By that time, propeller specialists and companies struggled for their place in the industry, and after a period of uncertainty, they found it with the turboprop, whose application was proved for regional trips in which the use of a turbojet was not profitable. It seemed that the race for speed ruled the aviation world, but it turned out that even though these engines could be very efficient at supersonic speeds, they were aerodynamically inefficient. In the airline business, especially, a bigger and faster plane was not interesting enough if the burnt fuel was a lot higher. Now, the fuel consumption was the dominant parameter. The birth of the turbofan was therefore justified. Improved efficiency not only allows airlines to save money on fuel, but also, as a consequence, concedes the airplanes to fly further. The oil crisis in the 70s, together with the growing concern over the environmental impact of aviation which has been growing substantially during the past 30 years, pushed further investigation to try to optimize the engines to reduce fuel consumption. Decision making on optimal engine cycle selection, needs now to consider mission fuel burn, direct operating costs, engine and airframe noise, emissions and global warming impact, indeed, a challenge. The composite materials and new technologies help to achieve significant weight and fuel reduction and experiments are taking place today to show that this is the right step ahead. It is difficult to say which of the many researching ways will lead to viable solutions but indeed this effort to achieve an increased efficiency in terms of fuel consumption is pushing the industry further still. One of the potential improvement lines, which has risen interest, specially due to the significant increase in the engine efficiency, is the development of state-of-art technology for the transmission system in geared turbofans. Pratt&Whitney with their PW1000G geared turbofan family of engines, introduce themselves as the leaders but with the close look of Rolls-Royce and their UltraFan.

This thesis starts with a revision on the evolution of aircraft engines and its dependency on fuel consumption. Continuing, a comparison between existing gearboxes used in turboprops and geared turbofans, to finalise with an individual design of an epicyclic gearbox for both aircraft engines, using KissSoft.

Keywords: turboprop, turbofan, fuel consumption, geared turbofan, epicyclic gearbox.

2 Evolution of the engines

The invention of the turbojet engine was revolutionary in the world of aviation just before World War II. Up until that moment, piston engines driving a propeller were the dominant force, and still are in many of the small aircraft in use today. Nevertheless, in the early jet age (1950s and 1960s), speed ruled on aviation, and when the need of power started to increase, the need to look for more efficient engines aroused. The use that had been given to those aircrafts was enough until the date, however, its working principle became inconvenient. They were too bulky and heavy, limiting their possibilities due to the complex designs. Given that the thrust provided by the engine is proportional to the airflow rate, when trying to maximize that, and keeping in mind the fact that large thrust per unit size is a design objective, designers came up with the attempt of trying to increase it, reaching the origin of the turbojets engines, leading to lighter and smaller engines, providing a boost in aircraft speed, and expanding the whole flight envelope.

Although the propeller-driven aircraft is not nearly as efficient as the jet, there were still some drawbacks to consider. A suitable engine application requires a high overall efficiency, this is how its performance is evaluated. This is a strong function on the one hand, of the thermal efficiency¹, which in order to be high, a combination of a high compressor pressure ratio and a high inlet temperature in the turbine (Tit) is needed. This results, for a turbojet, in a high jet velocity. For sea level static ISA conditions, a typical jet velocity of an aircraft with a cruise speed of $M=0.85$ (flight speed of around 250 m/s), would be around 600 m/s [1]. But also, on the other hand, it is also function of a good propulsive efficiency, which involves having the aircraft's speed close to the jet velocity² (see appendix A for a detailed explanation of the overall efficiency). This was not a problem, as the objective was to fly as fast as possible. In the early 1970s, jet technology was developing at a tremendous pace, overcoming the speed of sound, reaching even Mach 2 with the Concorde [2], and aiming even for Mach 3. Nevertheless, the net assessment of the efficiency of a jet engine is the measurement of its rate of fuel consumption per unit of thrust generated, which is not only a strong function of the overall's efficiency, but also it is a strong function of the aircraft flight speed and the ambient temperature, among others. Many factors must be taken into account and the magnificence of supersonic airlines came together with an unbearable noise and high fuel consumption which made it impossible for supersonic to enter mass aviation. To transport ordinary travelers on such planes was the same as to take children to school on supercars, it was unreasonable, as money spent on fuel is a major expenditure in operating an airline (together with reliability and maintainability, as these also have a direct impact on the cost of operating commercial engines)³. That is why, in the late 1960s [3] an aircraft designed to fly in a more efficient way at more moderate speeds, started to conquer transport aviation. This was the origin of the turbofan, with which there were substantial improvements in efficiency for subsonic flight, as for the same thrust, a lower specific fuel consumption was achieved. The idea behind this engine is simple. In order for the propulsive efficiency to be high, the mass of air passing through the engine needs to be accelerated by only a small amount. With that in mind, the only way of achieving high thrust is to increase the amount of mass moving through the propulsion system, which leads to a large propulsion device, with the subsequent problem of the increased drag. This problem can be attenuated by slightly reducing the speed, which also grants for higher comfort to the passengers due to lower noise, but a compromise between size and efficiency became the issue at that point.

In the mean time, for low flight speeds, propellers (ingesting 20 to 30 times the airflow rate of the engine [4]) are more than able to handle the required propulsion, and in this aspect, piston engines, still show a better efficiency than gas turbines. Nevertheless, the progress in the design and construction of the latter ones lead their replacement by turboprops, gas turbines driving a

1

$$\eta_{th} = \frac{m_a \cdot [V_j^2 - V_a^2]}{2 \cdot m_f \cdot Q_{ci}} \quad (1)$$

2

$$\eta_p \approx \frac{2}{\frac{V_j}{V_a} + 1} \quad (2)$$

³On the other hand, in the military world, the engine fuel consumption parameter takes a decidedly second role to other aircraft performance parameters, such as agility, maneuverability, and survivability.

propeller, which provided for the same power production, with a lower engine mass. These engines were used mostly on regional commuter transportation, in which less fuel-efficient jet-powered aircraft were not as profitable. The turboprop concept, whose development preceded that of the turbofan (early 1940s [3]), was a step-change in power, reliability and efficiency and could be considered as an extension of this latter one, and when compared to piston-engine aircrafts, they offer a smoother flight with less noise and vibration, with better fuel efficiency. Nevertheless, since they first emerged, turboprop engines were perceived as a temporary compromise between outdated piston engines and advanced jet engines, and due to the fact that there was a popular resistance, related to the idea of the propeller-driven airplanes, and what it represented in terms of modernity and security, an avoidance phenomenon started to appear, and the development of these engines has basically been dictated by the oil prices. The higher the price, the more relevant the propeller-enabled engine development became.

Later on, the oil crisis in the 70's served as motivation for further investigation and development in aeronautics, always on the focus of looking for fuel savings in aircraft engines. High fuel consumption of jet engines, previously perceived as a perfectly acceptable compromise for speed, now turned out to be a serious problem. Long-range transportation by large aircraft remained profitable, but flights over short distances by regional vehicles were not often paying off. This economic environment stimulated work towards another reinvention of the propeller for an increase in fuel efficiency. The Advanced Turboprop Project, carried out by NASA, was one of the most important works at that time. A really ambitious new engine called "unducted fan" surfaced, nevertheless, this project took so long to be developed, that by the time it was ready to come out, the fuel prices had already fallen, and it was not worth it for the industry to continue investing. It never materialized. However, the growing environmental concern directly related with fuel consumption and the restless desire to reduce operating costs has been the constant motivation for a continuous research. Improving the propulsive efficiency is one of the most researched lines. With technological development, the engines received a new, improved design, and the geared turbofan is the near future (and present) of the jet engines, thanks to the development of the most powerful transmission for energy-efficient aircraft engines to the date.

There are a lot more pros than cons to modern aircraft compared to the older airliners. It is a fact that they fly slower, but the rest of their performance is much better, not only due to modern technology but also because of the different compromises that had been made. For airlines, the parameters of fuel consumption and life cycle of the aircraft are more important than the speed of flight. Historic trends in improving efficiency levels show that aircraft entering today's fleet are around 80% more fuel efficient than they were in the 1960s [3]. Furthermore, fuel consumption is not only money. Fuel tanks on the aircraft remain the same, and an increase in fuel consumption may result in a reduction of the range. It is cheaper for the airline to make the passenger more comfortable, than to speed up the aircraft. The World is ruled by economically optimal airliners with economically optimal performance and modern airplanes pursue precisely these goals through further investigation on a number of fronts such as technological innovation, operational efficiency, infrastructure improvement and economic measures.

2.1 Turbojet

In order to start from the beginning, a brief reminder of the working principle of the different engines. In appendix B, one can find schemes, images and a brief explanation of some of the existing engines that will be covered in these sections.

A turbojet is a reaction engine which works in accordance with Newton's third law of motion: "For every action there is an equal and opposite reaction". A typical air-breathing jet engine follows the Brayton thermodynamic cycle [5] with an inlet, a compressor, a combustion chamber, a turbine and an exhaust. Nevertheless, these engines require several additional components which are indispensable for the proper functioning as a whole, such as the starter engine or the hydraulic pumps among others, but they do not play a key role in the thermodynamic cycle.

As air is drawn into the inlet, it is heated and compressed by the compressor and sent to the combustion chamber, where fuel is added and ignited. The hot combustion gases are expanded in

the turbine, which extracts sufficient energy to drive the compressor. The gases are not expanded to atmospheric pressure, and this gauge pressure is converted into jet velocity (V_j) through a further expansion, by an acceleration through the nozzle. This remainder of the exhaust energy is what is used to produce the thrust, $F = \dot{m}_a \cdot [V_j - V_a]$.

For a given level of technology, the efficiencies of all the components are known, therefore, the only two independent parameters are the turbine inlet temperature (T_{it}) and the compressor pressure ratio (Π_c). The engine performance depends, hence, on component performance and those two parameters, whose optimum values in order to maximize the overall efficiency or the specific thrust (F/\dot{m}), strongly depend on a chosen flight velocity, V_a , and the ambient temperature, T_a . In figure 1, a representation of a turbojet thrust and fuel consumption variation with compressor pressure ratio, turbine inlet, and flight Mach number. The calculations are obtained from [4], and with given assumptions about component efficiency, fluid properties and engine conditions. Each flight Mach number is assumed to correspond to an different altitude and thus a different pair of T_a and P_a .

It is appreciated that for a given flight Mach number and a given T_{it} , the Π_c that maximizes specific thrust, does not minimize fuel consumption, therefore, a compromise needs to be found. This selection is not arbitrary at all. While a higher T_{it} increases the specific thrust, an increase of Π_c , does not always imply an increase of the efficiency. Therefore, the T_{it} has to be as high as possible within technology limitations and the overall pressure ratio has to be high as well to obtain a low TSFC, but taking into account the effect on the efficiency. Furthermore, the compressor pressure ratio required to minimize specific fuel consumption is much less for supersonic than for subsonic flight. Moreover, the overall efficiency potentially attainable with supersonic flight is significantly higher than in subsonic, and the optimum pressure ratio drops with increasing Mach number. Designers are always eager to make all the processes as efficiently as possible, taking all the factors into account, from physical factors such as the material (stress and temperature), to the aerodynamic limits (boundary layers).

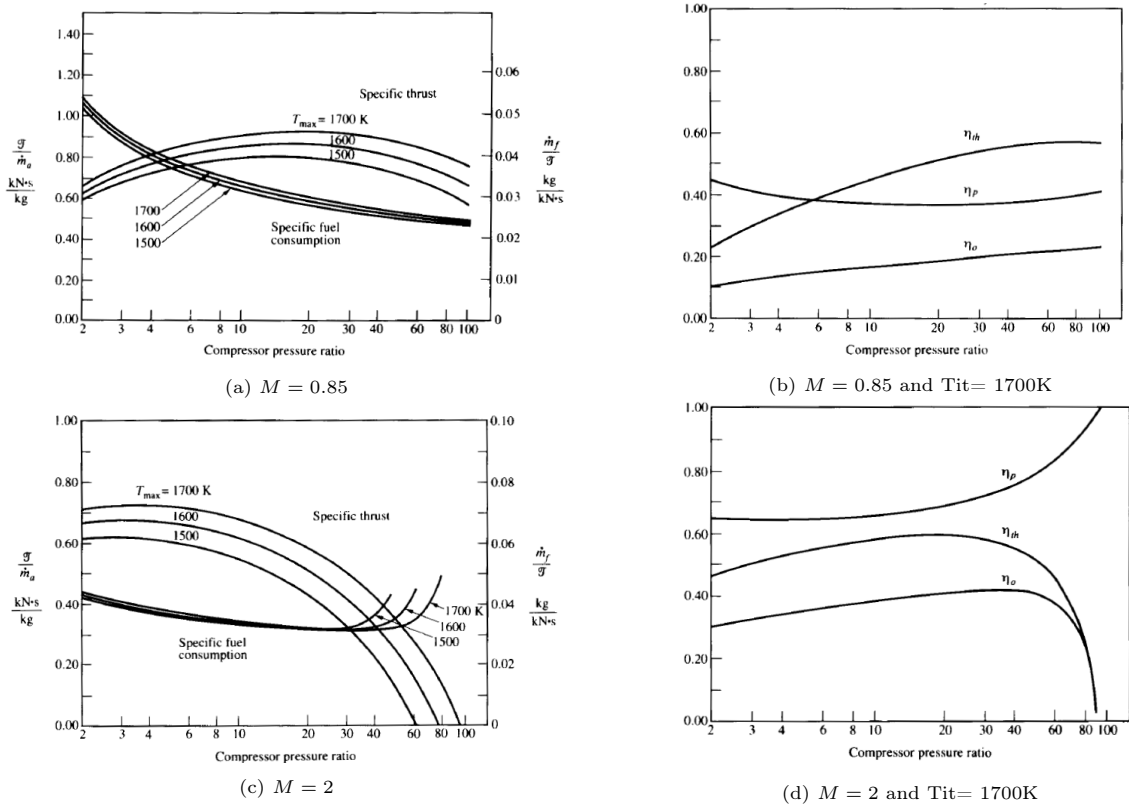


Figure 1: Turbojet cruise thrust, fuel consumption and efficiencies at different flight speed

2.2 Propeller

Aircraft propellers first emerged at the end of the 18th century, but it wasn't until 1903 when the Wright brothers created the first controlled, powered flight [6]. The advantages of propellers in terms of low-speed thrust, high propulsive efficiency and therefore, fuel efficiency were coupled with the smooth running and high reliability of the gas turbine. The propeller receives its driving power from the power generated by the turbine, thanks to the compression, combustion and expansion of the air, in a cycle such as that of the turbojet. The main difference between both engines is that the exhaust gases do not generally contain enough energy to create significant thrust, as most of the engine power is used to drive the propeller. Exhaust thrust in a turboprop is therefore, sacrificed in favour of shaft power, becoming around or less than 10% [7] of the total thrust.

The turboprop is characterized by a high efficiency, but its limitation on flight speed is a serious disadvantage. For that same reason, is why turboprops cannot fly at high altitudes⁴. The problem is that shock waves may form on the tips which reduce significantly the efficiency. Further information about this topic can be found in appendix D, but as a summary, on the one hand, the pressure rise in a compressor rotor depends upon the square of the linear velocity, " u ". An increase of the compressor pressure ratio benefits the thermal efficiency, and thus, even though we have seen that many parameters have an influence and there is always a balance to be found, to try to improve it, is a trend. At the same time, the linear speed of the fluid is the product of the rotational speed " N " and the radius " r ", and even though a high value of " u " is beneficial, the limiting factor in this case is the growth of compressibility effects because " u ", at the tip of a blade, where " r " gets its maximum value, can approach the local sound speed. Due to the stress limitations to which they would be submitted, the need of a gearbox is straightforward, to limit the tip speeds of the large-diameter propeller. In addition, mating the gas turbine with the propeller is a major technical hurdle, because the RPM of a gas turbine is about ten times greater than that appropriate for a propeller, and the gearbox need to be able to withstand it. The weight and reliability of such units reduces their attractiveness somewhat. The gearbox's design requires heavy development to ensure reliability and durability, and the need of the inclusion of this device, together with the fact that propellers are normally pitch controlled, which forces their hub bigger to accommodate the blade pitch mechanism and pipings, make this engine quite big in comparison with the turbojet. Furthermore, another issue due to that configuration is that the upstream of the intake disturbs the inlet flow, which leads to a non-uniform flow entering the compressor. Despite of all of this, the benefits that the propeller offers at low speeds and at takeoff due to the fact that the excess thrust is higher, and many other advantages which still accrue to a propeller-jet combination, make their use to be widespread today.

Another important characteristic of these engines, which specially affects those ones in which the gas turbine is smaller, is that they may suffer from efficiency penalties as the pressure ratio becomes high and the blade heights at the compressor exit become low. This is due to the clearances between the blade and the casing, making the aerodynamic losses too high. The size effect affects also the compressor configurations. That is why it is very common to find in these kind of engines a centrifugal compressor, with which small sizes perform better than in an axial one.

Lastly, for a given thrust, flight speed, and engine thermal efficiency, the minimum energy consumption is associated with the largest airflow through the propulsion unit. The propeller is therefore, the engine with the best consumption at low speeds, so far. However, the oil price has ruled the progress and technological advance on propellers, the higher the price, the more relevant the propeller-enabled engine development becomes. Once turbojets and turbofans appeared in the market, there has been a popular resistance, related to the idea of going back to propeller-driven airplanes, and what it represented in terms of modernity and security. Jet planes were more expensive, consumed more fuel, and were more demanding on infrastructure but had better flight performance in factors such as speed, range, and comfort, making them more attractive to the operators. This fact led to the lowest demand for turboprop airplanes at the beginning of the 2000s [6]. At the very beginning of the 21st century, the propeller-driven airplane prevailed as a niche. However, this century brought new challenges and priorities. Climate control and

⁴At high altitudes, an aircraft has to move at high speeds in order to generate enough lift to stay up, because density is low and lift is proportional to density and to the square of the velocity, so high velocity compensates for low density.

pollution are now much serious concerns. Propellers have a role again to play on the progress, and beyond efficiency, these engines have always offered benefits that the jet engine could not, such as, for example, better take-off and landing performances allow transporting passengers to and from regional, small airports.

2.3 Turbofan

The natural evolution of the turbojet when looking for a more efficient engine to fly at lower speeds was the turbofan. An engine which combines high thermal efficiency with a high propulsive efficiency. To reduce the high jet velocity, more energy has to be extracted from the turbine. Different possibilities were studied such as increasing the compressor pressure ratio or sending a higher mass flow rate, non of them turning out effective. The only viable solution was to add an extra compressor which did not feed air through the combustion chamber and the turbine. The design of the turbofan could, therefore, be considered as a compromise between the pure turbojet and the propeller engine [8].

Different configurations are possible (as it can be seen in appendix B), but the main principle is to add an additional compressor whose mass flow is separated from the remainder of the engine. The core of the engine is the same as that of the turbojet, and it is surrounded by a fan in the front, and an additional turbine to drive it, in the rear. The fan and the low pressure turbine are connected to an additional shaft, which goes through the core shaft due to mechanical reasons. In order to optimize the cycle, the two separate flow rates can be mixed again before going through the nozzle. This feature may also provide a reduction in jet noise emissions.

The turbofan, thus, has at least two separate compressors, both of them driven by a separate turbine. On the one hand, *low pressure compressor* (LPC), known usually as the fan, is driven by the *low pressure turbine* (LPT), running at a rotational speed, N_1 . The *high pressure compressor* (HPC), is driven by *high pressure turbine* (HPT), at a speed of N_2 . Furthermore, the existence of two separate mass flows means that there will be two different jet velocities, so the turbofan gets some of its thrust from the core and some from the fan. The ratio of these two flows is called the by-pass-ratio (BPR), an important design parameter in this kind of engines. This makes the turbofan more fuel efficient, as for the same amount of fuel flow rate (no fuel is added to the bypass stream), it generates more thrust than that with a turbojet at subsonic flight. This outweighs the reduction of V_{jp} : $F \approx \dot{m}_p \cdot (V_{jp} - V_a) + \dot{m}_s \cdot (V_{js} - V_a)$.

This effect is clearly more pronounced for higher BPRs. The order of magnitude of the jet velocity of the primary stream is 400 m/s [9], while for the secondary, it is typically around 300 m/s. Therefore, even though the addition of an extra compressor reduces significantly V_j , even when both of them are low, the thermal efficiency⁵, is still high. This explains the trend towards ever increasing the BPR of civil transport aircraft.

As for the turbojet, the Tit and the compressor pressure ratio⁶ (which in the product of the fan pressure ratio and the inner compressor pressure ratio) are two of the main design parameters in this engine. However, it has two additional parameters, the BPR mentioned, and the pressure ratio of the fan for the secondary stream, π_{FAN} . Again, a trade-off needs to be done in order to achieve the highest thrust and efficiency at the lowest fuel consumption. Having seen the number of parameters involved, their interdependence and the dependency on the flight velocity, this is not an easy task.

Besides, this lower speed allows not only improving fuel efficiency but also significantly reducing noise emissions, which is a very important topic for cities close to airports. The improved performance at low speeds, made the take-off and landings much easier and softer, improving not only the passengers' comfort but also improving the aircraft's structural efficiency. Older aircraft landed at higher speeds. The touch on the runway and braking were quite punishing, forcing engineers to install reinforced landing gears which took up space inside the aircraft and increased mass. Newer

⁵ $\eta_{th} = \frac{\dot{m}_p \cdot [V_{jp}^2 - V_a^2] + \dot{m}_s \cdot [V_{js}^2 - V_a^2]}{2 \cdot \dot{m}_f \cdot Q_{ci}}$

⁶ $\pi_o = \pi_F \cdot \pi_C$

airliners have softer, lighter, and more efficient gears.

To illustrate the performance improvement possible with bypass engines, Hill et al.[4] performs the same calculations as in the turbojet engine, following the same assumptions, with a BPR=5, and obtaining the results below:

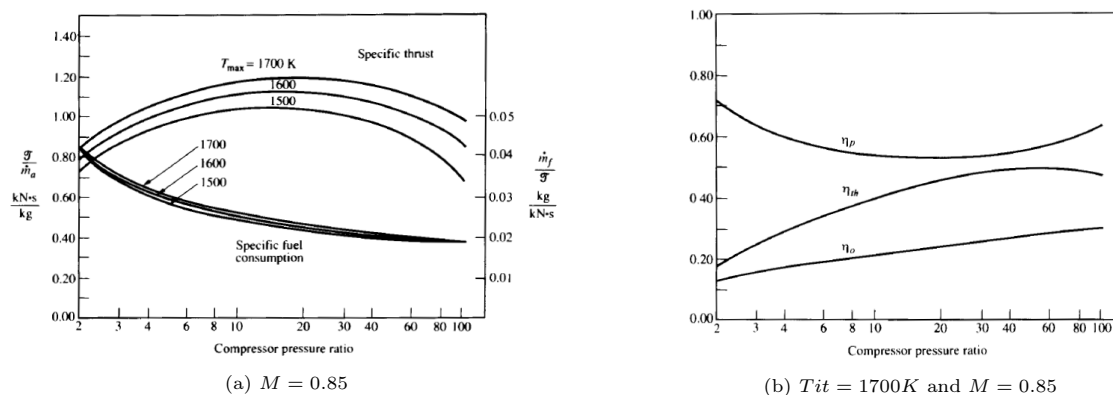


Figure 2: Turbofan cruise thrust, fuel consumption and efficiencies

The advantage of using a bypass rather than a turbojet engine for subsonic flights is evident, and the higher the T_{it} , and therefore V_j , the higher the benefit. Nevertheless there are some drawbacks. A BPR lower than 1 can be used up to Mach 2 [9], but high BPR turbofans cannot be used passed the transonic domain due to the increased drag and structural weight. Moreover, the question of optimum bypass ratio and optimum fan pressure ratio is not that arbitrary, as the difference in the pressure ratio of the inner section of the fan and the outer section, may also become a problem. This conflict between the optimum BPR and the optimum Π_o has been a focus of exploration and may even lead to further improvements in design of turbofans. One last consideration affecting the choice of the BPR is the problem that irradiates due to the mismatch between the rotational speed of the fan and its driving turbine in the absence of a geared power transmission, which limits its design. As the design of the turbofan engine was evolving, this last consideration became evident and quite a limiting factor, together with the reduced stiffness of the fan blades. Further information about this topic can be found in E.

3 Thrust-specific-fuel-consumption and its influence in engines' evolution

3.1 The concept of TSFC

As mentioned in the introduction, one of the parameters that has guided the evolution of aircraft engines has been fuel consumption, therefore, it is important to understand how it is measured and how it has been evolving over the years, as so the future trends to improve it. Probably, the most common parameter to make a reference to the fuel efficiency of a jet engine is the Thrust Specific Fuel Consumption. This parameter not only depends on the engine, but also on other factors such as, the length of the route, the weight of the aircraft, and the share of the airframe, and it is a combined impact of improvements in technology in these different areas which has allowed in average an annual increase in aircraft fuel efficiency of 2–2.5%, according to [10].

The ability to produce thrust with a minimum fuel expenditure is one of the main parameters that is considered to be a prime performance parameter in an engine. An engine that is incredibly fast but, consumes excessive amounts of fuel which disables long range trips or forces plane tickets to be extremely expensive to be able to afford its operation costs, are not worth it for airlines. It is therefore an important parameter to consider when selecting the power plant that matches the mission of the airplane, as it will directly affect the range and endurance of the plane. Hence, it is interesting to go a little bit deeper into the comparison of these engines, to see how the fuel efficiency of aircraft engines has evolved during the years, and how the future looks like.

The thrust specific fuel consumption TSFC, is the ratio of fuel flow rate per unit of thrust force produced, and it is one of the most important metrics employed in aviation as it indicates how efficiently the engine converts fuel into power: $TSFC = \frac{\dot{m}_f}{F}$.

This parameter allows comparing different engines regarding its performance and efficiency. While there is usually not a great variation in TSFC between engines within a specific class of power plants, there is a huge variation between the classes, as we will see now.

The jump from turbojets to turbofans to improve propulsive efficiency had a clear effect in fuel savings. When the primary flow rate is the same as the flow rate for a turbojet, and both engines have the same overall pressure ratio and turbine inlet temperature, the fuel flow rate remains the same. Since the thrust however increases significantly with BPR, especially for high BPRs, the TSFC of a turbofan will be significantly lower than that of a turbojet at subsonic flight. However, it is not that simple, because a larger fan diameter, at a given thrust, increases engine weight, which can partially, or even fully, negate any SFC benefits. The following picture shows orders of magnitude of typical TSFC values for turbojet and turbofan engines, obtained from [1].

Engine Type	Jet Velocity (m/s)	TSFC SLS TO (kg/hr/daN)	TSFC 35kft M 0.8 (kg/hr/daN)
Old Turbojet	600	1	≈ 1
New Turbojet	600	0.8	
LBPR Turbofan	500	0.6	
HBPR Turbofan (5-6)	350	0.4	0.65-0.58
VHBPR Turbofan (8-9)	300	0.35	0.57

Table 1: Typical TSFC values for turbojet and turbofan engines

Nevertheless, obtaining a lower TSFC is not only a function of the BPR. It also depends on the selection of an appropriate combination of the fan pressure ratio and bypass ratio which, indeed, it is not an easy task. To reduce the TSFC during subsonic cruise, a high BPR is selected, a high overall pressure ratio, a high TIT and finally, a moderate to low fan pressure ratio (depending on the BPR; lower values for higher BPR). The following figure shows the influence of the fan pressure ratio and bypass ratio on the fuel consumption of the engine. The figure clearly shows that an increase of the bypass ratio leads to a strong reduction in the SFC of the engine. The specific thrust however decreases as well, which means that the engine becomes significantly bigger for a

given thrust level. The figure also shows that the proper selection of fan pressure ratio is crucial. As shown, there is an optimum fan pressure ratio for each BPR. Deviating too much from this pressure ratio leads to a strong rise in SFC.

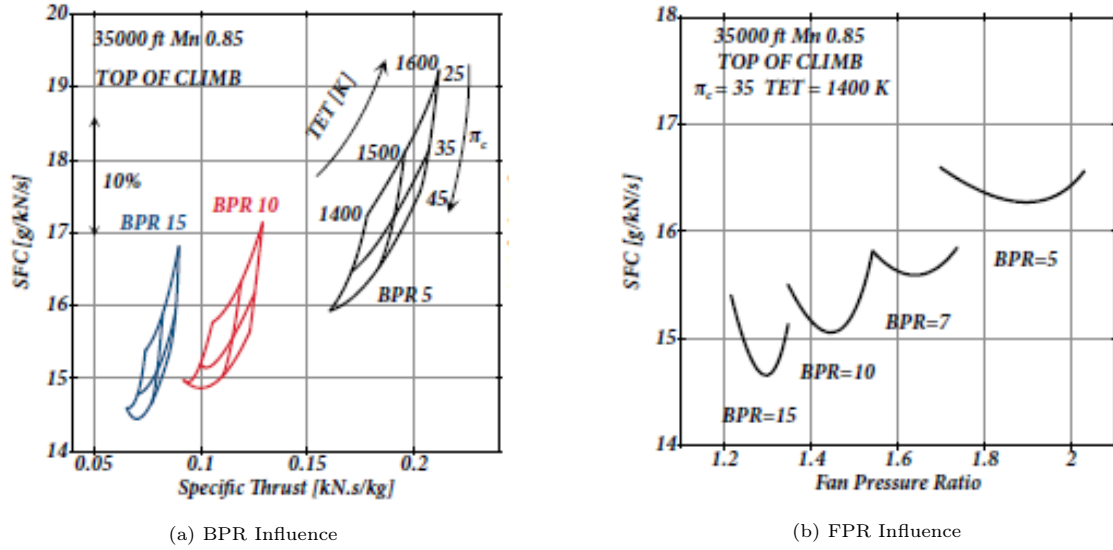


Figure 3: Influence of BPR and Fan Pressure Ratio on SFC for Typical Civil Engines [1]

On the other hand, turboprop engines generate both thrust and horse power, so a combined metric has to be defined to be able to make a comparison among engines. In order to do so, the equivalent shaft horse power combines the shaft horse power and the residual thrust into a single measure of the performance of a turboprop engine:

$$ESHP = SHP + \frac{F_{res} \cdot V_a}{\eta_p} \quad (3)$$

Since the ESHP is used to characterise the performance of a turboprop, it is logical to relate the specific fuel consumption to the ESHP, which is basically the ratio between the fuel flow to the equivalent shaft horse power (the power outtake of the engine). This parameter is usually known as the equivalent specific fuel consumption: $ESFC = \frac{\dot{m}_f}{ESHP}$.

In many books, this parameter is referred to as the break specific fuel consumption. Since the power of an aircraft equals the thrust times velocity ($P = T \cdot V$), the connection between PSFC (or ESFC) and TSFC is: $TSFC = ESFC \cdot V$.

As introduced with the turbofan, there are different parameters that cause variations in the TSFC. On the one hand, a higher engine rating implies an increase of the turbine inlet temperature T_{iT} and the compressor pressure ratio Π_c . The variation of both parameters results in a substantial increase of the thermal efficiency, which leads to a strong decrease in the thrust specific fuel consumption TSFC. On the other hand, jet engines benefit from a big temperature difference between maximum internal temperatures (limited by engine material) and outside air temperature. At lower outside temperatures, the thermal efficiency increases, leading to an increase in the overall efficiency, which leads to a reduction in the TSFC too. At higher altitudes the ambient temperature drops strongly, that is why, if possible, it is interest-

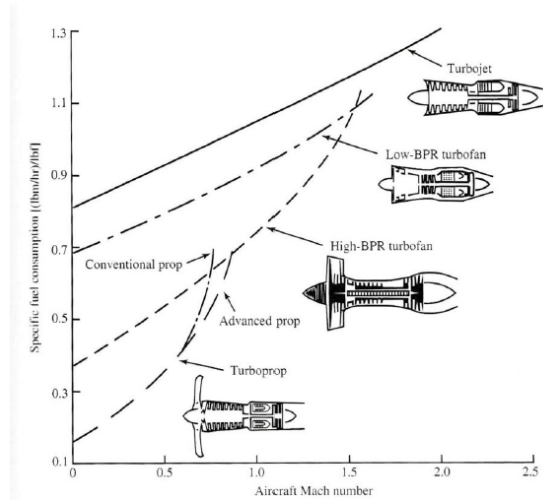


Figure 4: TSFC characteristics for different engines [11]

ing to fly high. From the tropopause onwards, the temperature and thus in principle also the TSFC, remains constant, so the variations of the TSFC with altitude will be very little. At high altitudes the TSFC can however rise slightly as a consequence of the decreasing Reynolds number (making the compressor efficiency to drop). Lastly, models such as that from Mattingly 1996 or Schulz 2007 [11] show a linear dependency between the speed and the TSFC during subsonic flight. When the flight velocity, V_a , increases at constant ambient conditions, the mass flow rate of the engine will increase. To keep the TiT constant, more fuel has to be injected to keep the fuel-to-air ratio constant. The fuel flow rate will thus increase proportionally with the air flow rate. This can be appreciated in the figure 4. Since we are only interested in subsonic flight, one may say that all types of engines are linearly dependent on the speed of the aircraft. A small exception would be the turboprop; however, these engines will usually not be operated above Mach 0.6 in which case the curve may still be seen as linear. Over that speed, they usually become too noisy and heavy. The pure turbojet, of the kind used in the early days of the jet propulsion, has very poor efficiency, worse even than low bypass turbofans. The high bypass turbofan, in comparison, has superb efficiency, something that explains their wide use in modern passenger transport aircraft.

Even though, the difference in TSFC is clear, it does not really make sense to compare two engines with different speed. Fuel efficiency differences can be explained largely by differences in aircraft operations, not only in technology.

3.2 Technological evolution to improve TSFC

According to [3], for commercial jetliners, the most important factors are aerodynamics and engine performance. The aerodynamic quality of the turbomachines has already reached a very high level and there is little room for further improvements. Or better said, lately, huge efforts usually make little effect. As for the latter one, we have seen that lowering engine SFC can be achieved by improving propulsive efficiency and thermal efficiency (either by reducing component losses or by improving the thermodynamic cycle). Also, it is clear that reducing engine weight results in a lower aircraft maximum take-off weight, which in turn leads to reduced thrust requirements for a given aircraft lift to drag ratio. Furthermore, reducing engine size, reduces drag and therefore also leads to reduced thrust requirements. A reduction in thrust requirements essentially results in lower fuel burn too, therefore it is an aim. Nevertheless, it is not that easy because the configuration of an engine is limited by the physical factors that, at the same time, limit the engine performance. Therefore, talking about an engine's configuration without mentioning those factors, does not make much sense. Basically there are two kinds: the material limits, related to stress and temperature levels, and aerodynamic limits related with the compressibility effects.

To start with, as mentioned several times, improvements in thermal efficiency, can be achieved mainly by increasing engine Overall Pressure Ratio (OPR) and TiT. This increase is limited due to the unbearable temperatures achieved which the materials cannot stand, therefore, this depends primarily on future advancements in material and cooling technology. Increasing turbine cooling flows for this purpose is also fairly limited, as cooling flows essentially represent losses in the thermodynamic cycle, and increasing them eventually leads to severe thermal efficiency deficits. Only mild improvements have been achieved so far and this seems to be a continuing trend; the potential introduction of ceramics would form a major improvement in the field, but substantially more research is still required before realising this. Also, the increase of this factor leads to higher flame temperatures which increase NO_x emissions.

Furthermore, the improvements in propulsive efficiency achieved with the design of the turbofan have a limit, because the larger the fan, the higher the engine weight which can partially, or even fully, negate any SFC benefits. On the one hand, that desire for minimum engine mass leads to highly stressed engine components as well as high peak temperatures. This directly affects engine items such as the turbine, as the largest stresses on turbine blades are due to centrifugal force⁷ and the allowable stress in these blades is directly related to the temperature at which they must operate. Thus, a compromise between the turbine blade stress and combustion temperature becomes also critical. On the other hand, as the size of the fan increases, the stress to which they are submitted does it to, and so the necessity of avoiding boundary layer separation due to the

⁷ $F_c = m \cdot w^2 \cdot R$

increase in the linear speed at their tip, for the same rotational speed. Therefore, the bigger the diameter, the lower the optimum speed. Hence, propulsive efficiency improvements are directly dependent on weight reduction technologies such as light weight fan designs and new shaft materials. Increasing engine bypass ratio aggravates the speed mismatch between the fan and the low pressure turbine, so another area of aeroengine improvement is increasing the mechanical transfer efficiency. The introduction of a gearbox, such as the one used in turboprops, can relieve this issue by permitting the design of these two components at their optimal speeds, and can, therefore, reduce engine weight, as well as improve component efficiency.

Improving core component efficiencies is clearly one way of improving the overall engine efficiency, nevertheless, modern designs are already quite aggressive and limited benefit may be reached, or better said, much effort turns out into little reward, at least in the last years. However, this last remark guides one to question about the reason of the appearance of a gearbox in any basic design of a propeller, while it would be a "strange" feature to find in a turbofan, at least if the most modern ones are not considered. Why would engineers not add it from the very first moment, if it, apparently, increases the overall efficiency?. If no GB is used, fans need to be smaller precisely because they will run with the speed of the low pressure turbine, and to convert the available power into thrust, they need a much higher solidity ratio, which translates into a higher wetted surface, which therefore increases friction losses. It seems unreasonable not to include it. This topic has been a focus of study for many designers and the conclusion is always the same: the inclusion of this device is always a complication and a component that can give trouble, therefore, if possible, it is avoided.

The complexity in the design of these GBs lies in the large power requirements. As a rule, these devices are very heavy relative to the engine, they generate too much heat and they do not live much. This already was an issue even in their implementation in turboprops, in which one of the largest power required was ≈ 11000 SHP in the NK-12. Furthermore, as the design power is increased, the specific weight will also increase, therefore, it becomes even more difficult to keep the weight in check. This is predominantly due to the reduction of the propeller speed as power goes up and the fact that the output torque increases faster than power. The effect of this trend which lead to higher specific weight, was an encouragement for the design of multiple torque-path gearboxes, instead of the simplest gear systems with just one gear. Nevertheless, it is important to keep in mind that the rotational speed efficiency benefits, can quickly be outweighed by the extra weight of the gearbox, unless it is extremely power dense. Moreover, even running at high efficiency, the waste heat produced would be in the order of several hundreds of kW, and the increase of loads on gears and bearings, promotes increased wear of details and heat release, reducing significantly their life. An issue to bear in mind.

For a propeller, the addition of a gearbox was quite straight forward. Propellers have bigger diameters than fans, as they are needed to provide sufficient push. Furthermore, most propellers are designed to rotate at constant speed, which would lead to a compressor surge (see appendix C) if connected directly to it. Therefore, the use of a GB allows to control the rotation speed of the different engine parts, closer to their optimum, developing more power thanks to making the engine to operate at higher RPM, while slowing down the propeller RPM, allowing it to push larger amounts of air at a slower velocity and preventing the efficiency decrease, was straight forward.

Apart from the difference in diameter, the design of the turbofan has the characteristic feature of having the fan enclosed in a duct, allowing its aerodynamics to be more controlled even with high flight numbers, such as high as $M=0.85$ [4]. The reason of this is that, the same way as the flow at the tip diameter of the first-stage compressor rotor, is limited to an allowable Mach number (and allowable turning angle), somewhat this happens with a fan or propeller. The detail mentioned about the existence of the duct in the turbofan engine, makes a great difference as the flow velocity approaching the blade can be greatly reduced by its design. Thus, a supersonic flight speed can be transformed, to a speed that will be low enough to avoid serious flow disruption due to shock waves near the rotor tip diameter (where the relative Mach number is highest). Having the fan enclosed by the inlet and composed of many blades, allows it to operate efficiently at higher speeds than a simple propeller.

Furthermore, for the turbofan, most engine designs have preferred to run the fan faster than ideally, reaching even a tip speed of above Mach 1, as it is beneficial to create thrust. There is no denying that having supersonic fan blade tips is best avoided, nevertheless, in these type of engines it is a price which is worth paying because a faster tip velocity means higher dynamic pressure, and the pressure difference between both sides of the fan blade grows with the square of their velocity. This makes the high thrust levels of modern turbofans possible. A proper question at this point would be to wonder why the same does not happen in a propeller. The reason is very simple. The bigger the diameter, the bigger the required torque needed to keep rotating it, that in addition to the increased drag due to the supersonic tips, makes it too complicated. It would be possible when the direction of flow at every station along the propeller blade is about equal to the local airfoil chord, which would be possible but not practical. On the other hand, in turbofans it is liable due to the existence of the intake, which creates constant flow conditions irrespective of flight speed. Propellers can turn at supersonic speeds, but since flow conditions are less controlled, the penalty for doing so is much higher than the penalty for a fan.

Lastly, in the past, with the first turbofan designs, the fan was small and rotated fast. The inclusion of the mentioned duct, allows its configuration not to be so demanding in the aerodynamic limit, as mentioned. However, the maximum tip speed of the fan blades is still limited. By increasing the size of the low pressure turbine and adding more stages to reach the required torque, the fan could be accommodated, avoiding the complication of adding a GB. Nevertheless, with the continued existing necessity to improve, new generation of high bypass turbofans require the fans to be much larger, hence, require too much torque to be driven, while at the same time lower RPM to be efficient. To slow the low pressure compressor-turbine shaft (LPC) or enlarge the turbines more, is an option, but not quite ideal as that leads to a loss in efficiency (higher drag and weight penalties). The inclusion of a gearbox in the turbofan engines started, thus, to be considered, but technological development needed to be done. The space limitations due to the fact that the GB in this engine must be inside the gas turbine, are indeed critical. This does not happen with the turboprops as, even though there are many possible configurations, the propeller is mounted outside the engine. Adding that to the fact that the power transmitted will be higher, this translates in the need of a very high power dense gearbox.

Introducing a gearbox allows, not only to make the rotational speed of the fan independent of that of the booster and the low pressure turbine, but also, to need fewer booster and LPT stages and at the same time maintain the low aerodynamic loading levels required for good efficiency. Gearboxes add weight, for sure, but that's compensated by the elimination of components in the engine core (supposedly). Also, the core engine parts that have been eliminated involve high cost materials, such as superalloys that can withstand high temperatures, while the gearbox materials are less exotic, providing a potential cost benefit. Clearly, the additional weight of power gearboxes competes with potential weight savings in the turbine. The other issue, as mentioned, is that the size of the gearbox implies challenges for the integration in the engine. It is important to balance these effects at an early stage of development, so a powerful pre-design methodology is required to estimate the gearbox mass and size. Testing has shown that GTF gearboxes must be at least 99.3% efficient to avoid that problem [12]. Most turbofans are designed with BPR of 5:1 or 6:1, and the geared turbofan demonstrates interesting and worth it, for applications with bypass ratios above 10, overcoming aerodynamic limitations for high speeds in fan; below this value, it just increases weight and complexity in the gearbox. Therefore, this does not compensate, even taking into consideration the theoretical performance improvements and engine specific fuel consumption reduction. Moreover, it is a must for the GTF gearbox to be very efficient in transmitting power. Even small inefficiencies such as gear tooth mismatch and bearing misalignment would generate enough heat to "cook" gearbox lubricating oil.

In 1970 the oil crisis served as the catalyst for renewed government interest in aeronautics, and NASA launched different ambitious projects, intended to conceive and develop novel technologies that would address this need for greater efficiencies in aviation, specially the propulsive efficiency.

On the one hand, one initiative was known as the NASA's Advanced Turboprop Project (ATP) (1976-1987). The dilemma was the following. On the one hand, when talking about turbofans, the optimum bypass ratio for flight Mach number 0.85 (with this flight Mach number, shocks in

the flow over the suction side of the wings remain rather weak), is between 10 and 15, and this optimum ratio increases with lowering of the flight Mach number. As the bypass ratio increases, the diameter of the fan does too, correspondingly. However, fuel savings might be realised with a somewhat lower flight Mach number (0.70–0.75) [13]. Then, shock losses disappear and a larger part of the wings can be operated with laminar boundary layers (shocks create the risk of separation of a laminar boundary layer). The optimum bypass ratio, thus, increases and the diameter of a turbofan for a large airliner may become impractically large. On the other hand, the speed limitation for propellers was already mentioned. The secret to an ultra-efficient engine was an extreme bypass ratio. A propeller would be more fuel-efficient than any jet, but propellers couldn't operate at high Mach numbers. Therefore, an effort needed to be put in upgrading the propeller-driven aircrafts, to make them more efficient at higher speeds and also make them less noisy. If this improvement was not achieved, propellers would not meet the airline's need for fuel saving.

I will not focus much on this topic, as it is out of the scope of this thesis, but the result of this project were highly swept propeller blades with supersonic tip speeds, so that engines with exposed propellers could power aircraft to speeds and cruising altitudes only attained by new turbojet and turbofan engines. The swept blades allowed to lower the Mach number of the velocity component perpendicular to the leading edge, as with backswept wings of an aeroplane. Increasing, thus, the efficiency at high speeds while lowering the related noise, in contrast to the standard straight-bladed propellers. This advancement allowed achieving the required Mach to have the potential fuel saving of 30% to 50% relative to existing turbofan engines [14]. The term propfan was used to refer to this engine, seen in figure 5a, and involved an increase in the number of blades (from the common propellers with 2 to 4 blades, to ones with 6, or up to 12), increasing the solidity and, as mentioned, with swept-back leading edges at the tips, to accommodate the large Mach numbers encountered. It was, basically, the response to the desire to incorporate the efficiency of the propeller, the high-speed capability of the turbofan and the reliability of the turbine engine. Anyways, with the technology established, the integration phase started in 1981. Different single-rotating prop fans of large scale were tested. Another variation of this propulsor involves the application of two concentric propellers on the same center-line, driven by the same primer mover, having the diameter of the forward propeller larger in order to avoid interference of the tip vortices with the rearward rotor. Such counter-rotating propellers are capable of significantly higher propulsive efficiency and higher disk loading⁸ than conventional propellers, as the contra-rotation concept allows avoiding post-swirl and reduces torque reaction, caused by rotation in just one direction. The diameter of the forward propeller is larger in order to avoid interference of the tip vortices with the rearward rotor. However, due to the public and industry perception of propellers and the concerns over the technical challenges, this project moved forward very slowly and in the meantime, in association with these efforts, General Electric developed their own technology, which was introduced in 1983. The design, which was a variation on the original propfan concept was bigger and more powerful than NASA's design, and it would fly earlier. It was basically a modified turbofan engine, with the fan placed outside the engine nacelle on the same axis as the compressor blades. It also involved two counter-rotating propellers that pushed the plane into the air, rather than pulling it through, as shown in figure 5b, achieving a 20% fuel conservation rate. The propeller blades were each mounted on either one of two sets of counter-rotating low-pressure turbine stages. The definition of the turboprop evolved, to open rotor or unducted fan as a preferred name for this engine. GE's UDF had a novel direct-drive arrangement, where the reduction gearbox was replaced by a low-speed seven-stage free turbine, with one set of turbine rotors driving the forward set of propellers, while the rear set was driven by the other set of rotors which rotated in the opposite direction. This was very well received for those who had been wary of issue-prone gearboxes. Their engine allowed for aircrafts in the 1980s to have a 15% fuel burn reduction relative to the low bypass turbofans of the era [15].

⁸Disk loading: Discharge velocity from the propeller. Ratio between propeller-induced velocity and free stream velocity.

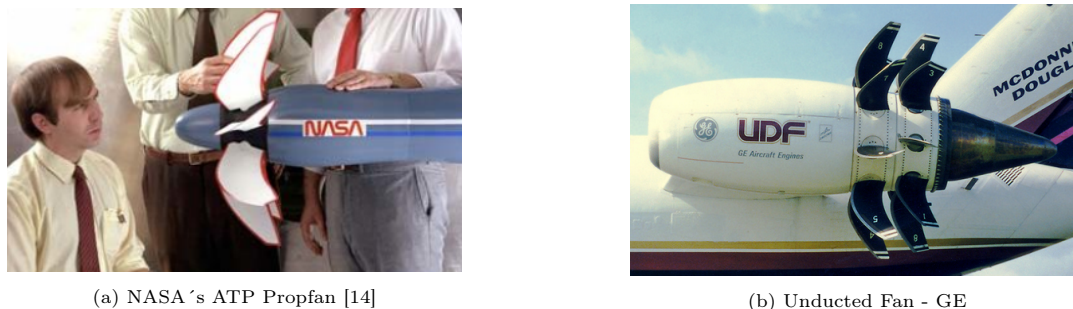


Figure 5: New technologies for the Turboprops

The difference among both technologies is further explained in F, nevertheless, the important aspect in our case is that in 1987, fuel prices started to decrease again, and those advanced technologies were no further "needed". It was more expensive for airlines, to change jet engines to advanced turboprops. Furthermore, despite all the efforts, these engines were still louder, which would dislike customers, and that was a risk that they were willing not to take, which, in turn, made the industry stick to what they had. Any product classified as "green", must deliver superior economic value to the customer above and beyond its favorable impact to the environment, otherwise, it would not "be successful", and this was the case. Nevertheless, all those tests run in turboprop engines, highlighted their problems. Not only the noise was an issue, but also the blade containment and the capability of the high-power gear drive system.

Since then, numerous feasibility studies have been published over the years focusing on future engine and aircraft designs that can reduce fuel consumption. One of the most resounded ones is the one carried-out by Pratt&Whitney. After the Prop-fan program, P&W undertook a 20-year study of worldwide gear experience, which helped to understand the areas of improvement to produce gear systems for Geared-Turbofan-engines. The combination of lower operating costs, high reliability, low noise and outstanding fuel efficiency, as mentioned before, made the product attractive and a good bet for research, and the transmission system of the engines was one of the potential significant improvements. This study was further motivated by the goals set by the Advisory Council for Aviation Research and Innovation in Europe (ACARE) [16], to reduce fuel consumption, noise and emissions. According to it, 20% of reduction in fuel consumption has to come and will come, from engine improvement, another 20% from aircraft improvement and 10% from air traffic management. It is interesting to note that although the work on UDFs ended in the early 1990s, the development of composite blade analysis and fabrication methods for that technology were incorporated into new large-diameter fan blades.

4 Geared turbofan

The use of gear systems in turbofan engines dates back to the early 1970s, with the oil crisis, with the introduction of the Lycoming ALF502 and the Garrett TFE731 (now made by Honeywell, but originally developed by Avco Lycoming and Garrett respectively). Therefore, the geared turbofan concept has already been highly proven in the civil aviation market. However, in those engines, the power transmitted nearly offsets the use of the gearboxes, as their BPR is too low, and it has not been until the appearance of the Pratt&Whitney PurePower PW1000G geared turbofan engine family in 2008, that this engine model has revolutionized the aviation market, as it is considered a model of innovation.

A definition of innovation is the creation of better or more effective products, processes, services, technologies, or ideas that are accepted by markets, governments, and society. The idea behind the geared turbofan was already accepted, liked, approved, but the technology was not advanced enough to make suitable for highly powerful engines. The P&W geared turbofan engine is not another traditional turbofan with a few incremental improvements, it is a model of innovation from the spinner to the tail cone, with the focal point in its gear system. They have been able to get the gearbox down to a scale where it makes the concept viable for large-aircraft applications, enabling a reasonable engine core and size. The P&W GTF combines existing jet engine technology with the well-established mechanical engineering technology of gears. This family of engines has significant improvements in aerodynamics, application of lightweight materials and efficiency gains with the high-pressure spool, low-pressure turbine, the combustor, engine controls and the engine health and maintenance monitoring systems. The heart of these engines is based on the gearbox design which improves the life, durability, and efficiency of aero gearboxes. By the step change in the basic engine architecture of the fan drive reduction gear, huge improvements are possible. This design resulted in a 50 to 75% reduction in engine noise over models of the time, a remarkable 12:1 bypass ratio and a 16 to 20% better fuel burn [17]. Furthermore, the compact, high-speed low-pressure system runs cooler and accomplishes more work with fewer stages, a design feature that helps reduce the number of airfoils and life-limited parts. Furthermore, the engine has many features that facilitate maintenance and reduce time and cost while the engine is in overhaul. A total technological and conceptual breakthrough.

In 2009, all stakeholders of the aviation industry committed to a set of ambitious climate action goals, and since then, an impressive number of technological solutions contributing to those goals have been proposed. In the line of what this paper is treating, it is interesting to talk about the Rolls-Royce Ultrafan. Rolls-Royce is expected to come out with a geared turbofan called UltraFan™ engine in 2025. The technology will come from their scalable three spools Advance engine which, at the same time, comes from their famous Rolls-Royce Trent family of engine (mentioned in appendix B), and it is expected to increase the bypass ratio from 11:1 to 15:1. The UltraFan™ engine will be equipped with variable pitch fan system which will provide weight save in nacelle to overcome bigger nacelle for longer fan blades. The aim is to provide better efficiency and lighter engine to compete with the GTF from P&W, in the narrow body and single aisle market. The UltraFan™ engine will also be used for the development of open-rotor engine by Rolls-Royce. This Ultra High Bypass Technology allows significant reductions in fuel burning, noise and hence, emissions.

In the following sections, I will be presenting the characteristics of the state-of-art gearboxes in both, propellers and turbofan engines, highlighting their differences. First of all, a brief introduction of the simple concept of a gearbox is going to be included, focusing on those characteristics and types that concern our case.

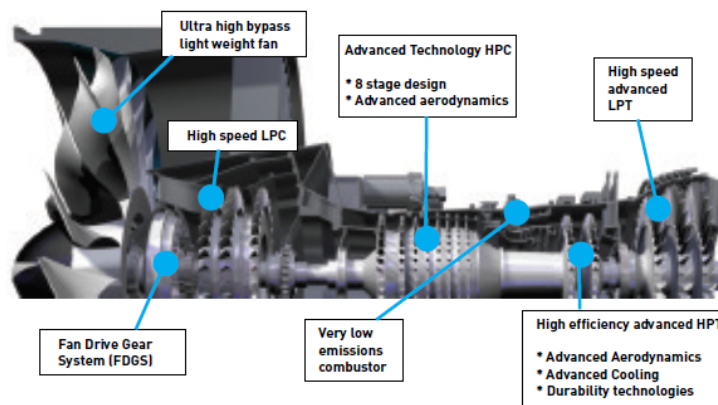


Figure 6: PurePower PW1000G Advanced Technologies

5 Types of gearboxes and gears in gas turbine engines

5.1 The concept of the gearbox

First of all, it is important to mention, in order to clarify the concepts, that any gas turbine counts with an accessory gearbox, or accessory drive, used to transmit mechanical power to different accessories. The module consists on the Main Gearbox (MGB) mounted on the engine core and externally mounted accessory components, on the forward and aft faces of the MGB. Its presence is essential for the operation of the engine, as it turns components in four systems, electrical, fuel, oil and hydraulic, and they usually handle between 400-500 hp [18].

The gearbox concerning this case is the drive gear that allows components to turn at speeds most efficiently for their individual operation. In fact, depending on the design and construction, a gear drive has three main functions: to increase torque from the driving equipment to the driven equipment; to reduce the speed generated by the motor; and/or to change the direction of the rotating shafts.

The heart of the gear drive is obviously the gears within it. They are toothed elements that operate in mated pairs, engaging one another. Each gear is attached to a machine shaft, therefore, when the driving gear rotates along with its shaft component, the driven gear rotates too, transmitting power. Apart from those two, there are more components to be considered in the whole assembly of a gearbox, such as bearings and a gearbox casing. Moreover, there are several types of gears, each of them offering different behaviors and advantages, which are classified based on the different design characteristics such as gear shape, tooth construction and design, and gear axis configuration. Furthermore, the assembly strongly depends on the type of gearbox and varies a lot on existing applications. Besides of the actual gearbox, an oil and cooling system is required, which is vital for the life of the GB. The requirements and specifications demanded by a particular motion or power transmission application determine the type of gear most suitable for each use.

In appendix G, one can find an explanation of the different possible classifications for gears, depending on the different design characteristics, and so the different type of gears available. Even though it is quite generic, an emphasis is put in those ones most used in our application case. The suitability of each type of gear and its exact design for a motion or power transmission application is dependent on the specifications and requirements of the application. Some of the principal factors which may be considered when designing and choosing a gear include the operational environmental conditions, the dimensional restrictions, the transmission requirements and the cost [19]. Furthermore, apart from those design characteristics, there are several other options which may be considered when designing and selecting a gear for a particular application, such as the construction material, surface treatments, number of teeth, tooth angle, lubricant method and type, among others.

In aviation, planetary gearboxes are the most common type of gearboxes used. They are able to transfer the largest torque and speed, in the most compact and light form. They basically can offer a higher power-to-weight ratio than a fixed axis shaft. The reason of the name is because of how the different gears move together which reminds to our planetary solar system. It consists in at least, three gears, a sun gear, a planet gear and a ring gear (seen as A,B and C correspondingly in figure 7). The sun gear is located in the center and engaged to the planet gears, which at the same time, on the other side (180 degrees opposite direction), mesh with the ring gear. The planet gears, themselves, are pinned to a carrier (D). Usually, it needs two or more planet gears to balance the load evenly. These main components make up a stage within a planetary gearbox, but for higher ratios double or triple stages can be found. Furthermore, there are different planetary gear systems: the planetary type itself, the star type and the solar planet. The difference between them is the transmission ratio and the direction of rotation which changes according to which member is fixed. In the picture and table below one can see the differences and the characteristics summarized:

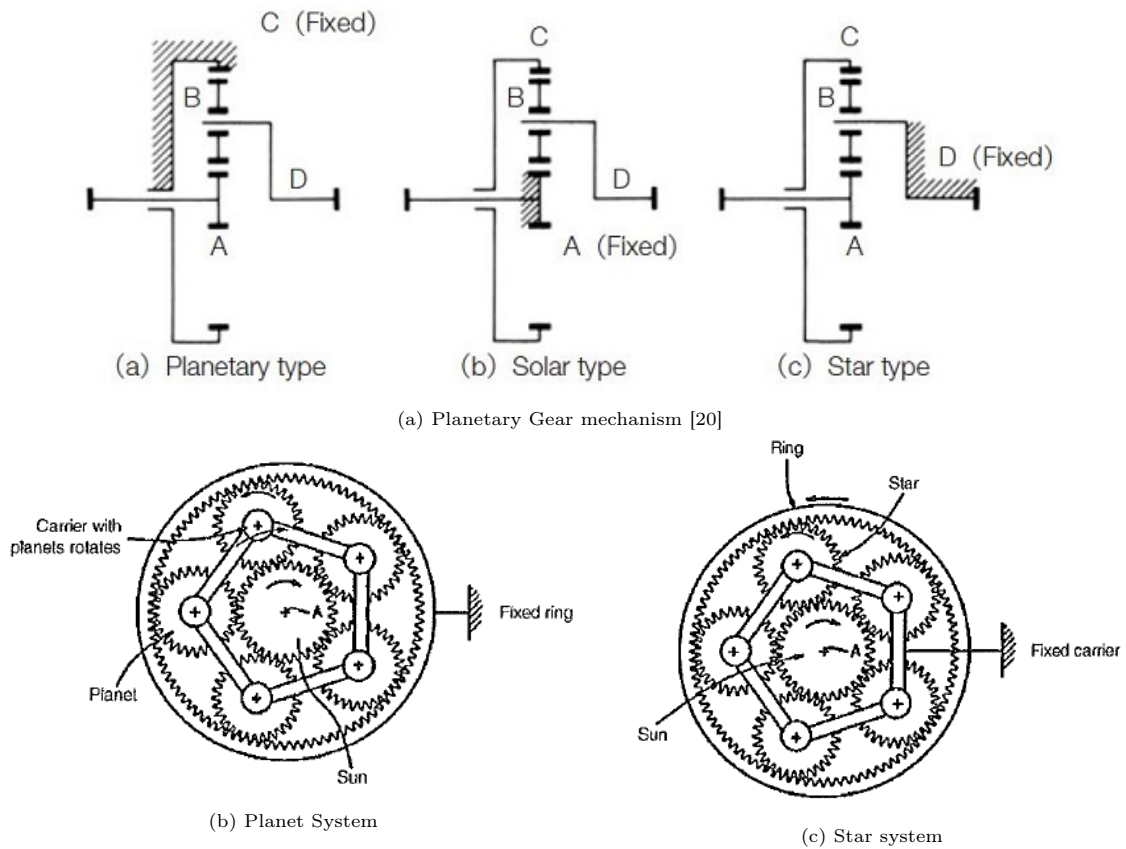


Figure 7: Planetary gear schemes

Arrangement	Fixed gear	Input gear	Output gear	Range of ratio input to output	Advantages/Challenges
Star	Carrier frame	Sun gear	Ring gear	3:1 - 11:1 (opposite direction)	Torque balances due to counter rotating
Planetary	Ring gear	Sun gear	Carrier frame	3:1 - 12:1 (same direction)	Stress carried by joints from carrier to planet gear
Solar	Sun gear	Ring gear	Carrier frame	1.2:1 - 1.7:1 (same direction)	Stress carried by joints from carrier to planet gear

Table 2: Types of arrangement for epicyclic gear systems

In the planetary type, the ring gear is fixed, being the input the sun gear and the output the planet carrier. In the solar type, the sun gear is fixed. In this case, the ring gear is the input and the carrier axis is the output. In both cases, the rotation of direction of the input and output axes are the same. Lastly, the star type has the carrier fixed with the planets gears rotating only on fixed axes. In a strict definition, this train loses the features of a planetary system and it becomes an ordinary gear train. The sun gear is an input axis and the internal gear is the output. In this case, input and output have opposite directions. This design is a highly efficient and effective way of transferring power. Part of the power is transferred as clutch power, resulting this in high efficiency and high power density. Nevertheless, for that to happen optimally, an even distribution of load on the individual branches of power must be ensured. Static overconstraint, manufacturing deviations and the internal dynamics of those transmission gears can ruin the environment. That is why the manufacturing process is quite complicated in comparison with other types of gears, and the choice of planetary gearbox type and the gearing ratio, should be defined by the outcome, and a careful balance between size, efficiency, performance and cost.

If the degree of reduction wanted is higher, a more complex planetary mechanism involving a sequential installation of planetary stages, can provide it. In this case, the output of the first planetary stage is connected to the input of the next, as a result of which the overall gear ratio is increased. For instance, simple planetary gears generally offer reductions as high as 10:1 [21], while a combination of various planetary stages in series, can achieve reductions many times higher. This scheme is the most compact and energy - intensive, as high stresses are distributed over two streams. That is why one of the important advantages of planetary transmissions is the multithreading of energy transmission. Its scheme can be seen in figure 8.

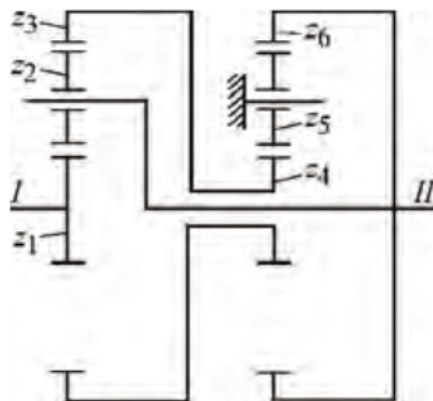


Figure 8: Planetary Gearbox with various stages

The main advantages of these systems is that thanks to the teeth, the gears cannot slip, therefore, an exact and high transmission ratio is maintained, large forces can be transmitted, and the number of turns a gear makes can be easily controlled. As many teeth are engaged at the same time, a high speed reduction is possible, and since the load is being transmitted among multiple gears, the torque capacity is increased. Furthermore, there is a direct relationship between loadability and torque density⁹. In the same line, as the load is divided, for the same amount of torque smaller gears are needed. The gearset design is also dependant on the gear ratio applied, as this factor has significant impact on load capacity. To explain it in an easy way, one gearset has a ratio of 3:1. The planets will be small compared to the sun gear. In fact, having too low gear ratios is not always possible, due to the fact that the pinion and outer ring gear would need to be nearly the same size, leaving no room for the planet gears. On the other hand, a set with a 10:1 ratio has relatively oversized planets, and therefore, load-carrying capacity is most limited by the sun. This goes together with the fact that a simple planetary stage will not offer a higher ratio, because pinion gears can be made only so small. The best balance of gear geometry is somewhere in between these extremes. That said, there is a limit to how many planets can be added. For example, the maximum number of planet gears in a system with a 10:1 ratio is 3.

This type of gear arrangement improves stability, rotational stiffness due to a balanced system and torque density, and all that, thanks to the increased number of gear contacts. This allows the gears to be more resistant to damage and to have higher durability. Three is the most typical number of planets, but all these benefits are upgraded as the number of planets are increased. However, it comes with a more complex and costlier manufacturing design. The precision in its design must be really high, otherwise, if the load taken up by the planets is not perfectly balanced, the operation may not be able to accept it, leading to a premature wear and failure. Furthermore, the compact design makes heat dissipation more difficult, which implies a need of cooling. Some other problems can also be found with the interference of the internal gear or the need of good lubrication.

When using planetary gears, one can also choose between spur or helical among other types, and this choice is certainly not arbitrary. Again, more information about the different types of gears can be found in appendix G. While in spur gears, the presence of bearing plays "just" a supporting role in the functioning of the gearbox, for the helical gears, which produce axial forces, the presence of a thrust bearing is crucial to withstand it (see appendix H). In a fixed-axis gearbox, those additional axial forces can be dealt with an up size of those bearings to accommodate them. Nevertheless, in planetary gear systems, there is usually little room for an up-size. Furthermore, its main functioning principle implies for the planets to split the torque input and transfer it to the output shaft, however, those bearings that support the planets in the carrier, need to be able to bear the whole impact of that torque transfer. A combination of small bearings that withstand high axial loads in a planetary gear system are not that easy to find, as these loads create tilting moment and uneven load distribution along the bearing, drastically lowering the bearings load carrying ca-

⁹Torque density is a measure of the torque-carrying capability of a mechanical component.

pability and life cycle, as seen in appendix H, and decreasing the efficiency of the system. Each design has to be treated individually, and the pros and cons of every choice need to be out-weighted.

Improving the overall efficiency of the GB, boosts its profits. Efficient power transmission systems ensure fuel economy which, therefore implies that less pollutant gases are emitted to the environment. Since power losses amount to heat generation within the gearbox, several gear failure modes such as scoring and fatigue can be directly influenced by the efficiency. Furthermore, improved efficiency of a gearing system can reduce the requirement on the capacity of the lubrication system and the gearbox lubricant and thereby reducing the operation cost, as it permits the oil flow to be reduced without affecting the temperature rise across the gearbox. Lower oil flow rates reduce oil pump energy losses. Reduced oil flow rate requirements also allow the weight and size of the lubrication and cooling system to be reduced. Depending on the application, different factors are more important than others, but the possibility to investigate different gearbox geometries and operating conditions in the preliminary stages of the design represents a clear advantage for engineers and can significantly contribute to finding the best design. There are different type of losses to be considered in gears, and their contributions to the power loss of the overall system strongly depend on the specific gearbox configuration. These losses can be divided in two groups. Firstly, the load dependent (friction induced) power losses caused primarily due to contacting surfaces of gears and bearings due to torque transmitted through the system which, at the same time can be divided into different sub-losses: sliding and rolling losses. The second group are independent of the load and are often referred to as spin power losses. These losses appear with the rotation of mechanical components, even without torque transmission.

Load dependent losses occur in the contact of the power transmitting components. The sliding losses occur when two surfaces slide against each other, and a large amount of frictional heat is generated alongside wear. In order to keep this loss at a minimum the gears are lubricated with oil or grease. Making the surfaces separated from each other and instead sliding against the lubricant. Lubricants are used for decreasing tooth friction but also for dissipating the heat generated. One can distinguish now, three different types of friction: dry friction (surfaces sliding directly against each other), lubricated friction (surfaces partially separated by a lubricant) and fluid friction (surfaces completely separated by oil). The fluid friction is the preferred type of friction from a loss minimization perspective. To achieve and maintain a fluid type friction the sliding velocity must be high enough to separate the two surfaces. If the speed is low the same effect can be achieved by using a lubricant with a higher viscosity. Or if the surface roughness is decreased a lubricant with a lower viscosity can be used. Furthermore, when two lubricated surfaces roll against each other a rolling loss is generated from the pressure build up in the lubricant as it is squeezed in between them. The higher the viscosity, the higher the rolling forces.

Spin losses, on the other hand, are related to lubricant viscosity and density, as well as immersion depth, the interaction of the moving components and the surrounding fluids (air, oil or a mixture of them), and also, the operating conditions and internal design of the gearbox casing. These losses's source come primarily from internal oil churning, windage and squeezing. Windage and churning are conceptually very similar to each other, but churning appears if the rotating components are partially submerged in an oil bath (dip lubrication), while windage appears under jet lubrication with the interaction of air/oil and air mixture and the rotating gears. Squeezing is a lower order of magnitude phenomena associated with the compression-expansion process by the meshing teeth. The contraction of the volume at the gear mesh implies an overpressure that induces a fluid flow primarily in the axial direction and this, for viscous fluids, means additional power losses and a decrease of the efficiency [22]. This type of losses can be controlled, for the most part, by careful design and construction.

The importance of the lubricant for the good life of the gears is clear, but not only that, it contributes to the cooling of the system, as mentioned, and the reduction in the operating temperature contributes to a better lubrication, less oil degradation and lower needs in maintenance. It is a win-win. Such increase in gearbox efficiency is possible through an improved gear tooth design and selecting the most suitable gear oil formulation.

Among the different type of gears or configurations that one can find in this industry, what they

all have in common, is that they are quite rigid and have high resistance against shock loads. As any part of the aircraft, the selection of materials involves multiple and challenging requirements that go beyond essential performance attributes (strength, durability, damage tolerance, and low weight). Materials must exhibit a set of demanding properties, be producible in multiple product forms and demonstrate consistent high quality. Furthermore, they must be both commercially available and affordable, and the list of materials meeting these requirements is not long. The gearboxes need to be of high efficiency at small overall dimensions and always striving for lowering the mass (even though, their mass makes a considerable proportion of the whole mass of the engine, and even in some cases, exceeds it); high reliability within the limits of installed service life, good manufacturability in production, repairability and serviceability. The high reliability of GBs is provided by sufficient safety coefficients and necessary rigidity of its elements, application of high-alloy steels made with large accuracy which tolerate large stresses, surface strengthening of contact surfaces, and the usage of automatic safety devices preventing overload of the GB [23]. All this, has to be combined with high accuracy, as the GBs are a source of torsional oscillations which can result in a breakage of the devices. These oscillations may arise because of inexactitudes caused by roughness in manufacturing of gear wheels, and also deformation of teeth under operation of loads in engagement, resulting in an alternation of pitch and angular speed causing high-frequency oscillations in a system. That is why trying to reduce these oscillations is the main focus of the designers. Increasing the coefficient of overlapping, with for example helical gears, are some of the factors that help reduce them, nevertheless, there are always drawbacks to be considered.

5.2 State-of-art gearboxes

Focusing on the turboprop and turbofan engines and having understood their design, in which it is clear that a parallel axis gear is applied, we will see that sometimes, in order to achieve the appropriate performance to comply the necessities, a serial arrangement of several gears are mounted together, being each of them an individual stage. The interesting part is that with multi-stage gearboxes a combination of different types of gears can be used. For example, when introducing standard gear reducers into a planetary train, the high-speed power might pass through an ordinary fixed axis gear set before the planetary reducer. Such a configuration, called an hybrid, is sometimes preferred as a simplistic alternative to additional planetary stages, or to lower input speeds that are too high for some planetary units to handle [21]. It also provides an offset¹⁰ between the input and output. If a right angle is needed, bevel gear may be sometimes attached to an inline planetary system. Having such options greatly expands the mechanical possibilities and one can reach their objectives in the most efficient way. This is where engineers "play", in order to reach the best design. Beyond all those complications and considerations needed to be taken into account in the design of the GB, another important factor to keep in mind is the heat produced due to the friction in engagements. In this type of application, the lubrication and cooling systems for heat rejection due to this issue are vital for the durability and well performance of the devices. The power "lost" due to friction losses and the pumping of oil and cooling to reject the heat produced can be reasonably high. Depending on the type of engine, the systems used may vary, and they play an important part in the gear type decision as a considerable part of the mass of the GB, is the mass of these systems.

It is already clear that the application of propellers (or fans) as movers of aircrafts together with gas turbines, justifies the necessity of the application of GBs of greater and smaller complexity, finding the difference essentially due to the different rotational frequencies among the different engines, and the power transmitted. As a background, some orders of magnitude for a particular version of the following engines, is shown bellow:

¹⁰An offset is the perpendicular distance between the axes.

Turboprops	Maximum Power (kW)	RPM - Power turbine and propeller	Type of gear
PW 120	1491	20000 / 1200	Placed out of the engine (three shafts)
Canada PT6	1450	30000 / 2200	Two stage planetary with helical involute
TP400	8251	8200 / 860	Offset 1st stage and planetary
Allison T56	2800	13800 / 1104	Spur set and planetary

Table 3: Order of magnitude for some turboprop engines

As it is appreciated, the GB can be a part of the engine or it can be mounted as an autonomous part. This is one of the features that play in favour in the turboprop engine, as there is not such a space limitation. The data shown in these tables is obtained from different sources such as [23] and [24], and helps us clearly see the difference among the power transmitted (Power = Torque x RPM) and the reduction ratios in both engines.

Geared turbofan	Static Thrust (kN)	RPM - LPT and Fan	Type of gear
TFE 731-2	15.6	19730 / 10970	Planetary with involute spur gears
Honeywell LF 507	31	7300 / 3200	Planetary with star arrangement
IAE Superfan V2500	133	5650 / 1900	Planetary with simple helical gears
PW1000G	160	15000 / 5000	Planetary Star system

Table 4: Order of magnitude for some Geared Turbofans

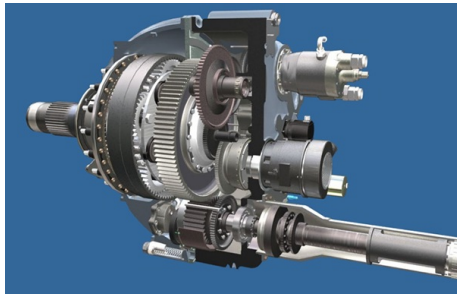
As expected, a bigger diameter of the propeller, involves a lower optimal speed. In the case of the turboprops, lowering the rotational frequency of the shaft of the propeller is reached by the application of gear ratios between 7 and 16. On the other hand, the gear ratio needed in a geared turbofan is typically lower than 3. Apart from that, the torque transmitted by the GB on both engines is far from similar, which is the main issue in geared-turbofans.

Having seen the requisites demanded for a GB in an aircraft engine, in this situation in which space and weight are an issue, but a large amount of speed reduction and torque are needed, planetary gear systems are indeed the right fit. This has been proven in tables 3 and 4, where nearly all the examples use this type of gear, and for that reason this thesis focuses on a comparative between the Epicyclic Gear Train configurations used in turboprops and turbofans. We will now go further into detail into some of these mentioned engines. Some of these engines are the ones mentioned in appendix B, thus particular information about them can be found there. As an advancement and in line with what was mentioned, the design of a GB is not that simple as just choosing a planetary type. Different arrangements and combinations are possible, and it is always worth it to keep them in mind. For sure, the small and light GBs transmitting powers from several hundreds up to several thousand kN, usually involve the construction of complex planetary transmissions, which in combination with others, can reach the expectations. In [25] a detailed study on gearbox types was performed for both, single and counter rotating propulsors. The study differentiated between inline and offset gearboxes and discussed different gearbox designs. The conclusions reached from that study were that for ducted engine concepts (such as turbofans) as well as for counter rotating applications, a planetary gearbox was found to be the superior solution. For single rotating propellers, a wide range of very different in service gearbox types was found, but the most common gearboxes contain a reduction spur stage and a planetary gear stage.

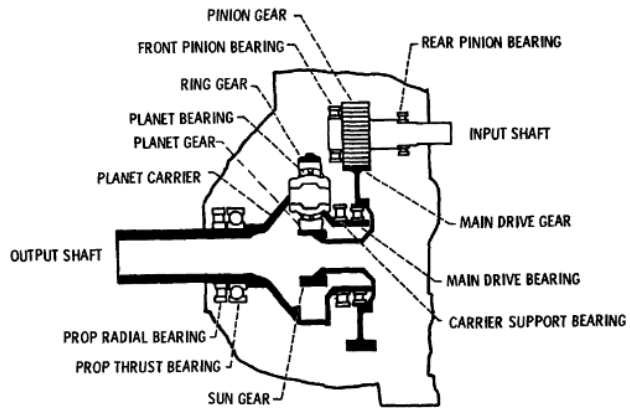
5.2.1 Gearboxes for turboprops

• Allison T56 - Single shaft turboprop

The Rolls-Royce T56 is a single-shaft engine with a modular design. The engine itself and its gearbox has evolved a lot during the years, being one of the leading large turboprop engines globally. It has been the focus for many development programs whose aim is to look for an improvement in power and fuel consumption through the incorporation of demonstrated technology while retaining its durability and cost effective design.



(a) Allison T56 gearbox



(b) Gearbox [26]

Figure 9: Gear Layout Arrangements

The T56 entered in production in the 1954, and its original gearbox came from an evolution of machines such as the T40. Over the years, there has been a number of engine development versions, which are grouped by series numbers, allowing to increase the maximum power delivered, through increases in pressure ratio and turbine temperature. During the late 1960s, a new gearbox design was presented after an engine enhancement program to reduce fuel consumption and decrease temperatures. Up until the date, it has been its last update in the GB design. The T56 family of engines uses an off-set gearbox arrangement, remotely mounted, rigidly attached to the power section with struts. This provides the design of some flexibility, allowing to use of the same basic propulsion system in different airframes. For example, airframes in which the propeller must be offset above the engine center line or those in which the propeller must be below the engine center line. In the table below, whose information is obtained from [27], the characteristics of both designs is shown. The total reduction to the propeller shaft is 13.54 to 1, for applications such as that in the Lockheed CP-140 Aurora, with a propeller's diameter of 4.11m. To avoid the use of a very large gear to get this reduction, two stages are used. The first stage is 3.125 to 1. The second planetary stage is 4.33 to 1, counting with 5 planets in the set. The T56 A-7 is an engine version from the Series III with an engine power of 3020 kW, while the T56 A-18 belongs to the series 3.5 and reaches a power of around 3400 kW.

Gearbox Feature	Early GB - T56 A-7	Mature GB - T56 A-18
1st stage gearing	Spur gear	Double helical
2nd stage gearing	Planetary spur gear	Planetary helical gear
Accessory gearing	Separable clamped components	Fewer parts

Table 5: Evolution of the T56 Gearbox

Nevertheless, despite the clear differences, there are some features that were kept from the first design. The use of a torquemeter is constant, and so the gear damper rings. These rings are used to reduce the vibration in the main drive bull gear, by locating them in the gear rim. Also, the gear cooling and lubrication by high-pressure jets directed to the out-of-mesh side, were kept. Moreover, the use of practical gear tooth such as the involute, and tolerances for production manufacture was a step forward in efficiency. All gears for the family of the T56 engine have always been designed for infinite life and many of them haven been operating for more than 10000 hours, which means more than 10^{11} cycles on the pinion gear teeth.

- PT6 - Two shafts turboprop

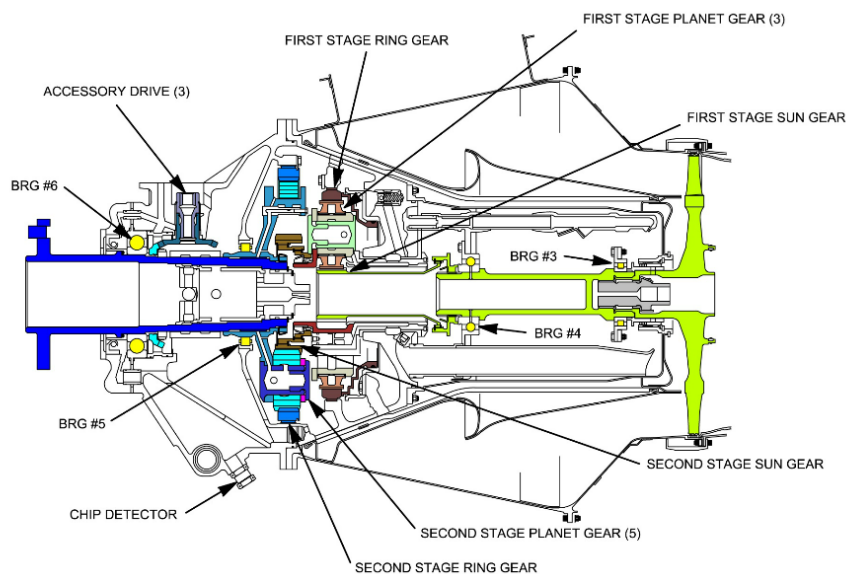


Figure 10: PT6 Reduction Gearbox Details [29]

The Pratt & Whitney Canada PT6 has spawned a wide family of turboprop and turbo-shaft engines since its first entrance in service in 1963. The original configuration has been maintained among the different versions, but thanks to the advancement in technology, different improvements have allowed to even triple the engine power from its original one, without suffering too much change, physically talking, reaching in its highest model 1450 kW. A brief evolution of the engine is shown in the table bellow (obtained from [28]):

Engine Model	PT6A-6	PT6A-68
Max. Power (kW)	456	1365
Power/Weight (kW/kg)	3.7	5.4
Max.gearbox power (kW)	410	1200
ESFC (kg/kW.hr)	0.39	0.30

Table 6: Evolution of the PT6

For propeller applications, such as the Antonov An-28 with a propeller's diameter of 2.8m, the engine counts with a two stage planetary epicyclic gearbox which provides an overall speed reduction by a factor between of 15:1 to 23:1 [28]. The first stage (5:1 reduction ratio) consists of a sun gear meshing with three planetary gears mounted in a carrier, coupled to the second stage gear. The outer ring gear of the first stage is helically splined into the gearbox, providing a means of measuring torque. The second stage (3:1 reduction ratio) is very similar to the first arrangement, but uses five planetary gears instead of three [29]. The output shaft is splined to the propeller shaft, which has a beveled ring gear attached to it for driving the propeller. This basic gearbox configuration has been maintained throughout the evolution of the PT6, except for the use of a star system in some models to reverse the rotational direction of the propeller. The development and application of technology to this gearbox configuration has enabled it to grow from 550 SHP to 1600 SHP without a commensurate growth in size or weight while maintaining reliability. In the pictures below one can clearly see the whole design.

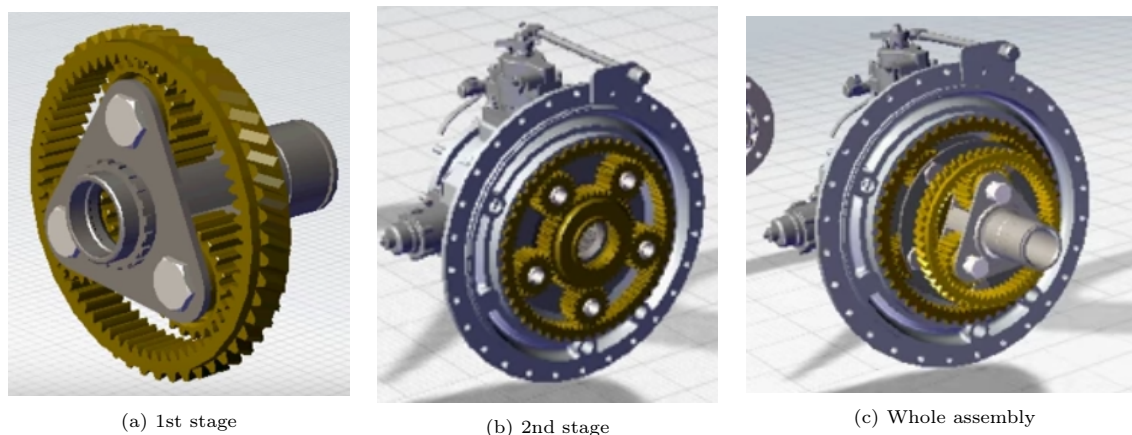


Figure 11: PT6 Gearbox

• PW100 - Three shafts turboprop

This family of engines is interesting to be analyzed, because the gearbox used is not a planetary type as the one we are focusing on. This is an example of the different possibilities that gears provide and a prove that every engine needs to be treated as unique.

PW100 is the name given to the third family of P&W engines. The designation of the whole family is like that, but actually there is no PW100 engine. The last two digits in PW1XX will indicated the take-off horsepower in hundreds. The engines are essentially the same, with, for the most part, a steady increase in power output, as well as slight variations in engine output speed and in the proportion of mechanical shaft horsepower vs. thrust produced. This engine, which entered in service in the mid 1980s, has powered regional turboprop aircraft from 1500kW to 4980kW, thanks to increasing the pressure ratio and the turbine inlet temperature, as well as the application of new technology, allowing to consume 25% to 40 % less fuel and produce up to 50% lower CO_2 emissions than similar sized jets [30]. The general configuration has been constant throughout the life of the engine program. It features a relatively unusual three-shaft engine configuration, it is a two-spool engine. Low pressure and high pressure compressors are powered independently by cooled turbine stages. A third shaft couples the power turbine to the propeller through a reduction gearbox, optimized to establish the best combination of engine and propeller efficiencies. This model is completely modular in its construction. Its modules, can be easily removed and replaced when needed, which makes maintenance a lot easier. A brief summary of the evolution of the PW100 engine is shown here:

Engine Model	PW120	PW127	PW150
Max.Power (kW)	1782	2457	4980
Power/Weight (kW/Kg)	4.27	5.11	7,22
Max.gearbox power (kW)	1491	2050	3781
ESFC (kg/kW.hr)	0.286	0.273	0.255

Table 7: Evolution of the PW100

The PW100 reduction gearbox is a two stage, offset design for turboprop applications with reduction ratios varying from 15.4:1 to 17.16:1, powering propellers of around 3.6m, such as that of the Antonov An-140. This basic gearbox configuration has been maintained throughout the evolution of the PW100 from the original PW115, to the newest PW150 reduction gearbox. The development and application of technology to this gearbox design has enabled this growth without a corresponding increase in weight. The first stage gears incorporate double helical gears for increased capacity and smoother running. The first stage torque from the input pinion is shared between two gears on opposite sides of the pinion. This reduces the loading on each gear mesh and balances the load on the input pinion bearings for increased life and reliability. The use of a double helical gear arrangement with the split torque path, means that the torque in the first stage is shared by four gear meshes. The torque is transferred from the first stage to the second stage gearing by means of two lay-shafts which provide both torsional and lateral flexibility to ensure

equalized gear load sharing and accommodating any misalignment. The two second stage pinions drive a bull gear¹¹ mounted directly on the propeller shaft. These are high contact ratio straight spur gears, which means that at least two gear teeth carry the load at any instant in time, to provide high load capacity combined with smooth running [31].

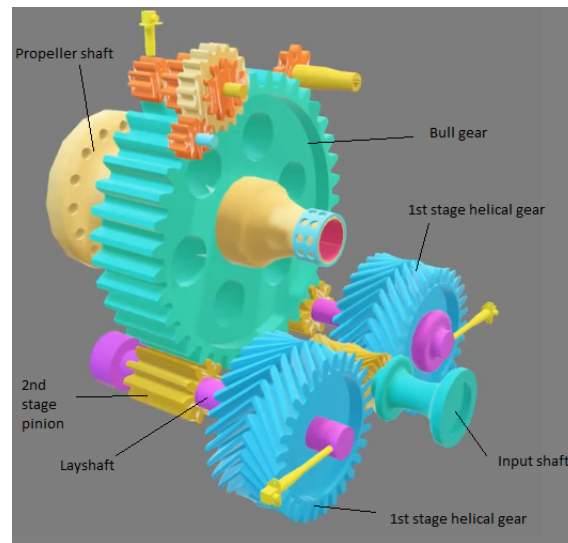


Figure 12: PW100 Reduction Gearbox Details

• Honeywell TPE 331 - Integral GB

The TPE 331 engine is a single-shaft turboprop appearing in applications such as the Antonov An-38, with a propeller's diameter of 2.85m. The originality of this engine is that it incorporates an integral gearbox. This means that the turbine rotor is directly mounted on the high-speed shaft of the gearbox, with no-bearings needed for the attachment. This has many benefits over the conventional separated gearbox, such as the fact that the high-speed couplings are eliminated, or the mentioned bearings. Also, the design ends up being more compact and lighter, something always positive, which together with the fact that many critical parts have been eliminated, the reliability is enhanced and the cost lowered. As it can be appreciated below, a planetary gearbox is employed, driven by a bull gear, engaged to the input shaft. Two stages of reduction are needed to accomplish the necessary ratio of the turbine-shaft-to-propeller speed. During the first design, two-stage planetary sets were considered, however the decision was made to use a combination of spur gear and single-stage planetary gear set. The principal advantage was the use of an offset design, whose benefits have already been mentioned. As it can be appreciated, a bull gear engaged to the input shaft drives the planetary gearbox, connected to the propeller. The choice of planetary gear was needed to meet the requirement to have the two propellers to turn in opposite directions if required. A relatively minor modification of making the ring gear stationary instead of the planetary gears provided the desired rotation.

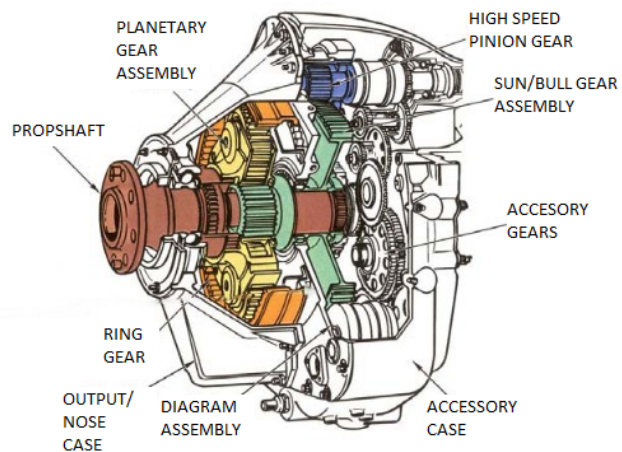


Figure 13: TPE 331 Reduction Gearbox Details

¹¹Bull gear:A toothed driving wheel that is the largest or strongest in the mechanism.

• NK-12 (the most powerful turboprop)

Being the difference in power demanded between turboprops and turbofans, one of the main reasons of having different gearbox designs, this state-of-art analysis could not miss the inclusion of the NK-12 engine, the most powerful turboprop until the date. This soviet engine from the 1950s, has had different versions over the years, with an upgrade in the power delivered, reaching a maximum of 11000 kW [32]. It powers the Tupolev Tu-95 bomber, with 5.6m diameter blades, and its derivatives such as the Tu-142 maritime patrol aircraft and the Tupolev Tu-114 airliner, which still holds the title of the world's fastest propeller-driven aircraft despite being retired from service in 1991. It also powered the Antonov An-22 Antei , the world's largest aircraft at the time, and several types of amphibious assault craft, such as the A-90. One of the main differences with the other engines mentioned, is that it drives two large four-bladed contra-rotating propellers, which increase the efficiency, but it can be noisier, heavier and mechanically more complex, so this advantage could be offset.

The NK-12 engine uses a differential planetary gearbox. Unlike the typical planetary gearboxes where one of the gears is fixed, here all three parts are moving: the turbine drives the sun, the planet pinion drives the front propeller, and the ring drives the rear propeller.

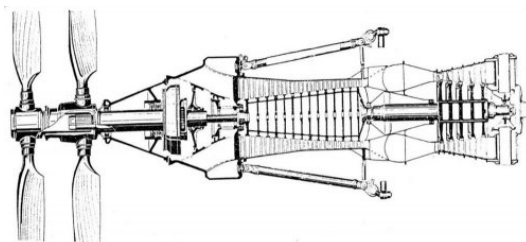


Figure 14: NK-12 turboprop

It does not come amiss to also come into detail into the gearbox of one of the projects developed for the propfan engine, as they are classified as something in between the turboprops and the turbofans. Even though none of these projects came to fruition, in the first decade of the 21st century, jet fuel prices began to rise again, and there was increased emphasis on engine/airframe efficiency to reduce emissions, which renewed interest in the propfan concept for jetliners. However, many limitations need to still be overcome.

• Progress D27

The Progress D-27 is a three-shaft contra-rotation engine with a tractor style, developed by the ukrainian Ivchenko Progress and launched in 1985. This engine powered the Antonov An-70, the first aircraft flight ever, which was completely powered by propfan engines, offering a 25%-30% reduction in fuel burn compared to the turbofans of the day. Furthermore, Ivchenko-Progress worked on derivatives based on the D-27 engine core, mostly within the 1988-1995 time frame, including also engines designed for turboshafts and high-bypass turbofans. The D-27's three-shaft uses the configuration of a fast running power turbine with a low number of stages, driving the propellers over a reduction gearbox. The gearbox is a planetary type with two concentric contra-rotating outgoing shafts and a reduction speed of 8.4:1 [23]. The planetary gear train is fitted with a sun gear driven by the rotor of the free power turbine, the planet gear driving the first propeller and the ring driving the second propeller. The eight-bladed front propeller, with a diameter of 4.5m receives most of the engine power output and provides most of the thrust, while the back propeller has only six blades. The shaft power is about 10 MW and the thrust is about 100 kN at sea level [33].



Figure 15: Antonov n-70

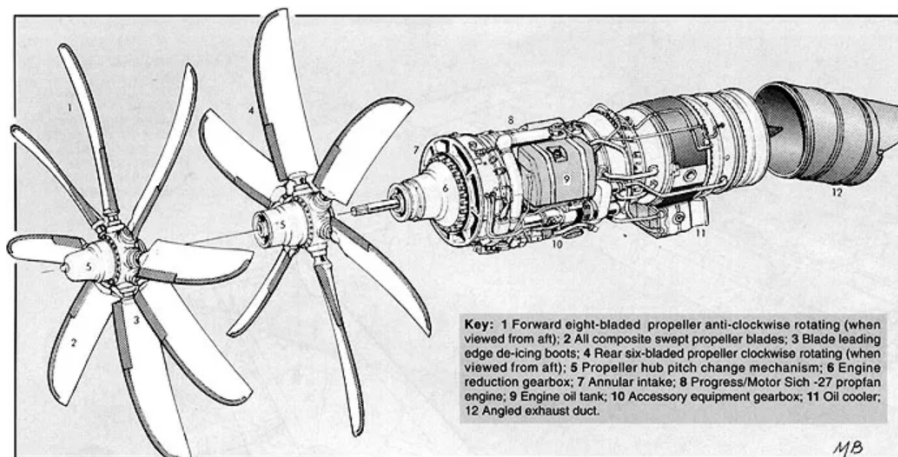


Figure 16: Progress D-27 turboprop

The future in the turboprops' gearboxes design

Gearboxes are designed based on the requirements needed in each case, and the next generation of turboprops will be defined by the current necessities. It is highly likely that a commercial turboprop will cruise at speeds common in current turbofans, where factors such as noise, power, desired life, maintainability, reliability and cruise speed will be an important consideration.

To start with, the predominant experience level for propeller type reduction gearing in the free World is up to 4,475 kW. A 8,950 kW gearbox was tested and this experience could probably be extrapolated to a 22,370 kW [27]. However, it is unlikely that the next generation of turboprops will operate at that high power level. Still, the most powerful turboprop engine is the mentioned Kuznetsov NK-12.

Furthermore, as to the life and reliability of the engine, orders of magnitude in the range of 25000 hrs and 40000 hrs, are circling around. The reliability of the GB is known to be vital. That is why, the inclusion of fault detection and health monitoring systems are a must. Multiple sensors and different evaluations techniques are an integral part of the design and development, as they provide real-time health information. Furthermore, the requirement for "on-condition" maintenance is in the list. This method of inspection allows to decide if maintenance is needed or not, instead of fixed times between overhauls. Maintainability requirements are reflected in a high degree of modularity, and life requirements show up in critical component material and size selection, as well as in multiple torque paths. As for the requirement for low noise, it manifests in helical gearing and multiple torque paths. Furthermore, to have good accessibility is crucial. This is a factor that has high weight on the design of the whole engine, not only on the gearbox.

The choice of arrangement selection may be affected by different factors too. On the one hand, the selection of an offset or an in-line gearbox depends on the inlet requirements, the accessory drive mounted, or the propeller control demanded. The benefit of using an in-line over the offset configuration is visible when weight and airframe interfaces are considered, if not, the latter one is usually the preferred one. As for the choice between remote or integral, it is an interesting trade-off. The weight and the cost are directly affected, but also, modularity for maintainability will be more difficult with a gear case integral with the power section front structure.

5.2.2 Gearboxes for turbofans

As mentioned, from the study in [25] and due to the power levels, the speeds, and the gear ratios involved, the conclusion is that planetary reduction gearboxes are considered to be the best choice, as well, for geared turbofans. As it will be seen in the state-of-art designs, no other configuration has been used in this type of engine. First of all, a revision of the firsts ever existing geared turbofans. Then, a detailed explanation of the breakthrough technology introduced by P&W and its direct competitor, Rolls-Royce.

• TFE - 731

This family of engines were the first geared turbofan for civil use applications, introduced in 1972. Different variants were developed ranging maximum thrusts from 15.6 kN to 21.1 kN, with a bypass ratio of 2.8:1 and a fan diameter of 1m. The gearbox used is of the planetary type with involute spur gears and a gear ratio of 1.8:1 [34], to power the fan for a 2.5 bypass ratio, which was very high for the time. In it, the fan shaft is linked to the ring gear and the input shaft is attached to the sun gear.

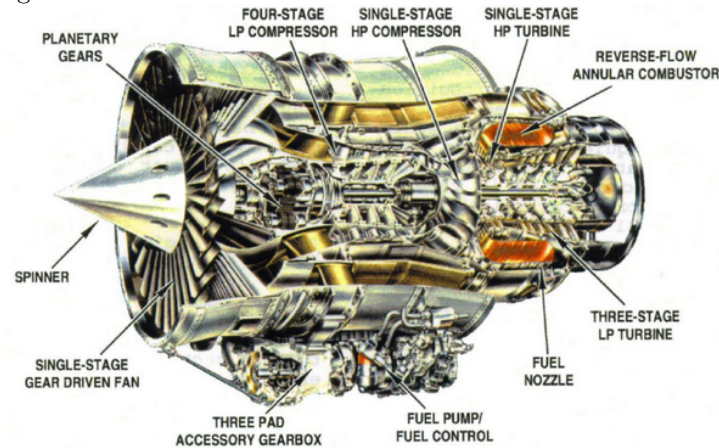


Figure 17: TFE 731 geared turbofan

• Lycoming ALF502

This engine is a geared turbofan engine produced by Lycoming Engines, whose first run was in 1980. Different variants were born from the original one, as improvements were achieved, reaching ranges of power of 30kN. The engine, with a bypass ratio of 5.7, and a fan diameter of 1.022m, counts with a single stage planetary gearbox in star arrangement with seven planets and is driven by the low pressure shaft. The gears are helical, and reach a gear ratio of 2.3:1.

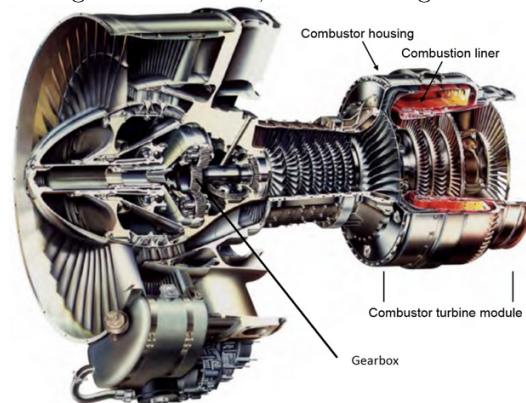


Figure 18: ALF502 geared turbofan

• IAE V2500 Superfan

The IAE V2500SF SuperFan was a design study for a high-bypass geared turbofan derived from the IAE V2500 in the 80s. The idea was to keep or even increase the maximum thrust of the original engine in the ranges of 124,5 kN to 142,4 kN, while having an 80% of the V2500's specific fuel consumption. Different design options were considered, until deciding that a single-rotation, variable blade pitch, geared fan, was the best option.

The fan, with a diameter of 2.72m and a bypass ratio of 18:1, was driven through a gearbox needed to provide 20000 SHP, which was a challenge. It turned out to be a derivation from the Rolls-Royce Tyne gearbox [35], concluding to be a planetary type with simple helical gears, and a

speed ratio of 3:1. This engine never got to become real after IAE suddenly cancelled the engine after recognising that the development timescale was unrealistic, given the technical challenges it faced.

These engines mentioned until the moment, are rather less powerful than the Pratt & Whitney's new offering, or even than the up-coming Rolls Royce Ultra Fan.

• PW1000G

As mentioned, after 20 years of research P&W developed a family of engines which have revolutionized the industry not only due to its whole design, but mainly, due to the advanced gear system design.

On the one hand, the first major difference with the previous engines mentioned is the power transmitted in such a compact way. In table 8, obtained from [36] one can see the specifications for the different models. Its clear that the thrust delivered is three or four times higher than the aforementioned engines, without considering the IAE V2500 SF.

Model	Static Thrust (kN)	BPR	Fan diameter (m)
PW1100G	110-160	12.5:1	0.206
PW1400G	120-140	12:1	0.206
PW1500G	85-104	12:1	0.185
PW1900G	76-102	12:1	0.185
PW1700G	67-76	9:1	0.142
PW1200G	67	9:1	0.142

Table 8: P&W geared turbofan models

In order to increase the efficiency, a higher bypass ratio was required, which certainly, involved a higher gear reduction ratio. The revolutionary part in this engine was that they have been able to create a gearbox, with enough reliability and durability, something needed to make the whole engine liable in a relatively small physical size, reducing the heat loss to a fraction of the transmitted power, and minimizing the lubrication and cooling systems, which was one of the biggest headaches in an engine of this size. By putting a 3:1 gearbox between the fan and the low-pressure spool, each spin at its optimal speed: 4,000–5,000 RPM for the fan and 12,000–15,000 RPM for the spool, with the high-pressure spool spinning at more than 20,000 RPM. Furthermore, P&W's GTF engines have accomplished these goals, with the overall maintenance cost of the engine being significantly reduced. The 30,000HP (22,000-kW) gearbox is designed as a lifetime item with no scheduled maintenance other than changing oil. Indeed, the design of this gearbox has been a challenge, but brings cleaner, quieter and more efficient high bypass ratio jet engines to the customer.

Lower gear ratios usually use a star system, while as the BPR increases, it is more interesting to use a planet system. After considering both options, P&W opted for a star system with 5 planets, as the BRP used allowed it and the counter-rotating effect possible with this configuration was aerodynamically favorable. Gears are double helical as the transmitted torque is huge and the speed is high.

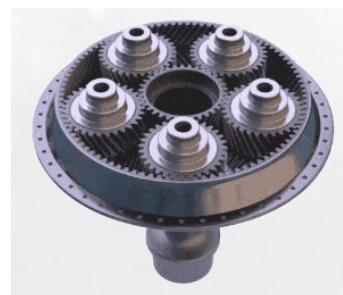


Figure 19: P&W gearbox for the geared Turbofan [37]

The big problem with this engine was how to manage the amount of heat produced in the Fan Drive Gear System (FGDS). As weird as it may sound, the biggest amount of heat loss was not produced due to the friction of the components, but due to churning excess oil. Therefore, much of their design effort went into getting lubrication oil quickly in and out of the unit, to prevent heat load buildup. A system of "baffle and gutter" was developed for this engine, allowing maximum efficiency, as it allowed to deliver oil to the gears and bearings for the needed lubrication and cooling, and at the same time, evacuate in a clean way. All that, accomplished in a compact way, and with a design that requires no additional maintenance than any other components of the engine.

An engine which offered amazing fuel savings but doesn't ensure long service life or needs overhauls every two days, with the complications that those involve, would not be really welcomed by the airliners. To achieve the reliability goals defined by the program, the FGDS had to hold, without any maintenance, for 30000 hours of flight [38]. The gearbox is made with high-strength gear steels in order to need "lower-maintenance". One of the main problems between overhauls was found to be with the bearings in the gearboxes. P&W found out in their study that most of the times, the failures for these bearing were not due to their undersizing, but due to the misalignment of the engine structure. In order to achieve the desired life, they developed an structure which allowed to isolate the gear system giving it enough flexibility for transient conditions, but in a controlled way, as too much flexibility can be as bad as too little. This can be appreciated in picture 20.

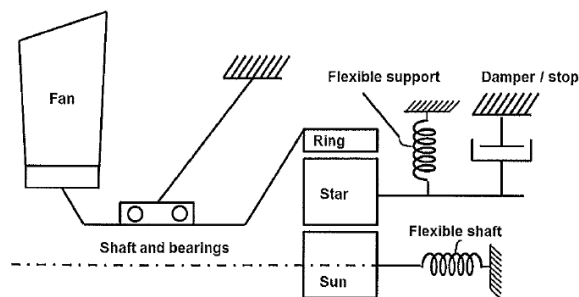


Figure 20: Load Isolation system for the FGDS

Furthermore, due to the power increase, the centrifugal loads to which the bearings were submitted, were unbearable with the usual bearings. Therefore load sharing between the gears needed to be optimised all the time, something that could be ruined if there were misalignment between the teeth, due to the manufacturing process or the working conditions. P&W made, thus, the decision to switch to journal bearings, which have higher capacity, and infinite life provided that they are supplied with the adequate lubrication. These journal bearings were a huge development hurdle, and continue to cause issues as power levels climb.

Certification of the first P&W geared turbofan, the PW1500G engine, occurred in February 2013, and since then, this family of engines continues to improve day by day, thanks to the continuous innovation and effort applied on it. They have enabled the most significant improvement in both noise and fuel burn in the last 20 years. However, as if it was not enough, the family never stops. If the 3:1 gear ratio is successful, they plan to move on to higher thrust models and therefore, to higher gear ratios. At a 4:1 ratio, for instance, the bypass ratio can be increased to 15:1. That would lead to potentially greater fuel savings, and possibly create a greater disruption in the jet engine market.

• Rolls-Royce UltraFan

As mentioned, in 2025, Roll-Royce is expected to come out with a geared turbofan that will directly compete with the GTF from P&W. This family of high-bypass geared turbofans, with a bypass of 15:1, will supposedly be more efficient and generating lower emissions than the PW1000G. Even though it is still under development, the company announced in 2017 that the gearbox designed to be used in this engine has already reached a record-breaking horsepower transmission.

The GB consist of a series of five planetary gears too, as it can be seen in figure 21, and it is sized to power 110–490 kN turbofans.



Figure 21: Rolls-Royce Power gearbox [39]

Other design aspects of the UltraFan noted by Rolls-Royce include a new core architecture with carbon-titanium fan blades and a composite engine case, to reduce weight. Ceramic-matrix composite parts are also used, to establish greater heat resistance, and promote engine efficiency by requiring less cooling air.

The future in geared turbofans

The pressure put over airlines to reduce harmful emissions increases everyday. Almost all passenger jets today are running on standard turbofans, but they are becoming outdated due to those increasing requirements. The P&W geared turbofan engine family, which has never stopped developing, is still considered the engine of the future, but with the close look of the Ultrafan from Rolls-Royce. For 2050, different studies are being devised, concepts and ideas in collaboration with universities and other research institutes, to look for revolutionary approaches that go beyond today's technology. Among the options under review for the engine, there are the use of highly efficient heat engines with extremely high pressures or the integration of recuperative elements to improve the thermodynamic cycle. They aim is to achieve an increase in the bypass ratio, from the current to as much as 20:1 by 2035. Moreover, further improving the core engine's thermal efficiency by increasing the pressure and temperature ratios. All improvements always have the same goal: improve efficiency and thereby minimize fuel consumption, emissions and noise.

6 Gearbox design with KissSoft

In the following section, I will be developing the design of a turboprop and a geared turbofan's gearbox using KissSoft, a modular calculation program for the design, optimization and verification of machine transmission elements according to international standards. This program allows to perform the sizing calculations of mechanical transmission elements, not only gears, but also bearings, belts and shafts. For this particular case, based on the analysis done and using the state-of-art information, a study of a typical configuration of an epicyclic GB for a TP and a GTF will be performed. The aim is to demonstrate with an example, those differences seen, in a broad sense, focusing only on the gears and assuming as many parameters as possible equal, in order to be able to perform a comparison between them.

Three factors dominate all aspects of an aircraft design. First, the need for the highest possible reliability due to the inherent higher risk and potentially catastrophic consequences of in-flight failure. Second, the need to minimise weight and volume of all components, resulting in high specific loading in all mechanisms. Therefore, there is always high specific power dissipation and the operating temperatures are high. Third, the extreme range of environmental conditions encountered from -60°C on the ground, or -80°C in the stratosphere, to over 200°C skin temperatures in supersonic aircraft [40]. Furthermore, turbofan engines fly higher than turboprops, that needs to be encountered, as the conditions to which they are submitted will be different. A gearbox design is therefore not less, and in fact its development and optimization has become a serious headache for engineers. While gearboxes offer many benefits to the engine in which they are implemented, they also introduce additional complexity. The detailed design of an aero-engine gearbox is a very complex process involving multiple disciplines. Integration issues, heat management, dynamic loads, vibration, maneuver loads, bending loads on the propeller shaft, weight, and other effects must be evaluated carefully to ensure a reliable operation. It is important to balance all those effects at an early stage of development, as the introduction of a gearbox has a strong influence on other engine components. In fact, when designing a gearbox, prior to running the qualification tests of the whole engine, many hours have to be spent in development on back-to-back rigs. In this kind of tests, the gearbox runs through different test cycles such as speed build-ups and long-term tests, at constant speed or with varying torques. Besides the efficiency, also the displacement of the gearbox, as well as temperatures and surface accelerations are gathered by different sensors. The total test time required is very significant, leading to be closely resembled to the time development associated with gas turbines themselves.

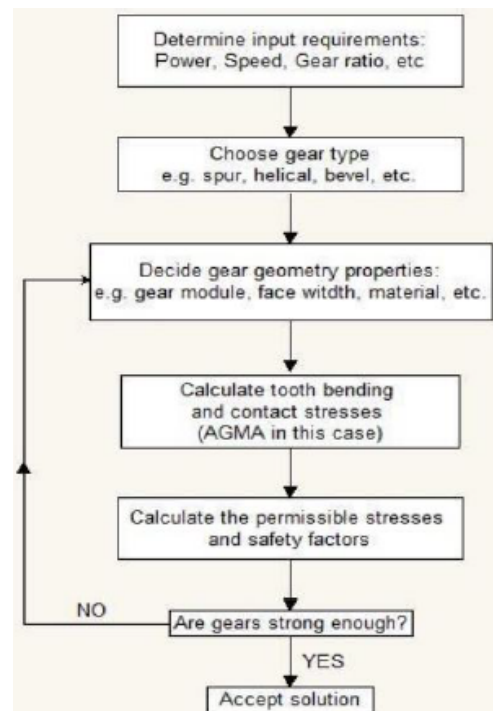


Figure 22: Phases in a gearbox design

6.1 Steps

The design process of a GB, as seen in figure 22, is a very iterative process, and engineers have several suitable calculation methods available for the sizing of the components. The process can be divided into three major phases. In the first phase, an initial gearbox geometry is derived from given specifications. In the second phase, a strength calculation is carried out for the resulting geometry. The occurring loads must be below the bearable loads. Several well established methods to calculate the loads for given gears are available in literature. The choice of the one to follow determines the final design. In the third phase, the results are evaluated and a variation and optimization of the geometry is performed. In the KissSoft software, the terms used to refer to these steps are rough sizing, followed by fine sizing and, finally, the modifications for optimizing.

• Rough sizing

In this step, different possible gear teeth configurations based on the data entered are proposed. The purpose of rough sizing is to ascertain the possible range of suitable solutions, defined by raw dimensions, all sized for the specified torque. Center distance and face-width are some of the dimensions that are estimated at this point of the design, and that will directly influence the overall size of the gearbox.

Furthermore, the design of the gearbox must comply with the criteria of sufficient strength in all components to ensure reliability. For that reason, the choice of the material and the lubricant is vital, as the torque capacity will strongly depend on it; together with the heat treatment received, and the gear quality. However, that is not the only consideration to make. There are different ways to define this demand. One of the two most common ones is to define minimum required safety factors for a given lifetime. This parameter, "lifetime", influences the permissible stress by making it dependent on the number of load cycles. Therefore, the design safety factors and the number of load cycles are interrelated.

Finally, after all the required inputs, the software defines different possible solutions that fulfill the requirements. The weight will be one of the most important outputs, as this will be roughly proportional to the manufacturing cost. Other important tooth parameters estimated such as, module, number of teeth, etc, for the required power and ratio, using the strength calculation according to the selected calculation standard, and to the predefined minimum safeties, are found. Thanks to the orders of magnitude of these parameters, at this early stage, it is possible to estimate the power density range of the gearbox variants, where clear differences among gearboxes will be appreciated.

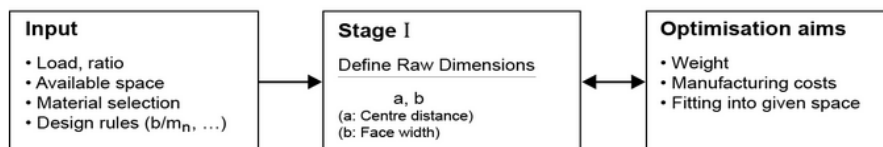


Figure 23: Phase I - KissSoft

• Fine sizing

This function is one of KissSoft's most powerful tools. It generates and displays all the possible geometry variants regarding the macrogeometry of the gear, for the specified face-width and center distance chosen in the rough sizing step. The solutions are displayed as graphics, so you can easily see the best possible macrogeometric variant for your purpose.

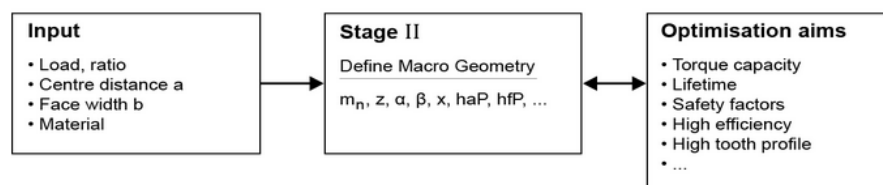


Figure 24: Phase II - KissSoft

The capability of this software is so high because it offers many tools to help size the design, on the basis of the orders of magnitude reached in the previous steps. However, before starting the fine sizing process, some data must be entered correctly to ensure the calculation returns the results one requires, such as for example, the reference profile. This choice can affect the whole complexity of the further manufacturing of the gear, as it is related with the manufacturing method of choice. The consideration of available tools in the early design stage can save a lot of effort in the later manufacturing steps. Evaluating different geometric solutions and eliminating non-feasible ones as soon as possible is a really important task.

• Optimization

After that, all the variants found in the fine sizing can be evaluated by a wide range of different criteria (accuracy of ratio, weight, strength, tooth contact stiffness deviation, etc.) and then, an optimization process can be performed depending on the chosen ones. The micro-geometry of the gear is defined here. The aim of this step is to specify flank line and profile modifications for optimal contact pattern, lower noise emissions and various other parameters, such as the GB's lower weight, which in our application, is critical.

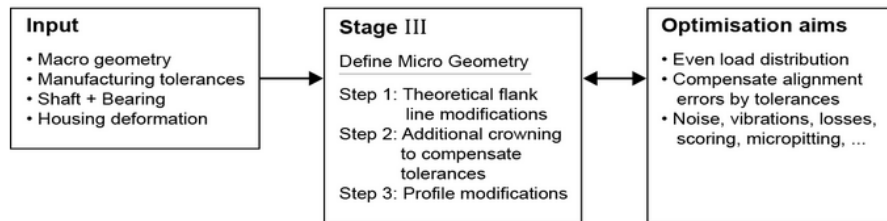


Figure 25: Optimization - KissSoft

7 Design procedure

7.1 Input parameters

The rough sizing, as its own name indicates, is rough. It begins with the definition of a few basic input data. In this section, all those parameters will be covered and the choices made will be explained.

In figure 26 one can see a basic scheme of this procedure. As it can be appreciated, there is no input required about the helix angle, the manufacturing process, the reference profile or a specification about the type of planetary configuration used, among others. Those parameters will be specified in the macrogeometry step, but still, this section will be used to explain them and the choices made will be detailed in their correspondent sections. At this point of the design, those parameters and many other are set by default by the software. Basically, the idea of the rough sizing is to be able to get an estimation of the final design, without having too many constraints, just having the minimal amount of inputs, used as guidance. After that, the calculation of configurations that satisfy those initial constrains within a certain range, are obtained.

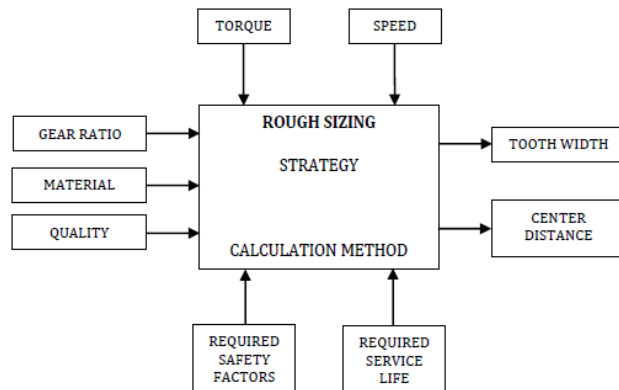


Figure 26: Rough sizing procedure

In this case, three designs will be carried out independently, and will receive the names "Turbo-prop", "GearedTurbofan 1" and "GearedTurbofan 2". As mentioned, in order to be able to make a good comparison between the devices, as many parameters as possible need to be equal, but the main input differences will be the gear ratio, the input RPM and the number of planets.

The interface of KissSoft is quite iterative. Through different sections of the interface, all the needed input parameters can be specified. It is divided in tabs which guide you to the final calculation, as steps to follow.

7.1.1 Basic data

In this section, some of the gear geometrical parameters are set. In appendix I, one can find the main parameters needed to define a gear design, with its correspondent definition.

To start with, the number of planets is defined. Here is where the first difference among designs is found:

GB	N ^o planets
Turboprop	3
GearedTurbofan 1	5
GearedTurbofan 2	5

Table 9: Number of planets in each of the designs

One of the main influences in the number of planets is the gear ratio, which as it will be seen later, and as it has been already seen in the SOA, it is a lot higher in turboprop's gearboxes than in gearedturbofan's. Thus the choice of number of planets is justified.

Continuing, the helix angle as default, is set as 0°, so for the rough sizing, we are considering spur gears for the three designs. It is logic to do it like that, as there is yet no information about

the gear, so it is very difficult to specify it. Furthermore, other inputs that can be defined at this point of the design are:

- Normal module, m_n .
- Center distance, a .
- Number of teeth, z .
- Facewidth, b .
- Profile shift coefficient.
- Normal pressure angle, α_n .

In order to get as many possible solutions in this initial step, these inputs are left for the software to define. The only consideration taken is regarding the normal pressure angle. The pressure angle gives the direction normal to the tooth profile. According to [41], normal pressure angles in use today range between 17.5° and 22.5° . Its definition affects the contact ratio and the length of line of action. As its value increases, the contact ratio and the length of line of action decreases. The contact ratio is an indication of the number of teeth in contact; and the line of action's length depends on the succession of contact points. In order for the system to be as smooth as possible, which is always desirable, the bigger these parameters, the better, and when one pair of teeth ends their iteration, a succeeding pair of teeth must come into engagement. Therefore, as a general rule, the higher the contact ratio, the less noise the gears will generate, the less sliding between the gears will happen, which maximizes pitting resistance, and the lower the possibility of backlash¹², minimizing the probability of scuffing. Nevertheless, it is important to mention that the backlash prevents binding and compensates for the effect of thermal expansion, machining and installation variation. A minimal amount of backlash is important in order to allow a space for the lubricant to enter the mesh. However, it also increases the amplitude of vibration, the meshing force and the impact of back of teeth, so a balance needs to be found. Taking only that in consideration, one could think that the lower the pressure angle the better. In fact, according to [42], historically, a common value of 14° was found in many gearsets, allowing reduced noise and low rate of wear. However, this was perfect for mechanism that did not need to transmit heavy loads, as this parameter also affects tooth strength. The higher the pressure angle, the higher the tooth strength and the load capacity. In applications such as the one in this paper, where both, noise and strength need to be optimized, an equilibrium needs to be found, and a value of 20° has been proven to be beneficial.

Continuing with the inputs at this point, the profile shift coefficient, even though for the reason explained before, it is going to be left to be selected by the software, it is important to mention some facts due to its relevance. The tooth profile is one side of a tooth in a cross section between the outside circle and the root circle of the gear. It refers to the curve of the intersection of a tooth surface and a plane or surface normal to the pitch surface, and the most common type of gear tooth profile is the involute gear tooth profile both, standard and corrected, so this is the choice.

The standard involute gear profile only depends on the number of teeth, pressure angle and pitch, which means that the majority of gear calculations can be output from those three pieces of gear data. In figure 27 one can see the difference in the profile depending on the number of teeth. For large number of teeth the gear tooth profile will look more like a rack (it becomes straighter) while with smaller number of teeth, it will have a large root fillet radius. This is influenced, mainly, by the interference among gears or among gears and gear cutting tools. From the standard involute, a profile shift can correct any inconvenience. The profile shift is the displacement between the production pitch circle and the tool reference line. In appendix J one can find more information about the benefits and drawbacks of the different profile shifted gears. A positive correction increases the tooth thickness and enlarges the center distance, while with a negative correction, the opposite occurs. It is thus, a way of adjusting the center distance of the gears when a failure occurs. The center distance is a critical parameter as it influences the contact ratio between the two gears, whose importance has already been introduced. Therefore, it is a known fact that the type of profile correction used will have a strong influence on the resulting transmission error and

¹²Backlash: the excess thickness of tooth space over the thickness of the mating tooth.

the degree of this influence may be determined by calculating the tooth loading during mesh. Furthermore, different criteria can be applied when selecting the degree of profile shift, however, at this point, the user is not allowed to specify it. It will be deeper seen in the fine sizing step. For the moment, no input is defined for this parameter.

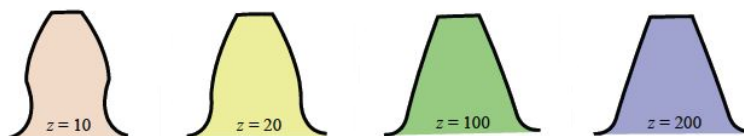


Figure 27: Tooth profiles varied by number of teeth

Continuing, the contact ratio, whose importance has been highlighted many times, by how it is influenced when defining other parameters, is directly related to how smooth the mesh is. It is an element that influences gear oscillation, noise, strength, rotation, and others. A contact ratio between 1 and 2 means that part of the time, two pairs of teeth are in contact and during the remaining time, just one pair is in contact. A bigger ratio between 2 or 3, means, therefore, that two or three pairs of teeth are in contact. This last type of gears are referred to as high contact ratio (HCR) and they are desirable but difficult to get. HCR gears have been used in many aircraft applications due to the advantages of increased durability rating, increased strength rating and reduced noise levels, however, these advantages, while noteworthy, have been overshadowed by concerns about susceptibility to scoring or other lubrication failures; lower efficiency; narrow top-lands; limited bearing capacity; gearbox thermal limitations; tooling costs; and uncertainty over rating methods. As any choice to be made in gear design, it is not arbitrary, and if the choice of using a HCR is selected, those disadvantages need to taken care of.

Furthermore, it is interesting to see that the total contact ratio, ϵ_γ , is defined as the sum of the transverse contact ratio, ϵ_α , and the overlap ratio, ϵ_β . The transverse contact ratio is the calculation resulting from dividing the length of path contact by the base pitch. On the other hand, the overlap ratio involves gears which have helix hands. For the rough sizing, in order to not complicate the design at this early stage, spur gear teeth are considered. Nevertheless, thanks to the sizing helps the software provides, in the following steps, an helix angle can be applied and thus, ϵ_β , will also gain importance and the calculation of the facewidth divided by normal pitch will have to be added for the transverse contact ratio. Knowing its formulae, it is clear that with no basic parameters defined, it is not possible to fix a contact ratio, however knowing that it is interesting to increase it, one can think of different means to do it: decrease the pressure angle, as mentioned; increase the number of teeth, which as it has not yet been defined, it is not possible; and increase the working tooth depth, which basically depends on the reference profile of choice. Nevertheless, when applying those considerations, the focus must be put in the whole performance of the gearset, as the drawbacks due to applying the HCR, may make the benefits, not worth it. Many works have been performed in this area, to see the effect of the different parameters in gear performance. The study performed in [43], for example, reaches a conclusion which is really interesting and can be applied in this case. In that scenario, the influence of various gear parameters on the mesh stiffness are investigated. The gear parameters concerned include pressure angle, helical angle, addendum coefficient and facewidth, among others. The comprehensive analysis of the mesh stiffness shows that contact ratios are the key factors affecting the fluctuation value of mesh stiffness when the gear parameters are changed. This means that the final value of the contact ratio, will be the most important one defining the mesh stiffness. Furthermore, the fluctuation value of mesh stiffness attains a minimum when the transverse contact ratio or overlap ratio is close to an integer, while it has an extreme maximum when the total contact ratio is approximate to an integer. This conclusion will, certainly help define these variables in the following steps.

7.1.2 Material

Proceeding, the material is also selected. For the application intended for these gears, the right choice of the material is vital for the good performance and long life of the devices. This choice is made based on a combination of many conditions such as load, speed, lubrication system, and temperature, plus the cost of producing the gear.

First of all, understanding the mechanical properties of the materials is vital for the right selection. The mechanical properties of a material are those which affect the mechanical strength and the ability of a material to be molded in a suitable shape. Nevertheless, the list is pretty long¹³. In order to make an informed decision but not make another thesis out of it, it is important to identify that some are more important than others when describing a material. In this particular application, the focus is put in:

- Strength: measures how much stress can be applied to an element before it deforms permanently or fractures.
- Hardness: measures a material's resistance to surface deformation. It is basically the ability to withstand friction, essentially abrasion resistance.
- Fatigue: expresses a material's ability to withstand cyclic stresses.
- Hardenability: ability of a material to attain the hardness by heat treatment processing. It is determined by the depth up to which the material becomes hard.

Modern gears are made from a wide variety of materials. Depending on the properties needed for the application, the choice is clearly different. Nevertheless, of all these, steel has the outstanding characteristics of high strength per unit volume and low cost per kg. Furthermore, even though this will be better understood as we move on in this "choice of material" step, this is also due, largely, to controllable heat treat distortion of these materials, which is performed to increase strength and life, that helps to reduce gear finishing costs. For those reasons, it is one of the most used materials. A well-controlled heat treatment produces the desirable surface and core properties for resistance to various failure modes. These failure modes include bending and contact fatigues, such as pitting and micropitting, and failures due to surface wear of gear teeth, like scuffing. Although both plain carbon and alloy steels with equal hardness, exhibit equal tensile strengths, alloy steels are preferred because of higher hardenability and the desired microstructures of the hardened case and core needed for high fatigue strength of gears. Over 90% of the gears used in industrial applications today are made from alloy steels [44]. Hence, this is the first choice made.

Micropitting refers to the formation of very small, micro-scale craters on the surface of the gear tooth flank due to the surface distress caused by excessive cyclic contact stress and/or when the lubrication film is not developed enough to separate high-points. It is different to the concept known as pitting, although the main difference is the size of the pits after surface fatigue. Pitting is one of the most common causes of gear failure, and while micropitting can affect all types of gears, it has become particularly troublesome in heavily loaded gears with hardened teeth. It is mainly characterised by the presence of fine surface pits and the occurrence of local plastic deformation and shallow surface cracks. It produces significant wear of the surfaces causing loss of profile of the teeth, leading to noise. Serious cases can precipitate scuffing and even complete fracture of the tooth. Scuffing, thus, is a severe type of adhesive wear which instantly damages tooth surfaces that are in relative motion. A severe form of scuffing is usually accompanied by considerable wear and as a result of that, the teeth become overloaded around the pitch line. A single overload can lead to a catastrophic failure. It affects, mainly, gears running at high speeds or at high temperatures. It is generally accepted a mild or light form of scuffing, provided it stops and the gears recover. Simple measures such as changing to a more efficient oil, operating the gears at less than service load until the completion of the running-in¹⁴ of the teeth or even removing bad spots on large teeth by hand can often be very effective in saving the gear drive from serious scuffing problems.

However, the decision involving the material selection does not end up here. The material endurance limits depend on material quality, the surface hardness and the heat treatment received. The material quality is another factor that strongly influences pitting resistance and bending strength, and itself may be influenced by the forming process, the cleanliness or purity of the substance, the sulfur content, and the grain size, among other things. Thus, the decision is not

¹³Some of the typical mechanical properties of a material include: strength, toughness, hardness, hardenability, brittleness, malleability, ductility, creep, resilience and fatigue.

¹⁴Running-in is the initial wear and plastic deformation of surfaces in contact, starting with the virgin state of the contacting surfaces as delivered from the manufacturing process and ranging for only a short period of time.

arbitrary. All these considerations must be taken into account.

Heat treatments are critical and complex processes that greatly impact how each gear will perform in transmitting power or carrying motion. They consist on heating cycles where the metal is subjected to controlled temperature changes in solid state. As mentioned, they optimize the performance and extend the life of gears in service by altering their properties. For any given type of heat treatment, the results affecting the properties can be tailored by modifying process parameters such as heating source, temperatures, cycle times, atmospheres, quench media, and tempering cycles to meet specific application requirements.

Apart from the choice of the heat treatment, which will produce a set of desired physical properties, it is important to minimize the distortion of dimensions. The degree of distortion depends on the material, the heat treat process and the equipment used. Steels with higher hardenability, in general, experience more heat treat distortion. On the other hand, lower hardenability steels exhibit low distortion but may not meet the design requirements. Many gears are machined into an oversized condition prior to heat treatment so that a planned amount of grind stock may be removed after the process in order to meet dimensional requirements. By selecting heat treatment processes where distortion is reduced, the amount of grind stock needed may be reduced to minimize machining on hardened surfaces after heat treatment and thereby reduce the overall costs of manufacturing. Also, heating may be employed to harden just the gear teeth only, which can be an effective method of reducing the distortion. However, the quality of gear geometry after heat treatment, deteriorates, to the extent that a finishing process becomes essential. Anyways, furthermore, it is important to bare in mind that removing too much of the outermost portion of a hardened gear that distorted excessively, will also negatively impact the fatigue properties and wear life performance. By this, the manufacturing of modifications is linked to the heat treatment/finishing process and should be considered in the design process, as it can greatly affect performance, ease of manufacture and economics of a component. An equilibrium needs to be found.

Many options exist for the heat treatment of gears. For an optimal design, one must have the knowledge of the various gear heat treat processes and understand the mechanism of heat treat distortion. According to [44], the major heat treat processes are:

•Through-hardening

In order to harden steel, the iron mix must contain a certain amount of carbon. In through hardening steel, there is a high level of carbon added to the iron mix. When the component is heat treated, it becomes hard all the way through, from the surface to the core, hence the term “through hardened”.

This process is generally used for gears that do not require high surface hardness, as through-hardened steel components are relatively brittle and can fracture under impact or shock loads. Typical gear tooth hardness, after through hardening, ranges from 32 to 48 HRC¹⁵ [44]. Most steels that are used for through-hardened gears have medium carbon (0.3–0.6%) and a relatively low alloy content (up to 3%). The purpose of alloy content is to increase hardenability. The higher the hardenability, the deeper is the through hardening of gear teeth. Since strength increases directly with hardness, this factor is interesting. High hardenability, however, has some adverse effect on the material ductility and impact resistance. The other drawback of this process is a lower allowable contact stresses than those in surface-hardened gears, which will be presented shortly. This tends to increase the size of through-hardened gears for the same torque capacity compared with those with surface hardened. Overall, through-hardened gears are used in gearboxes that require large gears that cannot be economically case or surface hardened, such as large marine propulsion gears and railway power transmission gears

Furthermore, all steel gears experience distortion during a heat treat process, we know that, but at least, distortion of through-hardened gears is not as severe as in the following other processes. Still, through-hardened gears, experience enough distortion that will eventually lower the

¹⁵HRC: Rockwell scale.

quality level of gears after heat treatment. This, thus, necessitates of a finishing operation for higher quality.

• Case hardening

This process produces a hard, wear resistance case or surface layer on top of a ductile, shock resistance interior (or core), which is advantageous under misalignment conditions. The idea behind the case hardening is to keep the core of the gear tooth at a level around 30 to 40 HCR [44] to avoid tooth breakage, while hardening the outer surface above HRC 55 [45] to increase the pitting resistance. In fact, the combination of a hard surface layer and a relatively liable inner core gives case-hardened steel superior crack and fracture resistance under shock loads.

Following, different processes to carry-out the case hardening are described, and after that, and analysis of the differences is made:

1. *Carburizing*

It is a process in which iron or steel is brought into contact with an environment of sufficient carbon potential, to cause absorption of carbon at the surface and, by diffusion, create a carbon concentration gradient between the surface and interior of the metal. The depth of penetration of carbon is dependent on temperature, time at each temperature and the composition of the carburizing agent. The objective is to secure a hard case and a relatively soft but tough core. For this process, low-carbon steels (up to a maximum of approximately 0.30% carbon), either with or without alloying elements, normally are used. After case carburizing, the gear teeth will have high carbon at the surface, with a hardness which lies in the range HRC 58 to 62, graduating into the low-carbon core of around 32 to 48 HCR [44]. Nevertheless, due to the fact that this process is developed at high temperatures, distortions are quite severe, meaning, a finishing process is required.

A vast majority of gears used in industrial applications today are carburized. It is because the process offers the highest power density and the highest torque-carrying capacity in a gearbox, through optimum gear design. In fact, the torque capacity of a carburized and hardened gear set, can be three to four times higher than that of a similar through-hardened gear set [44]. High surface hardness, high case strength, favorable compressive residual stress in the hardened case, and suitable core properties, based on appropriate grade of steel, result in the highest gear rating. Furthermore, carburized gears offer superior heat resistance compared with other case hardening processes. These gears are also capable of withstanding high shock load. The major disadvantage of carburizing is high heat treat distortion; although, recent advancements in carburizing have contributed greatly in controlling and minimizing this distortion.

2. *Nitriding*

It is a process used for alloy steel gears. The process primarily produces a wear and fatigue resistant surface on gear teeth and is frequently used in applications where gears are not subjected to high shock loads or contact. It is particularly useful for gears that need to maintain their surface hardness at elevated temperatures. Nitriding of gears can be done in either a gas or liquid medium containing nitrogen.

Through this method, gears do not require as much case depth as in carburized gears. This is due to the fact that nitriding is used basically to increase the wear life of gears under a moderate load. The depth of case and its properties are greatly dependent on the concentration and type of nitride-forming elements in the steel. In general, the higher the alloy content, the higher is the case hardness. However, higher alloying elements retard the N_2 diffusion rate, which slows the case depth development. Thus, nitriding requires longer cycle times to achieve a given case

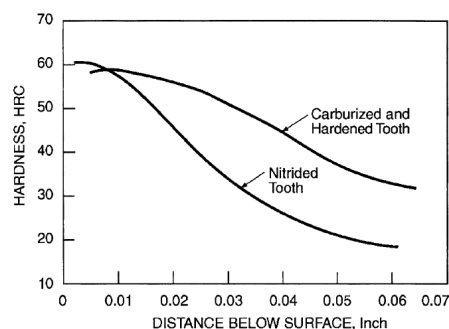


Figure 28: Hardness gradients for a carburized and a nitrided tooth [44]

depth than that required for carburizing. It is also to be noted that, higher case depth does not increase the contact fatigue life of nitrided gears in the same ratio as it does in carburized gears. This is due to the fact that hardness drops quickly below the surfaces of nitrided case, whereas, in a carburized case, the drop in hardness is very small. This can be appreciated in figure 28, where it is clear that the hardened case depth is significantly thinner than in carburized gears and it transitions to the core hardness immediately behind the case.

The major disadvantage of nitrided gears is their inability to resist shock loads due to the inherent brittleness of the case. Also, nitrided gears do not perform well in applications with possible misalignment during which the highly brittle nitrogen oxides on tooth edges breaks off and may go into the gear mesh.

This method, which is performed at a lot lower temperatures than carburizing, can be accomplished with a minimum distortion and with excellent dimensional control. Thus, while carburizing is the most effective surface-hardening method, nitriding excels when gear tooth geometry and tolerances before heat treating need to be maintained without any finishing operation. However, the quality of nitrided gear teeth is not as good as carburized gears, and grinding to improve tooth geometry is not recommended because this may detrimentally affect their load carrying capability. On the other hand, although, through-hardening is capable of maintaining close tooth dimensional tolerances too, the process cannot provide sufficient wear and pitting resistance. This is why nitriding is an alternative to carburizing especially for lightly loaded gears, which do not require high case depths, for which nitriding is not cost effective.

3. Carbonitriding

It is defined as a process in which carbon and alloy steel gears are held at a temperature above the transformation range, in a gaseous atmosphere of such composition, that allows steel to absorb carbon and nitrogen simultaneously and then it is cooled at a specific rate to room temperature, which produces the desired properties. The process primarily imparts a hard, wear-resistant case. A carbonitrided case has better hardenability than a carburized case. The addition of nitrogen has three important effects:

- It inhibits the diffusion of carbon, which favors production of a shallow case.
- It enhances hardenability, which favors attainment of a very hard case.
- Nitrides are formed, increasing the surface hardness further.

A case consisting of all nitrogen will have the highest hardenability but will not be as hard as an all-carbon case. For an optimum carbonitrided case, just sufficient nitrogen should be used, which gives the required hardenability. The balance should be found. Furthermore, distortion is far less than that of carburized gears because of lower process temperatures and shorter time cycles. Nevertheless, it is more than any nitriding process. The major advantage is, thus, that the hardenability of the case is significantly greater than any carburizing or nitriding process, and has a better wear resistance. On the other hand, the core often has low hardness. That is why, carbonitriding is limited to shallower cases in gears of low-duty cycle.

• Surface Hardening

Sometimes only the surface of the gears needs to be hardened, without altering the chemical composition of the surface layers. Surface hardness is primarily a function of carbon content. It also depends on alloy content, heating time, mass of the gear, and quenching considerations. The hardness achieved is generally between 53 and 55 HRC, and some of the most common processes are presented below:

1. Induction hardening

Surface hardening is possible to be achieved by very rapid heating with electrical induction for a short period, thus conditioning the surface hardening by quenching, provided the steel used contains sufficient carbon to respond to hardening. The depth to which the heated zone extends

depends on the frequency and power density of the current and on the duration of the heating cycle, which eventually controls the surface hardness and case depth that can be achieved.

Selective heating and, therefore, hardening, is accomplished by suitable design of the coils. Accurate heating to the proper surface temperature is a critical step. Inductor design, heat input, and cycle time must be closely controlled. Underheating results in less than specified hardness and case depth. Overheating can result in cracking. At the end of the heating cycle, the steel usually is quenched by water jets passing through the inductor coils. Precise methods for controlling the operation, such as the rate of energy input, duration of heating, and rate of cooling, are thus necessary. These features are incorporated in induction hardening equipments, which usually are operated entirely automatically.

In general, after induction hardening, the quality level of gears does not go down by more than one AGMA quality level. Thus, in most applications, induction-hardened gears do not require any post-heat-treat finishing except for high-speed applications. This method provides an alternative to carburizing and nitriding for large-sized gears, or gears that are not economically viable, and it has been used successfully on most gear types, specially when gear teeth require high surface hardness.

2. Flame hardening

This process is similar to induction hardening for heating the surface layers of steel above the transformation temperature by means of a high-temperature flame and then quenching. In this process, the gas flames impinge directly on the tooth surface to be hardened, and it can be applied differentially or on the whole surface of a workpiece. The final results are determined by the heat of the flame, the duration of the heating, and the speed, temperature of the quenching process, as well as the elemental composition of the target material. The rate of heating is very rapid, although not as fast as with induction heating. Furthermore, another difference is that, due to the fact that flame hardening is controlled by an open flame, it is a lot less precise than induction hardening.

The general application of flame hardening is to the tooth flanks only. Gears are flame hardened only when they are of large size and the quality requirement is lower.

In figure 29, it is depicted the hardness vs case depth in some of the processes mentioned. It is appreciated that carburized steels present the less steep change in hardness, as it goes deeper into the core. Each of these processes has its benefits and limitations when applied to gears. It is up to the gear design engineer to select a particular process for an optimal design, but indeed it is a tough challenge to find the optimal solution, as many considerations must be taken into account. In applications requiring high load capacity and long life for gears under occasional overload conditions, the carburizing followed by an adequate finish process may be selected, whereas nitriding, offering low distortion, may be the right choice for gears that are not subjected to very high load and do not require high quality. However, until recently, carburized and ground gears (which are gears submitted to a grinding process) were not considered economical because of high finishing cost. This concept was based on some inefficient carburizing equipment and processes. With the recent development of improved heat treat equipment and some high-quality carburizing grade steels, it is now possible to control and predict heat treat distortion during carburizing to the extent that finishing time is significantly reduced. In some cases, minor modifications of pre-heat treat gear-cutting tools (hobs, shaper cutters) help to compensate heat treat distortion to reduce this time even further. Hence, the use of carburized gears is increasing continually. After putting oneself into context, the choice of "**Steel, Grade 3, HRC58-64 (AGMA), case-hardened, carburized, AGMA 2001-C95**" is considered to be the most adequate in this case.

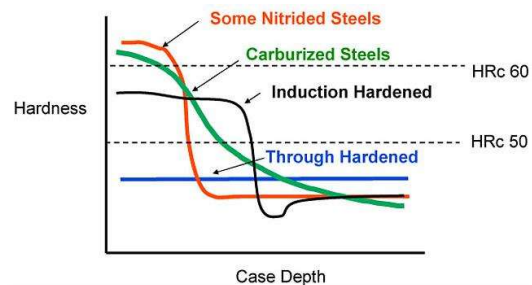


Figure 29: Comparison of hardening methods [44]

As it is appreciated, the gear steel is offered in three grades. The grade is a way of classifying metals based on all the different factors that can influence its properties and uses. A metal grade is usually determined by its chemical composition, its mechanical properties, or both, and it indicates the allowable contact stress, the strength that material can withstand and the quality. Steel grades for classification have been developed by a number of standards organizations, one of which can be seen here:

Steels	YS (MPa)	UTS (MPa)	El (%)	RA(%)
Grade 1	1210-1275	1520-1590	11-13	45-50
Grade 2	1415-1480	1550-1620	9-10	40-45
Grade 3	1760-1830	2240-2310	7-9	30-32

Table 10: Steel grades classification [46]

In this simple table, we can see the ranges for Yield Strength (YS), Ultimate Tensile Stress (UTS), the Elongation (El) and the Reduction Area (RA) , for the different grades.

The YS of a material is the stress at which a predetermined amount of permanent deformation occurs. The UTS is the point at which the material begins to break or tear. It is easily appreciated that the best characteristics for the type of application we are working with, are found in the Grade 3 types. Nevertheless, it is interesting to also have a look the other parameters. The El, which is a measure of the deformation that occurs before a material eventually breaks when subjected to a tensile load, for grade 3, shows that they break sooner (in length terms), than the other ones. Furthermore, the RA, which is a measure of the ductility¹⁶ of metals, shows that these types of metals are less prone to reduce their cross-sectional area when a tensile stress is applied. All these characteristics are the ones typically analysed in super-high strength steel, the ones needed in our case. The gearbox needs to be able to keep its original shape the longest the possible, any minimal change can critically affect the performance, thus, grade 3 is the right choice.

7.1.3 Manufacturing

The manufacturing process will determine the cost, quality, accuracy¹⁷ and manufacturing time, therefore, its importance is undoubtedly very relevant. It is also one of the most limiting constraints in the design process, as not all of the gears can be manufactured with every method. Therefore, it must be a considered choice and it is vital to have all the options on the table before making up one's mind.

It was mentioned that during the rough sizing step, the software does not take into account any inputs defined in the manufacturing tab. The choice of normal module, pressure angle and gear reference profile are directly linked to the tool geometry. Thus, manufacturing constraints may limit the number of feasible solutions, so it would be impractical to define it in such an early stage. Nevertheless, we will go now through the most common existing manufacturing options and when the time comes, the choice made will be explained.

Manufacturing of gears need several processing operations in sequential stages depending upon the material, type of gear and quality desired, which are:

- Performing the blank with or without teeth.
- Annealing the blank, if required (ie. forged or cast steels).
- Producing teeth or finishing the reformed teeth by machining.
- Full or surface hardening of the machined teeth (if required).
- Finishing process.

¹⁶Ductility:the ability of a metal to be easily bent or stretched.

¹⁷Gear tooth accuracy considerations include: involute profile, tooth alignment (lead), tooth spacing and tooth finish.

The art of gear manufacturing is, therefore, too broad and it could easily become a paper on its own. In figure 30, it is illustrated the 2 categories in which the different methodologies can be classified. On the one hand, forming means the use of plastic deformation to get the desired shape. It consist on directly casting, rolling, molding, drawing, extruding... the tooth forms in molten, powdered, or heat softened materials. Machining on the other hand, involves roughing and finishing operations, including removal material. This classification is not fixed, meaning, that a gear that is cut can have gone through a process of forming before.

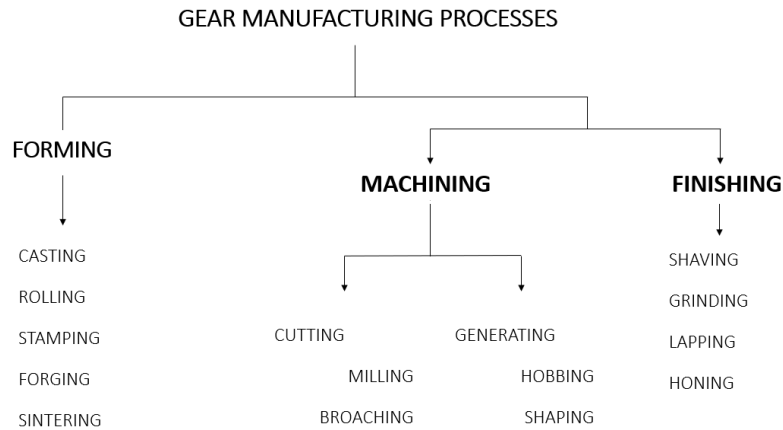


Figure 30: Gear manufacturing processes

1. Forming and machining

In all tooth-forming operations, the teeth on the gear are formed all at once from a mold or die into which the tooth shapes have been machined. The accuracy of the teeth is entirely dependent on the quality of the die or mold and in general is much less than the one that can be obtained from the other methods. Furthermore, most of these methods have high tooling costs, making them suitable only for high production quantities. For this reason, most of the gears are produced using machining process, and for that reason, our focus is put on those types of method.

When applying a machining method for gear manufacturing, one can find several routes. The most common one is performing the blank by casting, forging, extrusion..., followed by a pre-machining to prepare the blank to the desired dimensions, and then production of the teeth by machining and further finishing. Two types of gear tooth geometry are created by machining methods:

• Cutting

With this procedure, the profiles of the teeth are obtained as the replica form of the cutting tool. Therefore, the surface finish of the work piece obtained is completely based on the tool. Two machining operations can be employed to form cut gear teeth:

1. Gear Milling

The cutter called "form cutter" travels axially along the length of the gear tooth at the appropriate depth to produce it. After each tooth is cut, the cutter is withdrawn, the gear blank is rotated, and the cutter proceeds to cut another tooth. This method, more suited for large gear with large modules, is characterized by a low production rate and low accuracy and surface finish.

2. Gear Broaching

This type of operation is particularly applicable to internal teeth, but it can also be applied to external. The process is rapid and produces fine surface finish with high dimensional accuracy. However, because broaches are expensive and a separate broach is required for each size of gear,

this method is suitable mainly for high-quality production.

Another advantage, apart from the good finish, is its suitability for small gears, but the cost is an important consideration to take into account, as it may make it not worth it.

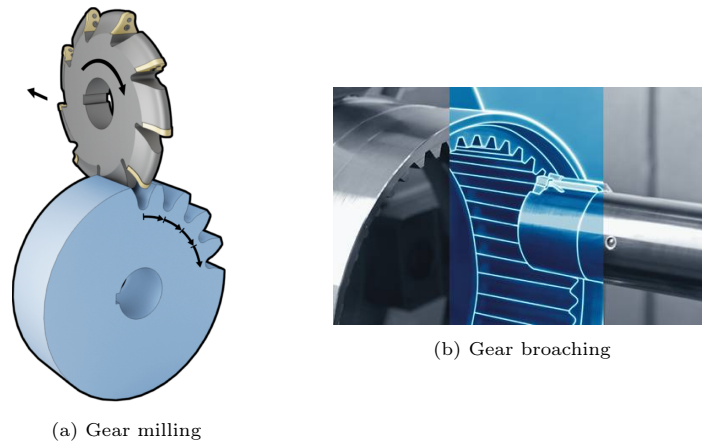


Figure 31: Forming methods

• Generation

In this case, the tooth profile is provided by a much simpler cutter tool, through rolling. The tooth flanks are obtained as an outline of the subsequent positions of the cutter, thanks to the relative motion between the work gear and the cutter during machining. This is the reason of the term "generating", as it refers to the fact that the shape of the gear tooth is not the shape of the cutting tool, but the combination of the motion of the work-piece and the cutting tool. Basically, it depends in the feed trajectory of the cutting tool. The cutter and blank behave as mating gears in working contact, and in this case, the surface finish of the work piece is partially based on the cutting tool. Here, one can find two machining processes too:

1. Gear hobbing

The gear teeth are progressively generated by a series of cuts with a helical cutting tool, called hob, which is like a worm cutter. The hob teeth are shaped to match the tooth shape and lapse, and are provided with grooves to make the cutting surface. All motions in hobbing are rotary, and the hob and gear blank rotate continuously as in two gears meshing until all teeth are cut.

Hobbing is a continuous process, which makes it fast, economical and highly productive, as its machine is much more rigid and strong than the shaping machines which will be explained later. It is a versatile method, being able to generate spur, helical and worm wheels, and most of the involute gears are produced like this thanks also, to its accuracy. It is the most accurate machining process since no repositioning of tool or blank is required and each tooth is cut by multiple hob teeth, averaging out any tool error. Its only limitation is that it cannot be used for internal gears unless a special tool is used.

2. Gear shaping

The cutter and gear blank are connected as gears, so that they will not roll together as the cutter reciprocates for cutting. First, the cutter must cut its way to the desired depth. The cutting tool travels axially across the gear blank. The cutter and gear blank then rotate slowly together as the gear teeth are cut in the gear blanks. Slightly more than one revolution of the work is required.

The limitation with this method is that both productivity and product quality are very low, thus, it is used, if at all, for making one or few teeth on a few gear or when required for repair and maintenance purpose. Furthermore, the rigidity obtained is lower compared to gear hobbing.

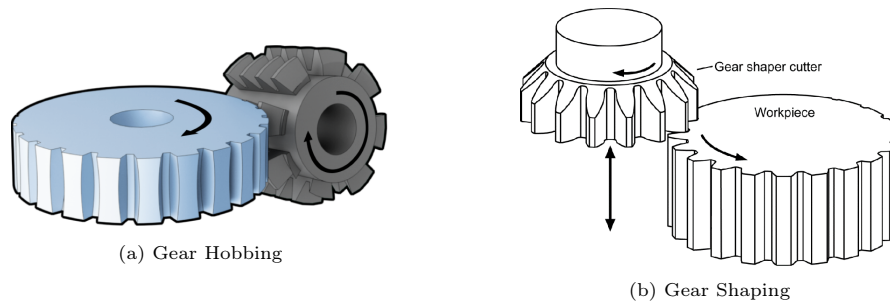


Figure 32: Generating methods

2. Surface finishing

Gear production by any of the processes described, together with the heat treatment to which the gears are submitted, means that the surface finish and dimensional accuracy may not be accurate enough for certain applications. For effective and noiseless operation at high speed, it is important for the profile of the teeth to be accurate, smooth and without irregularities, and this can be achieved with an appropriate finishing operation. Finishing operations typically remove little or no material, and are intended to accomplish the following:

1. Eliminate after effect of heat treatment and improve surface finish and/or hardness.
2. Correct error of profile and pitch, improving dimensional accuracy.
3. Ensure proper concentric of pitch circle and centre hole.

As shown, several finishing operations are available:

• Shaving

It is the most widely used method, as for the continuous production of large lots, it represents the best cost/performance ratio with high productivity. It is similar to gear shaping, but using accurate shaving tools to remove small amounts of material from a roughed gear, to correct profile errors and improve surface finish. It is a fast and rapid production process, but its main limitation is that it has no chance of removing the distortion caused by heat treatment.

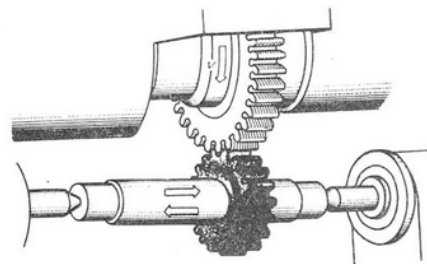


Figure 33: Gear Shaving

• Grinding

It is an abrasive method involving a grinding wheel of a particular shape and geometry, used for finishing the gear teeth. Usually, when high noiselessness and strict quality levels are required, the grinding operation is the best solution, especially in the case of hardened steels, where it may be difficult to keep the heat-treat distortion within acceptable limits. In fact, this method is usually performed after a gear has been cut and heat-treated to a high hardness, as it is necessary for the gears to be above 38HRC. At the expense, obviously, of a higher cost. Furthermore, this method requires special attention in order to avoid overheating, which could lead to gears cracking. Two basic methods for gear grinding are:

1. Form Grinding

The grinding wheel is dressed to the form that is exactly required on the gears. Due to that, it is considered really similar to the milling machining process. The teeth are finished one by one and after one tooth is finished, the blank is indexed to the next tooth space. This makes the process quite slow and less accurate.

Form grinding may be used for finishing straight or single helical spur gears, straight toothed bevel gears and worm wheels.

2. Generation Grinding

This method is based on the interacting motion between the grinding wheel and the gear being manufactured. The single or multi-ribbed rotating grinding wheel is reciprocated along the gear teeth as seen in figure 34. For finishing large gear teeth, a pair of thin dish type grinding wheels are used.

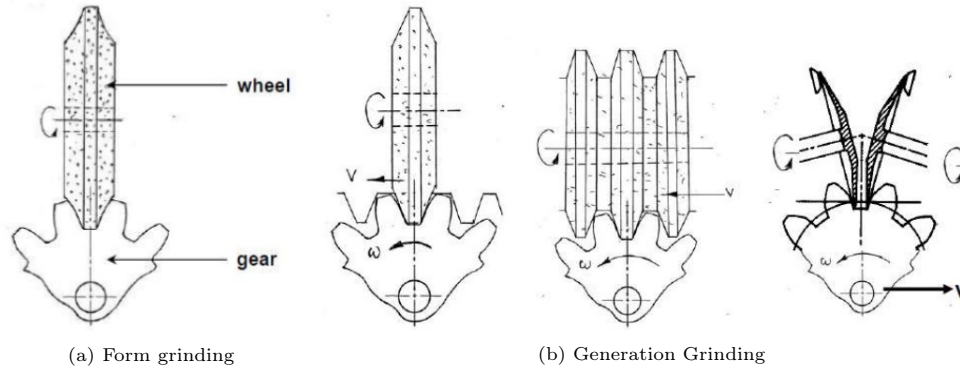


Figure 34: Grinding methods

Gear grinding is a finishing method which is generally known to be the most perfect way to end a high precision gear. They are an excellent design choice when quiet, strong gears are needed in your application.

• Lapping

This process is done, generally, in gears having a hardness higher than 45HRC, to remove burrs, abrasions and any small errors caused by heat treatment. In this process, the gear to be lapped is run under load in mesh with a gear shaped lapping tool or another mating gear of cast iron. An abrasive paste is introduced between the teeth under pressure, it is mixed with oil and made to flow through the teeth.

This process, typically, improves the wear properties of the gear teeth, and corrects the tooth spacing and any miss-concentricity created in the forming, cutting or in the heat treatment of the gears. Therefore, it is often applied to sets of hardened gears that must run silently in service.



Figure 35: Gear Lapping

• Honing

This process is carried out with a steel tool, really similar to that for gear shaving, having abrasive or cemented carbide particles embedded in their surface. The hones¹⁸ are rubbed against the profile generated on the tooth. It is suitable for finishing heat treated gears to a high level, perfect for applications where quiet, robust, and reliable gearing are required. This process is costlier than lapping but also much faster, therefore it is preferred for large quantity operations.

¹⁸Hone: A sharpening stone.

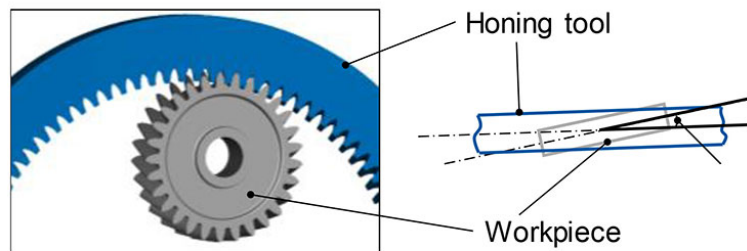


Figure 36: Gear Honing

In gear manufacturing the cost of production is clearly one of the factors which will push the choice of method in one way or another. However, for the purpose of this study, that is not relevant, therefore, the choice is not influenced by that, but by the accuracy of the processes. Thus, gear hobbing followed by a generation grinding finish seems to be the right choice. Once the rough sizing results are reached, I will come back to this point and specify the choice.

7.1.4 Reference Profile

The reference profile of the gear is directly linked to the cutter geometry, therefore, it is linked to the manufacturing method of choice and so, for the same reason why the manufacturing process was not defined, nor is this. The software will not take into account any input defined in this tab during the rough sizing.

Again, this choice can greatly influence the cost of the manufacturing process of the gears. On the one hand, using the available list of cutters (the software provides a data base with dozens) allows to save costs in the sense of making sure that it will ensure that no special cutter will be needed later on in the manufacturing process. However, if your design is unique, maybe no tool in that list provides your needed solution, and one is no willing to reject an optimal design over the cost. Therefore, when selecting it, it is a interesting to think of a cost-efficient process, if needed.

Anyways, with that in mind, KissSoft offers different possibilities. One can either define his/her own hobbing or pinion type cutter profile, or use a predefined type. The option of selecting constructed involute for precision engineering is also plausible. In that last case, the involute is defined directly together with a root radius. Having gone through the benefits of using an involute shape for the tooth, the instinct, or maybe the lack of knowledge, can push one to choose this last option. For sure, it is not a bad option. Nevertheless, it is not the only way to obtain an involute gear shape, as they can also be generated by rack type hob and shaper cutters, which, as mentioned, could allow to reduce manufacturing costs.

A basic rack defines the tooth profile of a gear with infinite diameter, and it is particularly useful for defining the parameters of a generating cutting tool. There are standard and non-standard basic rack tooth profiles. The standard back rack types have been established by gearing organizations, such as SO 53:1998, DIN 867:1986; JIB B 1701-1... etc, and gear manufacturers commonly have tools available to cut gears with the tooth proportions defined by these standard basic rack types.

In particular, the ISO-53 standard specifies the characteristics of the standard basic rack tooth profile for cylindrical involute gears (external or internal) for general and heavy engineering. The standard basic rack tooth profile defined constitutes a geometrical reference for a system of involute gears in order to fix the sizes of their teeth. As mentioned, it does not constitute a definition of a cutter, but a cutter may be defined from this standard basic rack tooth profile in order to realize a conforming profile. The proportions of the standard basic rack tooth profile are given in table 11:

Item	Standard basic rack value
Pressure angle, α_p	20°
Tip line - Datum line distance, h_{aP}	1m
Root line - Datum line distance, h_{fP}	1.25 m
Fillet radius, ρ_{fP}	0.38 m
Standard clearance, c_P	0.25 m

Table 11: Standard basic rack

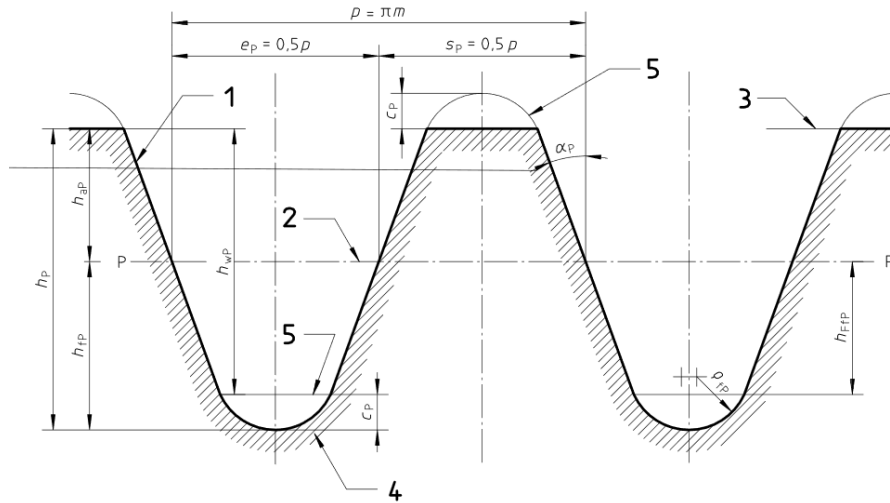


Figure 37: Standard rack profile

with,

1. Standard basic rack profile
2. Datum line
3. Tip line
4. Root line
5. Mating standard basic rack tooth profile

and where,

- s_p is the tooth thickness of a standard basic rack tooth;
- e_p is the spacewidth of a standard basic rack;
- p is the pitch;
- m is the module.

The rest of the parameters depend upon the ones defined.

By default, for the rough sizing, the software utilises this reference profile gear 1.25/0.38/1.0 ISO 53:1998 Profile A. Again, in the next step, it will be explained if we stick with this choice, or if it is more appropriate to use a different one.

7.1.5 Tolerances & Gear quality

The manufacturing tolerances must also be defined. This will clearly influence the geometry deviations, and they will affect the rating factors, which will directly affect the calculation. The software gives the possibility to define the tooth thickness tolerance for each gear in the planetary system, and also the center distance tolerance. There is no need to remind that these gears are designed for a critical application where the manufacturing process needs to be as close to "perfect" as possible, so the tolerances applied must be strict.

The software offers information about different standards, among which we can find the DIN 3967-1978. More information about this standard can be found in appendix K. It is important to bare in mind that small tooth thickness tolerances unfavourably affect the maintaining of the gear quality, since they unnecessarily limit the correction possibilities during manufacture. Therefore, a balance needs to be reached, between accuracy and some flexibility when manufacturing. KissSoft offers the classification shown in table 12 which helps make the decision. Due to the nature of our design the ab25 tolerance for turbogears, is selected for the tooth thickness in each gear (sun, planets and internal). Besides, it respects the note mentioned, and it is not the most demanding tolerance, "relaxing" the constraints for the manufacturing step. On the other hand, for the center distance tolerance, the choice is made based on the ISO 286-2 standard with js5. Further information about this standard can be found in appendix L.

Casted rims	a29, a30
Rims (normal backlash)	a28
Rims (tight backlash)	bc26
Turbo gears (high temperatures)	ab25
Polymer machines	c25, cd25
Locomotive gear trains	cd25
Standard mechanical engineering, heavy machinery, not reversing	b26
Standard mechanical engineering, heavy machinery, reversing	c25, c24, cd25, cd24, d35, d34, e25, e24
Automobiles	d26
Agricultural vehicles	e27, e28
Machine tools	f24, f25
Printing machines	f24, g24
Measuring gearboxes	g22

Table 12: Proposed tolerances in DIN 3967

The torque capacity strongly depends on the chosen gear materials, heat treatment and gear quality. The quality of a gear is the characteristic property which distinguishes the nature of its manufacturing tolerance. It is a comprehensive indicator of every facet of the gear makeup, and it provides a measure of the geometric accuracy of the teeth on a gear. Thus, it must be defined. There are numerous characteristics weighing on gear performance, and no single specification number covers them all. In this case, it is done according to AGMA 2015, which is the standard offered by default.

With this particular standard, the grade given to define the quality, depends on a comparison of its actual deviation, and the tolerance specified in the manufacturing process. Unless the appropriate gear quality level is used to calculate the power rating of a gear system and that quality level is, in fact, duplicated or exceeded in manufacturing [47], the unit produced may not have the desired life. The standard of use is important to mention, because the new AGMA 2015 standard is substantially different from the previous AGMA 2000-A88 standard, and it indeed needs to be explained to be understood, because accuracy grade numbers are reversed. A smaller grade number represents a smaller tolerance value and, as such, a higher quality gear. This is directly opposite to the typical standard and its previous version. The tolerance grades for the new standard are designated from A2 to A11. The highest quality gears are placed in the "high accuracy" group and have designations of A2-A5. "Medium accuracy" are designated as A6-A9, and "low accuracy" are A10-A11. Due to the critical application, the choice of an A2 quality is made.

7.1.6 Lubrication

The lubrication importance has already been highlighted when introducing the concept of gears, as a way of minimizing the losses generated in loaded gears and improving the overall efficiency. In fact, one of the main innovations which helped boost the efficiency of P&W gearedturbofan was the baffle and gutter system which allowed to deliver oil into the gears for cooling and lubricating in a way that minimized the losses. This has shown that, not only the lubricating oil is important, but also the whole system that makes it possible.

The engine oil system performs several important functions, which are vital for the continued operation of the engine and all its high speed rotating mechanisms, including:

- Lubrication of the engine's moving parts.
- Cooling of the engine by reducing friction.
- Carrying away contaminants (cleaning).
- Reducing noise.
- Material's protection.

As it can be seen, performing the lubrication of the gearbox is just one function, among many. Therefore, before choosing the type of lubricant to be used and the method to deliver it, which is what KissSoft gives the possibility for, it is important to engage with the whole lubricating system of the aircraft and to understand it.

When talking about aircraft's systems, they are all those required to operate an aircraft efficiently and safely. There are several basic aircraft systems that are universal, in fact, most aircraft have a standardized set of systems which diverge depending on their designed purpose. However, certain aircraft operations demand increasingly complex aircraft, and therefore systems. Furthermore, these systems need to be integrated and interconnected between each other, and it is the interrelationship between them that gives the vehicle its fighting edge, specially with the introduction of new technologies in these last years. However, this is also the cause of many of the development headaches. A general presentation of some of the main aircraft systems can be found in appendix M.

What concerns us here is the lubrication system, so a more detailed explanation is followed. To start with, a typical oil circuit is shown in figure 38. As it can be appreciated, different sensors can be included for pressure, temperature, oil level and cleanliness to be monitored. Monitoring of particles in the oil can be performed by regular inspection of a magnetic plug in the oil reservoir or by counting particles in the fluid in a particle detector. Any unusual particle density implies a failure somewhere in the rotating machinery and detection is essential to trigger a service or inspection. Furthermore, lubrication systems consist of either a wet-sump or dry-sump system.

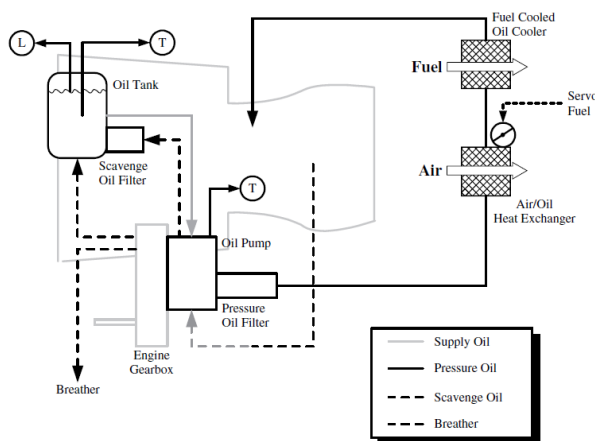
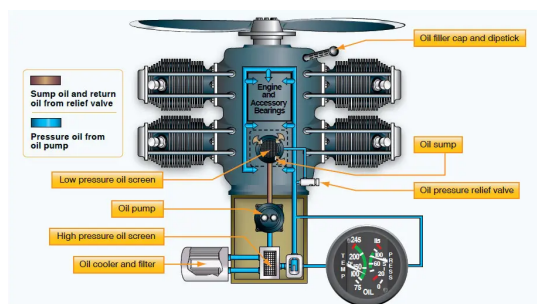
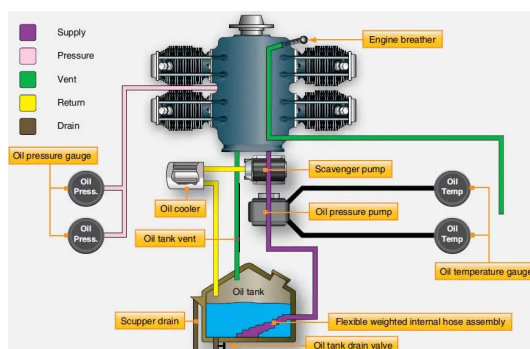


Figure 38: Typical oil circuit [48]



(a) Wet sump system



(b) Dry sump system

Figure 39: Oil systems

As it can be seen, the main difference between them is that wet sump systems maintain oil in reservoirs integral to the engine while dry sumps do not, leaving the sump "dry". The equipment pressurizes the oil from the oil tank and distributes it around the engine parts requiring lubrication with the oil pump, before cooling and filtering it, prior to returning it to the tank. These tanks are always larger than the oil it is meant to contain, to compensate for thermal expansion. One of the benefits of the dry sump system is that they allow a greater volume of oil to be supplied to the engine, which makes them more suitable for jet engines.

Adequately lubricating the elements will result in mechanical efficiency, reliability, low maintenance, and a long equipment life span. Therefore, the way that the oil reaches the different parts of the engines is vital. Some common lubrication methods are explained here, and one is more appropriate than other depending on the application:

- **Grease Lubrication**

This type of lubrication is appropriate for industrial gearbox systems that are open or closed, as long as they run at low speeds. Grease lubrication should not be used for continuous operation or high load gear drives. It should also be noted that grease lubrication has no cooling effect. A sufficient amount of grease must be used to ensure gear teeth are lubricated, but excess grease can result in power losses and viscous drag. Clearly, not appropriate for our application.

- **Splash lubrication (oil bath method)**

When applying it, the gears or another component within the gearbox dip into an oil bath. Through rotation, these components begin "splashing" the oil into necessary chambers and crevices that may contain additional gears or bearings in need of lubricant. Provisions must be made to ensure the gear teeth are not fully immersed in the bath. If teeth are immersed in the oil, excessive losses will result due to the oil being churned. This method is best for medium and high speed gears. In aviation, this method is never used by itself. If so, it is combined with the following method explained.

- **Forced oil circulation lubrication (pressure lubrication)**

It is considered the best way to lubricate gears. It is best suited for high speed industrial gearboxes. For this case, an oil tank, pump, filter, piping and other devices are needed. This the principal method for lubricating aircraft engines. There are different types inside this method:

- Drop method

An oil pump is used to drop the lubricant directly on the contact portion of the gears.

- Spray Method

An oil pump is used to spray the lubricating directly on the contact area of the gears through the use of nozzles. Extra care must be taken to ensure the oil reaches the contacting surfaces.

- Oil mist method

Lubricant is mixed with compressed air to form an oil mist that is sprayed against the contact region of the gears.

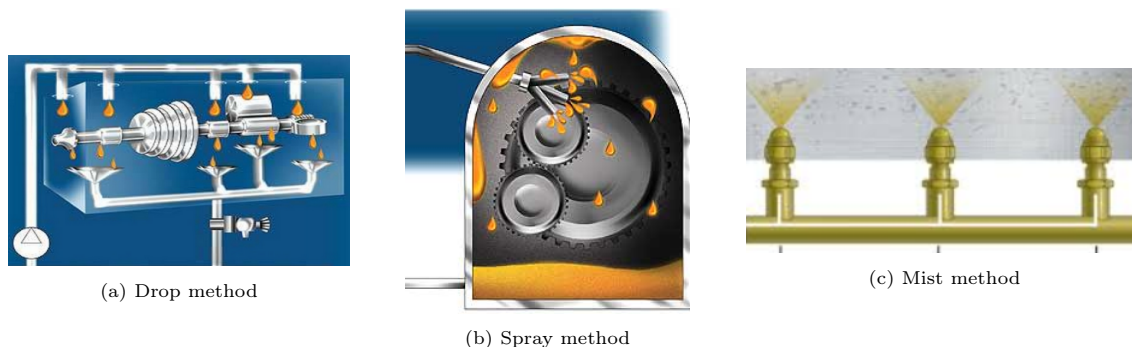


Figure 40: Forced oil circulation lubrication methods

Among the different methods offered in KissSoft, which are listed here, and knowing one of the main problems in these type of gears is the churning of the oil, the choice of oil injection is made (spray method).

- Oil bath lubrication
- Oil injection lubrication
- Grease lubrication
- Dry-run
- Completely immersed in oil

Once the lubrication system is clear, and so, the method to carry it out, the choice of lubricant must be made. The development of new more efficient aircraft engines, need the other areas of development to grow at the same speed, and lubricants are no less. Aviation lubricants must be extremely reliable, withstand high specific loadings and extreme environmental conditions within short times. Because of these factors, the lubrication requirements of aircraft are generally very critical. Nevertheless, according to [40], the recognition of the need for special lubricant in aircrafts appeared after the World War I, when aircraft started to fly higher and longer distances. The introduction and development of gas turbine engines, designed to significantly reduce fuel burn and reduce emissions, led, thus, to the development of new lubricants, becoming a huge challenge for both engine builders and oil formulators.

Lubrication of tooth contacts, both as a means of minimising surface damage and as a way of reducing friction due to sliding, is of crucial importance. Furthermore, the new, state-of-the-art technologies, stress lubricants more than ever before, increasing their demands. The extreme high temperatures to which they are submitted, cause oil residue to be reduced to carbon or coke, which leaves solid residues in the engine, implying constant overhauls, and decreasing efficiency. Furthermore, as mentioned, it is essential to be able to create a system facilitating the deliberation and evacuation of the oil. Proper filtration of the lubricant is also critical, as one of its functions is to clean the engine, as entrained particles can result in wear and material corrosion. The lubricant can make the difference between successful operation and failure not only for pitting, but also for scuffing and micropitting, and the cooling of the system.

Lubricants for the early gas turbine engines were essentially highly refined mineral oils. However, due to the increase in demand, the mineral-based lubricants of the day could not withstand such temperatures for sufficient lengths of time. The focus for lubricant development turned then, to ester-based synthetic lubricants. Compared with mineral lubricants, ester-based lubricants had better thermal and oxidative stability in addition to good low-temperature properties. Modern ester-based gas turbine lubricants consist of approximately 95% base oil. This has a dominant effect on the characteristics of the finished lubricant, in particular, the ones mentioned below. Further information about any of these characteristic can be found in O.

Density	Viscosity	Viscosity index, VI
Pour point	Thermal Stability	Oxidative stability
Coking propensity	Flash and fire points	Volatility
Shear stability	Lubricity	Hydrolytic stability
Elastomer compability	Acidity	Colour

Table 13: Lubricant 's characteristics

From the base oil formula, the wanted properties can be enhanced by additives in the finished product. For example, apart from the properties mentioned with ester-based oils, they also have other inherent properties such as good VI (and therefore no need of VI improved additives), solubility, detergency and dispersancy, affinity for metal surfaces, and they are more biodegradable than mineral oils. By adding certain components, specific properties can be improved, but one has to be careful, as performance improvements in one area can affect performance in another, thus, the main priorities to look for must be clear. Some of the most used additives in aircraft lubricants, together with the main drawbacks of adding them, are shown here:

- *Anti-oxidants*

One disadvantage of modern anti-oxidant packages is their tendency to be more aggressive towards elastomers, particularly in the older technology types used in engine construction.

- *Anti-wear and load carrying additives*

Improving the load-carrying capability of the lubricant for gears can make the lubricant more aggressive towards certain elastomer types, and can increase the coking propensity of the oil. Another disadvantage is that in the presence of water, this additive type reacts with unprotected magnesium alloy surfaces to produce a deposit which can build up and eventually shed, resulting in oil filter blockages. Furthermore, additives which improve load carrying in gears tend to increase rolling contact fatigue on bearing surfaces.

Anti-wear and load-carrying additives work by reacting with ferrous metal surfaces. The metal surfaces have to be sufficiently reactive themselves for the additive to work, but problems are encountered with more corrosion-resistant steels. These steels are designed to be chemically less reactive to inhibit corrosion and thus, this affects the ability of the anti-wear additive to react with the metal surface.

- *Corrosion Inhibitor additives*

Corrosion in lubricated systems can occur for a variety of reasons including static corrosion of steel components from the ingress of water or from the reaction with the lubricant, or due to degradation products of the lubricant and the metals in the system. As an example, ester-based lubricants have great affinity for water and can absorb several thousand ppm¹⁹ of water from the atmosphere during extended static periods. During periods of operation when the oil becomes heated the moisture is released from the lubricant into the airspace of the lubricated component. During long or frequent periods of operation this is not usually a problem; however, if the periods of operation are not long enough to expel the resulting moist air then, after shutdown, the water can condense onto the cold system components and cause corrosion.

However, as mentioned, corrosion inhibition is a fine balance of competition with the anti-wear/load-carrying capability of the lubricant. Like the anti-wear additive, the corrosion inhibitor is designed to react with the metal surface. Some corrosion inhibitors, compete with the anti-wear additive for the metal surface to the extent that the resulting lubricant has poorer anti-wear properties than non-corrosion-inhibited lubricants.

- *Anti-foam additives*

Foaming of the lubricant in a system can cause a variety of problems including loss of lubricant through overflowing of the resulting increased foam volume, oil pressure fluctuations because oil pumps cannot effectively pump a foam and also breakdown of lubrication because there

¹⁹ppm: parts per million.

is insufficient liquid lubricant to form the critical films. Dose rate and correct dispersion of the additive are critical because higher dose rates can cause foaming, rather than reducing it.

- *VI and lubricity additives*

This additives improve the viscosity-temperature behaviour of the lubricant. One potential disadvantage is the affect on oxidative and coking stability. Also, acids with higher molecular weight reduce lubricant volatility but adversely affect low temperature viscosity.

It is clear that formulating gas turbine lubricants is a complex business and also that they can be formulated to favour particular properties over others. It is the user of the lubricant who must define the requirements which the resulting lubricant must meet. Furthermore, lubricant's producers must be able to ensure the well performance of the oil, but testing every single experimental formulation is totally impractical. To avoid this problem, but at the same time, to be able to meet the requirement, lubricant specifications were born. As always, different classifications coexist, as it can be seen in the following table with some of the most common ones. Turbine lubricants are divided into various grades by the lubricant's kinematic viscosity at 100°C. The grades currently available are 3, 4, 5 and 7.5 cSt.

Specification	Issuing authority	Viscosity Grade	Lubricant class	Typical applications
SAE AS5780	SAE	5	SPC, HPC	TP, TJ, TF
MIL-PRF-7808	US Air force	3 and 4	n/a	TJ, APU
MIL-PRF-23699	US Navy	5	STD, CI, HTS	TP, TJ, TF
Def Stan 91-94	Uk MoD	3	n/a	TJ, APU
Def Stan 91-98	Uk MoD	7.5	n/a	TP
Def Stan 91-100	Uk MoD	5	High Load	TJ
Def Stan 91-101	Uk MoD	5	STD	TP, TJ, TF

Key: SPC = Standard Performance Capability; HPC = high- performance capability; STD = Standard; CI = Corrosion Inhibited; HTS = High Thermal Stability; TP = Turbo-Prop; TJ = Turbo-Jet; TF = Turbo-Fan; APU = Auxiliary Power Unit

Table 14: Turbine lubricants specifications

All of the above specifications define the performance of the lubricant as much as possible through the use of laboratory-based tests. The most widely used turbine lubricants, by far, are the 5 cSt grades covered by the US Navy specification, MIL-PRF-23699. It has been the industry standard for 5 cSt lubricants, apart from the high-load-type oils, used by both the US military and the civil aviation world for many years. There is not a single 5 cSt lubricant, again apart from the highload type, used in western aviation gas turbine engines that has not been tested and approved by this specification.

Coming back to our topic of application, the greatest challenge of aircraft lubricants is the heat. High temperature is the main factor responsible for degrading the lubrication and antiwear properties of aero-lubricating oils. Modern engine bulk lubricant temperatures can range between 80°C and 100°C for the system oil feed and peak at approximately 190°C on the scavenge side, with exposure to metal hot wall temperatures in the bearing chambers (see a brief explanation of how these bearing are lubricated in appendix N) between 300°C and 400°C [40]. Combining all this, with the constant desire to extend the time between major overhauls even further, then the enormity of the challenges these lubricants have to face becomes apparent. It is granted that a single charge of lubricant is not expected to last for that period, as lubricant is lost during operation and it must be regularly topped-up with fresh lubricant. The equilibrium of used lubricant/new lubricant that is reached must keep the engine lubricant system components sufficiently clean throughout this period. Although there are no combustion products for the lubricant to deal with, as in piston engines, it can still form coke deposits because of the high transient temperatures experienced, and spontaneous ignition in extreme cases. Any such deposits must be prevented from building up to the point at which they cause a blockage. The lubricant still has an important part to play in minimising the formation of these deposits in the first place and to be able to efficiently remove those that are formed. For the right choice of lubricant, engine usage, temperature, climate,

location and engine design are taken into consideration.

Oil viscosity or its readiness to flow under different temperatures is one of the most important properties. During a cold winter start, the oil will be thicker than during a warm start in summertime. Both cases demand that the oil pressure is attained within 30 seconds after start to prevent damage. The thermal stability of turbine engine lubricants is probably the single greatest challenge for both engine builders and oil formulators at present. This is also important to perform well the engine cooling. **Mobil Jet Oil II** [49] is a high performance aircraft-type gas turbine lubricant formulated with a combination of a highly stable synthetic base fluid and a unique chemical additive package. The combination provides outstanding thermal and oxidative stability to resist deterioration and deposit formation in both the liquid and vapour phases, as well as excellent resistance to foaming. This product is engineered for aircraft gas turbine engines used in commercial and military service requiring MIL-PRF-23699 level performance. Its usage extends gear and bearing life and reduces the engine maintenance, and for all those reasons this is the choice in this case. This is, thus, the choice made for this study. The properties used to define this lubricant are shown in the following table²⁰:

Properties	
Density oil at 15°C	1.0035 kg/dm ³
Viscosity at 40°C	27,6 mm ² /s
Viscosity at 100°C	5,1 mm ² /s
Viscosity at -40°C	11000 mm ² /s
Lower limit service temperature	-40 °C
Upper limit service temperature	204°C
Fire point	285°C
Flash point	270°C
Pour point	-59°C

Table 15: Properties for Mobil Jet Oil II

Furthermore, having mentioned that scuffing and micropitting are a big possibility, it is important to make sure that the lubricant will perform properly. In order to do that, different tests can be used. On the one hand, the micropitting test GF-C/8.3/90 consists of a load stage test performed on a back-to-back gear test rig. Here, the load is increased stepwise from load stage LS 5 to load stage LS 10 with a running time of 16h per load stage. The load stage in which the failure criterion is reached is called failure load stage and depending at which stage the system fails, it is classified as shown in table 16. Lubricants with a high micropitting load-carrying capacity reach the failure load stage > LS10. For that reason, this is our choice.

Description	Failure load stage	Micropitted area
Low micropitting load-carrying capacity	$\leq LS7$	Sometimes more than 50%
Medium micropitting load-carrying capacity	$LS 8 - LS 9$	About 30%
High micropitting load-carrying capacity	$\geq LS10$	Less than 20%

Table 16: Classification of test results of the micropitting test from [50]

If the load stage against micropitting is specified for the lubricant, the permitted specific lubricant film thickness λ_{GFP} can be calculated. It is calculated from the critical, specific lubricant film thickness λ_{GFT} which is a function of the temperature, oil viscosity, base oil and additive chemistry and can be calculated in the contact point of the defined test gears where the minimum, specific lubricant film thickness is found, and for the test conditions where the failure limit concerning micropitting has been reached. This then, makes it possible to define the safety against micropitting $S_\lambda = \lambda_{GFmin}/\lambda_{GFP}$, with λ_{GFmin} being the required smallest specific lubrication gap thickness,

²⁰1 cSt = 1mm²/s.

which is the specific film thickness where no micropitting risk is given. The calculation rules that, in order to prevent micropitting $\lambda_{GFmin} \geq \lambda_{GFP}$.

In the same path, the scuffing load capacity of gear oils is expressed in terms of FZG Scuffing Load Stage. FZG is the Technical Institute for the Study of Gears and Drive Mechanisms (Forschungsstelle für Zahnräder und Getriebebau) of the Technical University in Munich, where this test rig was developed. The several scuffing load tests performed on the FZG test rig serve for determining the extent to which gear lubricants help to prevent scuffing on the tooth faces at the lubrication gap. This is evaluated by loading the gears stepwise in 12 load stages for Hertzian stresses of 150–1800 N/mm². Each load stage is operated for 15 min at a pitch line velocity of 8.3 m/s with an initial oil temperature of 90°C, under conditions of dip lubrication without cooling. The gear flanks are inspected after each load stage for scuffing marks by visual inspection. Failure is considered if the faces of all the pinion teeth show a summed total damage width, which is equal to or exceeds one tooth width. The scuffing load capacity of a lubricant depends primarily on the base oils and additives used, and the consequent lubricant film thickness. The various scuffing load tests can be classified according to the occurring flash temperatures, which renders a list as follows [51]:

Scuffing load test	Flash temp. $\Delta \vartheta$ [K]
FZG (A/8.3/90) sls > 11	≈ 370
FZG (A/8.3/90) sls > 12	≈ 420
FZG (A/16.6/90) sls > 11	≈ 460
FZG (A/8.3/90) sls > 13	≈ 500
FZG (A/16.6/90) sls > 12	≈ 520
FZG (A/8.3/90) sls > 14	≈ 570
FZG (A/16.6/90) sls > 13	≈ 610
FZG (A10/16.6R/90) sls > 10 = API GL 4	≈ 620
FZG (S-A10/16.6R/90) ls 8 PASS = API GL 4	≈ 770
FZG (S-A10/16.6R/90) ls 9 PASS = API GL 5	≈ 950

Table 17: List for comparing the various FZG scuffing load tests

In this list, the requirements to be met by the lubricant in order to pass the tests increase from top to bottom. According to [52], the normal test procedure is the A/8.3/90 as standardised in DIN 51 354. However, our choice of lubricant presents ad flash temperature of 270°C (543. 17 K), which makes our the choice of test to be performed the FZG (A/16.6/90) sls > 12.

Once the test is performed, if the risk of scuffing is too high, one can increase the safety by changing the oil (choosing one with higher viscosity at high temperatures), adding a profile modification or modifying the profile shift distribution. Figure 41 shows the typical limits of the load-carrying capacity for case hardened gears according to Niemann. It clearly reflects the importance of testing the gear for each of them individually, as being "safe" from one type of failure is not a warranty of being safe from the others.

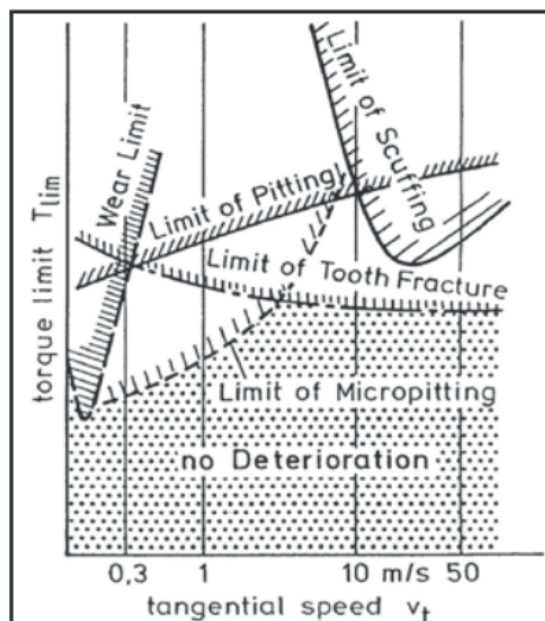


Figure 41: Typical limits of the load-carrying capacity for case hardened gears

7.1.7 Rating & factors

In the “Rating” section all the data regarding the loads in the three study cases of the gear pairs, is present. Power, torque, speed and required service life can be given as input. The only difference among designs will be the N_1 speed, the rest of parameters will be kept the same.

The designs are made to be able to transmit 10MW during, at least, 70000h of service (around 8 years). The driving gear is, of course, the sun gear, with a clockwise sense of rotation. The input speeds are the following:

GB	N_1 (RPM)
Turboprop	9000
Gearedfan 1	11000
Gearedfan 2	9000

Table 18: Input speed

Furthermore, to define the calculation method is essential, as many differences can be found in the final design depending on this choice. Rating standards exist because it is vital to know the load that will cause failure to the gearset. This load depends on many things, and it can only be determined by testing. However, testing to determine a safe load over the full life of a gearbox is not practical, and this is where standards come to place.

The rating standards provide minimum requirements that must be met for the rating to be valid. The gear cost can be minimized by just meeting these minimum requirements, however, by going beyond them, an extra margin of safety can be achieved. In fact, it is typical to try to assure that gears will be very reliable by the selection of a “conservative” rating standard or by increasing the required safety or service factors. The advantage of doing this is the supposedly lower chance of failure. However, if an adequately sized gearset does not fail, it means that it is already sufficiently reliable, and therefore, a larger gearset will not be more reliable. For low-speed sets, the only negative consequences of being “conservative” may be size, price, and slightly higher operating costs due to higher losses. For high-speed sets, being “conservative” can lead to high face widths or high pitch line velocities that can have significant negative consequences. Increased face width not only makes the gearset more sensitive to alignment, it is detrimental due to the heating of the oil, which it is transported across the face width as the contact line sweeps across. The further the oil travels across the face, the higher its temperature gets. Increased pitch line velocity leads to increased sliding velocities, which also leads to a higher temperature in the contact zone and higher risk of varnishing or scuffing. In some cases, high tooth temperatures may eventually distort the helix, affecting the load distribution across the tooth flanks. Therefore, rather than simply increasing the required service or safety factors, which will later be introduced, or specifying the use of a very conservative rating standard, every aspect of the gearbox should be carefully examined.

Said that, when reaching the point on having to make the choice of which standard to follow for the gear rating, it can become quite a headache. There are many different gear rating methods in use today, and they can give substantially different results for any given gearset, having them a huge impact on the size of the gearbox. Some of them are: AGMA 2001; AGMA 6011; AGMA 6013; ISO 6336; API 613; API 617; API 672; and API 677, which, according to [53], each of them is more appropriate to particular applications:

Standard	Applications
API 613	Special Purpose Gear Units for Petroleum, Chemical and Gas Industry Services.
ANSI/AGMA 2001-D04	Fundamental Rating Factors and Calculation Methods for Involute Spur and Helical Gear Teeth
ANSI/AGMA 6013-B16	Standard for Industrial Enclosed Gear Drives
ANSI/AGMA 6011-J14	Specification for High-Speed Helical Gear Units
ISO 6336-2006	Calculation of Load Capacity of Spur and Helical Gears
API 672	Packaged, Integrally Geared Centrifugal Air Compressors for Petroleum, Chemical, and Gas Industry Services
API 677	General-Purpose Gear Units for Petroleum, Chemical and Gas Industry Services.

Table 19: Applications according to the standard

As mentioned before, the gears designed are two planetary gearset, so when making this decision, the possible options of choice are narrowed. Furthermore, it is interesting to mention that the ANSI/AGMA 2001-D04 and the ISO 6336-2006 are the most common used standards. The AGMA standard, as its name states "American Gear Manufacturers Association", is mostly used by American manufacturers, and it is basically experience-based; while the ISO 6336-2006, which is more academically-based, is more commonly used in Europe. Both allow for wear, bending and pitting resistance with equation modifiers that are similar, but not identical. Even though the input data required for the calculations is quite similar in both cases, and the gear ratings are often fairly similar, there are a number of fundamental differences between them. For example, as curious facts, the ISO standard finds the calculation points for bending strength by fitting an equilateral triangle into the base of the tooth, whereas the AGMA method is to use the Lewis parabola; the ISO dynamic factor is based on shaft vibration and proximity to a critical speed based on a very simplistic model of the shaft, while the AGMA dynamic factor is based mainly on allowable single tooth pitch variation [53]. Many scientists have conducted studies to perform a comparison between both standards [53] [54]. Depending on the application, one is more conservative than the other, so in the end, it is a choice of the designer, and one just needs to have the knowledge that the results would be different. In this particular case, after a deep consideration, the choice of following the AGMA standard is made.

As introduced, this standard provides fundamental rating formulas applicable for rating the pitting resistance and bending strength of internal and external spur and helical involute gear teeth operating on parallel axes. The formulas evaluate gear tooth capacity as influenced by the major factors which affect gear tooth pitting and gear tooth fracture. The knowledge and judgment required to evaluate the various rating factors come from years of accumulated experience in designing, manufacturing, and operating gear units.

There are two major differences between the pitting resistance and the bending strength ratings. Pitting is a fatigue phenomenon which is a function of the stresses between two cylinders and is proportional to the square root of the applied tooth load. Bending strength is also a fatigue phenomenon related to the resistance to cracking at the tooth root fillet in external gears and at the critical section in internal gears. It is measured in terms of the bending (tensile) stress in a cantilever plate and is directly proportional to this same load. The difference in nature of the stresses induced in the tooth surface areas and at the tooth root is reflected in a corresponding difference in allowable limits of contact and bending stress numbers for identical materials and load intensities.

Proceeding, in order to predict the load capacity of gear drives, several methods can be found in the literature. Among these methods, the most common applied ones, use influence factors, as mentioned. Designing a 100% efficient gearbox is "impossible". There is so much casuistry to consider, and possible situations that need to be accounted for. The parameters that will be presented below, allow to consider a more realistic loading.

To start with, the overload factor K_o . This factor accounts for the operating characteristics of the driving and driven equipment. The dynamic response of the system results in additional gear tooth loads due to the relative accelerations of the connected masses of the driver and the driven equipment. Therefore, this factor is intended to make allowance for all externally applied loads in excess of the nominal tangential load W_t^{21} , accounting for the regularity and any uncertainty on the load.

There are many possible sources of overload which should be considered. Some of these are: system vibrations, acceleration torques, overspeeds, variations in system operation, split path load sharing among multiple prime movers, and changes in process load conditions. This overload can be just momentary, or more common, in any case, they are critical for the well-being of the gears.

As any load coming from load irregularity is not uniform at all and it can present also relevant shocks, it should be bigger than 1. According to DIN 3990/ISO 6336, the application factor (which is how this factor is referred to in older versions of the standard) can be established after analysing the working characteristics of the driving machine and driven machine in the following way:

Working characteristic of the driving machine	Working characteristics of the driven machine			
	Uniform	Light shocks	Moderate shocks	heavy shocks
Uniform	1	1.25	1.5	1.75
Light shocks	1.1	1.35	1.6	1.85
Moderate shocks	1.1	1.35	1.6	1.85
Heavy shocks	1.5	1.75	2	2.25 or higher

Table 20: Overload factor according to DIN 3990/ISO 6336

Due to the conditions to which aviation gears are submitted, the choice of an overload factor of 2.25 is made.

In this same line, the dynamic factor K_v takes into account internally generated gear tooth loads which are induced by non-conjugate meshing action of the gear teeth. It takes into account additional forces caused by natural frequencies in the tooth meshing. The conjugate action of the teeth consists on being able to give a strictly constant output/input velocity ratio for meshing gears. Without proper conjugate action, gears would suffer severe vibration, impact and noise problems, an even if the torque and speed of the gear are constant, significant vibration, and therefore, dynamic tooth forces, may exist. These forces appear, thus, from the relative accelerations between the gears as they vibrate in response to an excitation known as “transmission error”. Reducing the dynamic loading, affects directly the load loading and that, increases the life of the device. Accurate prediction of gear dynamic factors is necessary to be able to predict the fatigue life of gears. Thus, it is an important concern in gear design.

The dynamic factor is influenced by many parameters, from the environmental conditions, the geometry corrections applied on the gears, their size and geometry, of course, and the quality of the tooth. Moreover, all the deviations from the ideal gear tooth form and the ideal spacing, affect too. Some of the ways that can reduce it, consist on using involutes of circles to define the tooth shapes. This geometry is responsible for the smooth meshing of gears and minimal variation of speed and torque. Furthermore, using tooth profile modifications methods has been found to significantly affect tooth meshing stiffness [55]. Said that, as mentioned before, the profile shift coefficient, and also, the K_v factor are left to be calculated by the software, as needed, according to the selected calculation method. If considered, any modifications will be applied during the fine sizing step. It is known that standard-based calculations of gears dynamic factors have some limitations [56], but due to the early stage of the design, this is the most accurate at the moment.

21

$$W_t = \frac{2000 * T}{d} \quad (4)$$

The same is done with the load distribution factor, K_m . This factor modifies the rating equations to reflect the non-uniform distribution of the load along the lines of contact, which is influenced by many factors such as the manufacturing process or the assembly of the gears. Its magnitude depends on two components, the transverse load factor $K_{H\alpha}$, and the face load factor $K_{H\beta}$. The transverse load distribution factor accounts for the non-uniform distribution of load among the gear teeth which share the load, along the line of contact, which is due to the deviations from the ideal tooth profile. Standard procedures to evaluate the influence of the first one have not been established. Therefore, evaluation of the numeric value of the transverse load distribution factor is beyond the scope of the standard of choice and it can be assumed to be unity. On the other hand, the face load distribution factor accounts for the non-uniform distribution of load across the gearing face width, caused by mesh misalignment, and that is influencing the contact stress. This misalignment can be caused by elastic deformations of gears, shafts, and bearings as well as for manufacture and assembly deviations, bearing clearances or dynamic effects. The face load factor is defined as the peak load intensity divided by the average load intensity across the face width, and it is one of the most important items for a gear strength calculation. This factor is influenced by the length of gear shafts, the face width of the gears, the relative position of the gears over their shafts and the ratio between the pitch radii of the gears and the radii of their shafts. Therefore, its calculation is not arbitrary at all. The software offers different possibilities to calculate it. If one already knows the face load factor, one can add its own input. This is clearly not the case. Another way is to use the possibility given of "Calculation according to calculation method". The face load factor is then calculated according to the formulae used in the strength calculation standard method. Nevertheless, the formulae proposed in the standards for defining face load factor enable you to determine it very quickly but only empirically, and therefore not very accurately. For example, in the international standard for cylindrical gear rating, ISO 6336-1, using method C, some formulas are proposed to get a value for this factor. But the formulas are simplified, and the result is often not very realistic. Also AGMA 2001 proposes a formula, different from ISO 6336, but again not always appropriate. Therefore a note in AGMA stipulates that, even though, it is usually higher than it actually is, and therefore, the calculated value is on the conservative side, an analytical approach to determine the load distribution factor may be desirable. In the last edition of ISO 6336, a new annex E was added: "Analytical determination of load distribution". This annex is entirely based on AGMA 927-A01, and the calculation considers shaft misalignment due to bending, torsional deformation and manufacturing errors. Although the "Calculation according to ISO 6336 Annex E" method is very accurate, it requires quite a lot of time and effort, as it calculates any gapping in the meshing, and therefore defines the load distribution over the entire facewidth. To perform this calculation, one would need to know the exact dimensions of the shafts and support. It is out of the scope of this project to work on the design of those parts of the gearbox, and at this point of the design, we do not even the raw dimensions are calculated. To avoid any complications but being aware of the imprecision, the option, "Calculation according to calculation method" is used.

Furthermore, the mesh load factor, K_y takes into consideration the uneven load distribution across multiple planets. Depending on the number of planets and the application level, the value of this factor changes. According to AGMA 6123-C16, for high quality gear units such as ours, if the number of planets is 3, K_y should be 1, and if the number of planets are 5, it should be 1.19 or less. These are our inputs, thus.

Lastly, another fundamental part of the AGMA strength rating of gears is the geometry factor J. It evaluates the shape of the tooth, the position at which the most damaging load is applied, and the sharing of the load between oblique lines of contact in helical gears (not our case). Both the tangential (bending) and radial (compressive) components of the tooth load are included. The method applied for the calculation of this factor will be a graphical method for all gears.

7.1.8 Gear ratio, the safety factors and the input speed

The last three points to be defined before the rough sizing calculation are the gear ratio, the input speed and the safety factors.

For the first points, here, again, there will be a difference in the gearboxes designed for a turboprop engine and for a gearedturbopan.

GB	Gear ratio	Input speed (RPM)
Turboprop	9	9000
GearedTurbofan 1	2,5	11000
GearedTurbofan 2	2,2	9000

Table 21: Input speed and gear ratio

To lower gear ratio in the geared turbofans is obvious. The size of the fan is a lot smaller that that of the propeller, and therefore the speed limitation is less strict. Furthermore, the idea of performing these three simulations is because geared turbofans work at higher speeds than turboprops, so the difference seen in the Turboprop and the GearedTurbofan1 aim to have that into account. The inclusion of the GearedTurbofan2 with the same input speed as for the Turboprop looks for having as many parameters equal, as possible.

On the other hand, the safety factor established will be the same for all the designs. The required root safety for bending, S_F , and flank safety for pitting, S_H , are really interesting to be considered because they allow for safety and economic risk considerations along with other unquantifiable aspects of the specific design and application. They are intended to account for uncertainties or statistical variations in the design analysis, the material characteristics and the manufacturing tolerances, but also, they consider human safety risk, and the economic consequences of failure. The greater the uncertainties or consequences of these considerations, the higher the safety factor should be. A fixed value for this factors is difficult to define, and even in our standard of choice it is no specified. However, according to [57], for aircraft components, a safety factor above 1,5 is a proper choice, and therefore, for both cases, that is the input.

7.2 Rough Sizing

With all those inputs defined, the rough sizing step is calculated. As mentioned, at this point, the software offers all the possibilities that satisfy our demand. In appendix P, one can see the resulting windows at the end of the simulation, for the three designs. Here, one can already get an idea of the different orders of magnitude for the weight, the face-width, the center distance and the power density, among others. The differences in the designs is clear, and now it is easier to understand the difficulties mentioned when implementing the gearboxes for the geared turbofans. In the following table, the orders of magnitude of the main output parameters at this point, are shown for the three designs:

Design	Face-width, m	Center distance, m	Weight, kg	Power density, $T_{max}/W [Nm]$
Turboprop	220	380	1700	6
GearedTurbofan1	90	240	130	67
GearedTurbofan2	70	390	250	40

Table 22: Order of magnitude of the main parameters in the rough sizing step

These results are obtained considering the same power transmission, when in reality, that of the turbofans is usually higher than that of turboprops. In the easiest comparison (as they share more parameters equal), looking at the results obtained for the Turboprop and the GearedTurbofan2 (both designs have the same input speed but different gear ratio), the difference in size and power density is remarkable. Clearly, for the development of the gearbox for the fans, the design implies a very high power dense results. Furthermore, as a reminder, the gearboxes in the turboprops can be set or mounted outside the core of the engine, while in the geared turbofans, it is a requisite for it to be inside, something that limits its allowed size. This fact has not been considered when defining the inputs, nor will be considered later. However, it is interesting to know, because even without that constraint, the difference in the size of the resulting gearboxes is considerable, and it may even be necessary, in real life, to make them smaller, in the case of the gearedturboprops, or bigger, in the case of turboprops.

As to the results obtained for the GearedTurbofan1, when comparing them to those of the GearedTurbofan2, the differences are not that critical but still considerable. The change of a dif-

ferent (higher) input speed for the GTF1, with a subsequent increase in the reduction ratio, results in a higher power dense design. As mentioned, the GTF1 design would actually look more likely to the gearbox employed in the turbofans, as the working speeds there, are a lot higher than those in turboprop engines.

When looking at all the possible solutions, one must clearly make a choice, and indeed it is not arbitrary, as it will determine the inputs for the next steps. Different strategies can be applied during the search for the optimal solution for a given application. Minimising the weight and maximizing the power density of the gearing is and aim, but achieving both at the same time, with a high overall efficiency, is complicated. A nice trade-off is then looked for. Another important aspect to bear in mind are the safety factors. Even though it is known that they will change in the next steps, still, it is interesting to have higher values.

For the three designs the same criteria is applied. A solution with an average results for all the parameters mentioned in table 22 is selected. In appendix P, one can find the solution chosen for each design. The exact values will not be considered in the following steps. It will be seen later, but ranges will be defined, so it seemed like the right choice.

7.3 Fine Sizing

Starting from the selected rough sizing solution, one can proceed to the fine sizing calculation. This calculation allows to refine the design by taking into account more detailed parameters as gear module, profile shift, diameter constraints and other conditions. By iterating over these parameters, different possible solutions are provided. In figure 42 one can see the process depicted in a similar way to that shown in the rough sizing step.

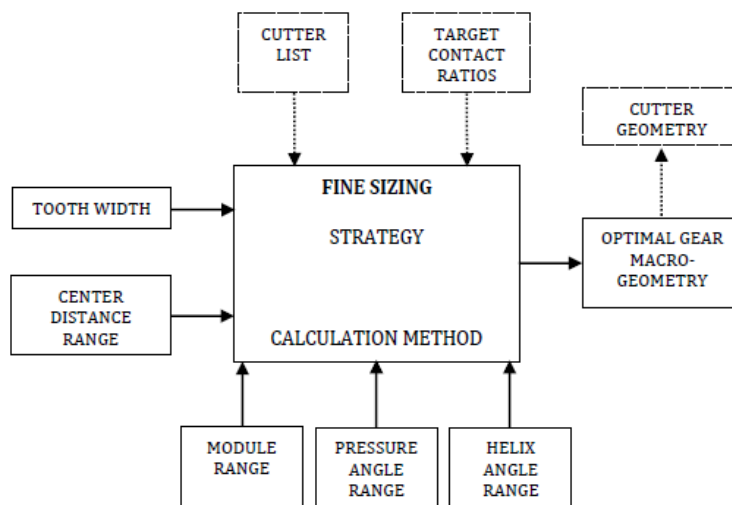


Figure 42: Fine sizing procedure

To start with, at this point, defining the manufacturing process will be determinant in the solutions obtained. It was already mentioned that during the rough sizing step the calculation is done without considering the manufacturing method. By default, the software uses a reference profile gear 1.25/0.38/1.0 ISO 53:1998 Profile A. As it can be appreciated in the picture, KissSoft offers two possible ways to proceed. One can either choose from the available cutter list provided (which includes hob cutters, shaper cutters and standard reference profiles), or define the contact ratio, and from this constraint, the software would iterate over the gear reference profile to get solutions. This last option, even though it is really tempting, as having deep tooth forms (or cylindrical gears with a high transverse contact ratio), can lead to a nearly constant stiffness, it can be a little "risky" because it can turn out in "impossible to get" profiles. However, there is no better solution, it depends on each case.

After having analysed all the manufacturing possibilities, it seemed that the right choice for this case was to use a hobbing method, followed by a grinding surface finish. However, after different iterations, it was concluded that choosing the hobbing process restricted quite a lot the number of possible solutions, due to the hob cutters available, and taking into account that I am not an expert in gear design probably, having to design the hob's dimensions is not the best choice. For that reason, the choice of continuing with the reference profile of choice in the first step, allowing the software to choose the most appropriate manufacturing method to provide it, is the choice. In the end, this procedure is going to be followed in all three designs, so that is not going to be a reason of difference. Nevertheless, for the finishing process, the grinding method is selected. Gears are usually manufactured with a grinding stock that will be removed in the grinding process to meet dimensional requirements. This grinding stock can also be defined. The software offers two possibilities: either to define it yourself or to use the Standard DIN 3972:1952, which will define a final machining stock. Due to the lack of experience, this last option is the chosen one.

Moreover, the type of planetary configuration to use, can also be defined. The rough sizing results were obtained considering a planetary type arrangement, with the ring gear held stationary. However, for the gear ratios employed, specially those for the geared turbofan designs, it is more appropriate to use a star configuration, with the planet carrier being fixed. This allows to take profit of the counter-rotating movement of the sun and the ring. Thus, for all three designs, this consideration is specified.

For the rest of the main parameters, KissSoft provides a large number of aids to help size gears. This sizing tool is really helpful for non-expert designers, as it allows one not to be forced to input an specific value, but to predefine ranges. Thanks to this tool, parameters such as the helix angle for designing helical gears instead of spur ones, can be defined. This way, one can benefit from the lower loading impact and the load sharing that these type of gears offer.

Other essential functions can be specified, such as if undercut wants to be allowed or the criteria to follow when sizing the profile shift coefficient. To start with, depending on the size of the gears and on the manufacturing method of choice, undercut may be necessary to avoid interferences. For those reasons, the undercut is allowed. As to the profile shift coefficient, depending on the criteria chosen, the KissSoft system proposes suitable profile shift coefficients. It can be calculated to achieve the minimum sliding velocity, or for optimal specific sliding, or for maximum root or flank safety, among others. The importance of lowering the sliding losses has been emphasised. Therefore, the choice of the profile shift is based on trying to reach its optimum value.

Furthermore, in the fine sizing step it is allowed to limit the value of the specific sliding velocity, the ratio between the sliding velocity and the rolling velocity of the mating tooth flanks. Its optimal value would be 1, which is clearly difficult to get, but it can be improved with profile modifications. Thus, the limit is put in $\zeta_{max} < 2$.

Proceeding from the RS results, and with the last updated input choices, the software systematically varies gearing parameters, filters the variants and with a simple algorithm it can sort and extract the best solutions and present them in a list or graphic overview. All the variants found by this process, which can be over 1000, can be evaluated by a wide range of different criteria (accuracy of ratio, weight, strength, tooth

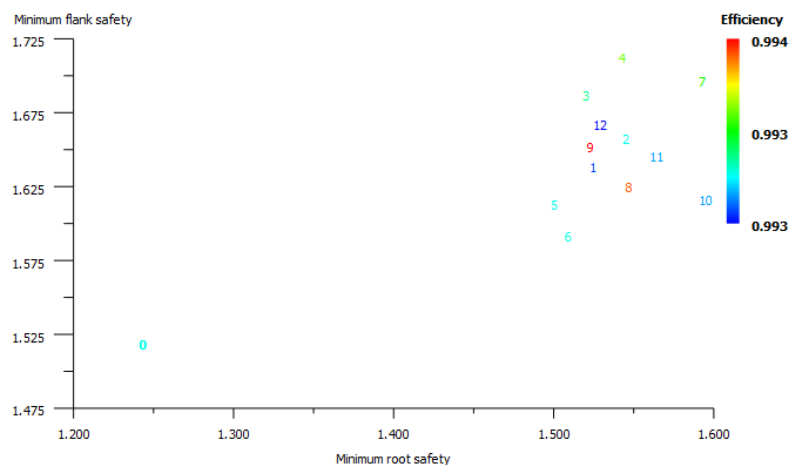


Figure 43: Example of the graphic presentation of the fine sizing results, base in the flank and root safety

contact stiffness deviation, efficiency, noise levels etc.). The main challenge is to be able to identify the non-feasible ones and to find the optimum. The following picture illustrates the final stage of a fine sizing step, where only several best solution candidates remain.

With a similar procedure to the one followed in rough sizing, limiting the number of solutions and with the strict criteria of not allowing any solution to have a safety factor lower than the 1.5 established; or with a deviation from the requested gear ratio too large; or with a specific sliding (wear, friction) too high, the best solution for each of the three designs is reached.

7.4 Modifications

The last step when dimensioning gears, once the standard gear parameters are defined, is to include any modifications that can be made to improve the performance. As mentioned during the rough sizing step, it is known that deflections during loading and manufacturing errors result in tooth geometries different than the ideal involute form, which results in gears not performing as they should in theory. This happens specially in high loaded gears, due to the high tooth deflections under performance. This can cause increased excessive contact pressures at the tooth tip and root, which ultimately result in an increase in noise and premature failure. To reduce these effects, profile and lead modifications can be applied to ensure proper meshing to achieve an optimized tooth contact pattern. However, these are not the only causes for applying modifications. For example, as the planets are usually the smaller gear member, compared to the ring, their tooth strength is generally lower than that of the larger gear. To provide increased strength, reduce undercutting and improve operating characteristics, the dedendum of a pinion tooth may be decreased and the addendum increased correspondingly. If the aim is to keep the center distance the same, they must be changed proportionally. Thus, tooth strengths are brought into balance and wear life of the gear set extended. This is just an example of many of the existing possibilities, and even though there is a whole other world in terms of modifications, in this case, the ones applied will be the simplest ones, as the idea is not to reach the most optimized design, but still, it is interesting to have the knowledge.

Going back to the point, after the fine sizing step, once there is a completely defined gear macro-geometry, an advanced analysis of the gears can be performed, and the optimization process of the tooth form can start. Here is where one of the most powerful tools in KissSoft takes on an important role. The contact analysis tool allows to simulate the real contact condition of a gear pair, in order to evaluate it and get precise information on the load distribution, to be able to calculate the tooth deformation. It is an amazing complement to the strength calculation as it allows to consider individual modifications and to take the system's equilibrium into account in every meshing position. This analysis allows to calculate certain parameters which are vital to understand the performance of the gear designed:

- The normal force that occurs during meshing.
- The actual path of contact under load.
- The transmission error, stress curves, flash temperature, specific sliding, power loss, heat generation, lubricant gap thickness, required safety against micro pitting, wear, and others.

The calculation method followed in this procedure is determined on the basis of the tooth stiffness calculation according to Weber/Banaschek and allows to optimize load distribution by analyzing the effectiveness of gear modifications. These modifications are aimed to optimize the load distribution, reduce noise by eliminating contact shock, reduce the irregularity of the loads acting on the gear during meshing (i.e. PPTE, peak-to-peak transmission errors²²), therefore achieving a more regular meshing, which would lower the contact temperature, improving the load-carrying capacity and the wear risk of the meshing. Basically, modifications, if applied in the right way, optimize the design turning it more efficient.

For the microgeometry design in KissSoft, a sizing function applies, again, modifying variables and supplying the essential results for optimizing the design on the basis of the contact analysis.

²²A perfect involute gear pair with infinite stiffness has no transmission error.

In this point, the choice of modification parameters is directly linked to the final machining process chosen. However, even though this shows the potential of the software, it is not that arbitrary, and the modifications cannot be sized in any way, as there are different types, and not all of them are favourable in our case.

To start with, as mentioned, the most common types of modifications are: profile modifications or tooth trace (or flank or lead) modifications. Both modification types are defined separately, but can be superimposed. On the one hand, flankline modifications are usually applied to compensate shaft bending and torsion, misalignment's due to manufacturing errors, bearing clearance, deformation and influence of the housing. There are different types of flank line modifications, as seen in figure 44:

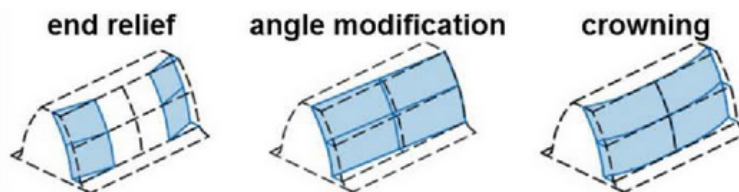


Figure 44: Tooth flank modifications

Optimal flankline modifications will normally increase the torque capacity of the gearbox due to a more even load distribution along the flank, thus reducing the face load factor, $K_{H\beta}$. Under optimal conditions the face load factor would be equal to one. Starting from the results obtained in the fine sizing, the objective is to try to reduce it. Nevertheless, it is a difficult procedure, as the key problem is how to get the precise deflections and the choice of which ones to apply. An excessive amount of tooth trace modification can result in deterioration of tooth contact. Thus, this has led to many studies [58] to try to find a way to optimize it. According to [59], typically, a helix angle modification is applied to compensate shaft misalignments, and a crowning to compensate the random manufacturing errors and torsional effects. If these two basic modification types are correctly combined, the load distribution can become theoretically perfectly uniform.

It is clear that analysing these type of modifications is a little bit outside of the scope of this thesis, as the idea is to design a planetary gear, not the whole gearset, so it is difficult to take into account shaft bending, for example. However, thanks to the sizing tool, a small consideration can be taken into account, as in the KissSoft manual itself is explained [60], when working with planets systems, this proposed tooth trace modification can be used to compensate for a misalignment of the planet and the sun and to take into account the effect of torsion on a particular gear.

Regarding tooth profile modification, they achieve a lower gear noise (thanks to the reduced transmission error), lower contact temperature, smooth normal force distribution and higher wear resistance. Furthermore, profile modification will directly influence the backlash, with the pros and cons mentioned about its application. It is also important to say that it is well known from literature that profile corrections are very important for spur gears, less so for helical gears. The reason is that helical gears and their helix angle, shift the meshing contact from the left to the right side of the gear. So a gear pair with a sprung helix overlap ratio, ϵ_β , bigger than 1 also has, along with a badly designed profile correction, a very good PPTE.

There are different types, as it can be appreciated in figure 45. Each combination used is aimed for a different result, which will vary depending on the whole gearset. For example, gears with high contact ratio show very different characteristics when using profile corrections that a standard-reference-profile. Clearly, not an easy task to find the optimum. According to [55], and I have indeed witnessed it, in literature, few conclusions about the effect of different profile corrections can be found. Some agreements have been reached, but indeed, nothing can be applied in a general way.

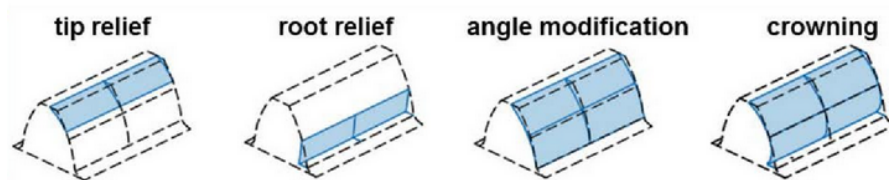


Figure 45: Type of profile modifications

Tip and root relief corrections mainly influence the high contact stresses that occur at the tooth corners (the entering and exiting regions) and the transmission errors, which is directly related to the noise level. Tip relief is much more popular than root modification, mainly due to the fact that near the base circle the curvature is rapidly changing, but anyways, when applied, they are usually included in both gears of a mesh. Furthermore, crowning allows the gear to maintain contact in the central region of the tooth and permits avoidance of edge contact with consequent lower load capacity. Crowning also allows a greater tolerance in the misalignment of gears in their assembly, maintaining central contact. The crowning should not be larger than necessary as otherwise it would reduce dimensions of tooth contact, thus weakening durable strength. Lastly, angle modification can help compensate for profile angle error, resulting from the manufacturing process, which affects the pressure angle. Figure 46 shows graphically the main parameters to define a profile modification:



Figure 46: Profile modification parameters

with, C_{aa} the amount of tip relief, L_{Ca} the length of the tip relief, C_{af} the amount of root relief and L_{Cf} the length of the root relief. Furthermore, inside each type of those profile modifications, one can find different types depending on the curvature applied on the correction and on the amount of material removed: short or long linear corrections, short or long in arc form, short or long progressive, fully crowned profile and more.

As for the optimal length of the profile correction, as it can be seen the following in table²³ obtained from [55], opinions differ. The reason is possibly due to the fact that the effect of long or short profile corrections depend also (among other factors) on the transverse contact ratio of the gear pair, as it will be seen later.

Author	Short Profile correction	Long Profile correction
Niemann	Avoid corner contact and no effect on TE	Avoid corner contact and reduces TE
Linke	Avoid corner contact and reduce TE	Avoid corner contact and reduce TE, but it is worse for low load
Houser	Avoid corner contact and no effect on TE	Avoid corner contact and reduce TE considerably at low load, but it is worse for low load
Smith	Reduces TE for low load	Reduces TE for high load

Table 23: Effects of short or long profile modification in literature

It is also astonishing that in literature, few or no indications are given for the best type of curve to use for the profile correction. The simplest way to find it is with a linear type, but some benefits can be found from using an arc-like or any of the other ones mentioned, which include a curve rather than a line, as the pressure angle of the profile do not have an instant change at the starting point of the modification (even though it is not discussed whether this type of curve has a major influence or transmission error). In the table itself, each author uses a different type of

²³Corner contact between gear teeth mainly occurs when the teeth just make contact or interfere with the root of the teeth. The corner contact promotes deviation from the intended line of contact.

modification. According to [55] Linke and Houser are using a parabolic correction, Smith is using profile crowning and Niemann, most probably, a linear correction.

Using [55] as reference, they performed a study in order to see the effect of different type of curves of the profile corrections on PPTE, depending on the contact ratio, and taking into account different torque levels. This is what helped to choose the type of modifications to apply in this case study. It is clear that PPTE is proportional to the torque. The bending of the tooth increases with the torque and the transmission error increases accordingly. It was already mentioned that, when increasing the contact ratio, a higher stiffness is achieved, and also lower stiffness variation and lower PPTE. However, this is only applied for gears with no profile correction. When applying a correction, the PPTE is not proportional to the torque and the PPTE of high-tooth gears is less reduced when compared to normal gears, but still it is smaller. This shows that each case must be studied independently, because you may even get a worse performance of the gearset, if profile modifications are not applied in the right way.

The conclusions achieved with their study were:

- With the exception of gears with a very high contact ratio, $\varepsilon_\alpha > 2.4$, the short correction is always worse than no correction at all.
- All gear sets above 80% of nominal torque have a significantly reduced TE. Only for low load (60% and less of nominal torque) will the TE increase as compared to the gear set with no correction.
- When using short profile correction in standard gears $\varepsilon_\alpha < 2$, the form of the curve has no major influence on the TE, but for high-tooth, the arc-like curve is much preferred.
- With a long profile, there is no significant difference between the effects of different curves.
- The reduction obtained in the flash temperature, which will directly influence the wear risk, are similar for short and long profile corrections.
- The flash temperature decrease is smaller with lower contact ratio, and reaches its optimum with $\varepsilon_\alpha = 2$

The results obtained for the short and long profile correction (which clearly were in line with some of the conclusions drawn by the mentioned authors, such as Niemann and Houser), related with the TE, were really positive, but care has to be taken with the transverse contact ratio in the three designs.

Furthermore, apart from these standard modifications, KissSoft allows also to define the so called topological modifications where each point on the tooth flank has its own amount of modification. These kind of modifications are much more difficult to produce than the standard modifications, and for this case study, will not be applied. With this analysis, the choice of applying tip and root relief, linear, long profile modifications and helix angle modifications in the three designs, is made. Thanks to the software's sizing tool, the same procedure is applied for all.

7.5 Results

Finally, all the inputs have been defined and the results can be analyzed. In appendix Q, one can find the detailed reports, obtained from KissSoft. Here, a brief summary of the main important parameters will be shown:

• **General information**

Gearbox design	Turboprop	Gearedfan 1	Gearedfan 2
Power (kW)	10000		
Power loss (kW)	71.536	74.731	43.217
Total efficiency	0.993	0.993	0.996
Number of planets	3	5	5
Speed sun (RPM)	9000	11000	9000
Speed ring	-988.4	-4,376.3	-4,164.9
Gear ratio	-9.105	-2.514	-2.161
Torque sun (Nm)	10,610.3	8,681.2	10,610.3
Torque planets (Nm)	107,220.172	30,501.439	33,538.398
Torque internal gear (Nm)	96,609.8	21,820.3	22,928.1
System Service life (h)	122,690	> 1,000,000	198,963

Table 24: General information about the gears

With the following simple calculation,

$$Power(W) = Torque(Nm) * 1000 * \pi * \frac{RPM}{30} \quad (5)$$

one can easily check that the transmitted power is close to 10MW. Still, nor the efficiency or the power loss, nor any other considerations are taken into account in that case.

Another really important consideration to make is the power losses in the system, as they will directly influence the efficiency. As mentioned, there are two types of losses. The ones that are directly depending on the transmitted power and the ones that are independent from the applied load. In the case of planetary gearboxes, the major contributions to the losses are given by the sliding between the teeth and by the churning losses of the planet carrier that is revolving inside the lubricant. As a reminder, this last consideration was one of the main focus in P&W design.

In the field of precision planetary gearboxes, the fundamental target of gear design is to maximize the efficiency. Many researches [61] show that an improvement of the efficiency, in particular a reduction of the meshing losses due to sliding, can be obtained by reducing the module of the gears, together with other modifications of the tooth form (pressure angle, profile shift). In the following tables, the module of the different gearboxes will be detailed, and it will show that that of the GearedTurbofan2, is the smallest one. This may be one of the reason of its lower power losses.

Furthermore, being the weight one of the most important factors in aviation, at this point one can appreciate the detail for the different gears. As expected from the results in the rough sizing, the total mass of the GB is a lot higher in the Turboprop than in the GearedTurbofans, which has direct effect on power density. Furthermore, table 25 is the perfect reflection of the problems mentioned in the introduction of gears in aircraft engines. The increased weight as the gear ratio increases can make its implementation not worth it. However, there are various solutions for reducing the mass of a gear. The most common is choosing a webbed gear design, with the implementation of lightning holes or spokes, furthering weight reduction. This will not be done in this calculation as this is out of the scope of the project, but it is interesting to know as it is typically done when the weight is critical.

Gearbox design	Turboprop	Gearedfan 1	Gearedfan 2
Sun gear mass (kg)	28.02	27.496	59.868
Planet mass (kg)	419.907	15.601	20.682
Internal gear mass (kg)	206.468	30.702	24.594
Total mass (kg)	1,494.209	136.204	187.873

Table 25: Weight of the gears

• Tooth geometry

In this section, the detail about the main parameters of the gears are shown. To start with, as known, the reference profile used was the 1.25/0.38/1.0 ISO 53:1998 Profil A. Nevertheless, that is without taking into account the finish process which is undertaken later. The reference profile of the final tooth form is shown in table 26:

Parameter	Turboprop	Gearedfan 1	Gearedfan 2
Dedendum	1.183	1.169	1.159
Addendum	1	1	1
Root radius factor	0.38	0.38	0.38

Table 26: Reference profile of the final tooth form

Continuing, the main information about the dimensions:

Turboprop	Sun	Planets	Internal Gear
Normal module (mm)	7		
Center distance (mm)	348		
Number of teeth	19	77	-173
Facewidth (mm)	228.8	223.3	228.8

Table 27: Tooth geometry - TP

GearedTurbofan1	Sun	Planets	Internal Gear
Normal module (mm)	5.75		
Center distance (mm)	196.8		
Number of teeth	37	28	-93
Facewidth (mm)	90.13	88	90.13

Table 28: Tooth geometry - GTF1

GearedTurbofan2	Sun	Planets	Internal Gear
Normal module (mm)	4.5		
Center distance (mm)	320.75		
Number of teeth	87	51	-188
Facewidth (mm)	60.49	58.92	60.49

Table 29: Tooth geometry - GTF2

Gears characteristics	Turboprop	Gearedfan 1	Gearedfan 2
Sun			
Profile shift coefficient	0.4935	0.466	-0.1769
Tooth thickness (module)	1.93	1.91	1.442
Tip diameter (mm)	156.398	235.205	410.893
Root diameter (mm)	125.834	210.266	391.462
Tooth height (mm)	15.282	12.470	9.716
Planets			
Profile shift coefficient	0.3693	0.4804	0.3437
Tooth thickness(module)	1.8396	1.9205	1.821
Tip diameter (mm)	568.259	182.26	248.619
Root diameter (mm)	537.694	157.32	229.188
Tooth height (mm)	15.282	12.47	9.716
Internal gear			
Profile shift coefficient	-1.2321	-1.4286	-1.0470
Tooth thickness (module)	0.6739	0.5321	0.8068
Tip diameter (mm)	1,236.915	553.725	872.323
Root diameter (mm)	1,267.480	578.664	891.754
Tooth height (mm)	15.282	12.470	9.716

Table 30: Gears characteristics

It is evident what it was mentioned in the introduction. As the gear ratio is increased, the whole size of the GB is bigger. This can be appreciated in table 30, when comparing the value of the root diameter of the internal gear for the TP and the GTF2 designs. The value obtained for the GTF1 is due to the effect of the increased speed. With a higher speed, for the same power, the torque is lower, as seen in table 24, so the GB is not that demanded. This is further appreciated when calculating the power density of each part.

With all the information gathered, the power density of the different gears can be calculated. In order to make a fast and easy comparison, an approximated calculation is going to be performed. The power density of a gear is defined as:

$$Powerdensity = \frac{Power}{Volume} \quad (6)$$

For the power, the perfect situation of 10MW is considered. For the volume, the approximation of a cylinder with the "tip diameter" value (for the planets and the sun) and the "root diameter" (for the internal gear) value from table 30, and the "facewidth" value from tables 27, 28 and 29, is performed. The results are shown below:

Power density (kW/m ³)	Turboprop	GearedTurbofan 1	GearedTurbofan 2
Sun gear	2,275,054	2,553,569	1,246,720
Planets	58,858	871,113	600,212
Internal gear	34,640	416,473	264,689

Table 31: Power density for the different gears

The value shown for the planets is for each of the planets involved in the transmission. Table 24 is again, an example of the difficulties that the P&W engineers face when designing the gearbox for the PW1000G engine due to its incredibly demanding power density. As a reminder, this family of engines uses gearboxes rated between 12,000 kW and 24,000 kW, with a gear ratio of 3:1. Or the one underdevelopment by Rolls-Royce, whose aim is to transfer more than 70,000 kW.

• Gear pairs information

With all the geometry given, it is also interesting to calculate the gear ratio for each pair of gears and confirm the defined overall ratio. Depending on the choice of arrangement for the planetary gear, and on which component is held stationary, the ratio of input rotation to output rotation is dependent upon the number of teeth in each gear in a different way. In this case, where the planet

carrier is held stationary, the sun gear is used as the input and the ring gear is the output. The gear ratio can be calculated as:

$$Gear - ratio = -\frac{N_r}{N_s} \quad (7)$$

, with N_r and N_s being the number of teeth in the ring and sun gears. If this formula is applied in the three designs, the gear ratios of 9.105, 2.514 and 2.161 will be reached for the Turboprop, GearedTurbofan1 and GearedTurbofan2. The negative sign in the gear teeth for the internal gear, represents the sense of rotation. If the sun gear rotates in a clockwise sense, it has been seen that the ring gear must rotate in the opposite way.

Continuing, the importance of the contact ratio, has been mentioned several times. The bigger the overlap, the better, as it means the system will be running smoother. In table 32 one can clearly see in the three designs, an overall contact ratio higher than two, which classifies them as HCR gears. Furthermore, also in the three designs, the overlap contact ratio is close to an integer, allowing to make profit of the consequent benefits, as mentioned.

Gear pairs information	Turboprop	Gearedfan 1	Gearedfan 2
Gear pair 1			
Gear ratio	4.053	1.321	1.706
Transverse contact ratio	1.492	1.480	1.672
Overlap ratio	1.937	1.096	1.008
Total contact ratio	3.429	2.585	2.68
Gear pair 2			
Gear ratio	-2.247	-3.321	-3.686
Transverse contact ratio	1.702	1.474	1.672
Overlap ratio	1.937	1.096	1.008
Total contact ratio	3.639	2.570	2.680

Table 32: Gear pairs information

• General influence factors

In the following table, a selection of relevant information which directly affect the life and performance of the gears.

	Sun	Planets	Internal Gear
Turboprop			
Number of load cycles	113,400	9,327.3	12,454.3
Safety factor, Bending	2.256	1.515/1.892	3.034
Safety factor, Pitting	1.667	1.765/5.401	5.365
GearedTurbofan1			
Number of load cycles	231,000	61,050	91,903.2
Safety factor, Bending	2.313	1.69/1.674	3.029
Safety factor, Pitting	1.678	1.730/2.821	2.795
GearedTurbofan2			
Number of load cycles	189,000	64,482.4	87,462.8
Safety factor, Bending	2.042	1.528/1.528	2.349
Safety factor, Pitting	2.173	2.227/3.384	3.361

Table 33: General influence factors

It is known that the calculation was performed with a minimum safety factor for both, bending and pitting of, 1.5. As a reminder, those factors help asses the safety of the design with a simple calculation:

$$Safety - Factor = \frac{Strength - of - material}{Maximum - stress - applied} \quad (8)$$

When this ratio becomes inferior to 1, this is when there is danger. From there, the higher the better. As seen, in our calculation, the minimum required is more than accomplished. There is a

slight increase in tooth root and flank safety factors thanks to the modifications applied. Although small, this improvement allows a change in gears' center distance and profile shift coefficients to achieve a more efficient meshing.

The number of load cycles for each of the different gears, is also interesting to mention. As seen, the most critical one is that of the planets of the Turboprop design. Special attention would be required to improve it.

Lastly, the service factor is included in the AGMA standards to include the combined effects of overload, reliability, life and other application related factors, and it is calculated using the type of gearbox, the expected service duty, and the type of application. Stated another way, service factors are variables that determine how capable a reducer is when it comes to accounting for unique but predictable factors such as frequent starts and stops, reversing, shock, or failure mitigation. This factor is actually the ratio of power a gear can mechanically handle, to the power required in the application it is designed for. The three designs were performed as precision enclosed gear units with an application in turbo gears. Theoretically, the higher, the better, as it provides an additional capacity to the gears and allows them to operate withing the specific conditions of the application, however, it can also be seen as how oversized the gearbox is when it comes to handling the application load. Its knowledge is essential to avoid premature wear or damage.

Service factor for gearset	Turboprop	Geared Turbofan 1	Geared Turbofan 2
Sun-Planets	3.409	4.524	4.092
Planets-Ring	4.257	4.482	4.092

Table 34: Service factors

- **Micropitting, scuffing and wear**

Thanks to the tests defined, some results about the micropitting, scuffing and wear probability were reached. As it can be seen, the scuffing and micropitting, which can be considered as serious cases of gear wear, are well taken care off, however, the risk of wear is still there and it is an issue which would involve more depth studied modifications to improve them.

Safety against micropitting	Turboprop	Geared Turbofan 1	Geared Turbofan 2
Sun-Planets	9.143	14.822	24.921
Planets-Ring	29.182	23.338	42.243

Table 35: Safety against micropitting

	Turboprop	Geared Turbofan 1	Geared Turbofan 2
Probability of wear (%)	83.053	37.345	12.637
Probability of scuffing (%)	< 5	< 5	< 5

Table 36: Safety against micropitting

- **Material**

A last point, the information regarding the surface hardness is the same for the three designs and the three gears. A more detailed list of parameters is shown below:

Surface hardness	Turboprop	Gearedfan 1	Gearedfan 2
Surface hardness(N/mm^2)	HRC 60		
Allowable bending stress number (N/mm^2)	515		
Allowable contact stress number (N/mm^2)	1,895		
Tensile strength (N/mm^2)	1,035		
Yield point (N/mm^2)	887		
Young's modulus (N/mm^2)	206,843		
Roughness average value DS, flank (μm)	0.63		
Roughness average value DS, root (μm)	2.40		
Mean roughness height, Rz, flank (μm)	5		
Mean roughness height, Rz, root (μm)	16		

Table 37: Surface hardness

7.6 3D Graphics

The following graphics help visualize the main different dimensions and the proportions. The scale used in each image is different, the idea is to be able see the detail.

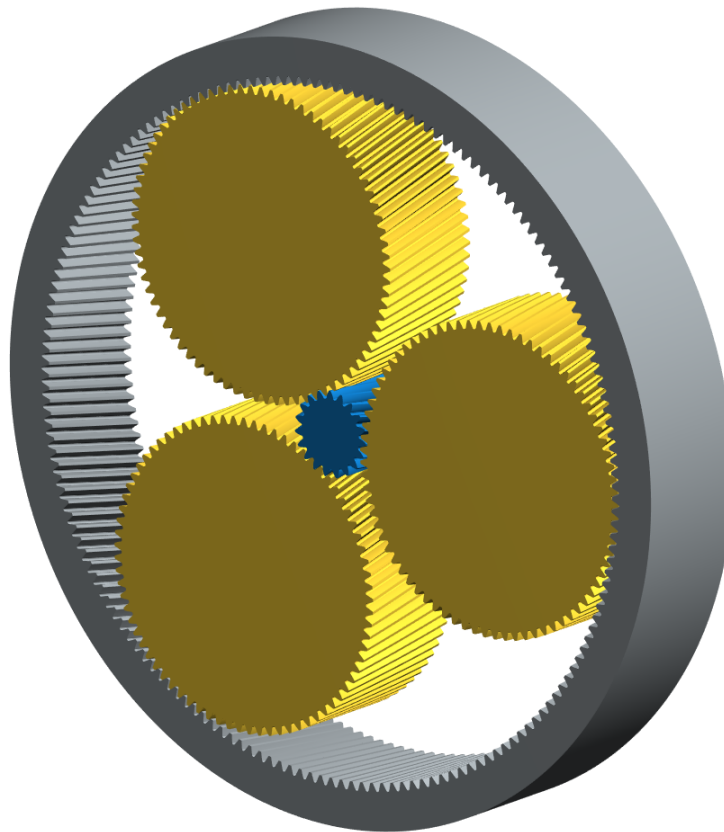


Figure 47: Turboprop's final 3D model

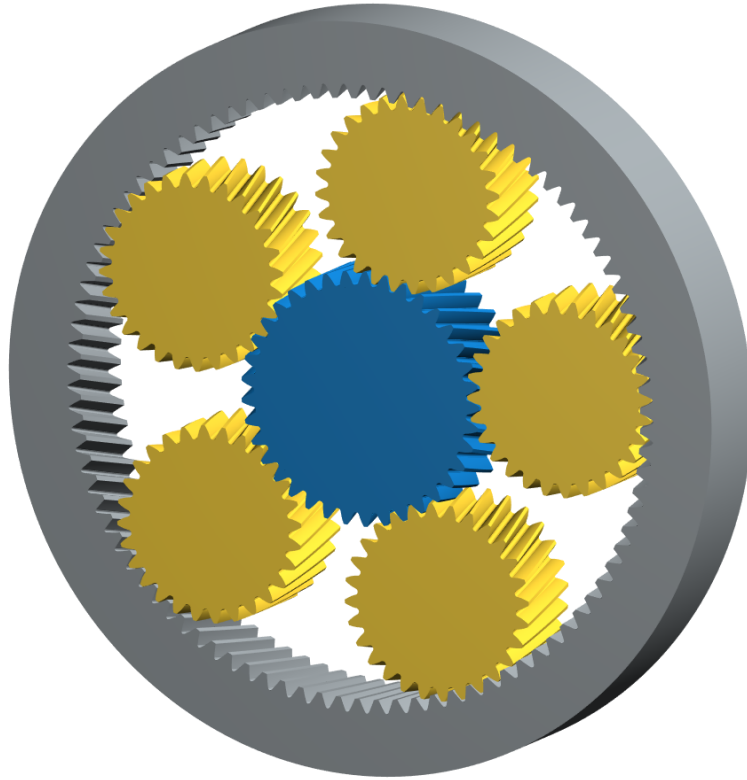


Figure 48: GTF1's final 3D model

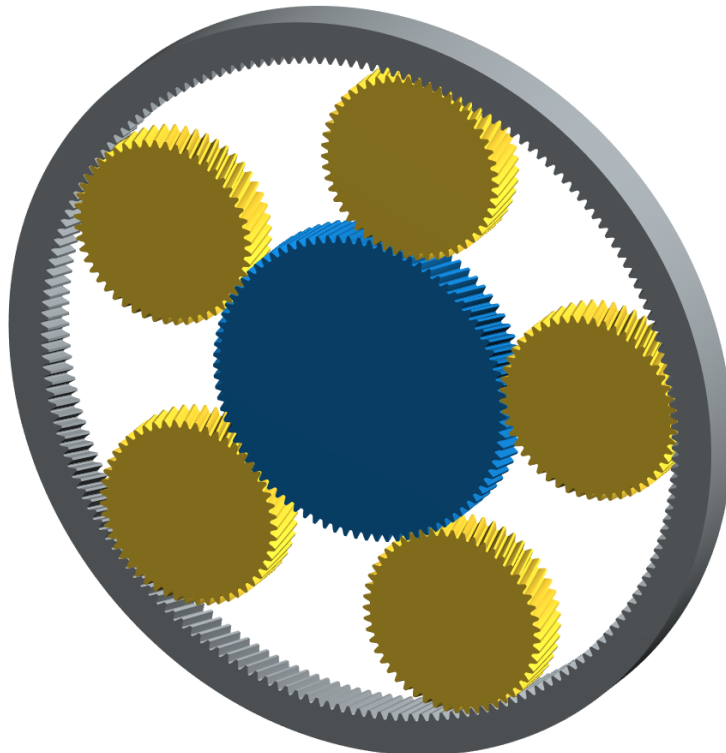


Figure 49: GTF2's final 3D model

8 Conclusion

Aviation has always been a high-tech industry, and continuous progress in the development of new technologies is vital for a sustainable growth of the industry. Nevertheless, as nearly everything in this World, economics interests are the main factors that have driven the advances, shifting the balance one way or another. It was in the 80's when fuel prices started to drop and, despite all the efforts that had been put on developing an engine such as the propfan, which would have performed in a much cleaner way than the engines of the time, it almost drop into oblivion, due to the fact that it was costlier to change all the engine's fleet that to keep working with the already implemented ones.

Nevertheless, in the last few years, the industry is experiencing a turning point, not only due to economical motivations, but also due to a set of ambitious climate action goals focused on the reduction of emissions. Meeting these goals is one of the major challenges for today's aviation sector, and an impressive number of technological solutions contributing to them have been proposed and many related projects have been initiated. Among them, one must distinguish two types. The "evolutionary" developments, those that can be fixed on a classical tube-and-wing aircraft configuration with jet fuel-powered turbofan engines, meaning the possibility of a short-term implementation in today's aircraft fleet. Within the next 15 to 20 years, all new technologies for commercial aircraft will still be evolutionary, as radically new configurations will require more time to reach technical maturity. These last ones mentioned are the "revolutionary" new aircraft configurations and propulsion systems, whose implementation would mean an important financial investment, and for which the economical framework must be very favorable. The additional benefits but also the challenges must be considered together with fuel savings when establishing a business case for radically new aircrafts.

Continuous progress is being achieved in all areas of evolutionary technologies, namely aerodynamics, materials and structures, propulsion and aircraft equipment systems. In recent, one of the most significant contributions to fuel burn reduction comes from the employment of engines with a higher by-pass-ratios, in which the use of a gearbox to make the front fan spin at its optimal speed, allowing to optimize its performance has turned out into a fierce competition to deliver tomorrow's aircraft with engines that are much lighter, quieter and more energy-efficient than the conventional turbofan engines used presently. Geared engines have flown for decades, one has only to look for a turboprop engine, but Pratt&Whitney is the first engine maker to build them in a scale capable of being fit inside a turbofan's engine, with a relatively light weight, transmitting the required power, and with a viable needed maintenance. Those design difficulties have been exposed and demonstrated in this paper, with the design and comparison of three gearboxes for turboprop and turbofan engines, using the KissSoft software.

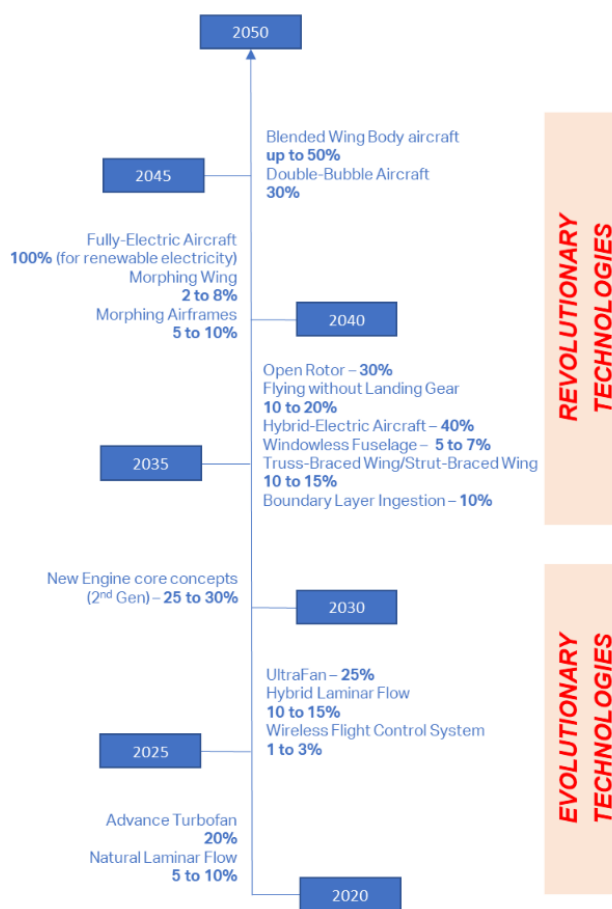


Figure 50: Timeline of expected future fuel efficiency improvements compared to predecessor aircraft or engine of the same category [62]

A Overall efficiency in jet engines

The performance of an aircraft engine is evaluated through the overall efficiency (η_0). This global efficiency is tied to both the fuel economy and aircraft range, and gives an indication of the applicability of a certain engine for a specific operating condition. It quantifies the relationship between work output and energy input, being the fraction of the fuel thermal power, which is converted into the thrust power of the aircraft. For mechanical propulsion systems like jet engines and propeller-based propulsion, it is traditionally split into two parts: thermal efficiency and propulsive efficiency. They measure the internal performance and thrust production efficiency of the engine in flight, respectively.

The thermal efficiency of the engine quantifies the ability of the engine to convert the thermal energy of the fuel, to mechanical power imparted to the engine airflow. It is an indicative of the efficiency of a non-flying engine, and is a cycle-dependent parameter which is thermodynamically restricted to the Carnot efficiency for an ideal engine, which basically indicates that the efficiency of a combustion engine cannot be greater than the temperature ratio between the temperature increase from ambient (t_a) to the maximum temperature t_{max} of the process, divided by the maximum temperature.

$$\eta_{th,carnot} = \frac{t_{max} - t_a}{t_{max}} \quad (9)$$

This is one of the reasons why turbojets have a higher thermal efficiency than propellers. As altitude increases, so does the thermal efficiency, as the temperature is lower, and the heat capacity also changes slightly with humidity and temperature, but little enough that we can consider it constant for this purpose.

The thermal efficiency of a jet engine can be defined as:

$$\eta_{th} \approx \frac{\dot{m}_a \cdot [V_j^2 - V_a^2]}{2 \cdot \dot{m}_f \cdot Q_{ci}} \quad (10)$$

In the case of turboprops, or any propeller-driven engine, the thermal efficiency is defined as the following equation, on the other hand:

$$\eta_{th,prop} = \frac{P_{shaft}}{\dot{m}_f \cdot Q_{ci}} \quad (11)$$

The thermal efficiency can be improved but that action is usually accompanied by more complexity and weight. System's complexity is linked with issues of reliability and maintenance, and the system's weight relates to extra cost and market acceptability. A successful engine is therefore not always the engine with the highest thermal efficiency but the one with the best overall system performance and cost to meet the customer's requirements in an optimum manner.

On the other hand, whereas the thermal efficiency quantifies the internal efficiency of the engine, the propulsive efficiency quantifies the efficiency of the conversion of the kinetic energy imparted to the air when it passes through the engine, into propulsive power. The propulsive efficiency is an external efficiency that depends on the actual operating point of the engine and is influenced by the amount of energy wasted in the propelling nozzle(s). It is defined as follows:

$$\eta_p \approx \frac{2}{\frac{V_j}{V_a} + 1} \quad (12)$$

This equation shows that in order for the propulsive efficiency to be high, V_j needs to be as close as possible to V_a . Nevertheless, an air-breathing jet engine cannot produce thrust if the jet velocity is not faster than the flight velocity. For practical reasons 100% propulsive efficiency is therefore not possible. However, to make it high, the fluid needs to be accelerated only by a small amount. In that situation, thrust is very small unless the mass of air moved is high.

The propulsive efficiency of a turboprop engine, on the other hand, is defined as the fraction of the mechanical power that is converted into total thrust power (the sum of propeller and engine nozzle thrust):

$$\eta_{p,prop} = \frac{F \cdot V_a}{P_{shaft}} \quad (13)$$

The following picture shows a comparison of the propulsive efficiency in the different engines mentioned in this paper. It clearly shows that turboprop engines are the most efficient at low speeds. Turbofan engines are the engine of choice for the higher subsonic to low transonic speed range, whereas the turbojet is mostly suited for (low) supersonic speeds.

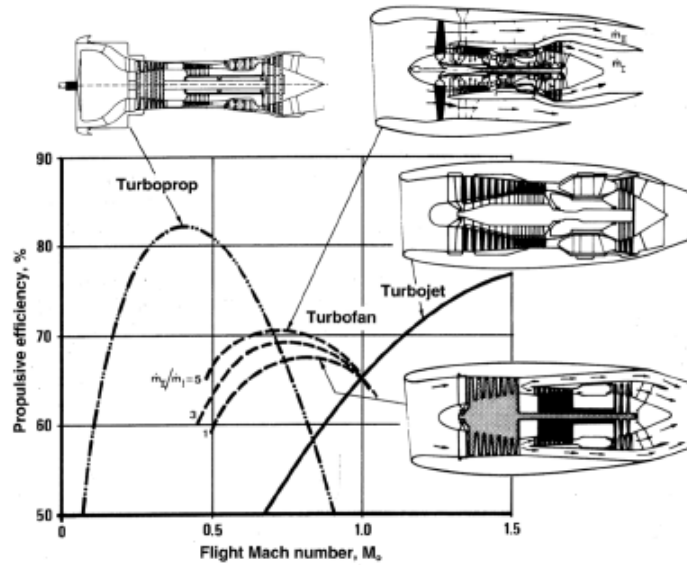


Figure 51: Propulsive Efficiency for Turboprop, Turbojet and Turbofan Engines [1]

The overall efficiency is simply the product of these two:

$$\eta_o = \eta_{th} \cdot \eta_p = \frac{F \cdot V_a}{\dot{m}_f \cdot Q_{ci}} = \frac{V_a}{TSFC \cdot Q_{ci}} \quad (14)$$

B Turbojet, Turboprop and Turbofan

B.1 State-of-the-art turbojets

A scheme of a simple turbojet engine would be:

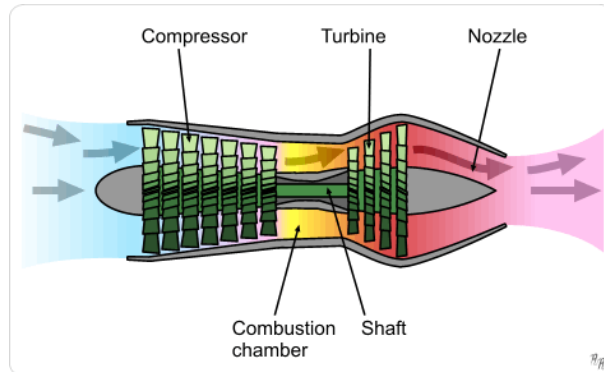


Figure 52: Scheme of a basic turbojet engine

Some example of State-of-Art turbojet with distinctive features are mentioned below.

- **SINGLE-SHAFT TURBOJET**

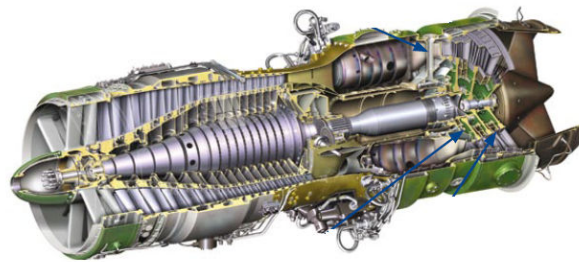


Figure 53: Rolls-Royce Avon 200

A simple turbojet configuration consists on a compressor and its driving turbine riding on a single shaft, and it was the choice for early turbojets. The Rolls-Royce Avon was the first axial flow jet engine designed and produced by Rolls-Royce. Introduced in 1950, the engine went on to become one of their most successful post-World War II engine designs. It remained in production for 24 years, and even now it is still produced with the version Avon 200 as a 21,480 shp power-source to run electricity generators and other high power requirement devices. Until the moment, it was used in a wide variety of aircraft, both military and civilian, as well as versions for stationary and maritime power [63].

- **DUAL-SHAFT TURBOJET**

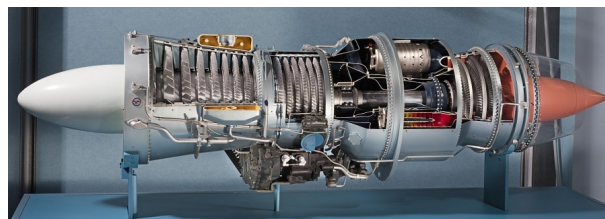


Figure 54: Pratt & Whitney JT3C (J57)

Another common turbojet configuration consists on two-shafts. A low-pressure compressor and its driving turbine ride on an inner driveshaft, while a high-pressure turbine rides on

a concentric outer driveshaft connected to a separate high-pressure turbine. In this fashion each compressor-turbine set is free to rotate at a different rotational speed appropriate to the desired performance characteristics.

The Pratt & Whitney J57²⁴ was designed to a relatively high overall pressure ratio to help improve both thrust-specific fuel consumption and specific thrust. During its development, they realised that throttling a single high pressure ratio compressor would cause stability problems as, due to the fact that the outlet area of a compressor is significantly smaller than that in its inlet, when operating at low throttle and acceleration settings, the compressor could surge (see appendix C) as the air taken at the front cannot get at the back, causing an important drop in thrust. Among the different possibilities considered to solve that problem, while General Electrics incorporated a variable geometry in the first few stages of the compressor (in their engine J79, for example), P&W opted for the two spool arrangement, allowing not only to develop an engine able to handle adequately any throttle setting, but also, by putting two compressors in series, one of which supercharges the other, they achieve a higher overall pressure ratio. This was the origin of this two-shaft engine, which since then, it has been upgraded steadily to achieve higher thrust levels [64]. Its most powerful model developed 19,600 pounds of thrust with after-burning [65].

B.2 State-of-the-art turboprops

There are two main configurations for turboprop, with one single shaft or two. A third type of configuration with three shafts can sometimes be found, but it is less common due to the mechanical complexity. Here are some examples of both.

- **Single shaft**

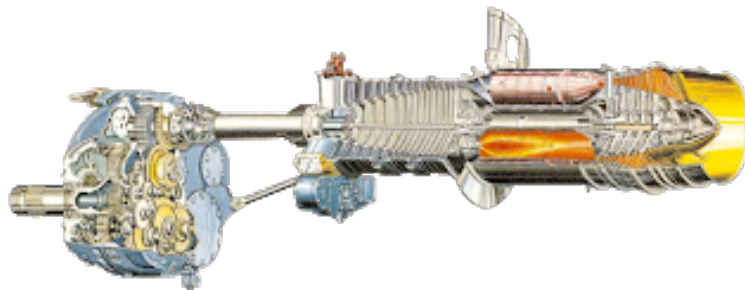


Figure 55: Rolls-Royce Allison T56

In the single shaft engine, the turbine is connected to the compressor and the propeller via a gearbox. The Allison T56 in the picture, is an american single-shaft, modular design turboprop manufactured by Rolls-Royce. It is a robust, reliable turboprop engine operating in military and civil aircraft worldwide considered the world-leading largest turboprop engine. The gearbox has two stages of gear reduction, features a propeller brake and is connected to the power section by a torquemeter assembly. Rolls-Royce demonstrated a 13% fuel savings on T56 engine enhancements, and together with the reduced fuel consumption, this enhancement package allows T56 engines to operate at significantly lower turbine temperatures, extending parts life and improving reliability by 22% [66].

- **Two shafts**

Another option is found with the two shaft configuration, where the propeller receives its power from a so called "free turbine" or "power turbine", whose connection is also via a gearbox. This configuration allows great flexibility and diversity of application, as well as

²⁴With the company designation: JT3C.

ease of hot end inspection and maintenance. The advantage of this configuration over the one shaft's is its flexibility in meeting a range of performance demands. Most of the turboprop engines work at constant speed, which demands thus for the shaft to rotate at constant speed regardless of the required output power, this limits the operating range considerably. In order to avoid compressor surge, a free turbine which can operate at lower rotational speeds than the gas generator, allows a lighter and less complex gearbox.

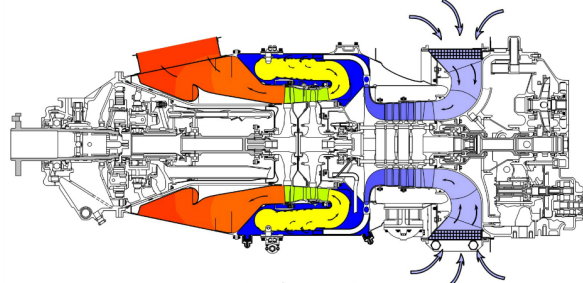


Figure 56: Pratt & Whitney Canada PT6

The Pratt & Whitney Canada's PT6 is a turboprop aircraft engine which entered service in the mid-1960's. Since then, the application of new technology, has enabled low cost development of engines approaching 1500 kW. The introduction of electronic controls, improved power-to-weight ratio, higher cycle temperature and reduced specific fuel consumption. Many variants of the PT6 have been produced, but not only as turboprops, also for helicopters, land vehicles, hovercraft, boats, as auxiliary power units and for industrial uses. However, the original configuration has been maintained throughout the engine family, which was the key for rapid development with low risk and cost.

B.3 State-of-the-art turbofans

To possible configurations of the turbofan are shown below:

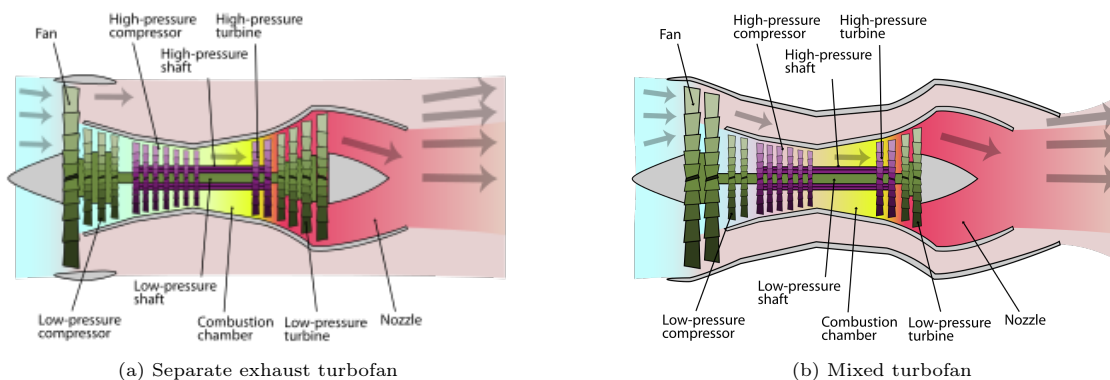


Figure 57: Two possible configurations for the Turbofan

Before getting into some distinctive features of existing turbofans, it is important to mention that, the pressure ratio experimented in the HPC is much higher than that in the LPC, and when a high overall pressure ratio²⁵ is used, such as in civil transport, the importance of the different height in the front and the back of the HPC becomes evident, which affects the efficiency. In order to try to optimize it, different solutions have been performed:

- **Three spools turbofan**

One of them is to split the high pressure section into two compressors resulting in a quite complex structure, as there are now three compressors with different rotational speeds. An example of this would be the RB211, from the Rolls-Royce Trent family of engines.

²⁵ $\Pi_o = \Pi_F \cdot \Pi_{HPC}$.

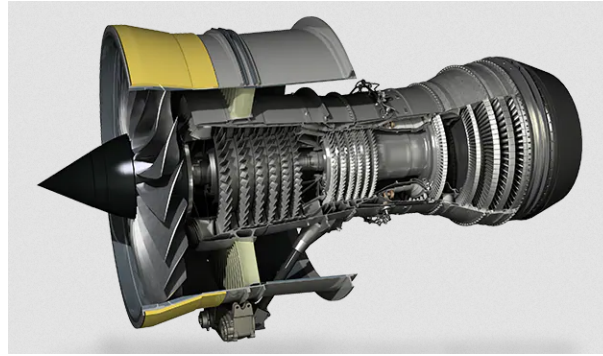


Figure 58: Rolls-Royce RB211

This engine was the first three-spool engine produced, and turned Rolls-Royce from a significant player in the aero-engine industry into a global leader. In fact, to build around the three-shaft design concept is unique to Rolls-Royce. They were introduced with the entry into service of the first of the RB211 series in the 1970s. In this type of configuration, each shaft has a compressor on its forward end and a turbine on its aft end. This design permitted each compressor to run nearer its optimum speed and efficiency, and to reduce the number of blades and other parts required in the engine. In the Boeing 757 this engine-aircraft combination has achieved record breaking fuel economy. An important feature of this engine is the use of wide-chord fan blades. These blades have no need for the span shroud or "snubbers", as mentioned in appendix E, commonly used on turbofan blades to prevent vibrations. Eliminating these flow-obstructive features, appears to have provided a 1% to 2% improvement in fan efficiency and up to a 4% reduction in thrust specific fuel consumption [4].

- **Booster configuration**

Another solution to the mentioned problem, is to keep the number of spools but making the first part of the HPC, to be attached to the fan. This part is known as the booster. This configuration, due to its simplicity compared to the other one, is used more often in engines such as the PW4000, CF6, GE90 and more.

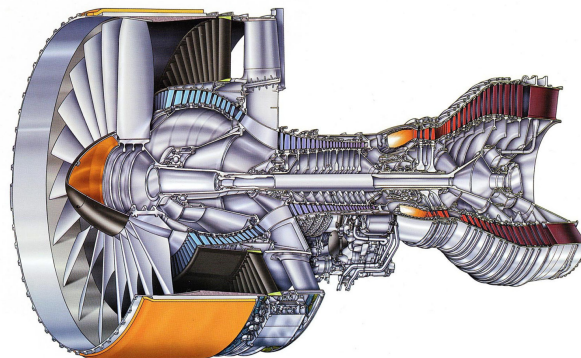


Figure 59: Pratt & Whitney PW4000

The Pratt & Whitney PW4000 is a family of high-bypass turbofan aircraft engines. The manufacturer offers dependability, low cost of ownership and low emissions for this family of engines now in service with 75 operators worldwide. The PW4000 family is approved for 180min Extended-range Twin-engine Operations (ETOPS) routes, giving aircraft equipped with PW4000 engines the ability to fly across oceans or barren terrain up to 3h from the nearest suitable airport [67]. Moreover, this engine is one of the quietest on the market.

C Compressor Surge

First of all, a differentiation between compressor stall and compressor surge needs to be done. On the one hand, a compressor stall is a local disruption of the airflow. It occurs when there is an imbalance between the air flow supply and the airflow demand. Basically, when there is a pressure ratio which is incompatible with the compressor rotational speed. In this situation, the compressor continues providing compressed air, but with reduced effectiveness. The rotational stall may be momentary, or may be steady, as the compressor finds a working equilibrium between stalled and unstalled areas. Many times it can be recovered, but some others can lead to a complete compressor stall, producing surge. On the other, a compressor surge is a complete disruption of the airflow, leading to a total loss of compression, requiring adjustments in the fuel flow to recover normal operation. This situation results in the air flowing through the compressor to slow down or even to stagnate, and sometimes even in a reversal flow, known as "backfire", with the expulsion of previously compressed air, out through the engine intake. It happens when the compressor exceeds the limit of its pressure rise capabilities or if it is highly loaded such that it does not have the capacity to absorb a momentary disturbance, creating a rotational stall which can propagate in less than a second to include the entire compressor. The compressor will recover to normal flow once the engine pressure ratio reduces to a level at which the compressor is capable of sustaining stable airflow. This situation is very dangerous, causing many vibrations and accelerating engine wear and possible serious damage.

Compressors are designed to work in a particular manner and up to a certain pressure ratio in what is called "the operating line". This line is located in the margin between the surge line and the choke line in the compressor map, as seen in figure 60. If the operating point goes beyond the surge line, the flow will break down and become unstable. On the other hand, if it goes below the choke line, the operation would become very inefficient, but not impossible. The condition of choking occurs when the compressor operates at a very high mass flow rate, and it cannot be increased, as some parts of the compressor have reached mach 1.

Various things can occur during the operation of the engine to lower the surge pressure ratio or raise the operating pressure ratio, leading to a decrease in the surge margin. The ingestion of foreign objects for example, can lead to lowering the surge line, while dirt and wear can lead to increasing compressor tip clearances and raising the operating line, all this can cause stalling or surging. In the case study, when an aircraft operates outside its design envelope or flies during critical atmospheric conditions, this can also lead to surge.

Nevertheless, the main point of this topic is to realise, based on the compressor map, that when the compressor rotational speed is reduced, when no Gearbox is used in the connection, therefore, the compressor margin is decreased, making the possibility of breakdown more liable during flight.

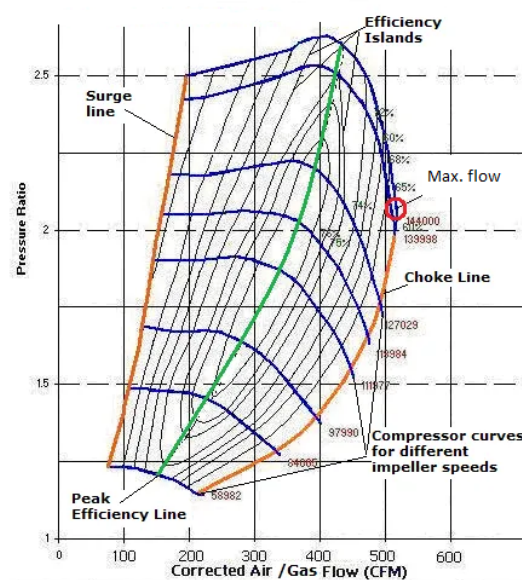
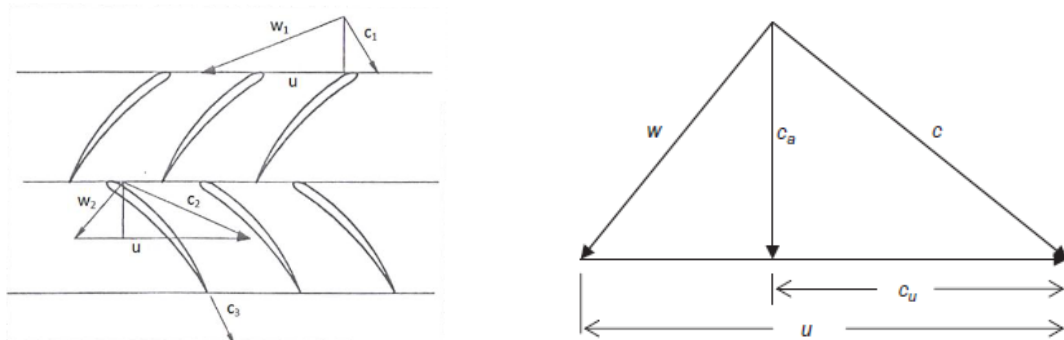


Figure 60: Compressor map

D Velocity components in turbomachines

The velocity triangle is the diagram which represents the various components of velocities of a working fluid in a turbomachine.



(a) Bidimensional scheme of the velocity triangle of a compressor [69]

(b) Relationship between components [15]

Figure 61: Velocity triangle

These components can be defined as:

- u = Blade linear speed
- c = Absolute speed
- w = Relative speed

The relationship between components is:

$$\bar{u} + \bar{w} = \bar{c} \quad (15)$$

The compressor power is defined as:

$$P_c = \dot{m}(u_2 c_{2,u} - u_1 c_{1,u}) \quad (16)$$

And the work done on the fluid per unit mass is:

$$W_c = \frac{P_c}{\dot{m}} = (u_2 c_{2,u} - u_1 c_{1,u}) \quad (17)$$

From trigonometry one can reach the following relationship:

$$W_c = \frac{1}{2} \cdot [(c_2^2 - c_1^2) + (u_2^2 - u_1^2) + (w_2^2 - w_1^2)] \quad (18)$$

Representing the first term $(c_2^2 - c_1^2)/2$, the increase in absolute velocity due to the rotor's work, which may be converted into a pressure increase.

The second term, $(u_2^2 - u_1^2)/2$ represents the centrifugal effect. In this case, the Euler equation can be applied:

$$\rho \omega^2 r = \frac{\delta p}{\delta r} \quad (19)$$

,yielding

$$p_2 - p_1 = \frac{1}{2} \rho \omega^2 (r_2^2 - r_1^2) = \frac{1}{2} \rho (u_2^2 - u_1^2) \quad (20)$$

E Evolution of fan technology

One of the main limitations of the turbofan lies in the dimensions of the fan blades. If we are considering a constant blade chord, the stiffness of the blade will reduce and its mass will increase, as it gets bigger, producing a reduction in the natural frequency²⁶, which results in problems due to vibrations. In order to solve that problem, two solutions entered the market:

- **Part-span shrouds or snubbers**

A snubber is a damper used to prevent blade flutter on narrow-chord fan blades. These blades are placed perpendicular to the main blade and interlock when the engine is rotating forming a solid ring, as one can see in figure 62a. This increases significantly the stiffness of the blades, but at the cost of reduced efficiency (up to 4% compared to wide chord blades) [1], as it impedes airflow, yielding to high fuel consumption.

- **Wide chord fan blades**

Due to the drawback of loss of efficiency with the addition of the snubbers, a new generation of wide chord fan blades was introduced. This new mechanism simultaneously increased the blade chord for mechanical stability, reducing the number of blades by approximately one third. This has been achieved at reduced weight with a hollow titanium construction and an internal core. The reduced number of blades also increases the flow area between the blades, thereby increasing the air mass through the fan. The evolution of the fan blades is appreciated in figure 62b.

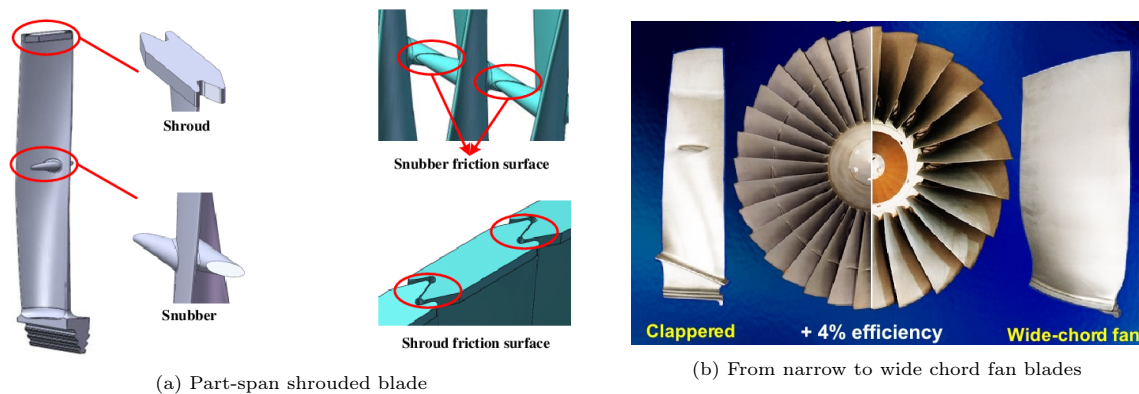


Figure 62: Fan blades

²⁶ $w_n = \sqrt{k/m}$

F NASA's technology vs GE in the propfan design

Both teams offered propellers with two rows of blades spinning in opposite directions to reduce losses due to "swirl"²⁷. Furthermore, the thin blades and sweep-back improved efficiency at transonic speeds, just as they did on an airplane wing. This particular design, allowed to reduce the diameter of the fans. Both designs would be installed on the airplane's tail, not under the wings, to allow room for the propeller disc and to keep noise out of the cabin.

The big difference between the two designs was how the propellers were driven. In order to transfer power to the propeller, NASA's team saw no problem with driving the radical new propellers via a 13-to-1 reduction gearbox, similar to the ones they'd used for years on the T56 turboprop. Nevertheless, this opinion was not shared among the GE's team, who clearly disliked gearboxes, which were known to be heavy and costly to maintain. The UDF blades were powered directly and gearlessly by a turbine, driven by hot gas from the engine. The two rows of propeller blades were each anchored to multiple rows of turbine blades.

Furthermore, the conventional turbines used are very large due to the fact that they have a lot of stages which are needed to support their functioning speed, and each rotating stage is followed by a fixed "stator," turning the flow so it hit the next turbine wheel at the right angle to convey force. This results in a huge engine, heavy and difficult to maintain. What was unique in GE's design, was that, the counter-rotating turbine stages were interlaced; the direction of spinning of each row of blades was the opposite of the direction of the stages immediately upstream and downstream of it. The design had no stators, and the relative velocity between each stage was doubled. Counter-rotation effectively doubled the turbine's rpm, so the turbine could be made smaller, simpler, and more efficient. The mechanics involved to achieve this were quite interesting. The front propeller and the front half of each stage are attached to a rotating outer casing which encloses the turbine rotor blades, while the back propeller and the back half of each stage are attached conventionally to a central shaft.

In the second half of the decade of the 80's, demonstrators for both engines were flown, revealing important results but also showing needed improvements such as the noise levels (still). However, in the end, no business came for any offering, as the fuel prices decreased again and the price of the new engines could not be justified.

²⁷Swirl:energy wasted in imparting spin to the air behind the airplane.

G Type of gears

Following, different design characteristics of gears are presented, emphasising those ones that are most used in the industry:

- **Gear shape**

A simple way of categorizing gears is by the overall shape of the gear-body. Most of the known gears are circular, meaning that the tooth are arranged around a cylindrical gear body with a circular face; nevertheless, there are non-circular available with elliptical, triangular and squared-shape faces. The difference between both of them lies on the gear ratio expressed. While the circular ones offer constancy in both rotatory speed and torque, meaning for a given input, the system provides the same output; in a non-circular gear variable speed and torque ratios are available. The latter ones allow full filling special motion requirements, such as variable rotational speed or reversing motion.

- **Gear tooth design**

Another way of classifying gears is by the design and construction options available for the teeth. On the one hand, the teeth (also called cogs), can be either cut directly in the gear blank or inserted separately. The advantage of employing gears with separated tooth components is the ability to individually replace the teeth rather than replacing the whole gear component, reducing the overall cost of gear maintenance. The arrangements of their placement, either in the inner or outer surface of the gear body, in mated pairs, largely determines the motion of the driven gear. When both gears are of the external type, both the driving and driver gear rotate or move in opposite directions. If an specific application requires for both to rotate in the same direction, an idler gear, such as that in figure 63a, is employed. Otherwise, if one of the mated pairs is an internal gear and the other one is external, both gears will rotate in the same direction, so the need of an idler gear for that purpose is eliminated. Furthermore, when space is an issue, this second type is more suited, as both gears with their components can be arranged close together.



Figure 63: Gear teeth Placement

Lastly, another way of classifying in terms of teeth configuration, is by the tooth profile. The cross-sectional shape of the teeth, affects and influences the gear's performance characteristics, including the speed ratio and friction. There are a large number of profiles, nevertheless, the most common ones are the involute, trochoid and cycloid. Throughout industry, the majority of gears produced employ the involute tooth profile both because of its ease of manufacturing and its smoothness of operation, as its design consists on fewer curves, making its manufacturing process easier. The trochoid and cycloid profiles are more rarely used. They are designed for more specialized applications such as pumps of clocks, and they offer a greater tooth durability and elimination of interference, but at a higher manufacturing cost.

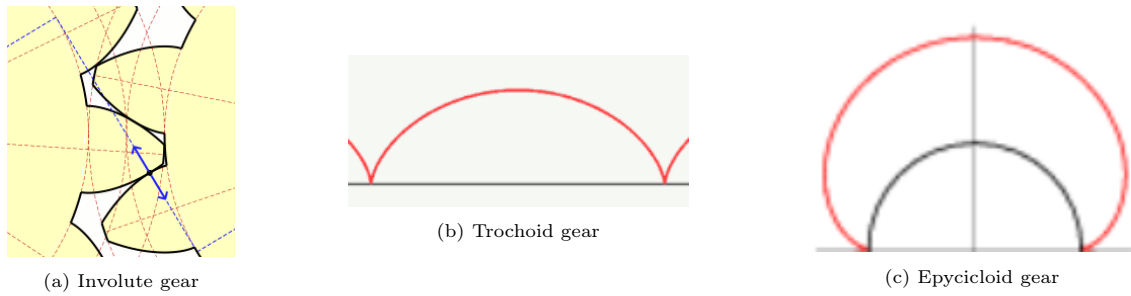


Figure 64: Gear tooth profile

• Axes configuration

As the name states, this classification refers to the orientation of the axis, which can be either parallel, intersecting or non of those. In the cases studied in this thesis, it is easier to link the gears used in them, to the parallel axis configuration. On the other hand, an example of intersecting gears would be the ones used in a turbo shaft.

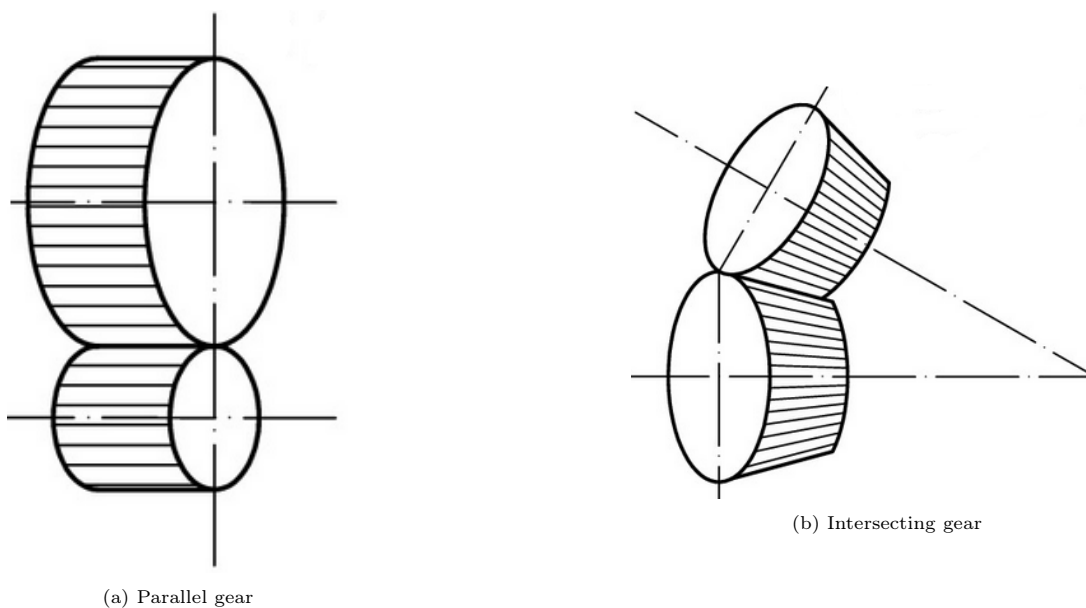


Figure 65: Classification according to the axes configuration

Based on the presented characteristics, there are different types of gears available. Some of the typical ones used in aviation are the following:

◦ Spur Gears

This is the most common type of gear employed. They are constructed with straight teeth parallel to the gear's shaft on a circular gear body, using the parallel axes configuration in mated pairs. The simplicity of the design allows for both a high degree of precision and easier manufacturing. Other characteristics of spur gears include lack of axial load, high-speed, high-load handling, and high efficiency rates. Nevertheless, there are some disadvantages to take into account such as the amount of stress experienced by the gear teeth, which limits the loading capacity, and the noise produced during high-speed applications [19].

Depending on the application, they can be mated with another spur gear or an internal gear, creating a planetary gear system, as seen in 69b. Depending on the application and other pertinent factors, a variety of speed transmission ratios may be produced, along with the desired rotational direction. For example, two differently sized spur gears can be used to change torque and rpm.



Figure 66: Spur Gear

o Helical Gears

Helical gears are similar to spur gears in construction and application, nevertheless their teeth are angled. The advantage of these characteristics, is the fact that the loading impact against the teeth is lower, as they come to contact gradually. Furthermore, more than one teeth pair are in contact at the same time, allowing some load sharing. Thanks to this, the reduction of noise and vibration is considerable. There is one fundamental requirement for any gearing: for a smooth run/torque transmission, before one pair of gear teeth leaves the mesh (leaves the contact), another pair of teeth must enter into contact.

However, "all that glitters is not gold" and there are some drawbacks that need to be mentioned. The difference in the teeth design makes the manufacturing process costlier than spurs. Furthermore, even though they can manage greater load capacities, they work less efficiently, in addition to the fact that they produce axial load which needs to be supported by thrust bearings (an implication of this issue can be found in appendix H), and sliding at the point of tooth contact, which adds friction. As the angle of the teeth increases, so does those effects.

There is another possibility for these gears, the called double helical gear. They were created to overcome the high axial thrust associated with the single ones. They consists on two opposite orientations of teeth together, usually along the middle of the gear. The axial thrust produced by the left-hand tooth is nullified by the right-hand tooth, thus eliminating the need for a thrust bearing. As in the case of single helical gears, double helical gears also provide smooth and silent operation at all speeds. They are chosen in applications with high transmission loads and rotational speeds.

The choice of helical gears for an application is interesting when the gearbox needs to run as smoothly and quietly as possible. Nevertheless, if it is needed to maximize the gearbox's torque density or working life under higher loads, spur gears are more adequate.



(a) Single Helical Gear



(b) Double Helical Gear

Figure 67: Helical Gears

o Bevel Gear

In this case, they are coned-shaped gears typically used to transmit motion and power between intersecting shafts, such as in the turbo-shaft of an helicopter. As in the case of spur gears, there

is no gradual contact between the teeth, therefore, they are submitted to high stress, affecting the durability and service life, and producing excessive noise.



Figure 68: Bevel Gear

The gears presented are the simplest way one can find them, two mated pair of gears that mesh together and transmit torque, representing a gear stage. However, the speed reduction needed in the cases studied in this thesis, would imply needing huge single-stage gearboxes. Multi-stage gearboxes or split torque gear systems, offer the advantage of dividing the desired transmission ratio into several smaller gear stages, thereby increasing the contact ratio. Each of the gears have a transmission ratio assigned, nevertheless, this assembly results in the reduction in gear speed causing an increase in available torque and hence allowing to use smaller gears. A direct advantage of this load sharing is the increase of good and longer life for the gears and its bearings. This option allows to increase power density, however, it is important to keep in mind that as the number of gear stages increases, the efficiency of the overall gearbox is reduced. In this situation, their arrangement is crucial for the appropriate performance. This is where the differences in needs among engines make the gearboxes' design different.

Lastly when thinking about gears, probably the first thing that comes to mind are the traditional fixed axis gear arrangement. In that particular case, the axis of rotation of the gears remain fixed, their mutual location does not change, as the gears only rotate around their axis. Nevertheless, there are ways to design a more efficient gear arrangement which allows more energy to be transmitted and converted into torque, rather than energy lost in heat, such as the Planetary Gear system (figure 69b), also known as Moving axis gear systems. In this case, some axis of the gears can move in relation to other axis, as their location is not fixed. In the pictures below, one can clearly differentiate both layouts. Considering just one stage, in the fixed axis configuration, both shafts are parallel but not in line, while in the Planetary Gear layout, they are coaxial. In order to have two in line shafts, at least, two-stages are needed in the fixed axis arrangement.

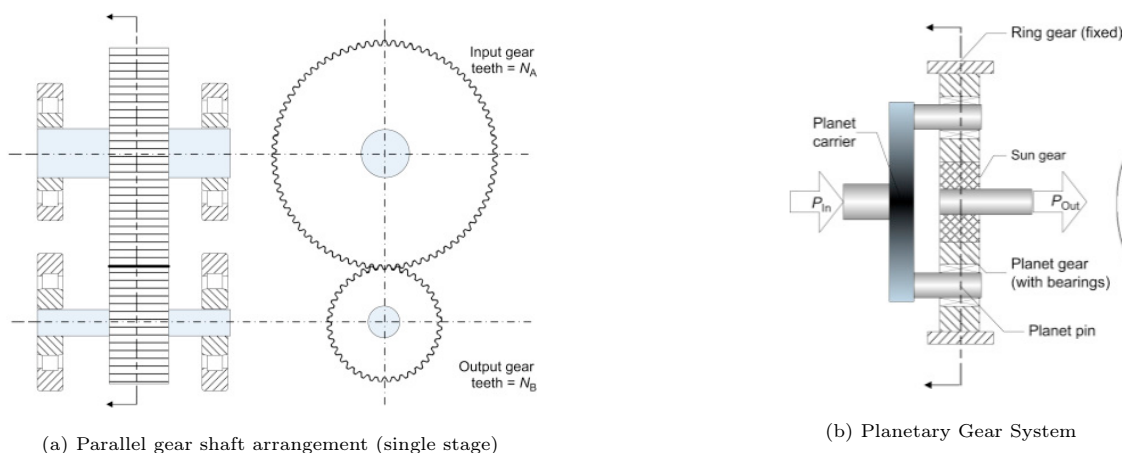


Figure 69: Gear Layout Arrangements

H Tilting moment and uneven load distribution in bearings in Helical Planetary GB

In its simplest form, the choice between spur gears or helical gear is "easy" to make. Being both of them the most common types of gears, they can often be used for the same types of applications. However, those drawbacks that come with their design are the reason of the difference. While spur gears are highly efficient and produce a lot of power, they tend to vibrate much, to be too loud, and the high impact to which the teeth are submitted, decreases their life cycle. However, it is important to mention, that due to the simple design, the manufacturing process is not expensive. Therefore, they are a right choice, when those factors are not an issue. On the other hand, the helical gears design allows the teeth to engage, to be more gradual and smoother, increasing their durability. That comes at the expense of costlier manufacturing process, and more importantly, to the existence of axial forces and sliding in the tooth contact, as one can see in figure 70.

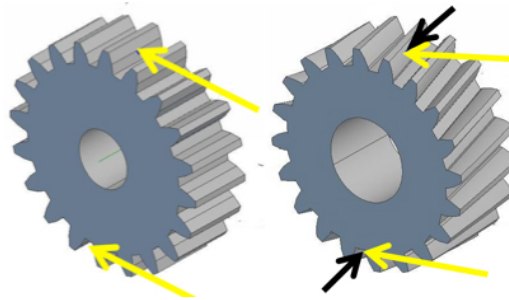


Figure 70: Forces applied in Spur gears and Helical gears

In fixed axis gearboxes, those drawbacks mentioned are just a small inconvenience for helical gears. An appropriate bearing selection, using larger size bearings or, using bearings that can carry high axial loads such as angular contact or tapered roller bearings, may be enough to get one through that problem, as the bearings in the fixed axis system have the only function of supporting the rotating gear shafts, so that is something that can be achieved.

In the case of the planetary gear system, in the usual case of the sun gear shaft being the driver, and the carrier shaft being the driven one, the forces transmitted from the planets to the carrier, are achieved through the planet's bearings. Therefore, now, these bearings have an active "transferring torque function". The high load applied (which are the reason of using planetary GB), and the limited space, which makes it not possible to use robust bearing, forces the usage of compact needle roller bearings [70], such as the one in figure 71. There is another option of using tapered roller bearing, as they can withstand axial forces better, but with the problem of being of a bigger size.



Figure 71: Needle Roller bearing

These bearings work well for high radial loads evenly distributed along the length of the needle, therefore, their application is appropriate in spur planetary GB. Nevertheless, when talking about helical gears, where axial loads appear, their use is not as well suited. As seen in figure 70, the axial forces created in the gear mesh are opposite to each other. The direction in the axial force in the sun/planet mesh is opposite of the force in the planet ring gear mesh, hence the planet is subjected to a significant tilting, the magnitude of which is axial force times gear pitch diameter

²⁸. This creates a strongly “skewed,” uneven load distribution along the needle rollers.

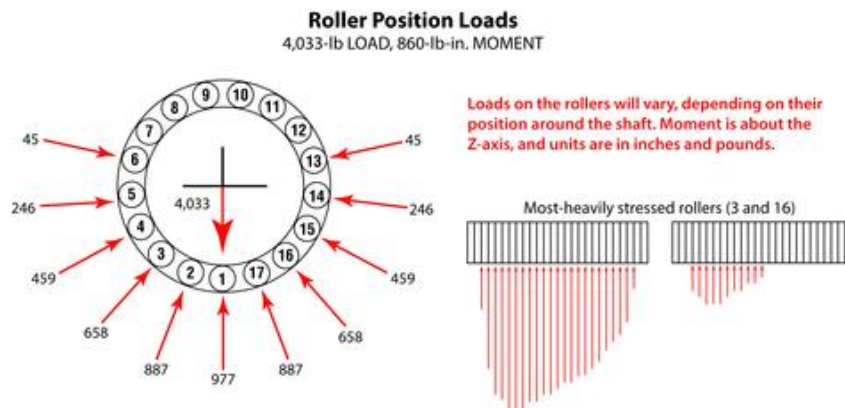


Figure 72: Load distribution [71]

The implication is that the loadability and life of the helical planetary gearbox is reduced drastically in comparison to spur planetary gearbox. In planetary gears the needle bearings are directly involved in the torque transfer and torque generation. Therefore, the needle bearing life and loadability have a strong limiting influence upon the torque rating of the planetary gearbox.

The choice of helical or spur, depends just on the application, specially, if the space is limited, and if the vibrations and noise must be decreased.

²⁸The pitch diameter of a gear (also known as the effective diameter), refers to the width of the cylinder as it intersects the midpoint of the major and minor diameters, known as the pitch line.

I Main design parameters in Gears

In the picture bellow, some of the main design parameters are represented and named:

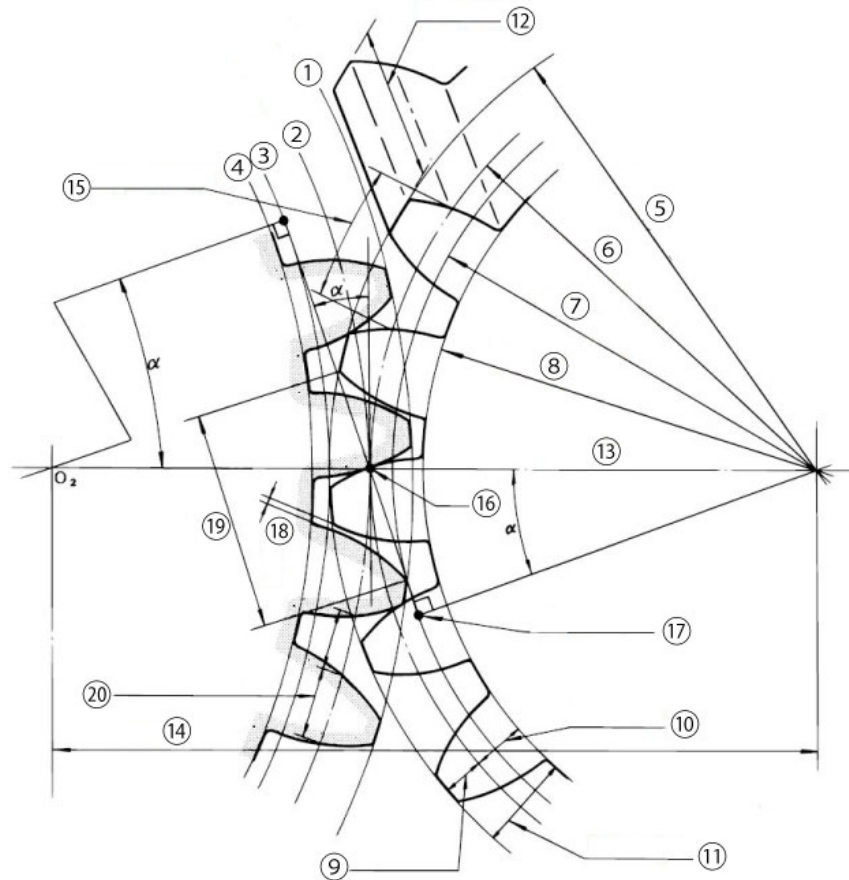


Figure 73: Design parameters for gears

1. Tip circle

The circle concentric with the reference circle and obtained by connecting the tooth tips. Its correspondent diameter can be seen in number 4.

2. Reference circle

Also known as pitch circle diameter. This diameter is the base for almost all gear calculations. The reference diameter of two meshing gears are always tangential to each other. Its correspondent diameter (d) can be seen in number 6.

3. Base circle

Circle from which the involute portion of the tooth profile is derived. The tangent lines to the involute curve and the base circle have the characteristic of being always perpendicular to each other. Its correspondent diameter d_a can be seen in number 7, and can be calculated as $d_a = d + 2 * m_n$.

4. Root circle

The circle concentric with the reference circle and obtained by connecting the bottoms of the teeth is called the root circle. Its correspondent diameter (d_f) can be seen in number 8, and can be calculated as $d_f = d - 2,5 * m_n$. It is, basically, the diameter of a circle around the bottom of the gear tooth spaces.

9. Addendum

Height of the tooth above the pitch circle.

10. Dedendum

Depth of the tooth below the pitch circle.

11. Tooth depth

Represents the height of the gear. It is calculated by the addendum circle radius minus the dedendum circle radius.

12. Facewidth

Length of the teeth in the axial direction.

13. Center line

The line connecting the center of the gears meshing.

14. Center distance

The length of gear tooth.

15. Reference pitch (p)

Distance between corresponding points on adjacent teeth. It is calculated by $p = \pi * m$.

16. Pitch point

The point of contact between two pitch circles.

17. Interference point**18. Backlash**

Amount by which the width of a tooth space exceeds the thickness of the engaging gear tooth.

19. Line of action or generating line

It is the tangent to the two base circles of the gear mesh. Another way to define it, is as the line that follows the force, which is perpendicular to the tangent at any point of the curve, irrespective of the mounting distance of the gears. Its length is limited by the succession of points of contact.

From those parameters, many others can be calculated such as:

- **Module (m)**

It is the index used to represent the tooth size. It is the ratio of the reference diameter to the number of teeth.

- **Pressure angle, α**

Describes the direction of the force created by the driving gear upon its mate. More precisely, it is the angle at a pitch point between the line of action (which is normal to the tooth surface) and the planet tangent to the pitch surface.

J Profile shifted gears

The reasons for applying profile shifts in the gears are related with improving the dynamic behaviour of the loads and therefore, improving the efficiency. Nevertheless, it is not that easy, there are limits in profile shifting, for both positive correction and negative correction.

In the case of the positive correction, whose modification can be appreciated in figure 74, the effects can be the following:

- It forms a tooth profile that has more bending strength, as the tooth thickness becomes thicker at the root.
- The contact ratio becomes smaller, as the working pressure angle becomes larger by the increase of the center distance, something that can have a direct effect on the carrying capacity of the gears.
- If too much shifting is applied, the tooth width at the tip gets smaller, and the tooth tip may become too sharpen.

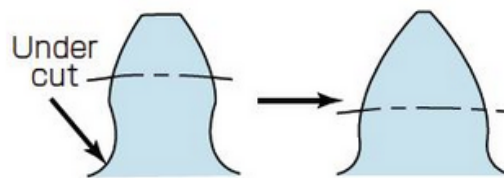


Figure 74: Effect of applying a positive shifted correction

On the other hand, when a negative correction is applied:

- It forms a tooth profile that has less bending strength, as the tooth thickness becomes thinner at the root, due to the increased root fillet radius.
- The contact ratio becomes larger, as the working pressure angle becomes smaller by the decrease of the center distance.
- Undercut may occur, which depending on the case it can have really negative effects. On the one hand, undercut is necessary in small gears, otherwise, the teeth would interfere. But sometimes, it appears just due to the fact that the generating tool sweeps out its paths, and removes some of the profile. It is important to keep in mind that, an undercut weakens the tooth and shortens the lines of contact, with its effect on loadability.

K DIN 3967-1978

The tooth thickness tolerances according to DIN 3967-1978, are shown here:

Reference diameter (mm)		Tolerance series									
over	up to	21	22	23	24	25	26	27	28	29	30
—	10	3	5	8	12	20	30	50	80	130	200
10	50	5	8	12	20	30	50	80	130	200	300
50	125	6	10	16	25	40	60	100	160	250	400
125	280	8	12	20	30	50	80	130	200	300	500
280	560	10	16	25	40	60	100	160	250	400	600
560	1 000	12	20	30	50	80	130	200	300	500	800
1000	1 600	16	25	40	60	100	160	250	400	600	1000
1600	2 500	20	30	50	80	130	200	300	500	800	1300
2500	4 000	25	40	60	100	160	250	400	600	1000	1600
4000	6 300	30	50	80	130	200	300	500	800	1300	2000
6300	10 000	40	60	100	160	250	400	600	1000	1600	2400

Figure 75: Tooth thickness tolerances according to ISO 286-2

L ISO Tolerances for Shafts according to ISO 286-2

ISO Tolerances for Shafts (ISO 286-2)																				
Nominal Shaft Sizes (mm)																				
over	3	6	10	18	30	40	50	65	80	100	120	140	160	180	200	225	250	280	315	355
inc.	6	10	18	30	40	50	65	80	100	120	140	160	180	200	225	250	280	315	355	400
micrometres																				
a12	-270 -390	-280 -430	-290 -470	-300 -510	-310 -560	-320 -570	-340 -640	-360 -660	-380 -730	-410 -760	-460 -860	-520 -920	-580 -980	-660 -1120	-740 -1200	-820 -1280	-920 -1440	-1050 -1570	-1200 -1770	-1350 -1920
d6	-30 -38	-40 -49	-50 -61	-65 -78	-80 -96	-100 -119	-120 -142					-145 -170			-170 -199			-190 -222		-210 -246
e6	-20 -28	-25 -34	-32 -43	-40 -53	-50 -66	-60 -79	-72 -94					-85 -110			-100 -129			-110 -142		-125 -161
e13	-20 -200	-25 -245	-32 -302	-40 -370	-50 -440	-60 -520	-72 -612					-85 -715			-100 -820			-110 -920		-125 -1015
f5	-10 -15	-13 -19	-16 -24	-20 -29	-25 -36	-30 -43	-36 -51					-43 -61			-50 -70			-56 -79		-62 -87
f6	-10 -18	-13 -22	-16 -27	-20 -33	-25 -41	-30 -49	-36 -58					-43 -68			-50 -79			-56 -88		-62 -98
f7	-10 -22	-13 -28	-16 -34	-20 -41	-25 -50	-30 -60	-36 -71					-43 -83			-50 -96			-56 -108		-62 -119
g5	-4 -9	-5 -11	-6 -14	-7 -16	-9 -20	-10 -23	-12 -27					-14 -32			-15 -35			-17 -40		-18 -43
g6	-4 -12	-5 -14	-6 -17	-7 -20	-9 -25	-10 -29	-12 -34					-14 -39			-15 -44			-17 -49		-18 -54
g7	-4 -16	-5 -20	-6 -24	-7 -28	-9 -34	-10 -40	-12 -47					-14 -54			-15 -61			-17 -69		-18 -75
h4	-0 -4	-0 -4	-0 -5	-0 -6	-0 -7	-0 -8	-0 -10					-0 -12			-0 -14			-0 -16		-0 -18
h5	-0 -5	-0 -6	-0 -8	-0 -9	-0 -11	-0 -13	-0 -15					-0 -18			-0 -20			-0 -23		-0 -25
h6	-0 -8	-0 -9	-0 -11	-0 -13	-0 -16	-0 -19	-0 -22					-0 -25			-0 -29			-0 -32		-0 -36
h7	-0 -12	-0 -15	-0 -18	-0 -21	-0 -25	-0 -30	-0 -35					-0 -40			-0 -46			-0 -52		-0 -57
h8	-0 -18	-0 -22	-0 -27	-0 -33	-0 -39	-0 -46	-0 -54					-0 -63			-0 -72			-0 -81		-0 -89
h9	-0 -30	-0 -36	-0 -43	-0 -52	-0 -62	-0 -74	-0 -87					-0 -100			-0 -115			-0 -130		-0 -140
h10	-0 -48	-0 -58	-0 -70	-0 -84	-0 -100	-0 -120	-0 -140					-0 -160			-0 -185			-0 -210		-0 -230
h11	-0 -75	-0 -90	-0 -110	-0 -130	-0 -160	-0 -190	-0 -220					-0 -250			-0 -290			-0 -320		-0 -360
h12	-0 -120	-0 -150	-0 -180	-0 -210	-0 -250	-0 -300	-0 -350					-0 -400			-0 -460			-0 -520		-0 -570
j5	+3 -2	+4 -2	+5 -3	+5 -4	+6 -5	+6 -7	+6 -9					+7 -11			+7 -13			+7 -16		+7 -18
j6	+6 -2	+7 -2	+8 -3	+9 -4	+11 -5	+12 -7	+13 -9					+14 -11			+16 -13			+16 -16		+18 -18
j7	+8 -4	+10 -5	+12 -6	+13 -8	+15 -10	+18 -12	+20 -15					+22 -18			+25 -21			+26 -26		+29 -28
js5	+2.5 -2.5	+3 -3	+4 -4	+4.5 -4.5	+5.5 -5.5	+6.5 -6.5	+7.5 -7.5					+9 -9			+10 -10			+11.5 -11.5		+12.5 -12.5
js6	+4 -4	+4.5 -4.5	+5.5 -5.5	+6.5 -6.5	+8 -8	+9.5 -9.5	+11 -11					+12.5 -12.5			+14.5 -14.5			+16 -16		+18 -18
js7	+6 -6	+7.5 -7.5	+9 -9	+10.5 -10.5	+12.5 -12.5	+15 -15	+17.5 -17.5					+20 -20			+23 -23			+26 -26		+28.5 -28.5
k5	+6 +1	+7 +1	+9 +1	+11 +2	+13 +2	+15 +2	+18 +3					+21 +3			+24 +4			+27 +4		+29 +4
k6	+9 +1	+10 +1	+12 +1	+15 +2	+18 +2	+21 +2	+25 +3					+28 +3			+33 +4			+36 +4		+40 +4
k7	+13 +1	+16 +1	+19 +1	+23 +2	+27 +2	+32 +2	+38 +3					+43 +3			+50 +4			+56 +4		+61 +4
m5	+9 +4	+12 +6	+15 +7	+17 +8	+20 +9	+24 +11	+28 +13					+33 +15			+37 +17			+43 +20		+46 +21
m6	+12 +4	+15 +6	+18 +7	+21 +8	+25 +9	+30 +11	+35 +13					+40 +15			+46 +17			+52 +20		+57 +21
m7	+16 +4	+21 +6	+25 +7	+29 +8	+34 +9	+41 +11	+48 +13					+55 +15			+63 +17			+72 +20		+78 +21

Figure 76: Shaft tolerances according to ISO 286-2

M Aircraft's systems interaction

Some of the main aircraft systems are:

- Flight control systems: designed to move the flight control surfaces, allowing the pilot to maintain or change attitude as required, to control an aircraft's direction in flight.
- Landing gear systems: essential system that allows the aircraft to start from the gate, taxi to the runway, take off and land safely. Aircraft landing gear supports the entire weight of an aircraft during landing and ground operations. They are attached to primary structural members of the aircraft.
- Hydraulic systems: are required for high speed flight and large aircraft to convert the crews' control system movements to surface movements. The reason of using these systems is that they are able to transmit a very high pressure or force with a small volume of fluid and in a reliable way. The hydraulic system is also used to extend and retract landing gear, operate flaps and slats, operate the wheel brakes and steering systems.
- Electrical systems: network of components that generate, transmit, distribute, utilize and store electrical energy. Depending upon the aircraft, generators or alternators are used to produce electricity. These are usually engine driven but may also be powered by an APU (auxiliary power unit), a hydraulic motor or a Ram Air Turbine (RAT)²⁹.
- Engine bleed air system: bleed air is compressed air taken from the compressor stage of a gas turbine engine upstream of its fuel-burning sections. It is used for several purposes which include cabin pressurisation, cabin heating, boundary layer control (BLC), ice protection and pressurisation of fuel tanks.
- Avionic systems: these encompass a wide range of electrical and electronic systems that include flight instruments, radios, and navigation systems.
- Environmental control systems (ECS): provide cabin pressurisation and heating while also providing cooling for electronic systems such as radar.
- Fuel system: designed to store and deliver aviation fuel to the propulsion system and to the APU if equipped. Fuel systems differ greatly due to different performance of the aircraft in which they are installed.
- Propulsion systems: these encompass engine installations and their controls. Here we can find the induction system or the ignition system among others.
- Lubrication system: used to assist the smooth and healthy operation of rotating machinery parts.

The advancement in technologies and in avionics has allowed to go a step forward in the integration and interrelation of aircraft's systems. In a real sense some of these developments are challenging the way that aircraft systems are engineered for the first time since World War II, and a key enabler in many of these developments is the advent of high power, and reliable power electronics.

It is the integration of major aircraft systems and the increased interrelationship and interdependence between them, that is driving the increasing adoption of high-speed digital data buses. The use of Commercial-of-the-Shelf (COTS) digital data buses greatly facilitate the interchange of data and control, that characterises the functional integration of these systems; on more recent aircraft these data buses also carry a significant amount of health monitoring and maintenance data. The ease with which component and subsystem performance information can be gathered and transmitted to a central or distributed computing centre has led to the emergence of prognostics and health monitoring systems that do much more than simply record failures. They now examine trends in system performance to look for degradation and incipient failures in order to schedule cost-effective maintenance operations. This is an important aspect of improvement in the

²⁹RAT: small turbine that is installed in an aircraft and used as an alternate or emergency hydraulic or electrical power source.

maintenance of aircraft systems, reducing the incidence of No Fault Found component replacement actions.

Following, different examples will be shown to understand this issue. To start with, figure 77 illustrates at a top level, the power generation (hydraulic and electrical), environmental control and fuel systems of a modern combat aircraft.

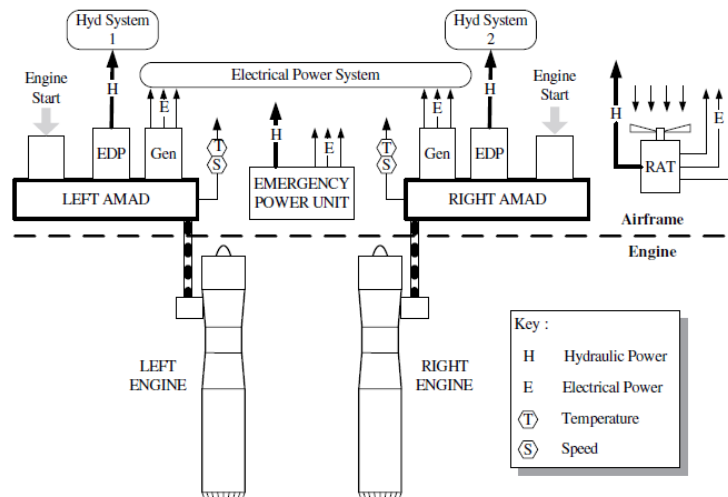


Figure 77: Typical military aircraft top-level power generation system [48]

The engines of the typical military fast jet accessory drive shafts that power Aircraft Mounted Accessory Drives (AMADs) are mounted within the airframe. In the simplest implementation, these accessory drives power Engine Driven Pumps (EDPs) to pressurise the aircraft centralised hydraulic systems. They also drive the electrical power generators that provide electrical power to the electrical distribution system. Most accessory drives will also have an air turbine motor powered by high-pressure air, which allows the AMAD and the engine to be cranked during engine start, the start process being powered by high-pressure air. Most aircrafts also possess an emergency power unit or Ram Air Turbine (RAT) to provide emergency supplies of electrical and hydraulic power. Once started, the engine provides bleed air for the aircraft systems as well as primary thrust to maintain the aircraft in flight, as seen in figure 78.

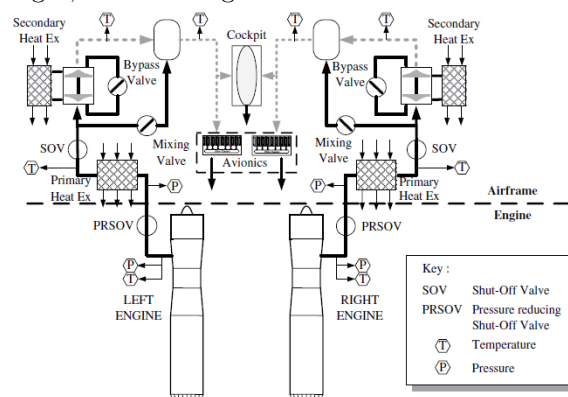


Figure 78: Typical military aircraft top-level environmental control [48]

One of the primary functions of the bleed air extracted from the engine is to provide the means by which the aircraft Environmental Control System (ECS) is driven. Bleed air taken from the engine compressor is reduced in pressure and cooled through a series of heat exchangers and an air cycle machine to provide cool air for the cockpit and the avionics cooling system. Suitably conditioned bleed air is used to pressurise the cockpit to keep the crew in a comfortable environment and may also be used to pressurise hydraulic reservoirs and aircraft fuel tanks, among other aircraft systems.

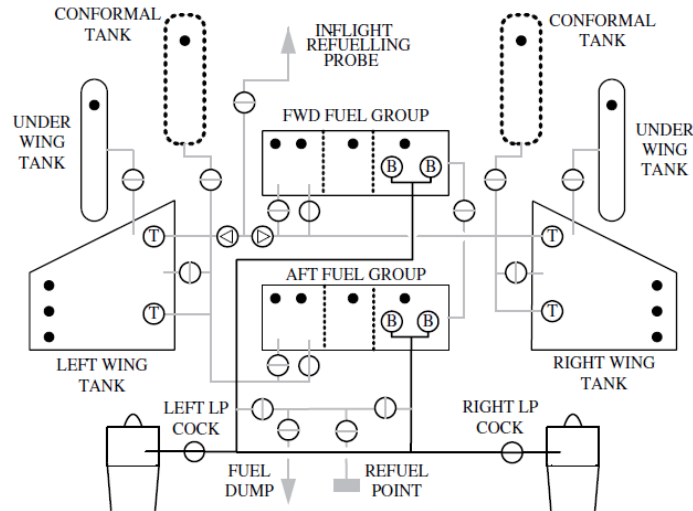


Figure 79: Typical military aircraft top-level fuel system [48]

Continuing, the aircraft fuel system as shown in figure 79, is fundamental to supply fuel to the engines to maintain thrust and powered flight. Fuel feed to the engines is pressurised by using electrically powered booster pumps to prevent fuel cavitation. This is usually an engine HP pump-related problem associated with inadequate feed pressure which manifests particularly at high altitude. Electrical power is used to operate the transfer pumps and fuel valves that enable the fuel management system to transfer fuel around the aircraft during the various phases of flight. In some cases, bleed air, again suitably conditioned, is used to pressurise the external fuel tanks, facilitating fuel transfer inboard to the fuselage tank groups.

Another situation of systems interaction can be found in how various systems operate together to reject waste heat from the aircraft. Figure 80 depicts the interaction of several major systems. The diagram illustrates how a total of eight heat exchangers across a range of systems use the aircraft fuel and ambient ram air as heat sinks into which waste heat may be dumped.

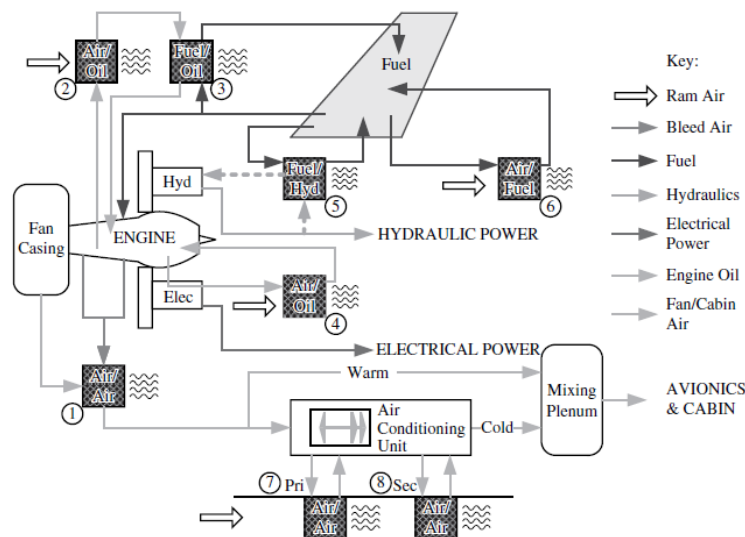


Figure 80: Typical civil systems interaction – heat exchange between systems [48]

Starting with the engine:

1. Air extracted from the engine fan casing is used to cool bleed air tapped off the intermediate or high pressure compressor (depending upon engine type).
2. Air is used to cool engine oil in a primary oil cooler heat exchanger.
3. Fuel is used to cool engine oil in a secondary oil cooler heat exchanger.
4. The electrical Integrated Drive Generator (IDG) oil is cooled by air.
5. The hydraulic return line fluid is cooled by fuel before being returned to the reservoir.
6. Aircraft fuel is cooled by an air/fuel heat exchanger.
7. Ram air is used in primary heat exchangers in the air conditioning pack to cool entry bleed air prior to entering the secondary heat exchangers.
8. Secondary heat exchangers further cool the air down to temperatures suitable for mixing with warm air prior to delivery to the cabin.

These have been just a couple of cases. As it can be seen, systems interaction is a complex matter which can determine the overall performance of the aircraft. One system failing can lead to a drastic ending. The interconnectedness of systems in the modern aircraft means that systems do not stand alone: their performance must be considered in the light of interaction with other systems, and as making a contribution to the performance of the aircraft as a whole.

In a very simple fashion, figure 81 sums up in a schematic way the power generation (hydraulic and electrical), environmental control and fuel system functional interrelation. It is not difficult to understand how complex modern aircraft systems have become to satisfy the aircraft overall performance requirements. If one system fails to perform to specification, then the aircraft as a whole will not perform correctly.

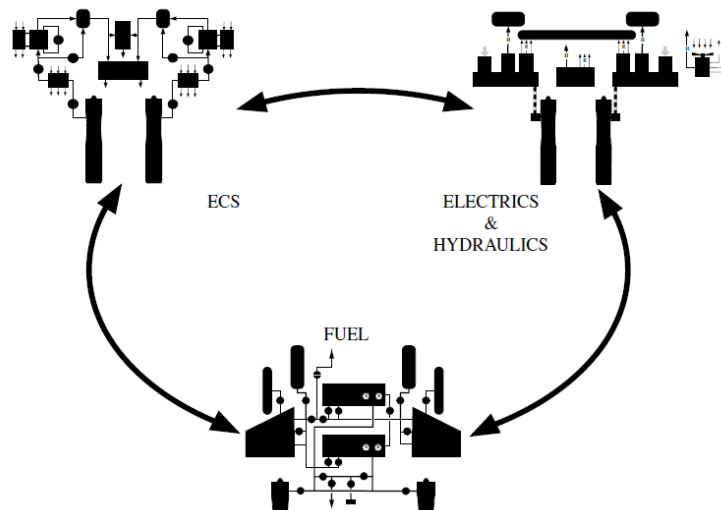


Figure 81: Typical aircraft systems interaction [48]

N Bearing chamber in jet engines

Bearings are used for supporting the shafts of the turbo fan engines and carrying the loads. Ball as well as roller bearings are used depending on the thrust/load application. The following pictures show, in a simplistic way, their location in a jet engine and in a lubrication system.

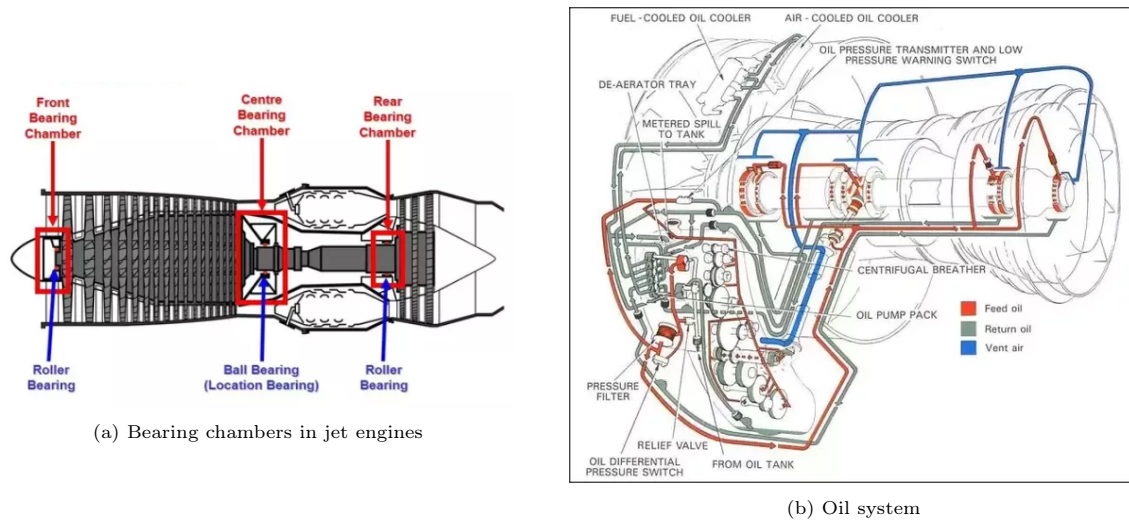


Figure 82: Bearing chambers

The importance of keeping the bearings well lubricated does not need to be highlighted and getting into this topic is out of the scope of this paper. But a little knowledge never hurts. Bearings are lubricated inside a bearing sump, which is sealed. Often labyrinth type seals are used together with air, which is also holding back the oil. Air and oil have to be separated and the air is eventually vented over board. Some oil is lost along in various paths causing oil consumption. This system needs rigorous design and maintenance for it to be optimized.

O Lubricants Characteristics

Lubricants have a wide range of properties that impact their physical and chemical properties. Knowing about these properties is important in determining which lubricant is best for which situation. Some of the most important are:

Density	Viscosity	Viscosity index, VI
Pour point	Thermal Stability	Oxidative stability
Coking propensity	Flash and fire points	Volatility
Shear stability	Lubricity	Hydrolytic stability
Elastomer compability	Acidity	Colour

1. **Viscosity:** A lubricant's "internal resistance to flow". Higher viscosity lubricants are thick and don't flow, while lower viscosity lubricants have a closer consistency to water and do flow.
2. **Viscosity Index:** The rate of change in viscosity with changes in temperature. In other words, how much viscosity changes, as temperature changes.
3. **Pour Point:** The lowest temperature at which a lubricant will flow like a liquid.
4. **Thermal Stability:** the ability of a fluid to resist breaking down under heat stress. When this happens, the molecular bonds start to break, which results in a change in the fluid's physical properties.
5. **Oxidation Stability:** Oxidation is a reaction that occurs when oxygen is combined with lubricating oil. Variables such as high temperatures, water and acids will accelerate the rate of oxidation. The life of a lubricant is reduced as temperatures increase, leading to varnish and sludge. This property is also linked to corrosion. Construction metals in the lubrication system can catalyse lubricant's oxidation, and when this happens, corrosion of metals can happen.
6. **Coking propensity:** tendency to produce carbonaceous deposits when exposed to high temperatures.
7. **Flash Point:** The temperature at which a lubricant (which is already vapor) will ignite when heated and mixed with air, but a flame is not sustained.
8. **Fire Point:** The temperature, slightly higher than the flash point, where the vapor will continue to burn for at least five seconds after the ignition source has been removed.
9. **Volatility:** the resistance of an oil to evaporation under high-temperature operating conditions. This is important for an engine lubricant because the loss of lower molecular weight components can significantly impact the viscosity. Low volatility means that less oil evaporates during operation. An oil with high volatility increases the volume of oil consumed by the engine, and the loss can change the oil's effectiveness as a lubricant.
10. **Shear stability:** property of an oil to resist the action of shear forces and the related mechanical destruction by breaking and tearing. It can be described as the resistance to changes in viscosity.
11. **Lubricity:** the measure of the reduction in friction and/or wear, by a lubricant.

12. Hydrolytic stability: the ability of a lubricant and its additives to resist chemical decomposition in the presence of water.
13. Elastomer compability: this property's main importance lies in the fact that lubricants need to be compatible with the materials that they are in contact with. In gas turbines, one of those materials are elastomers, specially the ones used in oil seals. An equilibrium is difficult to be found, because certain lubricants, particularly those formulated to give higher thermal stability, can be aggressive to certain elastomers. This is not a failing of the lubricant any more than a failing of any specific elastomer type. In fact, elastomer manufacturers have developed elastomers that are more resistant to degradation by advanced lubricant formulations.
14. Acidity: is an indicator of oil serviceability. Oil oxidation causes acidic byproducts to form. It is useful for monitoring as high acid levels can indicate excessive oil oxidation or depletion of the oil additives and can lead to corrosion of the internal components.

P Rough sizing solutions

The following picture shows the pop-up windows appearing at the end of the rough sizing simulation. A clear image of the order of magnitude for the main parameters, for the different designs, is reached. The result chosen as an input for the following step, is marked as blue:

Nr.	a [mm]	b ₁ [mm]	b ₂ [mm]	b ₃ [mm]	m _s [mm]	α _s [°]	z ₁	z ₂	z ₃	i	SF _{max}	SF _{min}	T _{1 max} [Nm]	P _{max} [kW]	η	W [kg]	T _{max} /W [Nm]
1	364.000	225.795	220.045	225.795	12.000	20.000	14	45	-109	8.786	1.909	1.532	11072.092	10435.201	0.991	1618.371	6.841
2	364.000	254.786	249.036	254.786	12.000	20.000	14	45	-109	8.786	1.917	1.502	10671.175	10023.301	0.991	1844.633	5.767
3	376.000	228.800	223.300	228.800	11.000	20.000	15	52	-120	9.000	1.676	1.502	10642.398	10030.224	0.993	1750.236	6.080
4	376.000	247.647	242.147	247.647	11.000	20.000	15	53	-120	9.000	1.590	1.497	10564.092	9956.422	0.992	1920.142	5.554
5	388.000	194.692	189.442	194.692	9.000	20.000	19	65	-152	9.000	1.342	1.504	10665.601	10052.092	0.994	1522.515	7.005
6	388.000	210.424	205.174	210.424	9.000	20.000	19	66	-152	9.000	1.332	1.502	10635.010	10023.260	0.994	1652.339	6.436
7	388.000	224.819	219.569	224.819	9.000	20.000	19	67	-152	9.000	1.282	1.498	10581.156	9972.504	0.993	1772.654	5.969
8	400.000	184.684	180.184	184.684	8.000	20.000	22	76	-176	9.000	1.161	1.502	10643.018	10030.808	0.995	1511.615	7.041
9	400.000	220.201	215.701	220.201	9.000	20.000	20	68	-160	9.000	1.506	1.497	10571.346	9963.259	0.994	1847.919	5.721
10	400.000	208.422	203.922	208.422	10.000	20.000	18	61	-144	9.000	1.586	1.499	10596.243	9966.724	0.993	1766.223	5.999

(a) Turboprop

Nr.	a [mm]	b ₁ [mm]	b ₂ [mm]	b ₃ [mm]	m _s [mm]	α _s [°]	z ₁	z ₂	z ₃	i	T _{1 max} [Nm]	P _{max} [kW]	η	W [kg]	T _{max} /W [Nm]
17	238.000	93.955	91.830	93.955	4.500	20.000	86	20	-129	2.500	8662.028	9977.940	0.987	133.558	64.856
21	241.000	90.915	88.790	90.915	4.500	20.000	86	19	-129	2.500	8669.644	9986.713	0.988	131.947	65.705
1	230.000	99.476	97.351	99.476	4.000	20.000	92	20	-138	2.500	8698.223	10019.634	0.988	129.979	66.920
10	234.000	100.607	98.482	100.607	4.500	20.000	84	19	-126	2.500	8673.031	9990.614	0.988	138.423	62.656
7	234.000	97.471	95.346	97.471	4.000	20.000	94	21	-141	2.500	8668.774	9985.711	0.989	131.269	66.038
33	245.000	89.941	87.941	89.941	4.500	20.000	88	20	-132	2.500	8674.835	9992.693	0.989	134.460	64.516
12	238.000	85.243	83.118	85.243	4.000	20.000	96	21	-144	2.500	8694.996	10015.917	0.989	118.456	73.403
15	238.000	90.129	88.004	90.129	4.500	20.000	84	19	-126	2.500	8717.709	10042.080	0.990	128.212	67.994
5	230.000	102.359	100.234	102.359	4.500	20.000	82	19	-123	2.500	8656.151	9971.171	0.990	136.717	63.315
13	238.000	95.224	93.099	95.224	4.000	20.000	96	22	-144	2.500	8643.668	9956.790	0.990	132.261	65.353
28	245.000	85.577	83.577	85.577	4.000	20.000	98	22	-147	2.500	8694.634	10015.499	0.990	125.430	69.318
24	245.000	81.971	79.971	81.971	3.500	20.000	112	25	-168	2.500	8689.089	10009.112	0.990	117.688	73.832
2	230.000	100.625	98.500	100.625	4.000	20.000	92	21	-138	2.500	8694.510	10015.126	0.990	131.466	66.133
11	234.000	100.667	98.542	100.667	4.500	20.000	84	20	-126	2.500	8673.203	9990.818	0.991	138.865	62.458
23	241.000	85.339	83.214	85.339	4.500	20.000	86	21	-129	2.500	8689.321	10009.379	0.991	124.518	69.784
22	241.000	91.558	89.433	91.558	4.500	20.000	86	20	-129	2.500	8660.633	9976.334	0.991	133.001	65.117
6	230.000	99.012	96.887	99.012	4.500	20.000	82	20	-123	2.500	8704.111	10026.416	0.991	132.739	65.573
34	245.000	90.093	88.093	90.093	4.500	20.000	88	21	-132	2.500	8674.772	9992.620	0.991	135.039	64.239
8	234.000	98.196	96.071	98.196	4.000	20.000	94	22	-141	2.500	8658.593	9973.984	0.991	132.390	65.402
18	241.000	88.143	86.018	88.143	4.000	20.000	96	22	-144	2.500	8709.929	10033.118	0.991	125.466	69.420
32	245.000	86.500	84.500	86.500	4.500	20.000	86	20	-129	2.500	9107.757	10491.383	0.992	129.909	70.109
9	234.000	95.459	93.334	95.459	4.000	20.000	94	23	-141	2.500	8697.740	10019.077	0.992	129.144	67.349
14	238.000	95.616	93.491	95.616	4.000	20.000	96	23	-144	2.500	8638.775	9951.155	0.992	133.113	64.898
16	238.000	91.175	89.050	91.175	4.500	20.000	84	20	-126	2.500	8701.902	10023.872	0.992	129.877	67.047
3	230.000	101.318	99.193	101.318	4.000	20.000	92	22	-138	2.500	8671.322	9988.646	0.992	132.564	65.413
29	245.000	85.500	84.500	85.500	4.000	20.000	98	23	-147	2.500	8685.707	10005.216	0.992	126.874	68.460
25	245.000	85.788	83.788	85.788	3.500	20.000	112	26	-168	2.500	8691.439	10011.819	0.992	123.163	70.568
4	230.000	101.931	99.806	101.931	4.000	20.000	92	23	-138	2.500	8662.838	9978.873	0.993	133.783	64.753
19	241.000	89.122	86.997	89.122	4.000	20.000	96	23	-144	2.500	8695.512	10016.510	0.993	126.988	68.475
30	245.000	87.199	85.199	87.199	4.000	20.000	98	24	-147	2.500	8671.336	9988.662	0.993	128.173	67.653
31	245.000	87.757	85.757	87.757	4.000	20.000	98	25	-147	2.500	8663.817	9980.001	0.993	129.469	66.912
20	245.000	87.437	85.437	87.437	3.500	20.000	112	27	-168	2.500	8692.813	10014.820	0.994	127.833	67.854
26	245.000	86.500	84.500	86.500	3.500	20.000	112	27	-168	2.500	8664.012	9980.225	0.994	124.354	69.672
27	245.000	87.437	85.437	87.437	3.500	20.000	112	28	-168	2.500	8668.130	9984.969	0.994	126.017	68.785

(b) GearedTurbopan 1

Nr.	a [mm]	b ₁ [mm]	b ₂ [mm]	b ₃ [mm]	m _s [mm]	α _s [°]	z ₁	z ₂	z ₃	i	T _{1 max} [Nm]	P _{max} [kW]	η	W [kg]	T _{max} /W [Nm]
24	393.000	68.926	67.301	68.926	3.500	20.000	203	19	-247	2.217	10646.667	10034.247	0.988	247.962	42.937
10	378.000	72.344	70.469	72.344	3.500	20.000	196	20	-239	2.219	10624.169	10013.044	0.990	239.836	44.298
7	378.000	71.639	69.764	71.639	3.500	20.000	194	19	-236	2.216	10626.478	10015.219	0.990	238.455	44.564
11	378.000	79.760	77.635	79.760	3.500	20.000	197	19	-238	2.208	10570.793	9962.738	0.990	265.696	39.785
32	401.000	67.063	65.500	67.063	2.750	20.000	266	24	-319	2.199	10628.748	10017.389	0.990	247.027	43.027
28	393.000	73.780	72.155	73.780	3.500	20.000	204	19	-246	2.206	10601.921	9992.075	0.990	265.616	39.914
31	393.000	75.129	73.504	75.129	3.500	20.000	205	19	-245	2.195	10598.104	9988.478	0.991	270.476	39.183
25	393.000	70.005	68.380	70.005	3.500	20.000	203	20	-247	2.217	10623.132	10012.067	0.991	251.014	42.321
14	386.000	75.290	73.665	75.290	3.500	20.000	200	19	-240	2.200	10575.178	9966.870	0.991	261.490	40.442
41	408.000	60.582	59.019	60.582	2.750	20.000	269	26	-326	2.212	10620.163	10009.268	0.991	229.575	46.260
9	378.000	77.226	75.351	77.226	3.500	20.000	195	19	-235	2.205	10623.944	10012.831	0.991	257.220	41.303
18	393.000	73.878	72.253	73.878	3.500	20.000	238	22	-287	2.206	10601.566	9991.740	0.991	263.141	40.289
29	393.000	71.149	69.524	71.149	3.500	20.000	204	20	-246	2.206	10599.380	9989.680	0.991	255.120	41.547
35	401.000	71.389	69.826	71.389	3.000	20.000	243	22	-292	2.202	10598.891	9989.220	0.991	264.806	40.025
4	395.532	69.790	67.900	69.790	3.772	20.000	190	19	-229	2.205	10607.208	9997.058	0.992	254.500	41.679
38	408.000	58.511	56.948	58.511	2.750	20.000	268	27	-327	2.220	10623.695	10012.597	0.992	221.038	48.063
15	393.000	70.625	69.000	70.625	3.000	20.000	237	23	-288	2.215	10622.638	10011.601	0.992	250.646	42.381
21	393.000	75.279	73.654	75.279	3.000	20.000	239	22	-286	2.197	10597.568	9987.972	0.992	268.134	39.523
8	378.000	73.096	71.221	73.096	3.500	20.000	194	20	-236	2.216	10622.316	10011.297	0.992	242.497	43.804
12	386.000	76.256	74.631	76.256	3.000	20.000	234	22	-281	2.201	10554.664	9947.537	0.992	261.967	40.290
26	393.000	68.120	66.495	68.120	3.500	20.000	203	21	-247	2.217	10661.358	10048.093	0.992	243.331	43.814
23	393.000	76.													

Q KissSoft results

Turboprop



KISSsoft Release 2020 A.1

KISSsoft – student license (not for commercial use)

File

Name : Turboprop

Changed by: marti on: 01.04.2021 at: 12:44:48

Calculation of a helical planetary gear stage

Drawing or article number:

Gear 1: 0.000.0
 Gear 2: 0.000.0
 Gear 3: 0.000.0

Calculation method

AGMA 2101-D04 (Metric Edition)

		----- Sun -----	Planets -----	Internal gear ---
Number of planets	[p]	1	3	1
Power (kW)	[P]	10000.000		
Transmitted power (hp)	[P]	13410.200		
Transmitted power (ft*lb/s)	[P]	7375600.0		
Speed (1/min)	[n]	9000.0		-988.4
Speed difference for planet bearing calculation (1/min)	[n2]		2220.8	
Speed planet carrier (1/min)	[nSteg]		0.0	
Torque (Nm)	[T]	10610.3	0.0	96609.8
Torque Pl.-Carrier (Nm)	[TSteg]		107220.172	
Overload factor	[Ko]		2.25	
Distribution factor	[Kv]		1.00	
Required service life (h)	[H]		70000.00	
Gear driving (+) / driven (-)		+	-/+	-
Working flank gear 1:		Right flank		
Gear 1 direction of rotation:		Clockwise		
Gear 3 direction of rotation:		counterclockwise		
Gearbox type:		Precision enclosed gear units		

Tooth geometry and material

Geometry calculation according to

ISO 21771:2007

		----- Gear 1 -----	Gear 2 -----	Gear 3 ---
Center distance (in, mm)	[a]	13.7008,348.000		
Center distance tolerance	ISO 286:2010 Measure js5			
Normal Diametral Pitch (1/in)	[Pnd]	3.62857		
Normal module (in, mm)	[mn]	0.27559, 7.0000		
Normal pressure angle (°)	[αn]	20.0000		
Helix angle at reference circle (°)	[β]	11.0000		
Number of teeth	[z]	19	77	-173
Facewidth (mm)	[b]	228.80	223.30	228.80
Hand of gear		right	left	left

Planetary axles can be placed in regular pitch.:

120 °

	[Q-AGMA2015-1-A2001]	A2	A2	A2
Accuracy grade				
Inner diameter (mm)	[di]	0.00	0.00	
External diameter (mm)	[di]			0.00
Inner diameter of gear rim (mm)	[dbi]	0.00	0.00	
Outer diameter of gear rim (mm)	[dbi]			0.00

Material

Gear 1

Steel, Grade 3, HRC58-64(AGMA), Case-carburized steel, case-hardened
AGMA 2001-C95

Gear 2

Steel, Grade 3, HRC58-64(AGMA), Case-carburized steel, case-hardened
AGMA 2001-C95

Gear 3

Steel, Grade 3, HRC58-64(AGMA), Case-carburized steel, case-hardened
AGMA 2001-C95

Surface hardness	----- Gear 1 -----		Gear 2 -----		Gear 3 ---	
	HRC 60		HRC 60		HRC 60	
	(lb/in ²), (N/mm ²)		(lb/in ²), (N/mm ²)		(lb/in ²), (N/mm ²)	
Allowable bending stress number	[sat]	74694 , 515.0	74694 , 515.0	74694 , 515.0	74694 , 515.0	
Allowable contact stress number	[sac]	274846 , 1895.0	274846 , 1895.0	274846 , 1895.0	274846 , 1895.0	1895.0
Tensile strength (N/mm ²)	[σB]	1035.00	1035.00	1035.00	1035.00	
Yield point (N/mm ²)	[σS]	887.00	887.00	887.00	887.00	
Young's modulus (N/mm ²)	[E]	206843	206843	206843	206843	
Poisson's ratio	[ν]	0.300	0.300	0.300	0.300	
Roughness average value DS, flank (μm)	[RAH]	0.63	0.63	0.63	0.63	
Roughness average value DS, root (μm)	[RAF]	2.40	2.40	2.40	2.40	
Mean roughness height, Rz, flank (μm)	[RZH]	5.00	5.00	5.00	5.00	
Mean roughness height, Rz, root (μm)	[RZF]	16.00	16.00	16.00	16.00	

Information on pre-machining

Gear reference profile

1:

Reference profile	1.25 / 0.38 / 1.0 ISO 53:1998 Profil A	
Final machining stock (mm)	[q]	0.160
Dedendum coefficient	[hfP*]	1.250
Root radius factor	[pfP*]	0.380 (pfPmax*= 0.472)
Addendum coefficient	[haP*]	1.000
Tip radius factor	[paP*]	0.000
Protuberance height coefficient	[hprP*]	0.000
Protuberance angle	[αprP]	0.000
Tip form height coefficient	[hFaP*]	0.000
Ramp angle	[αKP]	0.000
		not topping

Gear reference profile

2:

Reference profile	1.25 / 0.38 / 1.0 ISO 53:1998 Profil A	
Final machining stock (mm)	[q]	0.160
Dedendum coefficient	[hfP*]	1.250
Root radius factor	[pfP*]	0.380 (pfPmax*= 0.472)

Addendum coefficient	[haP*]	1.000
Tip radius factor	[paP*]	0.000
Protuberance height coefficient	[hprP*]	0.000
Protuberance angle	[αprP*]	0.000
Tip form height coefficient	[hFaP*]	0.000
Ramp angle	[αKP]	0.000
	not topping	

Gear reference profile

3:

Reference profile	1.25 / 0.38 / 1.0 ISO 53:1998 Profil A		
Final machining stock (mm)	[q]	0.160	
Dedendum coefficient	[hfP*]	1.250	
Root radius factor	[ρfP*]	0.380	(ρfPmax* = 0.472)
Addendum coefficient	[haP*]	1.000	
Tip radius factor	[paP*]	0.000	
Protuberance height coefficient	[hprP*]	0.000	
Protuberance angle	[αprP*]	0.000	
Tip form height coefficient	[hFaP*]	0.000	
Ramp angle	[αKP]	0.000	
	not topping		

Reference profile of the final tooth form:

Dedendum reference profile	[hfP*]	1.183	1.183	1.183
Tooth root radius Refer. profile	[ρfP*]	0.380	0.380	0.380
Addendum Reference profile	[haP*]	1.000	1.000	1.000
Protuberance height coefficient	[hprP*]	0.000	0.000	0.000
Protuberance angle (°)	[αprP*]	0.000	0.000	0.000
Tip form height coefficient	[hFaP*]	0.000	0.000	0.000
Ramp angle (°)	[αKP]	0.000	0.000	0.000

Data for final machining:

Depth of immersion	[hgrind*]	0.999	0.999	0.826
Addendum coefficient Pinion type cutter	[haP0grind*]			1.193
Radius at cutter head	[rgrind*]	0.100	0.100	0.100
Grinding only flank (0), flank & root (1)		0	0	0

Generation grinding (0), form grinding (1)	0	0	0
Type of profile modification:	for high load capacity gearboxes		
Tip relief (µm)	[Ca L/R]	6.0 / 6.0	6.0 / 6.0 5.0 / 5.0
Root relief (µm)	[Cf L/R]	6.0 / 6.0	6.0 / 6.0 5.0 / 5.0
Lubrication type	Oil injection lubrication		
Oil grade, Own Input	Mobil Jet Oil II		
Lubricant base	Synthetic oil based on Ester		
Oil nominal kinematic viscosity at 40°C (mm²/s)	[v40]	27.60	
Oil nominal kinematic viscosity at 100°C (mm²/s)	[v100]	5.10	
Specific density at 15°C (kg/dm³)	[ρ]	1.004	
Oil temperature (°C)	[TS]	70.000	

Gear pair 1

Overall transmission ratio	[itot]	-9.105
Gear ratio	[u]	4.053
Transverse module (mm)	[mt]	7.131
Transverse pressure angle (°)	[αt]	20.344
Working pressure angle (°)	[αwt]	22.745
	[αwt.e/l]	22.750 / 22.740
Working pressure angle at normal section (°)	[αwn]	22.356
Helix angle at operating pitch circle (°)	[βw]	11.179
Base helix angle (°)	[βb]	10.329
Reference center distance (mm)	[ad]	342.289
Pitch on reference circle (mm)	[pt]	22.403
Base pitch (mm)	[pbt]	21.005
Transverse pitch on contact-path (mm)	[pet]	21.005
Sum of profile shift coefficients	[Σxi]	0.8628
Transverse contact ratio	[εα]	1.492
Transverse contact ratio with allowances	[εα.e/m/l]	1.493 / 1.489 / 1.485
Overlap ratio	[εβ]	1.937
Total contact ratio	[εγ]	3.429

Total contact ratio with allowances	[$\epsilon_{y,e/m/i}$]	3.431 / 3.426 / 3.422
Length of path of contact (mm)	[$g_a, e/i$]	31.335 (31.368 / 31.186)
Length T1-A (mm)	[T1A]	14.277 (14.244 / 14.392)
Length T1-B (mm)	[T1B]	24.607 (24.607 / 24.572)
Length T1-C (mm)	[T1C]	26.629 (26.623 / 26.636)
Length T1-D (mm)	[T1D]	35.282 (35.250 / 35.397)
Length T1-E (mm)	[T1E]	45.612 (45.612 / 45.578)
Length T2-A (mm)	[T2A]	120.270 (120.270 / 120.188)
Length T2-B (mm)	[T2B]	109.940 (109.908 / 110.007)
Length T2-C (mm)	[T2C]	107.918 (107.892 / 107.944)
Length T2-D (mm)	[T2D]	99.265 (99.265 / 99.182)
Length T2-E (mm)	[T2E]	88.935 (88.903 / 89.002)
Length T1-T2 (mm)	[T1T2]	134.547 (134.515 / 134.579)
Minimal length of contact line (mm)	[Lmin]	334.880
Gear pair 2		
Overall transmission ratio	[i_{tot}]	-9.105
Gear ratio	[u]	-2.247
Transverse module (mm)	[m_t]	7.131
Transverse pressure angle (°)	[α_t]	20.344
Working pressure angle (°)	[α_{wt}]	22.745
	[$\alpha_{wt,e/i}$]	22.740 / 22.750
Working pressure angle at normal section (°)	[α_{wn}]	22.356
Helix angle at operating pitch circle (°)	[β_w]	11.179
Base helix angle (°)	[β_b]	10.329
Reference center distance (mm)	[a_d]	342.289
Pitch on reference circle (mm)	[p_t]	22.403
Base pitch (mm)	[p_{bt}]	21.005
Transverse pitch on contact-path (mm)	[p_{et}]	21.005
Sum of profile shift coefficients	[Σx_i]	-0.8628

Transverse contact ratio	[$\epsilon\alpha$]	1.702
Transverse contact ratio with allowances	[$\epsilon\alpha.e/m/l$]	1.710 / 1.703 / 1.696
Overlap ratio	[$\epsilon\beta$]	1.937
Total contact ratio	[$\epsilon\gamma$]	3.639
Total contact ratio with allowances	[$\epsilon\gamma.e/m/l$]	3.648 / 3.641 / 3.634
Length of path of contact (mm)	[$g_a, e/l$]	35.743 (35.924 / 35.628)
Length T1-A (mm)	[T1A]	84.527 (84.347 / 84.560)
Length T1-B (mm)	[T1B]	99.265 (99.265 / 99.182)
Length T1-C (mm)	[T1C]	107.918 (107.944 / 107.892)
Length T1-D (mm)	[T1D]	105.533 (105.352 / 105.565)
Length T1-E (mm)	[T1E]	120.270 (120.270 / 120.188)
Length T2-A (mm)	[T2A]	219.074 (218.926 / 219.074)
Length T2-B (mm)	[T2B]	233.812 (233.845 / 233.697)
Length T2-C (mm)	[T2C]	242.465 (242.523 / 242.407)
Length T2-D (mm)	[T2D]	240.080 (239.931 / 240.080)
Length T2-E (mm)	[T2E]	254.818 (254.850 / 254.703)
Length T1-T2 (mm)	[T1T2]	134.547 (134.579 / 134.515)
Minimal length of contact line (mm)	[Lmin]	384.048
Gear 1		
Lead height (mm)	[p_z]	2189.791
Axial pitch (mm)	[p_x]	115.252
Profile shift coefficient		
Information on pre-machining	[x]	0.5603
Information on final machining	[x]	0.4935
Tooth thickness, arc, in module	[s_n^*]	1.9300
Tip alteration (mm)	[k^*mn]	0.000
Reference diameter (mm)	[d]	135.489
Base diameter (mm)	[d_b]	127.038
Tip diameter (mm)	[d_a]	156.398

(mm)	[da.e/i]	156.398 / 156.358
Tip diameter allowances (mm)	[Ada.e/i]	0.000 / -0.040
Tip form diameter (mm)	[dFa]	156.398
(mm)	[dFa.e/i]	156.398 / 156.358
Root diameter (mm)	[df]	125.834
Generating Profile shift coefficient		
Information on pre-machining	[xE.e/i]	0.5211/ 0.5113
Information on final machining	[xE.e/i]	0.4543/ 0.4444
Generated root diameter with xE (mm)	[df.e/i]	125.284 / 125.147
(calculated with pre-machining tool)		
Root form diameter (mm)	[dFf]	130.395
(mm)	[dFf.e/i]	130.048 / 129.964
Internal toothing: Calculation dFf with pinion type cutter (z0=		
25 , x0=0.000)		
(calculated with final machining tool)		
Involute length (mm)	[l_dFa-l_dFf]	14.676
Addendum, $m_n(h_{aP}+x+k)$ (mm)	[ha]	10.454
(mm)	[ha.e/i]	10.454 / 10.434
Dedendum (mm)	[hf=mn*(hfP*-x)]	4.828
(mm)	[hf.e/i]	5.102 / 5.171
Tooth height (mm)	[h]	15.282
Virtual gear no. of teeth	[zn]	19.999
Normal tooth thickness at tip circle (mm)	[san]	3.353
(mm)	[san.e/i]	3.151 / 3.066
Normal tooth thickness at tip form circle (mm)	[sFan]	3.353
(mm)	[sFan.e/i]	3.151 / 3.066
Normal space width at root circle (mm)	[efn]	0.000
(mm)	[efn.e/i]	0.000 / 0.000

Gear 2

Lead height (mm)	[pz]	8874.416
Axial pitch (mm)	[px]	115.252
Profile shift coefficient		
Information on pre-machining	[x]	0.4361
Information on final machining	[x]	0.3693
Tooth thickness, arc, in module	[sn*]	1.8396

Tip alteration (mm)	[k*mn]	0.000
Reference diameter (mm)	[d]	549.088
Base diameter (mm)	[db]	514.838
Tip diameter (mm)	[da]	568.259
(mm)	[da.e/i]	568.259 / 568.189
Tip diameter allowances (mm)	[Ada.e/i]	0.000 / -0.070
Tip form diameter (mm)	[dFa]	568.259
(mm)	[dFa.e/i]	568.259 / 568.189
Root diameter (mm)	[df]	537.694
Generating Profile shift coefficient		
Information on pre-machining	[xE.e/i]	0.3812 / 0.3694
Information on final machining	[xE.e/i]	0.3144 / 0.3026
Generated root diameter with xE (mm)	[df.e/i]	536.925 / 536.760
(calculated with pre-machining tool)		
Root form diameter (mm)	[dFf]	541.613
(mm)	[dFf.e/i]	540.930 / 540.785
Internal toothing: Calculation dFf with pinion type cutter (z0=		
50 , x0=0.000)		
(calculated with final machining tool)		
Involute length (mm)	[l_dFa-l_dFf]	14.360
Addendum, $m_n(h_{aP^*}+x+k)$ (mm)	[ha]	9.585
(mm)	[ha.e/i]	9.585 / 9.550
Dedendum (mm)	[hf=mn*(hfP*-x)]	5.697
(mm)	[hf.e/i]	6.082 / 6.164
Tooth height (mm)	[h]	15.282
Virtual gear no. of teeth	[zn]	81.047
Normal tooth thickness at tip circle (mm)	[san]	5.274
(mm)	[san.e/i]	5.017 / 4.923
Normal tooth thickness at tip form circle (mm)	[sFan]	5.274
(mm)	[sFan.e/i]	5.017 / 4.923
Normal space width at root circle (mm)	[efn]	5.199
(mm)	[efn.e/i]	5.240 / 5.249

Gear 3

Lead height (mm)	[pz]	19938.623
Axial pitch (mm)	[px]	115.252
Profile shift coefficient		

Information on pre-machining	[x]	-1.1653
Information on final machining	[x]	-1.2321
Tooth thickness, arc, in module	[sn*]	0.6739
Tip alteration (mm)	[k*mn]	0.000
Reference diameter (mm)	[d]	1233.666
Base diameter (mm)	[db]	1156.713
Tip diameter (mm)	[da]	1236.915
(mm)	[da.e/i]	1236.915 /1236.810
Tip diameter allowances (mm)	[Ada.e/i]	0.000 / -0.105
Tip form diameter (mm)	[dFa]	1236.915
(mm)	[dFa.e/i]	1236.915 / 1236.810
Root diameter (mm)	[df]	1267.480
Generating Profile shift coefficient		
Information on pre-machining	[xE.e/i]	-1.2634/ -1.2830
Information on final machining	[xE.e/i]	-1.3302/ -1.3499
Generated root diameter with xE (mm)	[df.e/i]	1269.128 /1268.854
(calculated with pre-machining tool)		
Root form diameter (mm)	[dFf]	1263.792
(mm)	[dFf.e/i]	1265.639 /1265.389
Internal toothing: Calculation dFf with pinion type cutter (z0=		
50 , x0=0.000)		
(calculated with final machining tool)		
Involute length (mm)	[l_dFa-l_dFf]	14.526
Addendum, $m_n(h_{aP}+x+k)$ (mm)	[ha]	-1.625
(mm)	[ha.e/i]	-1.572 / -1.625
Dedendum (mm)	[hf=mn*(hfP*-x)]	16.907
(mm)	[hf.e/i]	17.594 / 17.731
Tooth height (mm)	[h]	15.282
Virtual gear no. of teeth	[zn]	182.092
Normal tooth thickness at tip circle (mm)	[san]	5.926
(mm)	[san.e/i]	5.425 / 5.285
Normal tooth thickness at tip form circle (mm)	[sFan]	5.926
(mm)	[sFan.e/i]	5.425 / 5.285
Normal space width at root circle (mm)	[efn]	3.941
(mm)	[efn.e/i]	3.853 / 3.835

Gear specific pair data Gear pair 1, Gear 1

Operating pitch diameter (mm)	[dw]	137.750
(mm)	[dw.e/i]	137.755 / 137.745
Active tip diameter (mm)	[dNa]	156.398
(mm)	[dNa.e/i]	156.398 / 156.358
Theoretical tip clearance (mm)	[c]	0.954
Effective tip clearance (mm)	[c.e/i]	1.453 / 1.326
Active root diameter (mm)	[dNf]	130.207
(mm)	[dNf.e/i]	130.258 / 130.193
Reserve (dNf-dFf)/2 (mm)	[cF.e/i]	0.147 / 0.072
Max. sliding velocity at tip (m/s)	[vga]	22.306
Specific sliding at the tip	[ζa]	0.519
Specific sliding at the root	[ζf]	-1.079
Mean specific sliding	[ζm]	0.519
Sliding factor on tip	[Kga]	0.344
Sliding factor on root	[Kgf]	-0.224
Roll angle at dFa (°)	[ξdFa.e/i]	41.143 / 41.112
Roll angle to dNa (°)	[ξdNa.e/i]	41.143 / 41.112
Roll angle to dNf (°)	[ξdNf.e/i]	12.982 / 12.849
Roll angle at dFf (°)	[ξdFf.e/i]	12.547 / 12.368
Diameter of single contact point B (mm)	[d-B]	136.237 (136.237 / 136.212)
Diameter of single contact point D (mm)	[d-D]	145.320 (145.289 / 145.432)
Addendum contact ratio	[ε]	0.904 (0.904 / 0.902)

Gear specific pair data Gear pair 1, Gear 2

Operating pitch diameter (mm)	[dw]	558.250
(mm)	[dw.e/i]	558.270 / 558.230
Active tip diameter (mm)	[dNa]	568.259
(mm)	[dNa.e/i]	568.259 / 568.189
Theoretical tip clearance (mm)	[c]	0.954
Effective tip clearance (mm)	[c.e/i]	1.345 / 1.216
Active root diameter (mm)	[dNf]	544.698
(mm)	[dNf.e/i]	544.741 / 544.677
Reserve (dNf-dFf)/2 (mm)	[cF.e/i]	1.978 / 1.873

Max. sliding velocity at tip (m/s)	[vga]	14.515
Specific sliding at the tip	[ζa]	0.519
Specific sliding at the root	[ζf]	-1.078
Mean specific sliding	[ζm]	0.519
Sliding factor on tip	[Kga]	0.224
Sliding factor on root	[Kgf]	-0.344
Roll angle at dFa (°)	[ξdFa.e/i]	26.770 / 26.751
Roll angle to dNa (°)	[ξdNa.e/i]	26.770 / 26.751
Roll angle to dNf (°)	[ξdNf.e/i]	19.810 / 19.788
Roll angle at dFf (°)	[ξdFf.e/i]	18.471 / 18.418
Diameter of single contact point B (mm)	[d-B]	559.826 (559.801 / 559.879)
Diameter of single contact point D (mm)	[d-D]	551.790 (551.790 / 551.730)
Addendum contact ratio	[ε]	0.588 (0.589 / 0.583)

Gear specific pair data Gear pair 2, Gear 2

Operating pitch diameter (mm)	[dw]	558.250
(mm)	[dw.e/i]	558.230 / 558.270
Active tip diameter (mm)	[dNa]	568.259
(mm)	[dNa.e/i]	568.259 / 568.189
Theoretical tip clearance (mm)	[c]	1.611
Effective tip clearance (mm)	[c.e/i]	2.482 / 2.285
Active root diameter (mm)	[dNf]	541.883
(mm)	[dNf.e/i]	541.903 / 541.771
Reserve (dNf-dFf)/2 (mm)	[cF.e/i]	0.559 / 0.420
Max. sliding velocity at tip (m/s)	[vga]	1.594
Specific sliding at the tip	[ζa]	0.057
Specific sliding at the root	[ζf]	-0.154
Mean specific sliding	[ζm]	0.107
Sliding factor on tip	[Kga]	0.025
Sliding factor on root	[Kgf]	-0.047
Roll angle at dFa (°)	[ξdFa.e/i]	26.770 / 26.751
Roll angle to dNa (°)	[ξdNa.e/i]	26.770 / 26.751
Roll angle to dNf (°)	[ξdNf.e/i]	18.821 / 18.774
Roll angle at dFf (°)	[ξdFf.e/i]	18.471 / 18.418

Diameter of single contact point B (mm)	[d-B]	551.790 (551.790 / 551.730)
Diameter of single contact point D (mm)	[d-D]	556.423 (556.286 / 556.447)
Addendum contact ratio	[ε]	0.588 (0.587 / 0.585)

Gear specific pair data Gear pair 2, Gear 3

Operating pitch diameter (mm)	[dw]	1254.250
(mm)	[dw.e/i]	1254.295 /1254.205
Active tip diameter (mm)	[dNa]	1236.915
(mm)	[dNa.e/i]	1236.915 /1236.810
Theoretical tip clearance (mm)	[c]	1.611
Effective tip clearance (mm)	[c.e/i]	2.090 / 1.930
Active root diameter (mm)	[dNf]	1264.007
(mm)	[dNf.e/i]	1264.033 /1263.914
Reserve (dNf-dFf)/2 (mm)	[cF.e/i]	0.862 / 0.678
Max. sliding velocity at tip (m/s)	[vga]	12.084
Specific sliding at the tip	[ζa]	0.133
Specific sliding at the root	[ζf]	-0.060
Mean specific sliding	[ζm]	0.107
Sliding factor on tip	[Kga]	0.047
Sliding factor on root	[Kgf]	-0.025
Roll angle at dFa (°)	[ξdFa.e/i]	21.688 / 21.703
Roll angle to dNa (°)	[ξdNa.e/i]	21.688 / 21.703
Roll angle to dNf (°)	[ξdNf.e/i]	25.232 / 25.247
Roll angle at dFf (°)	[ξdFf.e/i]	25.413 / 25.444
Diameter of single contact point B (mm)	[d-B]	1247.661 (1247.685 /1247.575)
Diameter of single contact point D (mm)	[d-D]	1252.413 (1252.299 /1252.413)
Addendum contact ratio	[ε]	1.114 (1.123 / 1.111)

General influence factors

----- Gear 1 ----- Gear 2 ----- Gear 3 ---

Calculated with the operating pitch circle:

Nominal circumferential force (lb)	[Wt,Ftw]	11544.09 (51350.66 N)
Nominal circumferential force (lb)	[Wt,Ftw]	11544.09 (51350.66 N)

Axial force (lb)	[Faw]	2281.38	(10148.10	N)	
Axial force (lb)	[Faw]	2281.38	(10148.10	N)	N)
Axial force, total (N)	[Fatot = p*Fa]	6844.15	(30444.31	N)	
Axial force, total (N)	[Fatot = p*Fa]	6844.15	(30444.31	N)	N)
Radial force (lb)	[Frw]	4839.64	(21527.79	N)	
Radial force (lb)	[Frw]	4839.64	(21527.79	N)	N)
Net face width of narrowest member (in)	[F,b]	8.79	(223.30	mm)	
Net face width of narrowest member (in)	[F,b]	8.79	(223.30	mm)	mm)
Circumferential force per in (lb/in)	[w]	1313.12	(229.96	N/mm)	
Circumferential force per in (lb/in)	[w]	1313.12	(229.96	N/mm)	N/mm)
Pitch line velocity (ft/min)	[vt]	12778.18	(64.91	m/s)	
Pitch line velocity (ft/min)	[vt]	12778.18	(64.91	m/s)	m/s)
Gearbox type:	Precision enclosed gear units				
Mesh alignment factor	[Cma]	0.173	0.173		
Mounting procedure:	Contact improved by adjusting at assembly				
Mesh alignment correction factor	[Ce]	0.800			
Gearing:	without longitudinal flank modification				
Lead correction factor	[Cmc]	1.000	1.000		
Pinion proportion factor	[Cpf]	0.234	0.122		
Pinion proportion modifier	[Cpm]	1.000	1.000		
Small offset	[s1/s < 0.175]				
Face load distribution factor	[Cmf]	1.373	1.261		
Load distribution factor	[Km]	1.373	1.261		
Transmission accuracy level number	[Av]	3			
Dynamic factor introduced:					
Dynamic factor	[Kv]	1.100			
Number of load cycles (in mio.)	[NL]	113400.0	9327.3	12454.3	

Tooth root load capacity

	----- Gear 1 -----	Gear 2 -----	Gear 3 --	
Rim thickness factor	[KB]	1.000	1.000	1.000
Size factor	[KS]	1.000	1.000	1.000
Limiting Variation in action (in/10000)	[LimVarAc]	6.0	5.0	
Load sharing:				
0 = No, Loaded at tip, 1 = Yes, Loaded at HPSTC		0	0	
Calc. as helical gear (0) / as LACR (1)		0	0 / 0	0

Load angle (°)	[φnL]	34.34	24.49	/24.49	21.09		
Determination of factor Y by graphical method							
Calculated with generating profile shift coefficient	[xE.m]	0.4493	0.3085		-1.3400		
Height of Lewis parabola (in)	[hF]	0.518	0.507	/0.507	0.524		
Height of Lewis parabola (mm)	[hF]	13.163	12.884	/12.884	13.320		
Tooth thickness at critical section (in)	[sF]	0.595	0.625	/0.625	0.704		
Tooth thickness at critical section (mm)	[sF]	15.119	15.870	/15.870	17.886		
Radius at curvature of fillet curve (in)	[ρF]	0.041	0.035	/0.035	0.036		
Radius at curvature of fillet curve (mm)	[ρF]	1.036	0.901	/0.901	0.909		
Helical factor	[Ch]		1.24		1.24		
Helix angle factor	[Kψ]		0.96		0.96		
Tooth form factor Y	[Y]	0.658	0.637	/0.637	0.756		
Stress correction factor	[Kf]	1.771	1.869	/1.869	1.965		
Bending strength geometry factor J	[J]	0.557	0.511	/0.586	0.661		
Bending stress number (lb/in ²)	[st]	28529.8	31095.2	/24900.022071.8			
Bending stress number (N/mm ²)	[st]	196.7	214.4	/171.7	152.2		
Stress cycle factor	[YN]	0.862	0.901		0.896		
(for general applications)							
Allowable bending stress number (lb/in ²)	[sat]	74694.4	74694.4		74694.4		
Allowable bending stress number (N/mm ²)	[sat]	515.0	515.0		515.0		
Temperature factor	[KT]	1.000	1.000		1.000		
Reliability factor (99.00 %)	[KR]		1.000				
Reverse loading factor	[-]	1.000	0.700		1.000		
Effective allow. b.s.n. (lb/in ²)	[sateff]	64374.2	47110.8	/ 47110.866955.6			
Effective allow. b.s.n. (N/mm ²)	[sateff]	443.8	324.8	/324.8	461.6		
Allowable transmitted power (hp, kW)	[Pat]	20172.6	,15042.58	13544.8	,10100.32 / 16914.8	,12613.31	27120.4 , 20223.56
Note: Allowable transmitted power Patcalculated including the following values: Ko, KR, SFmin							
Allowable transmitted power at unity service factor (hp, kW)	[Patu]	68082.4	,50768.70	45713.8	,34088.59 / 57087.6	,42569.91	91531.4 , 68254.51
Note: Allowable transmitted power Patu calculated with Ko=1, KR=1, SFmin=1							
Transmittable power including SFmin (-, kW)	[Patu/SFmin]	45388.3	,33845.80	30475.9	,22725.72 /38058.4	,28379.94	61020.9 , 45503.01
Note: Transmittable power including SFmin calculated with Ko=1, KR=1							
Unit load (lb/in ²)	[UL]		4764.76		4764.76		
Allowable unit load (lb/in ²)	[Uat]	7167.4	4812.6	/ 6009.99636.0			
Required safety factor	[SFmin]	1.500	1.500		1.500		
Safety factor, Bending	[sateff/st]	2.256	1.515	/1.892	3.034		

Yield strength factor	[Ky]	0.50		
Core hardness (HV)	[HV]	316	316	316
Core hardness (HB)	[HB]	300	300	300
Allowable yield strength number (lb/in ²)	[say]	111800.00	111800.00	111800.00
Stress correction factor	[Kf]	1.771	1.869 / 1.869 1.965	
Maximum peak tangential load (lb, N)	[Wmax]	25974.20	,115538.98	25974.20 , 115538.98
Load distribution factor (overload)	[Kmy]	1.20		
Safety for yield strength	[Syield]	4.38	4.24 / 4.86	5.77
	[Syield = say*Ky / (Wmax*Pd*Kmy/F/J/Kf)]			

Note: The calculation is performed with coefficient Kf and the core hardness in HB.
 The core hardness value in the database can differ considerably from the actual hardness.
 The value must be checked in critical cases..

Flank safety

		----- Gear 1 -----	Gear 2 -----	Gear 3 -----
		(√lb/in), (√N/mm)	(√lb/in), (√N/mm)	
Elastic coefficient	[Cp]	2290.00	,190.20	2290.00 , 190.20
Size factor	[Ks]	1.000	1.000	1.000
Load sharing ratio	[mN]		0.667	0.581
Helical overlap factor	[Cψ]		1.000	1.000
Geometry factor I	[I]		0.244	0.517
		(lb/in ²), (N/mm ²)	(lb/in ²), (N/mm ²)	
Contact stress number	[sc]	133052.4	,917.4	43482.9 , 299.8
Stress cycle factor (for general applications)	[ZN]	0.807	0.854	0.849
Surface condition factor	[Cf]	1.000	1.000 / 1.000	1.000
Hardness ratio factor	[CH]	1.000	1.000 / 1.000	1.000
Temperature factor	[KT]	1.000	1.000	1.000
Reliability factor	[KR]	99.000 {ZS.CRAGMA}		
Allowable contact stress number (lb/in ²)	[sac]	274846.4	274846.4	274846.4
Allowable contact stress number (N/mm ²)	[sac]	1895.0	1895.0	1895.0
Effective allow. c.s.n. (lb/in ²)	[saceff]	221739.2	234851.9	/234851.9 233295.4
Effective allow. c.s.n. (N/mm ²)	[saceff]	1528.8	1619.2	/1619.21608.5
Allowable transmitted power (hp)	[Pac]	16553.7	(12344.02 kW)	18569.4 (13847.14 kW)/173863.1 (129648.86 kW) 171566.1 (127935.98 kW)

Note: Allowable transmitted power Pacalculated including the following values: Ko, KR, SHmin

Allowable transmitted power at unity service factors (hp)	[Pacu]	83803.2 (62491.62 kW)	94007.8 (70101.17 kW)	880182.1 (656347.38 kW)	868553.3 (647675.88 kW)
Note: Allowable transmitted power Pacu calculated including the following values: Ko=1, KR=1, SHmin=1					
Transmittable power including SHmin (hp)	[Pacu/SHmin ²]	37245.9 (27774.05 kW)	41781.3 (31156.07 kW)	391192.0 (291709.95 kW)	386023.7 (287855.95 kW)
Note: Allowable transmitted power Pacu/SHmin ² calculated including the following values: Ko=1, KR=1					
Contact load factor (lb/in ²) (N/mm ²)	[K]	301.9	2.081		
Allowable contact load factor (lb/in ²)	[Kac]	838.4	940.5	967.1	954.4
Required safety factor	[SHmin]	1.500	1.500	1.500	1.500
Safety factor (Pitting)	[saceff/sc]	1.667	1.765	5.401	5.365
Service factors:					
Service factor for tooth root	[KSF]	5.077	3.409	4.257	6.825
Service factor for pitting	[CSF]	6.249	7.010	65.63564	7.68
Service factor for gear set	[SF]		3.409	4.257	
Note: Service factors calculated with Ky=1, Ko=1, KR=1, SFmin=1, SHmin=1					
Transmittable power including required service factors KSFmin, CSFmin (hp)		30475.90	(22725.72 kW)		
KSFmin =		1.50	CSFmin = 2.25		
Note: Service factors calculated with Ko=1, KR=1, SFmin=1, SHmin=1					
The equations used for Pat, Pac, Pacu, Patu, Pa are according AGMA2001.					

Micro pitting according to ISO/TS 6336-22:2018

Pairing Gear	1 -2 :		
Calculation of permissible specific film thickness			
Lubricant load according to FVA Info sheet 54/7		10, Mobil Jet Oil II	
Reference data FZG-C Test:			
Torque (Nm)	[T1Ref]	265.100	
Line load at contact point A (N/mm)	[FbbRef,A]	236.300	
Oil temperature (°C)	[θOilRef]	90.000	
Tooth mass temperature (°C)	[θMRef]	137.638	
Contact temperature (°C)	[θBRef,A]	309.560	
Lubrication gap thickness (µm)	[hRef,A]	0.016	
Specific film thickness in test	[λGFT]	0.031	
Material coefficient	[WW]	1.000	
Permissible specific film thickness	[λGFP]	0.043	

Interim results in accordance with	ISO/TS 6336-22:2014		
Coefficient of friction	[μ _m]	0.047	
Lubricant factor	[XL]	1.300	
Roughness factor	[XR]	0.908	
Lubrication coefficient for lubrication type	[XS]	1.200	
Tooth mass temperature (°C)	[θM]	81.375	
Tip relief factor	[XCα(A)]	1.797	
Loss factor	[HV]	0.141	
Equivalent Young's modulus (N/mm ²)	[Er]	227300.000	
Pressure-viscosity coefficient (m ² /N)	[α38]	0.01000	
Dynamic viscosity (Ns/m ²)	[ηtM]	7.316	
Roughness average value (μm)	[Ra]	0.630	
Calculation of speeds, load distribution and flank curvature according to method B following ISO/TS 6336-22:2018			
Ca taken as optimal in the calculation (0=no, 1=yes)		1	1
Calculation at point (0:A, 1:AB, 2:B, 3:C, 4:D, 5:DE, 6:E, -1:No Point)		1	
Diameter (mm)	[dy]	132.855	563.964
Relative radius of curvature (mm)	[pred]	16.906	
Load sharing factor	[XY]	0.803	
Contact stress (N/mm ²)	[pH]	654.414	
Contact stress (N/mm ²)	[pdyn]	1206.266	
Minimal specific film thickness	[λGFY]	0.397	(hY= 0.250 μm)
Safety against micropitting	[Sλ(B)]	9.143	
For interim results, refer to file:	Micropitting_12.tmp		

Pairing Gear	2 -3 :		
Calculation of permissible specific film thickness			
Material coefficient	[WW]	1.000	
Permissible specific film thickness	[λGFP]	0.043	

Interim results in accordance with	ISO/TS 6336-22:2014		
Coefficient of friction	[μ _m]	0.017	
Lubricant factor	[XL]	1.300	
Roughness factor	[XR]	0.523	
Lubrication coefficient for lubrication type	[XS]	1.200	
Tooth mass temperature (°C)	[θM]	71.163	
Tip relief factor	[XCα(A)]	2.148	
Loss factor	[HV]	0.020	
Equivalent Young's modulus (N/mm ²)	[Er]	227300.000	

Pressure-viscosity coefficient (m ² /N)	[α38]	0.01000	
Dynamic viscosity (Ns/m ²)	[ηtM]	9.551	
Roughness average value (μm)	[Ra]	0.630	
Calculation of speeds, load distribution and flank curvature according to method B following ISO/TS 6336-22:2018			
Ca taken as optimal in the calculation (0=no, 1=yes)		1	1
Calculation at point (0:A, 1:AB, 2:B, 3:C, 4:D, 5:DE, 6:E, -1:No Point)		1	
Diameter (mm)	[dy]	546.660	1242.213
Relative radius of curvature (mm)	[pred]	66.445	
Load sharing factor	[XY]	0.740	
Contact stress (N/mm ²)	[pH]	317.021	
Contact stress (N/mm ²)	[pdyn]	559.990	
Minimal specific film thickness	[λGFY]	1.267	(hY= 0.798 μm)
Safety against micropitting	[Sλ(B)]	29.182	
For interim results, refer to file:	Micropitting_23.tmp		

The calculation of micropitting specified in ISO/TS6336-22 is not designed for use with internal toothing because it has not yet been subject to sufficient investigation. The results can only be used for information purposes.

Scuffing load capacity

Results from	AGMA 925-A03, Details see in the specific calculation sheet
Probability of wear (%)	[Pwear] 83.053
Probability of scuffing (%)	[Pscuff] 5% or lower

Measurements for tooth thickness

		Gear 1	Gear 2	Gear 3
Information on pre-machining				
Tooth thickness allowance (final machining) (mm)	[As.e/i]	-0.200 /-0.250	-0.280 /-0.340	-0.500 /-0.600
Input for final machining stock, per flank (mm)	[q]	0.160	0.160	0.160
Additional measure for pre-machining (mm)	[ΔAs_pre.e/i]	0.341 /0.341	0.341 /0.341	0.341 /0.341
Tooth thickness allowance (normal section) (mm)	[As_pre.e/i]	0.141 /0.091	0.061 /0.001	-0.159 /-0.259
Number of teeth spanned	[k]	3.000	10.000	-0.000
Base tangent length with allowance (mm)	[Wk.e/i]	56.121 / 56.074	206.101 /206.045	-0.000 / -0.000
Effective diameter of ball/pin (mm)	[DMeff]	14.000	12.000	-12.000

Diametral two ball measure (mm) [MdK.e/i] 162.968 /162.877 570.603 /570.456 1234.247 /1233.990

Information on final machining

Tooth thickness tolerance		DIN 3967 ab25	DIN 3967 ab25	DIN 3967 ab25
Tooth thickness allowance (normal section) (mm)	[As.e/i]	-0.200 /-0.250	-0.280 /-0.340	-0.500 /-0.600
Number of teeth spanned	[k]	3.000	10.000	-0.000
(Internal toothing: k = (Measurement gap number)				
Base tangent length (no backlash) (mm)	[Wk]	55.989	206.044	-0.000
Base tangent length with allowance (mm)	[Wk.e/i]	55.801 /55.754	205.781 /205.725	-0.000 /-0.000
Diameter of measuring circle (mm)	[dMWk.m]	138.383	553.201	-0.000
Theoretical diameter of ball/pin (mm)	[DM]	13.929	12.073	11.646
Effective diameter of ball/pin (mm)	[DMeff]	14.000	12.000	12.000
Radial single-ball measurement backlash free (mm)	[MrK]	81.611	285.285	616.816
Radial single-ball measurement (mm)	[MrK.e/i]	81.429 /81.383	284.939 /284.865	617.585 /617.457
Diameter of measuring circle (mm)	[dMMr.m]	142.126	553.368	1251.501
Diametral measurement over two balls without clearance (mm)	[MdK]	162.713	570.454	1233.580
Diametral two ball measure (mm)	[MdK.e/i]	162.349 /162.258	569.763 /569.614	1235.118 /1234.863
Measurement over pins according to DIN 3960 (mm)	[MdR.e/i]	162.858 /162.766	569.879 /569.730	-0.000 /-0.000
Measurement over 2 pins, free, according to AGMA 2002 (mm)	[dk2f.e/i]	162.325 /162.234	569.758 /569.609	0.000 /0.000
Measurement over 2 pins, transverse, according to AGMA 2002 (mm)	[dk2t.e/i]	163.344 /163.252	569.994 /569.845	0.000 /0.000
Measurement over 3 pins, axial, according to AGMA 2002 (mm)	[dk3A.e/i]	162.858 /162.766	569.879 /569.730	-0.000 /-0.000
Measurement over 3 pins with allowance (mm)	[Md3R.e/i]	0.000 /0.000	0.000 /0.000	-0.000 /-0.000
Note: Internal gears with helical teeth cannot be measured with rollers.				
Chordal tooth thickness in reference circle (mm)	[sc]	13.489	12.876	4.717
(mm)	[sc.e/i]	13.295 /13.247	12.599 /12.539	4.217 /4.116
Reference chordal height from da.m (mm)	[ha]	10.769	9.640	-1.603
Tooth thickness, arc (mm)	[sn]	13.510	12.877	4.717
(mm)	[sn.e/i]	13.310 /13.260	12.597 /12.537	4.217 /4.117
Backlash free center distance (mm)	[aControl.e/i]	347.404 /347.267	348.956 /349.150	
Backlash free center distance, allowances (mm)	[j]ta]	-0.596 /-0.733	0.956 /1.150	
dNf.i with aControl (mm)	[dNf0.i]	129.424	543.464 / 539.983	1266.396
Reserve (dNf0.i-dFf.e)/2 (mm)	[cF0.i]	-0.312	1.267 / -0.474	-0.503

Tip clearance (mm)	[c0.i(aControl)]	0.605	0.495 / 1.341	0.792
Center distance allowances (mm)	[Aa.e/i]	0.013 /-0.013	-0.013 /0.013	
Circumferential backlash from Aa (mm)	[jtw_Aa.e/i]	0.010 /-0.010	0.010 /-0.010	
Radial backlash (mm)	[jrw]	0.746 /0.583	1.163 /0.944	
Circumferential backlash, transverse section (mm)	[jtw]	0.622 /0.487	0.984 /0.797	
Normal backlash (mm)	[jrw]	0.563 /0.443	0.892 /0.724	
Torsional angle on input with output fixed:				
Total torsional angle (°)	[j.tSys]	1.3182/1.0856		

Toothing tolerances

		----- Gear 1 -----	Gear 2 -----	Gear 3 ---
Following	AGMA 2000-A88			
Accuracy grade	[Q-AGMA2000]	15	15	15
Pitch Variation Allowable (µm)	[VpA]	2.30	3.00	3.40
Runout Radial Tolerance (µm)	[VrT]	11.00	16.00	19.00
Profile Tolerance (µm)	[VphiT]	3.80	4.80	5.40
Tooth Alignment Tolerance (µm)	[VpsiT]	13.00	13.00	13.00
Composite Tolerance, Tooth-to-Tooth (µm)	[VqT]	3.20	2.90	2.90
Composite Tolerance, Total (µm)	[VcqT]	6.50	7.70	8.70

AGMA <-> ISO: VpA <-> fpbT, VrT <-> FrT, VpsiT <-> FbT, VqT <-> fidT, VcqT <-> FidT

		A2	A2	A2
According to AGMA 2015-1-A01 & 2015-2-A06	[Q-AGMA2015]			
Accuracy grade	[Q-AGMA2015]	A2	A2	A2
Single pitch deviation (µm)	[fptT]	2.70	3.20	3.70
Total cumulative pitch deviation (µm)	[FpT]	9.50	14.00	19.00
Profile form deviation (µm)	[ffaT]	3.20	3.90	4.60
Profile slope deviation (µm)	[fHaT]	2.60	3.20	3.80
Total profile deviation (µm)	[FαT]	4.20	5.00	6.00
Helix form deviation (µm)	[ffbT]	3.80	4.00	4.30
Helix slope deviation (µm)	[fHβT]	3.80	4.00	4.30
Total helix deviation (µm)	[FβT]	5.50	5.50	6.00
Single flank composite, total (µm)	[FisT]	10.00	15.00	23.00
Single flank composite, tooth-to-tooth (µm)	[fisT]	0.90	1.40	2.10
Radial composite, total (µm)	[FidT]	9.00	13.00	17.00

Radial composite, tooth-to-tooth (µm)	[fidT]	1.70	2.40	3.20
Following	AGMA 2015-2-B15			
Radial composite, total (µm)	[FidT]	30.00	(R20) 36.00	(R20) 36.00 (R20)
Radial composite, tooth-to-tooth (µm)	[fidT]	17.00	(R20) 16.00	(R20) 14.00 (R20)

Axis alignment tolerances (recommendation acc. to ISO TR 10064-3:1996, Quality

	2		
Maximum value for deviation error of axis (µm)	[fΣβ]	3.58	3.58
Maximum value for inclination error of axes (µm)	[fΣδ]	7.15	7.15

Modifying and defining the tooth form

Profile and tooth trace modifications for gear 1

Symmetric (both flanks)

- Tip relief, linear
Caa = 6.000 µm LCa = 1.473 *mn dCa = 145.337 mm
- Root relief, linear
Caf = 6.000 µm LCf = 1.528 *mn dCf = 136.237 mm
- Helix angle modification, tapered or conical
CHb = -35.609 µm
CHβ = -35.609 µm -> Right Tooth Flank β.eff = 11.0092° -right Left Tooth Flank β.eff = 10.9909° -right
- flankline crowning
Cb = 11.644 µm
rcrown = 561972 mm

Profile and tooth trace modifications for gear 2

Symmetric (both flanks)

- Tip relief, linear
Caa = 6.000 µm LCa = 2.100 *mn dCa = 556.454 mm
- Root relief, linear
Caf = 6.000 µm LCf = 2.325 *mn dCf = 551.790 mm

Profile and tooth trace modifications for gear 3

Symmetric (both flanks)

- Tip relief, linear
Caa = 5.000 µm LCa = 2.116 *mn dCa = -1247.717 mm

- Root relief, linear

Caf = 5.000 μm LCf = 2.350 *mn dCf = -1252.413 mm

Tip relief verification

Diameter (mm)	[dcheck]	156.218	568.049	-1237.055
Tip relief left/right (μm)	[Ca L/R]	5.9 / 5.9	5.9 / 5.9	4.9 / 4.9

Data for the tooth form calculation :

Calculation of Sun gear

Tooth form, Sun gear, Step 1: Automatic (pre-machining)

haP*= 0.976, hfP*= 1.250, pFP*= 0.380

Calculation of Planets

Tooth form, Planets, Step 1: Automatic (pre-machining)

haP*= 0.992, hfP*= 1.250, pFP*= 0.380

Calculation of Internal gear

Tooth form, Internal gear, Step 1: Automatic (pre-machining)

z0= 50, x0=0.0000, da0= 375.143 mm, a0= -446.924 mm

haP0*= 1.328, paP0*= 0.380, hfP0*= 0.967, pFP0*= 0.000

Supplementary data

Singular tooth stiffness (N/mm/ μm)	[c]	15.321	15.252	
Meshing stiffness (N/mm/ μm)	[cy]	20.972	23.278	
Mass (kg)	[m]	28.020	419.907	206.468
Total mass (kg)	[mGes]	1494.209		
Moment of inertia for system, relative to the input: calculation without consideration of the exact tooth shape				
Single gears (da+df)/2...di (kg*m ²)	[J]	0.06975	16.05006	84.72231
System (da+df)/2...di (kg*m ²)	[J]	4.02339		

Torsional stiffness at driving gear with fixed driven gear:

Torsional stiffness (MNm/rad)	[cr]	45.720	
Torsion when subjected to nominal torque (°)	[δcr]	0.013	
Mean coefficient of friction (as defined in Niemann)	[μ _m]	0.048	0.022
Wear sliding coef. by Niemann	[ζ _w]	0.774	0.182
Loss factor	[HV]	0.141	0.020
Meshing power (kW)		10000.000	10000.000
Gear power loss (kW)	[PVZ]	22.377	1.468
Total power loss (kW)		71.536	
Total efficiency		0.993	
Sound pressure level according to Masuda, without contact analysis	[dB(A)]	121.4	119.3

Service life, damage

Required safety for tooth root	[SFmin]	1.50
Required safety for tooth flank	[SHmin]	1.50

Service life (calculated with required safeties):

System service life (h)	[Hatt]	122690
Tooth root service life (h)	[HFatt]	1e+06 1.227e+05 1e+06
Tooth flank service life (h)	[HHatt]	1e+06 1e+06 1e+06

Note: The entry 1e+006 h means that the Service life > 1,000,000 h.

Damage calculated on the basis of the required service life (70000.0 h)

F1%	F2%	F3%	H1%	H2%	H3%
0.00	57.0542	0.0000	1.0273	0.0845	0.0000

Damage calculated on basis of system service life [Hatt] (122690.3 h)

F1%	F2%	F3%	H1%	H2%	H3%
0.00	100.0000	0.0000	1.8006	0.1481	0.0000

Remarks:

- Symbols used in []: [xx,yy] xx as used in AGMA 2001-D04, yy as used in AGMA 2101-D04
- Specifications with [e/i] imply: Maximum [e] and minimum value [i] for
Taking all tolerances into account
Specifications with [m] imply: Mean value within tolerance
- For the backlash tolerance, the center distance tolerances and the tooth thickness allowance are taken into account.
The maximum and minimum clearance according to
the largest or smallest allowances are defined.
The calculation is performed for the operating pitch circle.
 $s_{ateff} = sat \cdot KL / KT / KR \cdot K_{wb} / SF$ (SF = 1.0)
LACR = Spur gear or helical gear with $\epsilon\beta$ (mF) < 1.0
PSTC = Point of Single Tooth Contact
- Cycle factors YN, ZN are expanded over 10^{10} (following the method used by AGMA programm)

End of Report

lines: 923

GearedTurbofan 1



KISSsoft Release 2020 A.1

KISSsoft – student license (not for commercial use)

File

Name : GearedTurbofan 1

Changed by: marti on: 01.04.2021 at: 12:46:47

Calculation of a helical planetary gear stage

Drawing or article number:

Gear 1: 0.000.0
 Gear 2: 0.000.0
 Gear 3: 0.000.0

Calculation method AGMA 2101-D04 (Metric Edition)

		----- Sun -----	Planets -----	Internal gear ---
Number of planets	[p]	1	5	1
Power (kW)	[P]	10000.000		
Transmitted power (hp)	[P]	13410.200		
Transmitted power (ft*lb/s)	[P]	7375600.0		
Speed (1/min)	[n]	11000.0		-4376.3
Speed difference for planet bearing calculation (1/min)	[n2]		14535.7	
Speed planet carrier (1/min)	[nSteg]		0.0	
Torque (Nm)	[T]	8681.2	0.0	21820.3
Torque Pl.-Carrier (Nm)	[TSteg]		30501.439	
Overload factor	[Ko]		2.25	
Distribution factor	[Kv]		1.19	
	[KAeff = KA*Kgam]		2.68	
Required service life (h)	[H]		70000.00	
Gear driving (+) / driven (-)		+	-/+	-
Working flank gear 1:		Right flank		
Gear 1 direction of rotation:		Clockwise		
Gear 3 direction of rotation:		counterclockwise		
Gearbox type:		Precision enclosed gear units		

Tooth geometry and material

Geometry calculation according to

ISO 21771:2007

		----- Gear 1 -----	Gear 2 -----	Gear 3 ---
Center distance (in, mm)	[a]	7.7480,196.800		
Center distance tolerance	ISO 286:2010 Measure js5			
Normal Diametral Pitch (1/in)	[Pnd]	4.41739		
Normal module (in, mm)	[mn]	0.22638, 5.7500		
Normal pressure angle (°)	[αn]	20.0000		
Helix angle at reference circle (°)	[β]	13.0000		
Number of teeth	[z]	37	28	-93
Facewidth (mm)	[b]	90.13	88.00	90.13
Hand of gear		right	left	left

Planetary axles can be placed in regular pitch.:

72 °

	[Q-AGMA2015-1-A2001]	A2	A2	A2
Accuracy grade				
Inner diameter (mm)	[di]	0.00	0.00	
External diameter (mm)	[di]			0.00
Inner diameter of gear rim (mm)	[dbi]	0.00	0.00	
Outer diameter of gear rim (mm)	[dbi]			0.00

Material

Gear 1

Steel, Grade 3, HRC58-64(AGMA), Case-carburized steel, case-hardened
AGMA 2001-C95

Gear 2

Steel, Grade 3, HRC58-64(AGMA), Case-carburized steel, case-hardened
AGMA 2001-C95

Gear 3

Steel, Grade 3, HRC58-64(AGMA), Case-carburized steel, case-hardened
AGMA 2001-C95

Surface hardness	----- Gear 1 -----		----- Gear 2 -----		----- Gear 3 ---	
	HRC 60		HRC 60		HRC 60	
	(lb/in ²), (N/mm ²)		(lb/in ²), (N/mm ²)		(lb/in ²), (N/mm ²)	
Allowable bending stress number	[sat]	74694 , 515.0	74694 , 515.0	74694 , 515.0	74694 , 515.0	
Allowable contact stress number	[sac]	274846 , 1895.0	274846 , 1895.0	274846 , 1895.0	274846 , 1895.0	1895.0
Tensile strength (N/mm ²)	[σB]	1035.00	1035.00	1035.00	1035.00	
Yield point (N/mm ²)	[σS]	887.00	887.00	887.00	887.00	
Young's modulus (N/mm ²)	[E]	206843	206843	206843	206843	
Poisson's ratio	[ν]	0.300	0.300	0.300	0.300	
Roughness average value DS, flank (μm)	[RAH]	0.63	0.63	0.63	0.63	
Roughness average value DS, root (μm)	[RAF]	2.40	2.40	2.40	2.40	
Mean roughness height, Rz, flank (μm)	[RZH]	5.00	5.00	5.00	5.00	
Mean roughness height, Rz, root (μm)	[RZF]	16.00	16.00	16.00	16.00	

Information on pre-machining

Gear reference profile

1:

Reference profile	1.25 / 0.38 / 1.0 ISO 53:1998 Profil A	
Final machining stock (mm)	[q]	0.160
Dedendum coefficient	[hfP*]	1.250
Root radius factor	[ρfP*]	0.380 (pfPmax*= 0.472)
Addendum coefficient	[haP*]	1.000
Tip radius factor	[paP*]	0.000
Protuberance height coefficient	[hprP*]	0.000
Protuberance angle	[αprP]	0.000
Tip form height coefficient	[hFaP*]	0.000
Ramp angle	[αKP]	0.000
		not topping

Gear reference profile

2:

Reference profile	1.25 / 0.38 / 1.0 ISO 53:1998 Profil A	
Final machining stock (mm)	[q]	0.160
Dedendum coefficient	[hfP*]	1.250
Root radius factor	[ρfP*]	0.380 (pfPmax*= 0.472)

Addendum coefficient	[haP*]	1.000
Tip radius factor	[paP*]	0.000
Protuberance height coefficient	[hprP*]	0.000
Protuberance angle	[αprP*]	0.000
Tip form height coefficient	[hFaP*]	0.000
Ramp angle	[αKP]	0.000
	not topping	

Gear reference profile

3:

Reference profile	1.25 / 0.38 / 1.0 ISO 53:1998 Profil A		
Final machining stock (mm)	[q]	0.160	
Dedendum coefficient	[hfP*]	1.250	
Root radius factor	[ρfP*]	0.380	(ρfPmax* = 0.472)
Addendum coefficient	[haP*]	1.000	
Tip radius factor	[paP*]	0.000	
Protuberance height coefficient	[hprP*]	0.000	
Protuberance angle	[αprP*]	0.000	
Tip form height coefficient	[hFaP*]	0.000	
Ramp angle	[αKP]	0.000	
	not topping		

Reference profile of the final tooth form:

Dedendum reference profile	[hfP*]	1.169	1.169	1.169
Tooth root radius Refer. profile	[ρfP*]	0.380	0.380	0.380
Addendum Reference profile	[haP*]	1.000	1.000	1.000
Protuberance height coefficient	[hprP*]	0.000	0.000	0.000
Protuberance angle (°)	[αprP*]	0.000	0.000	0.000
Tip form height coefficient	[hFaP*]	0.000	0.000	0.000
Ramp angle (°)	[αKP]	0.000	0.000	0.000

Data for final machining:

Depth of immersion	[hgrind*]	0.984	0.984	0.697
Addendum coefficient Pinion type cutter	[haP0grind*]			1.259
Radius at cutter head	[rgrind*]	0.100	0.100	0.100
Grinding only flank (0), flank & root (1)		0	0	0

Generation grinding (0), form grinding (1)	0	0	0
Type of profile modification:	for high load capacity gearboxes		
Tip relief (µm)	[Ca L/R]	5.0 / 5.0	5.0 / 5.0
Root relief (µm)	[Cf L/R]	5.0 / 5.0	5.0 / 5.0
Lubrication type	Oil injection lubrication		
Oil grade, Own Input	Mobil Jet Oil II		
Lubricant base	Synthetic oil based on Ester		
Oil nominal kinematic viscosity at 40°C (mm²/s)	[v40]	27.60	
Oil nominal kinematic viscosity at 100°C (mm²/s)	[v100]	5.10	
Specific density at 15°C (kg/dm³)	[ρ]	1.004	
Oil temperature (°C)	[TS]	70.000	

Gear pair 1

Overall transmission ratio	[itot]	-2.514
Gear ratio	[u]	1.321
Transverse module (mm)	[mt]	5.901
Transverse pressure angle (°)	[αt]	20.483
Working pressure angle (°)	[αwt]	24.086
	[αwt.e/l]	24.093 / 24.080
Working pressure angle at normal section (°)	[αwn]	23.509
Helix angle at operating pitch circle (°)	[βw]	13.328
Base helix angle (°)	[βb]	12.204
Reference center distance (mm)	[ad]	191.791
Pitch on reference circle (mm)	[pt]	18.539
Base pitch (mm)	[pbt]	17.367
Transverse pitch on contact-path (mm)	[pet]	17.367
Sum of profile shift coefficients	[Σxi]	0.9464
Transverse contact ratio	[εα]	1.489
Transverse contact ratio with allowances	[εα.e/m/l]	1.490 / 1.486 / 1.482
Overlap ratio	[εβ]	1.096
Total contact ratio	[εγ]	2.585

Total contact ratio with allowances	[$\epsilon_{y,e/m/i}$]	2.586 / 2.582 / 2.578
Length of path of contact (mm)	[$g_a, \theta/i$]	25.857 (25.881 / 25.742)
Length T1-A (mm)	[T1A]	32.204 (32.180 / 32.272)
Length T1-B (mm)	[T1B]	40.694 (40.694 / 40.647)
Length T1-C (mm)	[T1C]	45.719 (45.705 / 45.733)
Length T1-D (mm)	[T1D]	49.571 (49.547 / 49.639)
Length T1-E (mm)	[T1E]	58.061 (58.061 / 58.014)
Length T2-A (mm)	[T2A]	48.112 (48.112 / 48.069)
Length T2-B (mm)	[T2B]	39.623 (39.598 / 39.694)
Length T2-C (mm)	[T2C]	34.598 (34.587 / 34.608)
Length T2-D (mm)	[T2D]	30.745 (30.745 / 30.702)
Length T2-E (mm)	[T2E]	22.256 (22.231 / 22.327)
Length T1-T2 (mm)	[T1T2]	80.317 (80.292 / 80.341)
Minimal length of contact line (mm)	[Lmin]	130.196
Gear pair 2		
Overall transmission ratio	[i_{to}]	-2.514
Gear ratio	[u]	-3.321
Transverse module (mm)	[m_t]	5.901
Transverse pressure angle (°)	[α_t]	20.483
Working pressure angle (°)	[α_{wt}]	24.086
	[$\alpha_{wt,\theta/i}$]	24.080 / 24.093
Working pressure angle at normal section (°)	[α_{wn}]	23.509
Helix angle at operating pitch circle (°)	[β_w]	13.328
Base helix angle (°)	[β_b]	12.204
Reference center distance (mm)	[a_d]	191.791
Pitch on reference circle (mm)	[p_t]	18.539
Base pitch (mm)	[p_{bt}]	17.367
Transverse pitch on contact-path (mm)	[p_{et}]	17.367
Sum of profile shift coefficients	[Σx_i]	-0.9464

Transverse contact ratio	[εα]	1.474
Transverse contact ratio with allowances	[εα.e/m/l]	1.481 / 1.476 / 1.470
Overlap ratio	[εβ]	1.096
Total contact ratio	[εγ]	2.570
Total contact ratio with allowances	[εγ.e/m/l]	2.577 / 2.571 / 2.566
Length of path of contact (mm)	[ga, e/l]	25.602 (25.721 / 25.534)
Length T1-A (mm)	[T1A]	22.511 (22.392 / 22.535)
Length T1-B (mm)	[T1B]	30.745 (30.745 / 30.702)
Length T1-C (mm)	[T1C]	34.598 (34.608 / 34.587)
Length T1-D (mm)	[T1D]	39.878 (39.759 / 39.902)
Length T1-E (mm)	[T1E]	48.112 (48.112 / 48.069)
Length T2-A (mm)	[T2A]	102.827 (102.733 / 102.827)
Length T2-B (mm)	[T2B]	111.062 (111.086 / 110.994)
Length T2-C (mm)	[T2C]	114.914 (114.949 / 114.879)
Length T2-D (mm)	[T2D]	120.194 (120.100 / 120.194)
Length T2-E (mm)	[T2E]	128.429 (128.453 / 128.361)
Length T1-T2 (mm)	[T1T2]	80.317 (80.341 / 80.292)
Minimal length of contact line (mm)	[Lmin]	128.990
Gear 1		
Lead height (mm)	[pz]	2971.197
Axial pitch (mm)	[px]	80.303
Profile shift coefficient		
Information on pre-machining	[x]	0.5474
Information on final machining	[x]	0.4660
Tooth thickness, arc, in module	[sn*]	1.9100
Tip alteration (mm)	[k*mn]	0.000
Reference diameter (mm)	[d]	218.346
Base diameter (mm)	[db]	204.542
Tip diameter (mm)	[da]	235.205

(mm)	[da.e/i]	235.205 / 235.159
Tip diameter allowances (mm)	[Ada.e/i]	0.000 / -0.046
Tip form diameter (mm)	[dFa]	235.205
(mm)	[dFa.e/i]	235.205 / 235.159
Root diameter (mm)	[df]	210.266
Generating Profile shift coefficient		
Information on pre-machining	[xE.e/i]	0.4996/ 0.4876
Information on final machining	[xE.e/i]	0.4182/ 0.4063
Generated root diameter with xE (mm)	[df.e/i]	209.716 / 209.579
(calculated with pre-machining tool)		
Root form diameter (mm)	[dFf]	213.596
(mm)	[dFf.e/i]	213.149 / 213.039
Internal toothing: Calculation dFf with pinion type cutter (z0=		
37 , x0=0.000)		
(calculated with final machining tool)		
Involute length (mm)	[l_dFa-l_dFf]	11.854
Addendum, $m_n(h_{ap}+x+k)$ (mm)	[ha]	8.430
(mm)	[ha.e/i]	8.430 / 8.407
Dedendum (mm)	[hf=mn*(hfP*-x)]	4.040
(mm)	[hf.e/i]	4.315 / 4.384
Tooth height (mm)	[h]	12.470
Virtual gear no. of teeth	[zn]	39.749
Normal tooth thickness at tip circle (mm)	[san]	3.720
(mm)	[san.e/i]	3.531 / 3.452
Normal tooth thickness at tip form circle (mm)	[sFan]	3.720
(mm)	[sFan.e/i]	3.531 / 3.452
Normal space width at root circle (mm)	[efn]	4.432
(mm)	[efn.e/i]	4.489 / 4.505

Gear 2

Lead height (mm)	[pz]	2248.473
Axial pitch (mm)	[px]	80.303
Profile shift coefficient		
Information on pre-machining	[x]	0.5618
Information on final machining	[x]	0.4804
Tooth thickness, arc, in module	[sn*]	1.9205

Tip alteration (mm)	[k*mn]	0.000
Reference diameter (mm)	[d]	165.235
Base diameter (mm)	[db]	154.788
Tip diameter (mm)	[da]	182.260
(mm)	[da.e/i]	182.260 / 182.214
Tip diameter allowances (mm)	[Ada.e/i]	0.000 / -0.046
Tip form diameter (mm)	[dFa]	182.260
(mm)	[dFa.e/i]	182.260 / 182.214
Root diameter (mm)	[df]	157.320
Generating Profile shift coefficient		
Information on pre-machining	[xE.e/i]	0.5140/ 0.5020
Information on final machining	[xE.e/i]	0.4326/ 0.4207
Generated root diameter with xE (mm)	[df.e/i]	156.771 / 156.634
(calculated with pre-machining tool)		
Root form diameter (mm)	[dFf]	160.763
(mm)	[dFf.e/i]	160.346 / 160.244
Internal toothing: Calculation dFf with pinion type cutter (z0=		
28 , x0=0.000)		
(calculated with final machining tool)		
Involute length (mm)	[l_dFa-l_dFf]	11.910
Addendum, $m_n(h_{aP}+x+k)$ (mm)	[ha]	8.512
(mm)	[ha.e/i]	8.512 / 8.489
Dedendum (mm)	[hf=mn*(hfP*-x)]	3.957
(mm)	[hf.e/i]	4.232 / 4.301
Tooth height (mm)	[h]	12.470
Virtual gear no. of teeth	[zn]	30.081
Normal tooth thickness at tip circle (mm)	[san]	3.387
(mm)	[san.e/i]	3.194 / 3.113
Normal tooth thickness at tip form circle (mm)	[sFan]	3.387
(mm)	[sFan.e/i]	3.194 / 3.113
Normal space width at root circle (mm)	[efn]	4.535
(mm)	[efn.e/i]	4.619 / 4.641

Gear 3

Lead height (mm)	[pz]	7468.143
Axial pitch (mm)	[px]	80.303
Profile shift coefficient		

Information on pre-machining	[x]	-1.3455
Information on final machining	[x]	-1.4268
Tooth thickness, arc, in module	[sn*]	0.5321
Tip alteration (mm)	[k*mn]	0.000
Reference diameter (mm)	[d]	548.816
Base diameter (mm)	[db]	514.118
Tip diameter (mm)	[da]	553.725
(mm)	[da.e/i]	553.725 / 553.655
Tip diameter allowances (mm)	[Ada.e/i]	0.000 / -0.070
Tip form diameter (mm)	[dFa]	553.725
(mm)	[dFa.e/i]	553.725 / 553.655
Root diameter (mm)	[df]	578.664
Generating Profile shift coefficient		
Information on pre-machining	[xE.e/i]	-1.4124/ -1.4267
Information on final machining	[xE.e/i]	-1.4937/ -1.5081
Generated root diameter with xE (mm)	[df.e/i]	579.598 / 579.433
(calculated with pre-machining tool)		
Root form diameter (mm)	[dFf]	575.976
(mm)	[dFf.e/i]	577.108 / 576.971
Internal toothing: Calculation dFf with pinion type cutter (z0=		
30 , x0=0.000)		
(calculated with final machining tool)		
Involute length (mm)	[_dFa-_dFf]	12.224
Addendum, $m_n(h_{aP}+x+k)$ (mm)	[ha]	-2.454
(mm)	[ha.e/i]	-2.419 / -2.454
Dedendum (mm)	[hf=mn*(hfP*-x)]	14.924
(mm)	[hf.e/i]	15.309 / 15.391
Tooth height (mm)	[h]	12.470
Virtual gear no. of teeth	[zn]	99.911
Normal tooth thickness at tip circle (mm)	[san]	4.944
(mm)	[san.e/i]	4.661 / 4.573
Normal tooth thickness at tip form circle (mm)	[sFan]	4.944
(mm)	[sFan.e/i]	4.661 / 4.573
Normal space width at root circle (mm)	[efn]	2.447
(mm)	[efn.e/i]	2.357 / 2.338

Gear specific pair data Gear pair 1, Gear 1

Operating pitch diameter (mm)	[dw]	224.049
(mm)	[dw.e/i]	224.061 / 224.038
Active tip diameter (mm)	[dNa]	235.205
(mm)	[dNa.e/i]	235.205 / 235.159
Theoretical tip clearance (mm)	[c]	0.537
Effective tip clearance (mm)	[c.e/i]	0.914 / 0.802
Active root diameter (mm)	[dNf]	214.443
(mm)	[dNf.e/i]	214.484 / 214.428
Reserve (dNf-dFf)/2 (mm)	[cF.e/i]	0.722 / 0.639
Max. sliding velocity at tip (m/s)	[vga]	33.004
Specific sliding at the tip	[ζa]	0.493
Specific sliding at the root	[ζf]	-0.974
Mean specific sliding	[ζm]	0.493
Sliding factor on tip	[Kga]	0.256
Sliding factor on root	[Kgf]	-0.280
Roll angle at dFa (°)	[ξdFa.e/i]	32.528 / 32.502
Roll angle to dNa (°)	[ξdNa.e/i]	32.528 / 32.502
Roll angle to dNf (°)	[ξdNf.e/i]	18.080 / 18.028
Roll angle at dFf (°)	[ξdFf.e/i]	16.796 / 16.686
Diameter of single contact point B (mm)	[d-B]	220.139 (220.139 / 220.104)
Diameter of single contact point D (mm)	[d-D]	227.303 (227.281 / 227.362)
Addendum contact ratio	[ε]	0.711 (0.711 / 0.707)

Gear specific pair data Gear pair 1, Gear 2

Operating pitch diameter (mm)	[dw]	169.551
(mm)	[dw.e/i]	169.559 / 169.542
Active tip diameter (mm)	[dNa]	182.260
(mm)	[dNa.e/i]	182.260 / 182.214
Theoretical tip clearance (mm)	[c]	0.537
Effective tip clearance (mm)	[c.e/i]	0.914 / 0.802
Active root diameter (mm)	[dNf]	161.061
(mm)	[dNf.e/i]	161.100 / 161.048
Reserve (dNf-dFf)/2 (mm)	[cF.e/i]	0.428 / 0.351

Max. sliding velocity at tip (m/s)	[vga]	36.139
Specific sliding at the tip	[ζa]	0.493
Specific sliding at the root	[ζf]	-0.974
Mean specific sliding	[ζm]	0.493
Sliding factor on tip	[Kga]	0.280
Sliding factor on root	[Kgf]	-0.256
Roll angle at dFa (°)	[ξdFa.e/i]	35.618 / 35.586
Roll angle to dNa (°)	[ξdNa.e/i]	35.618 / 35.586
Roll angle to dNf (°)	[ξdNf.e/i]	16.529 / 16.458
Roll angle at dFf (°)	[ξdFf.e/i]	15.491 / 15.345
Diameter of single contact point B (mm)	[d-B]	173.895 (173.872 / 173.959)
Diameter of single contact point D (mm)	[d-D]	166.555 (166.555 / 166.523)
Addendum contact ratio	[ε]	0.778 (0.779 / 0.775)

Gear specific pair data Gear pair 2, Gear 2

Operating pitch diameter (mm)	[dw]	169.551
(mm)	[dw.e/i]	169.542 / 169.559
Active tip diameter (mm)	[dNa]	182.260
(mm)	[dNa.e/i]	182.260 / 182.214
Theoretical tip clearance (mm)	[c]	1.402
Effective tip clearance (mm)	[c.e/i]	1.902 / 1.777
Active root diameter (mm)	[dNf]	161.203
(mm)	[dNf.e/i]	161.216 / 161.137
Reserve (dNf-dFf)/2 (mm)	[cF.e/i]	0.486 / 0.395
Max. sliding velocity at tip (m/s)	[vga]	14.378
Specific sliding at the tip	[ζa]	0.196
Specific sliding at the root	[ζf]	-0.375
Mean specific sliding	[ζm]	0.232
Sliding factor on tip	[Kga]	0.111
Sliding factor on root	[Kgf]	-0.100
Roll angle at dFa (°)	[ξdFa.e/i]	35.618 / 35.586
Roll angle to dNa (°)	[ξdNa.e/i]	35.618 / 35.586
Roll angle to dNf (°)	[ξdNf.e/i]	16.683 / 16.577
Roll angle at dFf (°)	[ξdFf.e/i]	15.491 / 15.345

Diameter of single contact point B (mm)	[d-B]	166.555 (166.555 / 166.523)
Diameter of single contact point D (mm)	[d-D]	174.127 (174.019 / 174.150)
Addendum contact ratio	[ε]	0.778 (0.778 / 0.776)

Gear specific pair data Gear pair 2, Gear 3

Operating pitch diameter (mm)	[dw]	563.151
(mm)	[dw.e/i]	563.179 / 563.122
Active tip diameter (mm)	[dNa]	553.725
(mm)	[dNa.e/i]	553.725 / 553.655
Theoretical tip clearance (mm)	[c]	1.402
Effective tip clearance (mm)	[c.e/i]	1.756 / 1.632
Active root diameter (mm)	[dNf]	574.712
(mm)	[dNf.e/i]	574.734 / 574.651
Reserve (dNf-dFf)/2 (mm)	[cF.e/i]	1.229 / 1.119
Max. sliding velocity at tip (m/s)	[vga]	2.547
Specific sliding at the tip	[ζa]	0.273
Specific sliding at the root	[ζf]	-0.244
Mean specific sliding	[ζm]	0.232
Sliding factor on tip	[Kga]	0.100
Sliding factor on root	[Kgf]	-0.111
Roll angle at dFa (°)	[ξdFa.e/i]	22.898 / 22.919
Roll angle to dNa (°)	[ξdNa.e/i]	22.898 / 22.919
Roll angle to dNf (°)	[ξdNf.e/i]	28.610 / 28.631
Roll angle at dFf (°)	[ξdFf.e/i]	29.184 / 29.218
Diameter of single contact point B (mm)	[d-B]	560.050 (560.070 / 559.996)
Diameter of single contact point D (mm)	[d-D]	567.542 (567.462 / 567.542)
Addendum contact ratio	[ε]	0.696 (0.703 / 0.694)

General influence factors

----- Gear 1 ----- Gear 2 ----- Gear 3 ---

Calculated with the operating pitch circle:

Nominal circumferential force (lb)	[Wt,Ftw]	3484.25	(15498.70	N)
Nominal circumferential force (lb)	[Wt,Ftw]		3484.25	(15498.70 N)

Axial force (lb)	[Faw]	825.41	(3671.62	N)	
Axial force (lb)	[Faw]	825.41	(3671.62	N)	
Axial force, total (N)	[Fatot = p*Fa]	4127.06	(18358.08	N)	
Axial force, total (N)	[Fatot = p*Fa]	4127.06	(18358.08	N)	
Radial force (lb)	[Frw]	1557.58	(6928.46	N)	
Radial force (lb)	[Frw]	1557.58	(6928.46	N)	
Net face width of narrowest member (in)	[F,b]	3.46	(88.00	mm)	
Net face width of narrowest member (in)	[F,b]	3.46	(88.00	mm)	
Circumferential force per in (lb/in)	[w]	1005.68	(176.12	N/mm)	
Circumferential force per in (lb/in)	[w]	1005.68	(176.12	N/mm)	
Pitch line velocity (ft/min)	[vt]	25402.18	(129.04	m/s)	
Pitch line velocity (ft/min)	[vt]	25402.18	(129.04	m/s)	
Gearbox type:	Precision enclosed gear units				
Mesh alignment factor	[Cma]	0.111	0.111		
Mounting procedure:	Contact improved by adjusting at assembly				
Mesh alignment correction factor	[Ce]	0.800			
Gearing:	without longitudinal flank modification				
Lead correction factor	[Cmc]	1.000	1.000		
Pinion proportion factor	[Cpf]	0.058	0.058		
Pinion proportion modifier	[Cpm]	1.000	1.000		
Small offset	[s1/s < 0.175]				
Face load distribution factor	[Cmf]	1.146	1.146		
Load distribution factor	[Km]	1.146	1.146		
Transmission accuracy level number	[Av]	3			
Dynamic factor introduced:					
Dynamic factor	[Kv]	1.100			
Number of load cycles (in mio.)	[NL]	231000.0	61050.0	91903.2	

Tooth root load capacity

	----- Gear 1 -----	Gear 2 -----	Gear 3 -----	
Rim thickness factor	[KB]	1.000	1.000	1.000
Size factor	[KS]	1.000	1.000	1.000
Limiting Variation in action (in/10000)	[LimVarAc]	5.0	5.0	
Load sharing:				
0 = No, Loaded at tip, 1 = Yes, Loaded at HPSTC		0	0	
Calc. as helical gear (0) / as LACR (1)		0	0 / 0	0

Load angle (°)	[φnL]	28.62	30.71 /30.71	22.45		
Determination of factor Y by graphical method						
Calculated with generating profile shift coefficient	[xE.m]	0.4122	0.4267	-1.5009		
Height of Lewis parabola (in)	[hF]	0.415	0.417 /0.417	0.422		
Height of Lewis parabola (mm)	[hF]	10.530	10.596 /10.596	10.709		
Tooth thickness at critical section (in)	[sF]	0.508	0.503 /0.503	0.639		
Tooth thickness at critical section (mm)	[sF]	12.906	12.774 /12.774	16.220		
Radius at curvature of fillet curve (in)	[ρF]	0.030	0.031 /0.031	0.030		
Radius at curvature of fillet curve (mm)	[ρF]	0.762	0.791 /0.791	0.773		
Helical factor	[Ch]		1.26	1.26		
Helix angle factor	[Kψ]		0.95	0.95		
Tooth form factor Y	[Y]	0.667	0.671 /0.671	0.973		
Stress correction factor	[Kf]	1.855	1.831 /1.831	2.083		
Bending strength geometry factor J	[J]	0.532	0.542 /0.537	0.685		
Bending stress number (lb/in ²)	[st]	27479.0	26964.2 /27216.221332.0			
Bending stress number (N/mm ²)	[st]	189.5	185.9 /187.6	147.1		
Stress cycle factor	[YN]	0.851	0.871	0.865		
(for general applications)						
Allowable bending stress number (lb/in ²)	[sat]	74694.4	74694.4	74694.4		
Allowable bending stress number (N/mm ²)	[sat]	515.0	515.0	515.0		
Temperature factor	[KT]	1.000	1.000	1.000		
Reliability factor (99.00 %)	[KR]		1.000			
Reverse loading factor	[-]	1.000	0.700	1.000		
Effective allow. b.s.n. (lb/in ²)	[sateff]	63564.0	45561.3 / 45561.364615.5			
Effective allow. b.s.n. (N/mm ²)	[sateff]	438.3	314.1 /314.1	445.5		
Allowable transmitted power (hp, kW)	[Pat]	20680.3	,15421.23 15106.2	,11264.63 / 14966.4	,11160.36	27080.2 , 20193.57
Note: Allowable transmitted power Patcalculated including the following values: Ky, Ko, KR, SFmin						
Allowable transmitted power at unity service factor (hp, kW)	[Patu]	83057.4	,61935.50 60670.3	,45241.57 / 60108.7	,44822.78	108760.9 , 81102.42
Note: Allowable transmitted power Patu calculated with Ky=1, Ko=1, KR=1, SFmin=1						
Transmittable power including SFmin (-, kW)	[Patu/SFmin]	55371.6	,41290.33 40446.9	,30161.05 /40072.5	,29881.85	72507.2 , 54068.28
Note: Transmittable power including SFmin calculated with Ky=1, Ko=1, KR=1						
Unit load (lb/in ²)	[UL]		4442.49	4442.49		
Allowable unit load (lb/in ²)	[Uat]	6850.9	5004.3 / 4958.08971.0			
Required safety factor	[SFmin]	1.500	1.500	1.500		
Safety factor, Bending	[sateff/st]	2.313	1.690 /1.674	3.029		

Yield strength factor	[Ky]	0.50		
Core hardness (HV)	[HV]	316	316	316
Core hardness (HB)	[HB]	300	300	300
Allowable yield strength number (lb/in ²)	[say]	111800.00	111800.00	111800.00
Stress correction factor	[Kf]	1.855	1.831 / 1.831 2.083	
Maximum peak tangential load (lb, N)	[Wmax]	7839.56	34872.07	7839.56 , 34872.07
Load distribution factor (overload)	[Kmy]	1.12		
Safety for yield strength	[Syield]	4.25	4.27 / 4.23	6.15
	[Syield = say*Ky / (Wmax*Pd*Kmy/F/J/Kf)]			

Note: The calculation is performed with coefficient Kf and the core hardness in HB.
 The core hardness value in the database can differ considerably from the actual hardness.
 The value must be checked in critical cases..

Flank safety

		----- Gear 1 -----	Gear 2 -----	Gear 3 -----
		(√lb/in), (√N/mm)	(√lb/in), (√N/mm)	(√lb/in), (√N/mm)
Elastic coefficient	[Cp]	2290.00	190.20	2290.00 , 190.20
Size factor	[Ks]	1.000	1.000	1.000
Load sharing ratio	[mN]		0.676	0.682
Helical overlap factor	[Cψ]		1.000	1.000
Geometry factor I	[I]		0.158	0.420
		(lb/in ²), (N/mm ²)	(lb/in ²), (N/mm ²)	(lb/in ²), (N/mm ²)
Contact stress number	[sc]	130032.3	896.5	79719.3 , 549.6
Stress cycle factor (for general applications)	[ZN]	0.794	0.818	0.811
Surface condition factor	[Cf]	1.000	1.000	1.000 / 1.000 1.000
Hardness ratio factor	[CH]	1.000	1.000	1.000 / 1.000 1.000
Temperature factor	[KT]	1.000	1.000	1.000
Reliability factor	[KR]	99.000		{ZS.CRAGMA}
Allowable contact stress number (lb/in ²)	[sac]	274846.4	274846.4	274846.4
Allowable contact stress number (N/mm ²)	[sac]	1895.0	1895.0	1895.0
Effective allow. c.s.n. (lb/in ²)	[saceff]	218140.1	224919.8	/224919.8 222813.7
Effective allow. c.s.n. (N/mm ²)	[saceff]	1504.0	1550.8	/1550.81536.2
Allowable transmitted power (hp)	[Pac]	16773.5	(12507.95 kW)	17832.4 (13297.52 kW) / 47444.4 (35379.07 kW) 46560.1 (34719.60 kW)

Note: Allowable transmitted power Paccalculated including the following values: Ky, Ko, KR, SHmin

Allowable transmitted power at unity service factors (hp) [Pacu] 101050.1 (75352.57 kW) 107429.0 (80109.25 kW) 285823.0 (213136.76 kW) 280495.2 (209163.87 kW)

Note: Allowable transmitted power Pacu calculated including the following values: $K_Y=1$, $K_o=1$, $K_R=1$, $S_{Hmin}=1$

Transmittable power including S_{Hmin} (hp) [Pacu/ S_{Hmin}^2] 44911.2 (33490.03 kW) 47746.2 (35604.11 kW) 127032.4 (94727.45 kW) 124664.5 (92961.72 kW)

Note: Allowable transmitted power Pacu/ S_{Hmin}^2 calculated including the following values: $K_Y=1$, $K_o=1$, $K_R=1$

Contact load factor (lb/in ²) (N/mm ²)	[K]	264.7	1.825
Allowable contact load factor (lb/in ²)	[Kac]	744.9	791.9 / 838.2 822.6
Required safety factor	[S_{Hmin}]	1.500	1.500 1.500
Safety factor (Pitting)	[saceff/sc]	1.678	1.730 / 2.821 2.795

Service Factors, with $K_Y= 1.000$:

Service factor for tooth root	[KSF]	6.194	4.524 / 4.482 8.110
Service factor for pitting	[CSF]	7.535	8.011 / 21.31420.916
Service factor for gear set	[SF]	4.524	4.482

Note: Service factors calculated with $K_Y=1$, $K_o=1$, $K_R=1$, $S_{Fmin}=1$, $S_{Hmin}=1$

Transmittable power including required service factors K_{SFmin} , C_{SFmin} (hp) 40072.48 (29881.85 kW)

$K_{SFmin} = 1.50$, $C_{SFmin} = 2.25$

Service Factors, with $K_Y= 1.190$:

Service factor for tooth root	[KSF]	5.205	3.802 / 3.767 6.815
Service factor for pitting	[CSF]	6.332	6.732 / 17.91117.577
Service factor for gear set	[SF]	3.802	3.767

Note: Service factors calculated with $K_o=1$, $K_R=1$, $S_{Fmin}=1$, $S_{Hmin}=1$

The equations used for Pat, Pac, Pacu, Patu, Pa are according AGMA2001.

Micropitting according to ISO/TS 6336-22:2018

Pairing Gear 1 -2 :

Calculation of permissible specific film thickness

Lubricant load according to FVA Info sheet 54/7 10, Mobil Jet Oil II

Reference data FZG-C Test:

Torque (Nm)	[T1Ref]	265.100
Line load at contact point A (N/mm)	[FbbRef,A]	236.300
Oil temperature (°C)	[θ_{OilRef}]	90.000
Tooth mass temperature (°C)	[θ_{MRef}]	137.638
Contact temperature (°C)	[$\theta_{BRef,A}$]	309.560

Lubrication gap thickness (µm)	[hRef,A]	0.016	
Specific film thickness in test	[λGFT]	0.031	
Material coefficient	[WW]	1.000	
Permissible specific film thickness	[λGFP]	0.043	
Interim results in accordance with ISO/TS 6336-22:2014			
Coefficient of friction	[µ _m]	0.040	
Lubricant factor	[XL]	1.300	
Roughness factor	[XR]	0.925	
Lubrication coefficient for lubrication type	[XS]	1.200	
Tooth mass temperature (°C)	[θM]	91.283	
Tip relief factor	[XCα(A)]	1.617	
Loss factor	[HV]	0.125	
Equivalent Young's modulus (N/mm²)	[Er]	227300.000	
Pressure-viscosity coefficient (m²/N)	[α38]	0.01000	
Dynamic viscosity (Ns/m²)	[ηtM]	5.800	
Roughness average value (µm)	[Ra]	0.630	
Calculation of speeds, load distribution and flank curvature according to method B following ISO/TS 6336-22:2018			
Ca taken as optimal in the calculation (0=no, 1=yes)		1	1
Calculation at point (0:A, 1:AB, 2:B, 3:C, 4:D, 5:DE, 6:E, -1:No Point)		5	
Diameter (mm)	[dy]	231.132	163.611
Relative radius of curvature (mm)	[ρred]	18.167	
Load sharing factor	[XY]	0.725	
(XY interpolated between XY(eps.b=0.8) and XY(eps.b=1.2) according ISO/TC60/WG6)			
Contact stress (N/mm²)	[pH]	527.579	
Contact stress (N/mm²)	[pdyn]	969.386	
Minimal specific film thickness	[λGFY]	0.643	(hY= 0.405 µm)
Safety against micropitting	[Sλ(B)]	14.822	
For interim results, refer to file:	Micropitting_12.tmp		
Pairing Gear 2 -3 :			
Calculation of permissible specific film thickness			
Material coefficient	[WW]	1.000	
Permissible specific film thickness	[λGFP]	0.043	
Interim results in accordance with ISO/TS 6336-22:2014			
Coefficient of friction	[µ _m]	0.026	
Lubricant factor	[XL]	1.300	

Roughness factor	[XR]	0.735	
Lubrication coefficient for lubrication type	[XS]	1.200	
Tooth mass temperature (°C)	[θM]	78.073	
Tip relief factor	[XCα(A)]	1.617	
Loss factor	[HV]	0.049	
Equivalent Young's modulus (N/mm ²)	[Er]	227300.000	
Pressure-viscosity coefficient (m ² /N)	[α38]	0.01000	
Dynamic viscosity (Ns/m ²)	[ηtM]	7.948	
Roughness average value (μm)	[Ra]	0.630	
Calculation of speeds, load distribution and flank curvature according to method B following ISO/TS 6336-22:2018			
Ca taken as optimal in the calculation (0=no, 1=yes)		1	1
Calculation at point (0:A, 1:AB, 2:B, 3:C, 4:D, 5:DE, 6:E, -1:No Point)		1	
Diameter (mm)	[dy]	163.694	556.836
Relative radius of curvature (mm)	[pred]	21.812	
Load sharing factor	[XY]	0.728	
(XY interpolated between XY(eps.b=0.8) and XY(eps.b=1.2) according ISO/TC60/WG6)			
Contact stress (N/mm ²)	[pH]	482.650	
Contact stress (N/mm ²)	[pdyn]	886.833	
Minimal specific film thickness	[λGFY]	1.013	(hY= 0.638 μm)
Safety against micropitting	[Sλ(B)]	23.338	
For interim results, refer to file:	Micropitting_23.tmp		

The calculation of micropitting specified in ISO/TS6336-22 is not designed for use with internal toothings because it has not yet been subject to sufficient investigation. The results can only be used for information purposes.

Scuffing load capacity

Results from	AGMA 925-A03, Details see in the specific calculation sheet
Probability of wear (%)	[Pwear] 37.345
Probability of scuffing (%)	[Pscuff] 5% or lower

Measurements for tooth thickness

Gear 1 Gear 2 Gear 3

Information on pre-machining

Tooth thickness allowance (final machining) (mm)	[As.e/i]	-0.200 /-0.250	-0.200 /-0.250	-0.280 /-0.340
Input for final machining stock, per flank (mm)	[q]	0.160	0.160	0.160
Additional measure for pre-machining (mm)	[ΔAs_pre.e/i]	0.341 /0.341	0.341 /0.341	0.341 /0.341
Tooth thickness allowance (normal section) (mm)	[As_pre.e/i]	0.141 /0.091	0.141 /0.091	0.061 /0.001
Number of teeth spanned	[k]	6.000	5.000	-0.000
Base tangent length with allowance (mm)	[Wk.e/i]	98.535 / 98.488	80.836 / 80.789	-0.000 / -0.000
Effective diameter of ball/pin (mm)	[DMeff]	10.500	11.000	-10.000
Diametral two ball measure (mm)	[MdK.e/i]	238.793 /238.685	187.289 /187.189	549.951 /549.805

Information on final machining

Tooth thickness tolerance		DIN 3967 ab25	DIN 3967 ab25	DIN 3967 ab25
Tooth thickness allowance (normal section) (mm)	[As.e/i]	-0.200 /-0.250	-0.200 /-0.250	-0.280 /-0.340
Number of teeth spanned	[k]	6.000	5.000	-0.000
(Internal toothing: k = (Measurement gap number)				
Base tangent length (no backlash) (mm)	[Wk]	98.403	80.704	-0.000
Base tangent length with allowance (mm)	[Wk.e/i]	98.215 /98.168	80.516 /80.469	-0.000 /-0.000
Diameter of measuring circle (mm)	[dMMw.k]	225.938	173.635	-0.000
Theoretical diameter of ball/pin (mm)	[DM]	10.421	10.738	9.447
Effective diameter of ball/pin (mm)	[DMeff]	10.500	11.000	10.000
Radial single-ball measurement backlash free (mm)	[MrK]	119.347	93.503	275.016
Radial single-ball measurement (mm)	[MrK.e/i]	119.130 /119.075	93.300 /93.249	275.427 /275.354
Diameter of measuring circle (mm)	[dMMr.m]	223.385	170.741	564.755
Diametral measurement over two balls without clearance (mm)	[MdK]	238.489	187.006	549.952
Diametral two ball measure (mm)	[MdK.e/i]	238.054 /237.945	186.601 /186.499	550.773 /550.629
Measurement over pins according to DIN 3960 (mm)	[MdR.e/i]	238.259 /238.150	186.601 /186.499	-0.000 /-0.000
Measurement over 2 pins, free, according to AGMA 2002 (mm)	[dk2f.e/i]	238.041 /237.932	0.000 /0.000	0.000 /0.000
Measurement over 2 pins, transverse, according to AGMA 2002 (mm)	[dk2t.e/i]	238.461 /238.351	0.000 /0.000	0.000 /0.000
Measurement over 3 pins, axial, according to AGMA 2002 (mm)	[dk3A.e/i]	238.259 /238.150	186.601 /186.499	-0.000 /-0.000
Measurement over 3 pins with allowance (mm)	[Md3R.e/i]	0.000 /0.000	0.000 /0.000	-0.000 /-0.000
Note: Internal gears with helical teeth cannot be measured with rollers.				
Chordal tooth thickness in reference circle (mm)	[sc]	10.978	11.036	3.060
(mm)	[sc.e/i]	10.782 /10.732	10.840 /10.791	2.779 /2.719
Reference chordal height from da.m (mm)	[ha]	8.549	8.676	-2.441

Tooth thickness, arc (mm)	[sn]	10.983	11.043	3.060
(mm)	[sn.e/i]	10.783 /10.733	10.843 /10.793	2.780 /2.720
Backlash free center distance (mm)	[aControl.e/i]	196.326 /196.207	197.361 /197.489	
Backlash free center distance, allowances (mm)	[jta]	-0.474 /-0.593	0.561 /0.689	
dNf.i with aControl (mm)	[dNF0.i]	213.581	160.276 / 160.251	576.216
Reserve (dNF0.i-dFf.e)/2 (mm)	[cF0.i]	0.216	-0.035 / -0.047	0.378
Tip clearance (mm)	[c0.i(aControl)]	0.218	0.218 / 1.225	0.953
Center distance allowances (mm)	[Aa.e/i]	0.010 /-0.010	-0.010 /0.010	
Circumferential backlash from Aa (mm)	[jtw_Aa.e/i]	0.009 /-0.009	0.009 /-0.009	
Radial backlash (mm)	[jrw]	0.603 /0.464	0.699 /0.551	
Circumferential backlash, transverse section (mm)	[jtw]	0.535 /0.412	0.630 /0.497	
Normal backlash (mm)	[jnw]	0.477 /0.369	0.561 /0.444	
Torsional angle on input with output fixed:				
Total torsional angle (°)	[j.tSys]	0.5871/0.4740		

Toothing tolerances

		----- Gear 1 -----	Gear 2 -----	Gear 3 ---
Following	AGMA 2000-A88			
Accuracy grade	[Q-AGMA2000]	15	15	15
Pitch Variation Allowable (µm)	[VpA]	2.40	2.30	2.80
Runout Radial Tolerance (µm)	[VrT]	12.00	11.00	14.00
Profile Tolerance (µm)	[VphiT]	3.80	3.60	4.40
Tooth Alignment Tolerance (µm)	[VpsiT]	6.50	6.40	6.50
Composite Tolerance, Tooth-to-Tooth (µm)	[VqT]	2.90	3.00	2.90
Composite Tolerance, Total (µm)	[VcqT]	6.90	6.60	8.00
AGMA <-> ISO: VpA <-> fpbT, VrT <-> FrT, VpsiT <-> FbT, VqT <-> fidT, VcqT <-> FidT				

According to AGMA 2015-1-A01 & 2015-2-A06

Accuracy grade	[Q-AGMA2015]	A2	A2	A2
Single pitch deviation (µm)	[fptT]	2.70	2.60	3.00
Total cumulative pitch deviation (µm)	[FpT]	10.00	9.50	14.00
Profile form deviation (µm)	[ffaT]	3.20	3.10	3.70
Profile slope deviation (µm)	[fhαT]	2.60	2.50	3.00

Total profile deviation (µm)	[FaT]	4.10	4.00	4.80
Helix form deviation (µm)	[ffβT]	2.90	2.90	3.20
Helix slope deviation (µm)	[fhβT]	2.90	2.90	3.20
Total helix deviation (µm)	[FβT]	4.10	4.00	4.40
Single flank composite, total (µm)	[FisT]	11.00	10.00	15.00
Single flank composite, tooth-to-tooth (µm)	[fisT]	1.00	0.90	1.40
Radial composite, total (µm)	[FidT]	10.00	9.50	13.00
Radial composite, tooth-to-tooth (µm)	[fidT]	1.80	1.70	2.40
Following	AGMA 2015-2-B15			
Radial composite, total (µm)	[FidT]	31.00	(R20) 30.00	(R20) 36.00 (R20)
Radial composite, tooth-to-tooth (µm)	[fidT]	16.00	(R20) 16.00	(R20) 16.00 (R20)

Axis alignment tolerances (recommendation acc. to ISO TR 10064-3:1996, Quality)

	2		
Maximum value for deviation error of axis (µm)	[fΣβ]	2.79	2.79
Maximum value for inclination error of axes (µm)	[fΣδ]	5.59	5.59

Modifying and defining the tooth form

Profile and tooth trace modifications for gear 1

Symmetric (both flanks)

- Tip relief, linear
Caa = 5.000 µm LCa = 1.472 *mn dCa = 227.323 mm
- Root relief, linear
Caf = 5.000 µm LCf = 1.863 *mn dCf = 220.139 mm
- Helix angle modification, tapered or conical
CHb = -2.455 µm
CHβ=-2.455µm -> Right Tooth Flank β.eff=13.0016°-right Left Tooth Flank β.eff=12.9984°-right
- flankline crowning
Cb = 0.803 µm
rcrown=1264644mm

Profile and tooth trace modifications for gear 2

Symmetric (both flanks)

- Tip relief, linear
Caa = 5.000 µm LCa = 1.428 *mn dCa = 174.147 mm

- Root relief, linear
 Caf = 5.000 μm LCf = 1.708 *mn dCf = 166.555 mm

Profile and tooth trace modifications for gear 3

Symmetric (both flanks)

- Tip relief, linear
 Caa = 5.000 μm LCa = 1.440 *mn dCa = -560.088 mm
 - Root relief, linear
 Caf = 5.000 μm LCf = 1.868 *mn dCf = -567.542 mm

Tip relief verification

Diameter (mm)	[dcheck]	235.044	182.099	-553.840
Tip relief left/right (μm)	[Ca L/R]	4.9 / 4.9	4.9 / 4.9	4.9 / 4.9

Data for the tooth form calculation :

Calculation of Sun gear

Tooth form, Sun gear, Step 1: Automatic (pre-machining)
 haP* = 0.970, hfP* = 1.250, pfP* = 0.380

Calculation of Planets

Tooth form, Planets, Step 1: Automatic (pre-machining)
 haP* = 0.970, hfP* = 1.250, pfP* = 0.380

Calculation of Internal gear

Tooth form, Internal gear, Step 1: Automatic (pre-machining)
 z0 = 30, x0 = 0.0000, da0 = 193.221 mm, a0 = -193.147 mm
 haP0* = 1.407, paP0* = 0.380, hfP0* = 0.838, pfP0* = 0.000

Supplementary data

Singular tooth stiffness (N/mm/ μm)	[c]	15.330	14.410
---	-----	--------	--------

Meshing stiffness (N/mm/μm)	[c _v]	20.950	19.534	
Mass (kg)	[m]	27.496	15.601	30.702
Total mass (kg)	[mGes]	136.204		
Moment of inertia for system, relative to the input: calculation without consideration of the exact tooth shape				
Single gears (da+df)/2...d _i (kg*m ²)	[J]	0.17052	0.05622	2.67313
System (da+df)/2...d _i (kg*m ²)	[J]	1.08448		
Torsional stiffness at driving gear with fixed driven gear:				
Torsional stiffness (MNm/rad)	[c _r]	28.527		
Torsion when subjected to nominal torque (°)	[δ _{cr}]	0.017		
Mean coefficient of friction (as defined in Niemann)	[μ _m]	0.045	0.037	
Wear sliding coef. by Niemann	[ζ _w]	0.735	0.343	
Loss factor	[HV]	0.125	0.049	
Meshing power (kW)		10000.000	10000.000	
Gear power loss (kW)	[PVZ]	11.257	3.689	
Total power loss (kW)		74.731		
Total efficiency		0.993		
Sound pressure level according to Masuda, without contact analysis				
	[dB(A)]	118.3	120.6	

Service life, damage

Required safety for tooth root	[SF _{min}]	1.50		
Required safety for tooth flank	[SH _{min}]	1.50		
Service life (calculated with required safeties):				
System service life (h)	[H _{att}]	>	1000000	
Tooth root service life (h)	[HF _{att}]	1e+06	1e+06	1e+06
Tooth flank service life (h)	[HH _{att}]	1e+06	1e+06	1e+06

Note: The entry 1e+006 h means that the Service life > 1,000,000 h.

Damage calculated on the basis of the required service life (70000.0 h)						
F1%	F2%	F3%	H1%	H2%	H3%	
0.00	0.2096	0.0000	0.7712	0.2038	0.0000	

Remarks:

- Symbols used in []: [xx,yy] xx as used in AGMA 2001-D04, yy as used in AGMA 2101-D04
- Specifications with [e/i] imply: Maximum [e] and minimum value [i] for
Taking all tolerances into account
- Specifications with [m] imply: Mean value within tolerance
- For the backlash tolerance, the center distance tolerances and the tooth thickness allowance are taken into account.

The maximum and minimum clearance according to the largest or smallest allowances are defined..

The calculation is performed for the operating pitch circle.

$$\text{sateff} = \text{sat} \cdot \text{KL} / \text{KT} / \text{KR} \cdot \text{Kwb} / \text{SF} \quad (\text{SF} = 1.0)$$

LACR = Spur gear or helical gear with $\epsilon\beta$ (mF) < 1.0

PSTC = Point of Single Tooth Contact

- Cycle factors YN, ZN are expanded over 10^{10} (following the method used by AGMA programm)

End of Report

lines: 928

GearedTurbofan 2



KISSsoft Release 2020 A.1

KISSsoft – student license (not for commercial use)

File

Name : GearedTurbofan 2

Changed by: marti on: 01.04.2021 at: 12:48:30

Calculation of a helical planetary gear stage

Drawing or article number:

Gear 1: 0.000.0

Gear 2: 0.000.0

Gear 3: 0.000.0

Calculation method

AGMA 2101-D04 (Metric Edition)

		----- Sun -----	Planets -----	Internal gear ---
Number of planets	[p]	1	5	1
Power (kW)	[P]	10000.000		
Transmitted power (hp)	[P]	13410.200		
Transmitted power (ft*lb/s)	[P]	7375600.0		
Speed (1/min)	[n]	9000.0		-4164.9
Speed difference for planet bearing calculation (1/min)	[n2]		15352.9	
Speed planet carrier (1/min)	[nSteg]		0.0	
Torque (Nm)	[T]	10610.3	0.0	22928.1
Torque Pl.-Carrier (Nm)	[TSteg]		33538.398	
Overload factor	[Ko]		2.25	
Distribution factor	[Kv]		1.19	
	[KAeff = KA*Kgam]		2.68	
Required service life (h)	[H]		70000.00	
Gear driving (+) / driven (-)		+	-/+	-
Working flank gear 1:		Right flank		
Gear 1 direction of rotation:		Clockwise		
Gear 3 direction of rotation:		counterclockwise		
Gearbox type:		Precision enclosed gear units		

Tooth geometry and material

Geometry calculation according to

ISO 21771:2007

		----- Gear 1 -----	Gear 2 -----	Gear 3 ---
Center distance (in, mm)	[a]	12.6280,320.750		
Center distance tolerance	ISO 286:2010 Measure js5			
Normal Diametral Pitch (1/in)	[Pnd]	5.64444		
Normal module (in, mm)	[mn]	0.17717, 4.5000		
Normal pressure angle (°)	[αn]	20.0000		
Helix angle at reference circle (°)	[β]	14.0000		
Number of teeth	[z]	87	51	-188
Facewidth (mm)	[b]	60.49	58.92	60.49
Hand of gear		right	left	left

Planetary axles can be placed in regular pitch.:

72 °

	[Q-AGMA2015-1-A2001]	A2	A2	A2
Accuracy grade				
Inner diameter (mm)	[di]	0.00	0.00	
External diameter (mm)	[di]			0.00
Inner diameter of gear rim (mm)	[dbi]	0.00	0.00	
Outer diameter of gear rim (mm)	[dbi]			0.00

Material

Gear 1

Steel, Grade 3, HRC58-64(AGMA), Case-carburized steel, case-hardened
AGMA 2001-C95

Gear 2

Steel, Grade 3, HRC58-64(AGMA), Case-carburized steel, case-hardened
AGMA 2001-C95

Gear 3

Steel, Grade 3, HRC58-64(AGMA), Case-carburized steel, case-hardened
AGMA 2001-C95

Surface hardness	----- Gear 1 -----		----- Gear 2 -----		----- Gear 3 ---	
	HRC 60		HRC 60		HRC 60	
	(lb/in ²), (N/mm ²)		(lb/in ²), (N/mm ²)		(lb/in ²), (N/mm ²)	
Allowable bending stress number	[sat]	74694 , 515.0	74694 , 515.0	74694 , 515.0	74694 , 515.0	
Allowable contact stress number	[sac]	274846 , 1895.0	274846 , 1895.0	274846 , 1895.0	274846 , 1895.0	
Tensile strength (N/mm ²)	[σB]	1035.00	1035.00	1035.00	1035.00	
Yield point (N/mm ²)	[σS]	887.00	887.00	887.00	887.00	
Young's modulus (N/mm ²)	[E]	206843	206843	206843	206843	
Poisson's ratio	[ν]	0.300	0.300	0.300	0.300	
Roughness average value DS, flank (μm)	[RAH]	0.63	0.63	0.63	0.63	
Roughness average value DS, root (μm)	[RAF]	2.40	2.40	2.40	2.40	
Mean roughness height, Rz, flank (μm)	[RZH]	5.00	5.00	5.00	5.00	
Mean roughness height, Rz, root (μm)	[RZF]	16.00	16.00	16.00	16.00	

Information on pre-machining

Gear reference profile

1:

Reference profile	1.25 / 0.38 / 1.0 ISO 53:1998 Profil A	
Final machining stock (mm)	[q]	0.140
Dedendum coefficient	[hfP*]	1.250
Root radius factor	[ρfP*]	0.380 (pfPmax*= 0.472)
Addendum coefficient	[haP*]	1.000
Tip radius factor	[paP*]	0.000
Protuberance height coefficient	[hprP*]	0.000
Protuberance angle	[αprP]	0.000
Tip form height coefficient	[hFaP*]	0.000
Ramp angle	[αKP]	0.000
		not topping

Gear reference profile

2:

Reference profile	1.25 / 0.38 / 1.0 ISO 53:1998 Profil A	
Final machining stock (mm)	[q]	0.140
Dedendum coefficient	[hfP*]	1.250
Root radius factor	[ρfP*]	0.380 (pfPmax*= 0.472)

Addendum coefficient	[haP*]	1.000
Tip radius factor	[paP*]	0.000
Protuberance height coefficient	[hprP*]	0.000
Protuberance angle	[αprP]	0.000
Tip form height coefficient	[hFaP*]	0.000
Ramp angle	[αKP]	0.000
	not topping	

Gear reference profile

3:

Reference profile	1.25 / 0.38 / 1.0 ISO 53:1998 Profil A		
Final machining stock (mm)	[q]	0.140	
Dedendum coefficient	[hfP*]	1.250	
Root radius factor	[ρfP*]	0.380	(ρfPmax* = 0.472)
Addendum coefficient	[haP*]	1.000	
Tip radius factor	[paP*]	0.000	
Protuberance height coefficient	[hprP*]	0.000	
Protuberance angle	[αprP]	0.000	
Tip form height coefficient	[hFaP*]	0.000	
Ramp angle	[αKP]	0.000	
	not topping		

Reference profile of the final tooth form:

Dedendum reference profile	[hfP*]	1.159	1.159	1.159
Tooth root radius Refer. profile	[ρfP*]	0.380	0.380	0.380
Addendum Reference profile	[haP*]	1.000	1.000	1.000
Protuberance height coefficient	[hprP*]	0.000	0.000	0.000
Protuberance angle (°)	[αprP]	0.000	0.000	0.000
Tip form height coefficient	[hFaP*]	0.000	0.000	0.000
Ramp angle (°)	[αKP]	0.000	0.000	0.000

Data for final machining:

Depth of immersion	[hgrind*]	0.975	0.975	0.838
Addendum coefficient Pinion type cutter	[haP0grind*]			1.161
Radius at cutter head	[rgrind*]	0.100	0.100	0.100
Grinding only flank (0), flank & root (1)		0	0	0

Generation grinding (0), form grinding (1)	0	0	0
Type of profile modification:	for high load capacity gearboxes		
Tip relief (µm)	[Ca L/R]	4.0 / 4.0	4.0 / 4.0 4.0 / 4.0
Root relief (µm)	[Cf L/R]	4.0 / 4.0	4.0 / 4.0 4.0 / 4.0
Lubrication type	Oil injection lubrication		
Oil grade, Own Input	Mobil Jet Oil II		
Lubricant base	Synthetic oil based on Ester		
Oil nominal kinematic viscosity at 40°C (mm²/s)	[v40]	27.60	
Oil nominal kinematic viscosity at 100°C (mm²/s)	[v100]	5.10	
Specific density at 15°C (kg/dm³)	[ρ]	1.004	
Oil temperature (°C)	[TS]	70.000	

Gear pair 1

Overall transmission ratio	[itot]	-2.161
Gear ratio	[u]	1.706
Transverse module (mm)	[mt]	4.638
Transverse pressure angle (°)	[αt]	20.562
Working pressure angle (°)	[αwt]	20.913
	[αwt.e/l]	20.919 / 20.908
Working pressure angle at normal section (°)	[αwn]	20.341
Helix angle at operating pitch circle (°)	[βw]	14.031
Base helix angle (°)	[βb]	13.140
Reference center distance (mm)	[ad]	320.006
Pitch on reference circle (mm)	[pt]	14.570
Base pitch (mm)	[pbt]	13.642
Transverse pitch on contact-path (mm)	[pet]	13.642
Sum of profile shift coefficients	[Σxi]	0.1668
Transverse contact ratio	[εα]	1.672
Transverse contact ratio with allowances	[εα.e/m/l]	1.674 / 1.667 / 1.659
Overlap ratio	[εβ]	1.008
Total contact ratio	[εγ]	2.680

Total contact ratio with allowances	[$\epsilon_{y,e/m/i}$]	2.683 / 2.675 / 2.668
Length of path of contact (mm)	[$g_a, \theta/i$]	22.804 (22.839 / 22.638)
Length T1-A (mm)	[T1A]	57.996 (57.961 / 58.082)
Length T1-B (mm)	[T1B]	67.158 (67.158 / 67.078)
Length T1-C (mm)	[T1C]	72.181 (72.159 / 72.203)
Length T1-D (mm)	[T1D]	71.638 (71.603 / 71.723)
Length T1-E (mm)	[T1E]	80.800 (80.800 / 80.720)
Length T2-A (mm)	[T2A]	56.498 (56.498 / 56.447)
Length T2-B (mm)	[T2B]	47.335 (47.300 / 47.450)
Length T2-C (mm)	[T2C]	42.313 (42.300 / 42.326)
Length T2-D (mm)	[T2D]	42.856 (42.856 / 42.805)
Length T2-E (mm)	[T2E]	33.693 (33.658 / 33.808)
Length T1-T2 (mm)	[T1T2]	114.494 (114.459 / 114.529)
Minimal length of contact line (mm)	[Lmin]	100.813
Gear pair 2		
Overall transmission ratio	[i_{tot}]	-2.161
Gear ratio	[u]	-3.686
Transverse module (mm)	[m_t]	4.638
Transverse pressure angle (°)	[α_t]	20.562
Working pressure angle (°)	[α_{wt}]	21.974
	[$\alpha_{wt,\theta/i}$]	21.969 / 21.980
Working pressure angle at normal section (°)	[α_{wn}]	21.370
Helix angle at operating pitch circle (°)	[β_w]	14.130
Base helix angle (°)	[β_b]	13.140
Reference center distance (mm)	[a_d]	317.687
Pitch on reference circle (mm)	[p_t]	14.570
Base pitch (mm)	[p_{bt}]	13.642
Transverse pitch on contact-path (mm)	[p_{et}]	13.642
Sum of profile shift coefficients	[Σx_i]	-0.7034

Transverse contact ratio	[εα]	1.672
Transverse contact ratio with allowances	[εα.e/m/l]	1.683 / 1.674 / 1.666
Overlap ratio	[εβ]	1.008
Total contact ratio	[εγ]	2.680
Total contact ratio with allowances	[εγ.e/m/l]	2.692 / 2.683 / 2.674
Length of path of contact (mm)	[ga, e/l]	22.805 (22.966 / 22.721)
Length T1-A (mm)	[T1A]	33.693 (33.532 / 33.726)
Length T1-B (mm)	[T1B]	42.856 (42.856 / 42.805)
Length T1-C (mm)	[T1C]	44.679 (44.692 / 44.667)
Length T1-D (mm)	[T1D]	47.335 (47.174 / 47.368)
Length T1-E (mm)	[T1E]	56.498 (56.498 / 56.447)
Length T2-A (mm)	[T2A]	153.714 (153.586 / 153.714)
Length T2-B (mm)	[T2B]	162.877 (162.910 / 162.793)
Length T2-C (mm)	[T2C]	164.701 (164.746 / 164.655)
Length T2-D (mm)	[T2D]	167.356 (167.228 / 167.356)
Length T2-E (mm)	[T2E]	176.519 (176.552 / 176.435)
Length T1-T2 (mm)	[T1T2]	120.021 (120.055 / 119.988)
Minimal length of contact line (mm)	[Lmin]	100.815
Gear 1		
Lead height (mm)	[pz]	5084.011
Axial pitch (mm)	[px]	58.437
Profile shift coefficient		
Information on pre-machining	[x]	-0.0859
Information on final machining	[x]	-0.1769
Tooth thickness, arc, in module	[sn*]	1.4420
Tip alteration (mm)	[k*mn]	0.000
Reference diameter (mm)	[d]	403.485
Base diameter (mm)	[db]	377.781
Tip diameter (mm)	[da]	410.893

(mm)	[da.e/i]	410.893 / 410.830
Tip diameter allowances (mm)	[Ada.e/i]	0.000 / -0.063
Tip form diameter (mm)	[dFa]	410.893
(mm)	[dFa.e/i]	410.893 / 410.830
Root diameter (mm)	[df]	391.462
Generating Profile shift coefficient		
Information on pre-machining	[xE.e/i]	-0.1714/ -0.1897
Information on final machining	[xE.e/i]	-0.2624/ -0.2807
Generated root diameter with xE (mm)	[df.e/i]	390.693 / 390.528
(calculated with pre-machining tool)		
Root form diameter (mm)	[dFf]	394.573
(mm)	[dFf.e/i]	393.947 / 393.814
Internal toothing: Calculation dFf with pinion type cutter (z0=		
50 , x0=0.000)		
(calculated with final machining tool)		
Involute length (mm)	[l_dFa-l_dFf]	8.699
Addendum, $m_n(h_{ap}+x+k)$ (mm)	[ha]	3.704
(mm)	[ha.e/i]	3.704 / 3.672
Dedendum (mm)	[hf=mn*(hfP*-x)]	6.012
(mm)	[hf.e/i]	6.396 / 6.479
Tooth height (mm)	[h]	9.716
Virtual gear no. of teeth	[zn]	94.550
Normal tooth thickness at tip circle (mm)	[san]	3.689
(mm)	[san.e/i]	3.430 / 3.344
Normal tooth thickness at tip form circle (mm)	[sFan]	3.689
(mm)	[sFan.e/i]	3.430 / 3.344
Normal space width at root circle (mm)	[efn]	3.685
(mm)	[efn.e/i]	3.750 / 3.765

Gear 2

Lead height (mm)	[pz]	2980.282
Axial pitch (mm)	[px]	58.437
Profile shift coefficient		
Information on pre-machining	[x]	0.4347
Information on final machining	[x]	0.3437
Tooth thickness, arc, in module	[sn*]	1.8210

Tip alteration (mm)	[k*mn]	0.000
Reference diameter (mm)	[d]	236.526
Base diameter (mm)	[db]	221.458
Tip diameter (mm)	[da]	248.619
(mm)	[da.e/i]	248.619 / 248.573
Tip diameter allowances (mm)	[Ada.e/i]	0.000 / -0.046
Tip form diameter (mm)	[dFa]	248.619
(mm)	[dFa.e/i]	248.619 / 248.573
Root diameter (mm)	[df]	229.188
Generating Profile shift coefficient		
Information on pre-machining	[xE.e/i]	0.3736/ 0.3583
Information on final machining	[xE.e/i]	0.2826/ 0.2674
Generated root diameter with xE (mm)	[df.e/i]	228.638 / 228.501
(calculated with pre-machining tool)		
Root form diameter (mm)	[dFf]	231.835
(mm)	[dFf.e/i]	231.377 / 231.264
Internal toothing: Calculation dFf with pinion type cutter (z0=		
50 , x0=0.000)		
(calculated with final machining tool)		
Involute length (mm)	[l_dFa-l_dFf]	9.103
Addendum, $m_n(h_{aP^*}+x+k)$ (mm)	[ha]	6.047
(mm)	[ha.e/i]	6.047 / 6.024
Dedendum (mm)	[hf=mn*(hfP*-x)]	3.669
(mm)	[hf.e/i]	3.944 / 4.012
Tooth height (mm)	[h]	9.716
Virtual gear no. of teeth	[zn]	55.426
Normal tooth thickness at tip circle (mm)	[san]	3.251
(mm)	[san.e/i]	3.063 / 2.989
Normal tooth thickness at tip form circle (mm)	[sFan]	3.251
(mm)	[sFan.e/i]	3.063 / 2.989
Normal space width at root circle (mm)	[efn]	3.499
(mm)	[efn.e/i]	3.545 / 3.557

Gear 3

Lead height (mm)	[pz]	10986.138
Axial pitch (mm)	[px]	58.437
Profile shift coefficient		

Information on pre-machining	[x]	-0.9561
Information on final machining	[x]	-1.0470
Tooth thickness, arc, in module	[sn*]	0.8086
Tip alteration (mm)	[k*mn]	0.000
Reference diameter (mm)	[d]	871.899
Base diameter (mm)	[db]	816.354
Tip diameter (mm)	[da]	872.323
(mm)	[da.e/i]	872.323 / 872.233
Tip diameter allowances (mm)	[Ada.e/i]	0.000 / -0.090
Tip form diameter (mm)	[dFa]	872.323
(mm)	[dFa.e/i]	872.323 / 872.233
Root diameter (mm)	[df]	891.754
Generating Profile shift coefficient		
Information on pre-machining	[xE.e/i]	-1.0690/ -1.0935
Information on final machining	[xE.e/i]	-1.1600/ -1.1844
Generated root diameter with xE (mm)	[df.e/i]	892.990 / 892.770
(calculated with pre-machining tool)		
Root form diameter (mm)	[dFf]	889.344
(mm)	[dFf.e/i]	890.701 / 890.496
Internal toothing: Calculation dFf with pinion type cutter (z0=		
50 , x0=0.000)		
(calculated with final machining tool)		
Involute length (mm)	[_dFa-_dFf]	9.183
Addendum, $m_n(h_{aP}+x+k)$ (mm)	[ha]	-0.212
(mm)	[ha.e/i]	-0.167 / -0.212
Dedendum (mm)	[hf=mn*(hfP*-x)]	9.927
(mm)	[hf.e/i]	10.436 / 10.546
Tooth height (mm)	[h]	9.716
Virtual gear no. of teeth	[zn]	204.314
Normal tooth thickness at tip circle (mm)	[san]	3.795
(mm)	[san.e/i]	3.425 / 3.311
Normal tooth thickness at tip form circle (mm)	[sFan]	3.795
(mm)	[sFan.e/i]	3.425 / 3.311
Normal space width at root circle (mm)	[efn]	2.785
(mm)	[efn.e/i]	2.732 / 2.720

Gear specific pair data Gear pair 1, Gear 1

Operating pitch diameter (mm)	[dw]	404.424
(mm)	[dw.e/i]	404.440 / 404.408
Active tip diameter (mm)	[dNa]	410.893
(mm)	[dNa.e/i]	410.893 / 410.830
Theoretical tip clearance (mm)	[c]	0.710
Effective tip clearance (mm)	[c.e/i]	1.097 / 0.972
Active root diameter (mm)	[dNf]	395.187
(mm)	[dNf.e/i]	395.237 / 395.166
Reserve (dNf-dFf)/2 (mm)	[cF.e/i]	0.712 / 0.610
Max. sliding velocity at tip (m/s)	[vga]	21.982
Specific sliding at the tip	[ζa]	0.289
Specific sliding at the root	[ζf]	-0.662
Mean specific sliding	[ζm]	0.357
Sliding factor on tip	[Kga]	0.115
Sliding factor on root	[Kgf]	-0.190
Roll angle at dFa (°)	[ξdFa.e/i]	24.509 / 24.485
Roll angle to dNa (°)	[ξdNa.e/i]	24.509 / 24.485
Roll angle to dNf (°)	[ξdNf.e/i]	17.618 / 17.581
Roll angle at dFf (°)	[ξdFf.e/i]	16.940 / 16.869
Diameter of single contact point B (mm)	[d-B]	400.948 (400.948 / 400.895)
Diameter of single contact point D (mm)	[d-D]	404.038 (404.013 / 404.098)
Addendum contact ratio	[ε]	0.632 (0.633 / 0.624)

Gear specific pair data Gear pair 1, Gear 2

Operating pitch diameter (mm)	[dw]	237.076
(mm)	[dw.e/i]	237.085 / 237.067
Active tip diameter (mm)	[dNa]	248.619
(mm)	[dNa.e/i]	248.619 / 248.573
Theoretical tip clearance (mm)	[c]	0.710
Effective tip clearance (mm)	[c.e/i]	1.212 / 1.082
Active root diameter (mm)	[dNf]	231.483
(mm)	[dNf.e/i]	231.550 / 231.463
Reserve (dNf-dFf)/2 (mm)	[cF.e/i]	0.143 / 0.043

Max. sliding velocity at tip (m/s)	[vga]	36.174
Specific sliding at the tip	[ζa]	0.398
Specific sliding at the root	[ζf]	-0.406
Mean specific sliding	[ζm]	0.357
Sliding factor on tip	[Kga]	0.190
Sliding factor on root	[Kgf]	-0.115
Roll angle at dFa (°)	[ξdFa.e/i]	29.234 / 29.208
Roll angle to dNa (°)	[ξdNa.e/i]	29.234 / 29.208
Roll angle to dNf (°)	[ξdNf.e/i]	17.494 / 17.416
Roll angle at dFf (°)	[ξdFf.e/i]	17.340 / 17.239
Diameter of single contact point B (mm)	[d-B]	240.844 (240.817 / 240.935)
Diameter of single contact point D (mm)	[d-D]	237.466 (237.466 / 237.429)
Addendum contact ratio	[ε]	1.040 (1.041 / 1.035)

Gear specific pair data Gear pair 2, Gear 2

Operating pitch diameter (mm)	[dw]	238.807
(mm)	[dw.e/i]	238.797 / 238.816
Active tip diameter (mm)	[dNa]	248.619
(mm)	[dNa.e/i]	248.619 / 248.573
Theoretical tip clearance (mm)	[c]	0.817
Effective tip clearance (mm)	[c.e/i]	1.471 / 1.313
Active root diameter (mm)	[dNf]	231.483
(mm)	[dNf.e/i]	231.503 / 231.389
Reserve (dNf-dFf)/2 (mm)	[cF.e/i]	0.119 / 0.006
Max. sliding velocity at tip (m/s)	[vga]	13.846
Specific sliding at the tip	[ζa]	0.152
Specific sliding at the root	[ζf]	-0.238
Mean specific sliding	[ζm]	0.171
Sliding factor on tip	[Kga]	0.072
Sliding factor on root	[Kgf]	-0.067
Roll angle at dFa (°)	[ξdFa.e/i]	29.234 / 29.208
Roll angle to dNa (°)	[ξdNa.e/i]	29.234 / 29.208
Roll angle to dNf (°)	[ξdNf.e/i]	17.451 / 17.351
Roll angle at dFf (°)	[ξdFf.e/i]	17.340 / 17.239

Diameter of single contact point B (mm)	[d-B]	237.466 (237.466 / 237.429)
Diameter of single contact point D (mm)	[d-D]	240.844 (240.718 / 240.870)
Addendum contact ratio	[ε]	0.866 (0.865 / 0.864)

Gear specific pair data Gear pair 2, Gear 3

Operating pitch diameter (mm)	[dw]	880.307
(mm)	[dw.e/i]	880.341 / 880.272
Active tip diameter (mm)	[dNa]	872.323
(mm)	[dNa.e/i]	872.323 / 872.233
Theoretical tip clearance (mm)	[c]	0.817
Effective tip clearance (mm)	[c.e/i]	1.173 / 1.035
Active root diameter (mm)	[dNf]	889.421
(mm)	[dNf.e/i]	889.448 / 889.354
Reserve (dNf-dFf)/2 (mm)	[cF.e/i]	0.673 / 0.524
Max. sliding velocity at tip (m/s)	[vga]	15.602
Specific sliding at the tip	[ζa]	0.192
Specific sliding at the root	[ζf]	-0.180
Mean specific sliding	[ζm]	0.171
Sliding factor on tip	[Kga]	0.067
Sliding factor on root	[Kgf]	-0.072
Roll angle at dFa (°)	[ξdFa.e/i]	21.559 / 21.577
Roll angle to dNa (°)	[ξdNa.e/i]	21.559 / 21.577
Roll angle to dNf (°)	[ξdNf.e/i]	24.766 / 24.783
Roll angle at dFf (°)	[ξdFf.e/i]	24.967 / 25.003
Diameter of single contact point B (mm)	[d-B]	878.948 (878.973 / 878.886)
Diameter of single contact point D (mm)	[d-D]	882.307 (882.211 / 882.307)
Addendum contact ratio	[ε]	0.805 (0.818 / 0.802)

General influence factors

----- Gear 1 ----- Gear 2 ----- Gear 3 ---

Calculated with the operating pitch circle:

Nominal circumferential force (lb)	[Wt,Ftw]	2359.21	(10494.27	N)
Nominal circumferential force (lb)	[Wt,Ftw]	2342.11	(10418.22	N)

Axial force (lb)	[Faw]	589.58	(2622.60	N)	
Axial force (lb)	[Faw]	589.58	(2622.60	N)	
Axial force, total (N)	[Fatot = p*Fa]	2947.92	(13113.01	N)	
Axial force, total (N)	[Fatot = p*Fa]	2947.92	(13113.01	N)	
Radial force (lb)	[Frw]	901.52	(4010.17	N)	
Radial force (lb)	[Frw]	945.05	(4203.78	N)	
Net face width of narrowest member (in)	[F,b]	2.32	(58.92	mm)	
Net face width of narrowest member (in)	[F,b]	2.32	(58.92	mm)	
Circumferential force per in (lb/in)	[w]	1016.95	(178.10	N/mm)	
Circumferential force per in (lb/in)	[w]	1009.58	(176.80	N/mm)	
Pitch line velocity (ft/min)	[vt]	37515.80	(190.58	m/s)	
Pitch line velocity (ft/min)	[vt]	37789.64	(191.97	m/s)	
Gearbox type:	Precision enclosed gear units				
Mesh alignment factor	[Cma]	0.097	0.097		
Mounting procedure:	Contact improved by adjusting at assembly				
Mesh alignment correction factor	[Ce]	0.800			
Gearing:	without longitudinal flank modification				
Lead correction factor	[Cmc]	1.000	1.000		
Pinion proportion factor	[Cpf]	0.041	0.041		
Pinion proportion modifier	[Cpm]	1.000	1.000		
Small offset	[s1/s < 0.175]				
Face load distribution factor	[Cmf]	1.119	1.119		
Load distribution factor	[Km]	1.119	1.119		
Transmission accuracy level number	[Av]	3			
Dynamic factor introduced:					
Dynamic factor	[Kv]	1.100			
Number of load cycles (in mio.)	[NL]	189000.0	64482.4	87462.8	

Tooth root load capacity

	----- Gear 1 -----	Gear 2 -----	Gear 3 -----	
Rim thickness factor	[KB]	1.000	1.000	1.000
Size factor	[KS]	1.000	1.000	1.000
Limiting Variation in action (in/10000)	[LimVarAc]	5.0	5.0	
Load sharing:				
0 = No, Loaded at tip, 1 = Yes, Loaded at HPSTC		0	0	
Calc. as helical gear (0) / as LACR (1)		0	0 / 0	0

Load angle (°)	[φnL]	22.64	26.24 /26.24	20.97		
Determination of factor Y by graphical method						
Calculated with generating profile shift coefficient	[xE.m]	-0.2715	0.2750	-1.1722		
Height of Lewis parabola (in)	[hF]	0.327	0.324 /0.324	0.339		
Height of Lewis parabola (mm)	[hF]	8.318	8.218 /8.218	8.600		
Tooth thickness at critical section (in)	[sF]	0.395	0.399 /0.399	0.450		
Tooth thickness at critical section (mm)	[sF]	10.030	10.137 /10.137	11.442		
Radius at curvature of fillet curve (in)	[ρF]	0.030	0.024 /0.024	0.023		
Radius at curvature of fillet curve (mm)	[ρF]	0.767	0.619 /0.619	0.588		
Helical factor	[Ch]		1.27	1.27		
Helix angle factor	[Kψ]		0.94	0.94		
Tooth form factor Y	[Y]	0.611	0.667 /0.662	0.756		
Stress correction factor	[Kf]	1.780	1.852 /1.852	1.955		
Bending strength geometry factor J	[J]	0.588	0.616 /0.612	0.662		
Bending stress number (lb/in ²)	[st]	31237.1	29785.8 /29785.327537.2			
Bending stress number (N/mm ²)	[st]	215.4	205.4 /205.4	189.9		
Stress cycle factor	[YN]	0.854	0.871	0.866		
(for general applications)						
Allowable bending stress number (lb/in ²)	[sat]	74694.4	74694.4	74694.4		
Allowable bending stress number (N/mm ²)	[sat]	515.0	515.0	515.0		
Temperature factor	[KT]	1.000	1.000	1.000		
Reliability factor (99.00 %)	[KR]		1.000			
Reverse loading factor	[-]	1.000	0.700	1.000		
Effective allow. b.s.n. (lb/in ²)	[sateff]	63791.5	45517.0 / 45517.064672.4			
Effective allow. b.s.n. (N/mm ²)	[sateff]	439.8	313.8 /313.8	445.9		
Allowable transmitted power (hp, kW)	[Pat]	18257.4	,13614.48 13661.9	,10187.62 / 13662.2	,10187.80	20996.5 , 15657.01
Note: Allowable transmitted power Patcalculated including the following values: Ky, Ko, KR, SFmin						
Allowable transmitted power						
at unity service factor (hp, kW)	[Patu]	73326.4	,54679.16 54869.7	,40916.05 / 54870.6	,40916.77	84327.3 , 62882.47
Note: Allowable transmitted power Patu calculated with Ky=1, Ko=1, KR=1, SFmin=1						
Transmittable power including SFmin (-, kW)	[Patu/SFmin]	48884.3	,36452.78 36579.8	,27277.37 /36580.4	,27277.85	56218.2 , 41921.65
Note: Transmittable power including SFmin calculated with Ky=1, Ko=1, KR=1						
Unit load (lb/in ²)	[UL]		5740.12	5698.53		
Allowable unit load (lb/in ²)	[Uat]	7814.9	5847.8 / 5805.68922.2			
Required safety factor	[SFmin]	1.500	1.500	1.500		
Safety factor, Bending	[sateff/st]	2.042	1.528 /1.528	2.349		

Yield strength factor	[Ky]	0.50		
Core hardness (HV)	[HV]	316	316	316
Core hardness (HB)	[HB]	300	300	300
Allowable yield strength number (lb/in ²)	[say]	111800.00	111800.00	111800.00
Stress correction factor	[Kf]	1.780	1.852 / 1.852 1.955	
Maximum peak tangential load (lb, N)	[Wmax]	5308.21	23612.10	5308.21 , 23612.10
Load distribution factor (overload)	[Kmy]	1.10 1.10		
Safety for yield strength	[Syield]	3.55	3.88 / 3.88	4.43
	[Syield = say*Ky / (Wmax*Pd*Kmy/F/J/Kf)]			

Note: The calculation is performed with coefficient Kf and the core hardness in HB.
 The core hardness value in the database can differ considerably from the actual hardness.
 The value must be checked in critical cases..

Flank safety

		----- Gear 1 -----	Gear 2 -----	Gear 3 ---
		(√lb/in), (√N/mm)	(√lb/in), (√N/mm)	
Elastic coefficient	[Cp]	2290.00	,190.20 2290.00	, 190.20
Size factor	[Ks]	1.000	1.000	1.000
Load sharing ratio	[mN]		0.584	0.584
Helical overlap factor	[Cψ]		1.000	1.000
Geometry factor I	[I]		0.185	0.421
		(lb/in ²), (N/mm ²)	(lb/in ²), (N/mm ²)	
Contact stress number	[sc]	100864.8	,695.4 66374.4	, 457.6
Stress cycle factor (for general applications)	[ZN]	0.797	0.817	0.812
Surface condition factor	[Cf]	1.000	1.000 / 1.000	1.000
Hardness ratio factor	[CH]	1.000	1.000 / 1.000	1.000
Temperature factor	[KT]	1.000	1.000	1.000
Reliability factor	[KR]	99.000		{ZS.CRAGMA}
Allowable contact stress number (lb/in ²)	[sac]	274846.4	274846.4	274846.4
Allowable contact stress number (N/mm ²)	[sac]	1895.0	1895.0	1895.0
Effective allow. c.s.n. (lb/in ²)	[saceff]	219149.2	224637.0 / 224637.0	223067.6
Effective allow. c.s.n. (N/mm ²)	[saceff]	1511.0	1548.8 / 1548.8	1538.0
Allowable transmitted power (hp)	[Pac]	28135.6 (20980.60 kW)	29562.4 (22044.53 kW)	68268.2 (50907.24 kW) 67317.6 (50198.41 kW)

Note: Allowable transmitted power Paccalculated including the following values: Ky, Ko, KR, SHmin

Allowable transmitted power at unity service factors (hp)	[Pacu]	169499.6	(126395.02 kW)	178095.0	(132804.54 kW)	411273.1	(306684.29 kW)	405546.6	(302414.04 kW)
Note: Allowable transmitted power Pacu calculated including the following values: Ky=1, Ko=1, KR=1, SHmin=1									
Transmittable power including SHmin (hp)	[Pacu/SHmin ²]	75333.2	(56175.56 kW)	79153.3	(59024.24 kW)	182788.0	(136304.13 kW)	180242.9	(134406.24 kW)
Note: Allowable transmitted power Pacu/SHmin ² calculated including the following values: Ky=1, Ko=1, KR=1									
Contact load factor (lb/in ²) (N/mm ²)	[K]	172.8	, 1.192						
Allowable contact load factor (lb/in ²)	[Kac]	815.8	857.2	/896.3	883.8				
Required safety factor	[SHmin]	1.500	1.500	1.500					
Safety factor (Pitting)	[saceff/sc]	2.173	2.227	/3.384	3.361				

Service Factors, with Ky= 1.000 :

Service factor for tooth root	[KSF]	5.468	4.092	/4.092	6.288
Service factor for pitting	[CSF]	12.640	13.280	/30.668	30.241
Service factor for gear set	[SF]		4.092	4.092	

Note: Service factors calculated with Ky=1, Ko=1, KR=1, SFmin=1, SHmin=1

Transmittable power including required service factors KSFmin, CSFmin (hp) 36579.79 (27277.37 kW)

KSFmin = 1.50 , CSFmin = 2.25

Service Factors, with Ky= 1.190 :

Service factor for tooth root	[KSF]	4.595	3.438	/3.438	5.284
Service factor for pitting	[CSF]	10.621	11.160	/25.772	25.413
Service factor for gear set	[SF]		3.438	3.438	

Note: Service factors calculated with Ko=1, KR=1, SFmin=1, SHmin=1

The equations used for Pat, Pac, Pacu, Patu, Pa are according AGMA2001.

Micropitting according to ISO/TS 6336-22:2018

Pairing Gear	1 -2 :		
Calculation of permissible specific film thickness			
Lubricant load according to FVA Info sheet 54/7	10, Mobil Jet Oil II		
Reference data FZG-C Test:			
Torque (Nm)	[T1Ref]	265.100	
Line load at contact point A (N/mm)	[FbbRef,A]	236.300	
Oil temperature (°C)	[θOilRef]	90.000	
Tooth mass temperature (°C)	[θMRef]	137.638	

Contact temperature (°C)	[θBRef,A]	309.560	
Lubrication gap thickness (µm)	[hRef,A]	0.016	
Specific film thickness in test	[λGFT]	0.031	
Material coefficient	[WW]	1.000	
Permissible specific film thickness	[λGFP]	0.043	
Interim results in accordance with ISO/TS 6336-22:2014			
Coefficient of friction	[µm]	0.033	
Lubricant factor	[XL]	1.300	
Roughness factor	[XR]	0.857	
Lubrication coefficient for lubrication type	[XS]	1.200	
Tooth mass temperature (°C)	[θM]	86.221	
Tip relief factor	[XCα(A)]	1.266	
Loss factor	[HV]	0.081	
Equivalent Young's modulus (N/mm²)	[Er]	227300.000	
Pressure-viscosity coefficient (m²/N)	[α38]	0.01000	
Dynamic viscosity (Ns/m²)	[ηtM]	6.511	
Roughness average value (µm)	[Ra]	0.630	
Calculation of speeds, load distribution and flank curvature according to method B following ISO/TS 6336-22:2018			
Ca taken as optimal in the calculation (0=no, 1=yes)		0	0
Calculation at point (0:A, 1:AB, 2:B, 3:C, 4:D, 5:DE, 6:E, -1:No Point)		6	
Diameter (mm)	[dy]	410.893	231.483
Relative radius of curvature (mm)	[pred]	24.417	
Load sharing factor	[XY]	0.613	
(XY interpolated between XY(eps.b=0.8) and XY(eps.b=1.2) according ISO/TC60/WG6)			
Contact stress (N/mm²)	[pH]	416.014	
Contact stress (N/mm²)	[pdyn]	755.189	
Minimal specific film thickness	[λGFY]	1.082	(hY= 0.681 µm)
Safety against micropitting	[Sλ(B)]	24.921	
For interim results, refer to file:	Micropitting_12.tmp		
Pairing Gear 2 -3 :			
Calculation of permissible specific film thickness			
Material coefficient	[WW]	1.000	
Permissible specific film thickness	[λGFP]	0.043	
Interim results in accordance with ISO/TS 6336-22:2014			
Coefficient of friction	[µm]	0.022	

Lubricant factor	[XL]	1.300	
Roughness factor	[XR]	0.696	
Lubrication coefficient for lubrication type	[XS]	1.200	
Tooth mass temperature (°C)	[θM]	74.730	
Tip relief factor	[XCa(A)]	1.741	
Loss factor	[HV]	0.034	
Equivalent Young's modulus (N/mm ²)	[Er]	227300.000	
Pressure-viscosity coefficient (m ² /N)	[α38]	0.01000	
Dynamic viscosity (Ns/m ²)	[ηtM]	8.672	
Roughness average value (μm)	[Ra]	0.630	
Calculation of speeds, load distribution and flank curvature according to method B following ISO/TS 6336-22:2018			
Ca taken as optimal in the calculation (0=no, 1=yes)		0	1
Calculation at point (0:A, 1:AB, 2:B, 3:C, 4:D, 5:DE, 6:E, -1:No Point)			
		1	
Diameter (mm)	[dy]	234.314	875.594
Relative radius of curvature (mm)	[pred]	31.651	
Load sharing factor	[XY]	0.590	
(XY interpolated between XY(eps.b=0.8) and XY(eps.b=1.2) according ISO/TC60/WG6)			
Contact stress (N/mm ²)	[pH]	358.664	
Contact stress (N/mm ²)	[pdyn]	651.081	
Minimal specific film thickness	[λGFY]	1.834	(hY= 1.155 μm)
Safety against micropitting	[SA(B)]	42.243	
For interim results, refer to file:	Micropitting_23.tmp		

The calculation of micropitting specified in ISO/TS6336-22 is not designed for use with internal toothing because it has not yet been subject to sufficient investigation. The results can only be used for information purposes.

Scuffing load capacity

Results from	AGMA 925-A03, Details see in the specific calculation sheet
Probability of wear (%)	[Pwear] 12.637
Probability of scuffing (%)	[Pscuff] 5% or lower

Measurements for tooth thickness

Gear 1 Gear 2 Gear 3

Information on pre-machining

Tooth thickness allowance (final machining) (mm)	[As.e/i]	-0.280 /-0.340	-0.200 /-0.250	-0.370 /-0.450
Input for final machining stock, per flank (mm)	[q]	0.140	0.140	0.140
Additional measure for pre-machining (mm)	[ΔAs_pre.e/i]	0.298 /0.298	0.298 /0.298	0.298 /0.298
Tooth thickness allowance (normal section) (mm)	[As_pre.e/i]	0.018 /-0.042	0.098 /0.048	-0.072 /-0.152
Number of teeth spanned	[k]	11.000	7.000	-0.000
Base tangent length with allowance (mm)	[Wk.e/i]	144.936 /144.880	91.003 / 90.956	-0.000 / -0.000
Effective diameter of ball/pin (mm)	[DMeff]	7.500	8.000	-7.500
Diametral two ball measure (mm)	[MdK.e/i]	411.876 /411.714	251.122 /251.005	871.531 /871.322

Information on final machining

Tooth thickness tolerance		DIN 3967 ab25	DIN 3967 ab25	DIN 3967 ab25
Tooth thickness allowance (normal section) (mm)	[As.e/i]	-0.280 /-0.340	-0.200 /-0.250	-0.370 /-0.450
Number of teeth spanned	[k]	11.000	7.000	-0.000
(Internal toothing: k = (Measurement gap number)				
Base tangent length (no backlash) (mm)	[Wk]	144.919	90.911	-0.000
Base tangent length with allowance (mm)	[Wk.e/i]	144.656 /144.600	90.723 /90.676	-0.000 /-0.000
Diameter of measuring circle (mm)	[dMWk.m]	403.181	238.421	-0.000
Theoretical diameter of ball/pin (mm)	[DM]	7.520	7.852	7.516
Effective diameter of ball/pin (mm)	[DMeff]	7.500	8.000	7.500
Radial single-ball measurement backlash free (mm)	[MrK]	205.947	125.504	435.567
Radial single-ball measurement (mm)	[MrK.e/i]	205.566 /205.483	125.269 /125.209	436.152 /436.048
Diameter of measuring circle (mm)	[dMMr.m]	401.039	239.411	882.448
Diametral measurement over two balls without clearance (mm)	[MdK]	411.828	250.893	871.134
Diametral two ball measure (mm)	[MdK.e/i]	411.066 /410.901	250.422 /250.304	872.304 /872.097
Measurement over pins according to DIN 3960 (mm)	[MdR.e/i]	411.131 /410.967	250.537 /250.419	-0.000 /-0.000
Measurement over 2 pins, free, according to AGMA 2002 (mm)	[dk2f.e/i]	411.061 /410.897	250.414 /250.296	0.000 /0.000
Measurement over 2 pins, transverse, according to AGMA 2002 (mm)	[dk2t.e/i]	411.197 /411.032	250.651 /250.532	0.000 /0.000
Measurement over 3 pins, axial, according to AGMA 2002 (mm)	[dk3A.e/i]	411.131 /410.967	250.537 /250.419	-0.000 /-0.000
Measurement over 3 pins with allowance (mm)	[Md3R.e/i]	0.000 /0.000	0.000 /0.000	-0.000 /-0.000
Note: Internal gears with helical teeth cannot be measured with rollers.				
Chordal tooth thickness in reference circle (mm)	[sc]	6.489	8.193	3.639
(mm)	[sc.e/i]	6.210 /6.151	7.995 /7.946	3.268 /3.188

Reference chordal height from da.m (mm)	[ha]	3.713	6.102	-0.193
Tooth thickness, arc (mm)	[sn]	6.489	8.194	3.639
(mm)	[sn.e/i]	6.209 /6.149	7.994 /7.944	3.269 /3.189
Backlash free center distance (mm)	[aControl.e/i]	320.097 /319.946	321.480 /321.645	
Backlash free center distance, allowances (mm)	[jta]	-0.653 /-0.804	0.730 /0.895	
dNf.i with aControl (mm)	[dNf0.i]	393.876	230.201 / 230.078	891.315
Reserve (dNf0.i-dFf.e)/2 (mm)	[cF0.i]	-0.035	-0.588 / -0.650	-0.409
Tip clearance (mm)	[c0.i(aControl)]	0.180	0.290 /0.596	0.152
Center distance allowances (mm)	[Aa.e/i]	0.013 /-0.013	-0.013 /0.013	
Circumferential backlash from Aa (mm)	[jtw_Aa.e/i]	0.010 /-0.010	0.010 /-0.010	
Radial backlash (mm)	[jrw]	0.817 /0.641	0.907 /0.717	
Circumferential backlash, transverse section (mm)	[jtw]	0.619 /0.486	0.738 /0.583	
Normal backlash (mm)	[jnw]	0.563 /0.443	0.666 /0.527	
Torsional angle on input with output fixed:				
Total torsional angle (°)	[j.tSys]	0.3776/0.3073		

Toothing tolerances

		----- Gear 1 -----	Gear 2 -----	Gear 3 ---
Following	AGMA 2000-A88			
Accuracy grade	[Q-AGMA2000]	15	15	15
Pitch Variation Allowable (µm)	[VpA]	2.60	2.30	2.90
Runout Radial Tolerance (µm)	[VrT]	12.00	10.00	14.00
Profile Tolerance (µm)	[VphiT]	3.80	3.50	4.20
Tooth Alignment Tolerance (µm)	[VpsiT]	4.90	4.80	4.90
Composite Tolerance, Tooth-to-Tooth (µm)	[VqT]	2.90	2.90	2.90
Composite Tolerance, Total (µm)	[VcqT]	7.90	7.30	8.90
AGMA <-> ISO: VpA <-> fpbT, VrT <-> FrT, VpsiT <-> FbT, VqT <-> fidT, VcqT <-> FidT				
According to AGMA 2015-1-A01 & 2015-2-A06				
Accuracy grade	[Q-AGMA2015]	A2	A2	A2
Single pitch deviation (µm)	[fptT]	2.70	2.60	3.20
Total cumulative pitch deviation (µm)	[FpT]	12.00	10.00	16.00
Profile form deviation (µm)	[ffaT]	3.30	3.00	3.80

Profile slope deviation (µm)	[fHαT]	2.70	2.40	3.10
Total profile deviation (µm)	[FαT]	4.20	3.90	5.00
Helix form deviation (µm)	[ffβT]	2.80	2.70	3.00
Helix slope deviation (µm)	[fHβT]	2.80	2.70	3.00
Total helix deviation (µm)	[FβT]	3.90	3.70	4.30
Single flank composite, total (µm)	[FisT]	13.00	11.00	19.00
Single flank composite, tooth-to-tooth (µm)	[fisT]	1.20	1.00	1.70
Radial composite, total (µm)	[FidT]	12.00	10.00	16.00
Radial composite, tooth-to-tooth (µm)	[fidT]	2.20	1.90	3.00
Following	AGMA 2015-2-B15			
Radial composite, total (µm)	[FidT]	34.00	(R20) 31.00	(R20) 36.00 (R20)
Radial composite, tooth-to-tooth (µm)	[fidT]	15.00	(R20) 15.00	(R20) 14.00 (R20)

Axis alignment tolerances (recommendation acc. to ISO TR 10064-3:1996, Quality

		2		
Maximum value for deviation error of axis (µm)	[fΣβ]		2.66	2.66
Maximum value for inclination error of axes (µm)	[fΣδ]		5.33	5.33

Modifying and defining the tooth form

Profile and tooth trace modifications for gear 1

Symmetric (both flanks)

- Tip relief, linear
Caa = 4.000 µm LCa = 2.027 *mn dCa = 404.066 mm
- Root relief, linear
Caf = 4.000 µm LCf = 2.514 *mn dCf = 400.948 mm
- Helix angle modification, tapered or conical
CHb = -0.325 µm
CHβ = -0.325 µm → Right Tooth Flank β.eff = 14.0003°-right Left Tooth Flank β.eff = 13.9997°-right
- flankline crowning
Cb = 0.106 µm
rcrown = 4302771 mm

Profile and tooth trace modifications for gear 2

Symmetric (both flanks)

- Tip relief, linear

Caa = 4.000 µm LCa = 2.031 *mn dCa = 240.864 mm
 - Root relief, linear
 Caf = 4.000 µm LCf = 2.077 *mn dCf = 237.466 mm

Profile and tooth trace modifications for gear 3
Symmetric (both flanks)

- Tip relief, linear
 Caa = 4.000 µm LCa = 2.050 *mn dCa = -878.996 mm
 - Root relief, linear
 Caf = 4.000 µm LCf = 2.336 *mn dCf = -882.307 mm

Tip relief verification
 Diameter (mm) [dcheck] 410.740 248.483 -872.413
 Tip relief left/right (µm) [Ca L/R] 3.9 / 3.9 3.9 / 3.9 3.9 / 3.9

Data for the tooth form calculation :

Calculation of Sun gear

Tooth form, Sun gear, Step 1: Automatic (pre-machining)
 haP* = 1.000, hfP* = 1.250, pfP* = 0.380

Calculation of Planets

Tooth form, Planets, Step 1: Automatic (pre-machining)
 haP* = 0.975, hfP* = 1.250, pfP* = 0.380

Calculation of Internal gear

Tooth form, Internal gear, Step 1: Automatic (pre-machining)
 z0 = 50, x0 = 0.0000, da0 = 243.594 mm, a0 = -324.643 mm
 haP0* = 1.301, paP0* = 0.380, hfP0* = 0.989, pfP0* = 0.000

Supplementary data

Singular tooth stiffness (N/mm/ μ m)	[c]	15.494	15.363	
Meshing stiffness (N/mm/ μ m)	[cy]	23.299	23.102	
Mass (kg)	[m]	59.868	20.682	24.594
Total mass (kg)	[mGes]	187.873		
Moment of inertia for system, relative to the input: calculation without consideration of the exact tooth shape				
Single gears (da+df)/2...di (kg*m ²)	[J]	1.20442	0.14755	4.98682
System (da+df)/2...di (kg*m ²)	[J]	4.41929		
Torsional stiffness at driving gear with fixed driven gear:				
Torsional stiffness (MNm/rad)	[cr]	52.622		
Torsion when subjected to nominal torque (°)	[δcr]	0.012		
Mean coefficient of friction (as defined in Niemann)	[μ _n]	0.040	0.033	
Wear sliding coef. by Niemann	[ζ _w]	0.552	0.287	
Loss factor	[HV]	0.081	0.034	
Meshing power (kW)		10000.000	10000.000	
Gear power loss (kW)	[PVZ]	6.419	2.225	
Total power loss (kW)		43.217		
Total efficiency		0.996		
Sound pressure level according to Masuda, without contact analysis	[dB(A)]	118.1	120.0	

Service life, damage

Required safety for tooth root	[SFmin]	1.50		
Required safety for tooth flank	[SHmin]	1.50		
Service life (calculated with required safeties):				
System service life (h)	[Hatt]	198963		
Tooth root service life (h)	[HFatt]	1e+06	1.99e+05	1e+06
Tooth flank service life (h)	[HHatt]	1e+06	1e+06	1e+06

Note: The entry 1e+006 h means that the Service life > 1,000,000 h.

Damage calculated on the basis of the required service life (70000.0 h)					
F1%	F2%	F3%	H1%	H2%	H3%
0.00	35.1824	0.0000	0.0000	0.0000	0.0000

Damage calculated on basis of system service life [Hatt] (198963.1 h)

F1%	F2%	F3%	H1%	H2%	H3%
0.00	100.0000	0.0000	0.0000	0.0000	0.0000

Remarks:

- Symbols used in []: [xx,yy] xx as used in AGMA 2001-D04, yy as used in AGMA 2101-D04
- Specifications with [e/i] imply: Maximum [e] and minimum value [i] for
Taking all tolerances into account
Specifications with [m] imply: Mean value within tolerance
- For the backlash tolerance, the center distance tolerances and the tooth thickness allowance are taken into account.
The maximum and minimum clearance according to the largest or smallest allowances are defined.
The calculation is performed for the operating pitch circle.
 $sateff = sat * KL / KT / KR * Kwb / SF$ (SF = 1.0)
LACR = Spur gear or helical gear with $\epsilon\beta$ (mF) < 1.0
PSTC = Point of Single Tooth Contact
- Cycle factors YN, ZN are expanded over 10^{10} (following the method used by AGMA programm)

End of Report lines: 931

List of Symbols

FS	Fine sizing
α_n	Normal pressure angle
ϵ_α	Transverse contact ratio
ϵ_β	Overlap contact ratio
ϵ_γ	Total contact ratio
η_o	Overall efficiency
η_p	Propulsive efficiency
η_{th}	Thermal efficiency
\dot{m}_a	Air flow
\dot{m}_f	Fuel flow
\dot{m}_p	Primary flow in the turbofan
\dot{m}_s	Secondary flow in the turbofan
\dot{m}_t	$m_p + m_s$
\dot{m}	$\dot{m}_a + \dot{m}_f$
λ_{GFP}	Permitted specific lubricant film thickness
λ_{GFT}	Specific lubricant film thickness
Π_c	Compressor pressure ratio
Π_F	Fan pressure ratio
Π_o	overall pressure ratio
ζ_{max}	Maximum specific sliding
ACARE	Advisory Council for Aviation Research and Innovation in Europe
AMAD	Aircraft Mounted Accessory Drive
APU	Auxiliary Power Unit
ATP	Advanced Turboprop Project
a	Center distance
b	Facewidth
c	Absolute speed
e_p	Spacewidth of a standard basic rack
ECS	Environmental Control System
EDP	Engine Driven Pump
El	Elongation
ESFC	Equivalent specific fuel consumption
ESHP	Equivalent shaft horsepower
F_{res}	Residual thrust
FGDS	Fan Gear Drive System

F	Thrust
GB	Gearbox
GTF	Geared turbofan
HPC	High Pressure Compressor
HPT	High Pressure Turbine
$K_{H\alpha}$	Transversed load factor
$K_{H\beta}$	Face load factor
K_m	Load distribution factor
K_o	Overload factor
K_v	Tangential load
K_Y	Mesh distribution factor
LPC	Low Pressure Compressor
LPT	Low Pressure Turbine
LS	Load Stage
m_n	Normal module
MGB	Main Gearbox
OPR	Overall Pressure ratio
p	Pitch
Q_{ci}	Lower heating value of the fuel
RAT	Ram AirTurbine
RA	Reduction Area
RS	Rough sizing
S_λ	Safety against micropitting
S_F	Root safety
S_H	Flank safety
s_p	Tooth thickness of a standard basic rack tooth
T_a	Ambient preassure
T_a	Ambient temperature
T_{it}	Turbine Inlet Temperature
TP	Turboprop
TSFC	Thrust specific fuel consumption
UDF	Unducted-fan
UTS	Ultimate Tensile Strength
u	Blade linear speed
V_a	Flight speed
V_j	Jet speed

W_t	Tangential load
w	Relative speed
YS	Yield Strength
z	N ^o of teeth

List of Figures

1	Turbojet cruise thrust, fuel consumption and efficiencies at different flight speed	4
2	Turbofan cruise thrust, fuel consumption and efficiencies	7
3	Influence of BPR and Fan Pressure Ratio on SFC for Typical Civil Engines [1]	9
4	TSFC characteristics for different engines [11]	9
5	New technologies for the Turboprops	14
6	PurePower PW1000G Advanced Technologies	15
7	Planetary gear schemes	17
8	Planetary Gearbox with various stages	18
9	Gear Layout Arrangements	22
10	PT6 Reduction Gearbox Details [29]	23
11	PT6 Gearbox	24
12	PW100 Reduction Gearbox Details	25
13	TPE 331 Reduction Gearbox Details	25
14	NK-12 turboprop	26
15	Antonov n-70	26
16	Progress D-27 turboprop	27
17	TFE 731 geared turbofan	28
18	ALF502 geared turbofan	28
19	P&W gearbox for the geared Turbofan [37]	29
20	Load Isolation system for the FGDS	30
21	Rolls-Royce Power gearbox [39]	31
22	Phases in a gearbox design	32
23	Phase I - KissSoft	33
24	Phase II - KissSoft	33
25	Optimization - KissSoft	34
26	Rough sizing procedure	35
27	Tooth profiles varied by number of teeth	37
28	Hardness gradients for a carburized and a nitrided tooth [44]	40
29	Comparison of hardening methods [44]	42
30	Gear manufacturing processes	44
31	Forming methods	45
32	Generating methods	46
33	Gear Shaving	46
34	Grinding methods	47
35	Gear Lapping	47
36	Gear Honing	48
37	Standard rack profile	49
38	Typical oil circuit [48]	51
39	Oil systems	51
40	Forced oil circulation lubrication methods	53
41	Typical limits of the load-carrying capacity for case hardened gears	57
42	Fine sizing procedure	63
43	Example of the graphic presentation of the fine sizing results, base in the flank and root safety	64
44	Tooth flank modifications	66
45	Type of profile modifications	67
46	Profile modification parameters	67
47	Turboprop's final 3D model	74
48	GTF1's final 3D model	75
49	GTF2's final 3D model	75
50	Timeline of expected future fuel efficiency improvements compared to predecessor aircraft or engine of the same category [62]	76
51	Propulsive Efficiency for Turboprop, Turbojet and Turbofan Engines [1]	78
52	Scheme of a basic turbojet engine	79
53	Rolls-Royce Avon 200	79
54	Pratt & Whitney JT3C (J57)	79

55	Rolls-Royce Allison T56	80
56	Pratt & Whitney Canada PT6	81
57	Two possible configurations for the Turbofan	81
58	Rolls-Royce RB211	82
59	Pratt & Whitney PW4000	82
60	Compressor map	83
61	Velocity triangle	84
62	Fan blades	85
63	Gear teeth Placement	87
64	Gear tooth profile	88
65	Classification according to the axes configuration	88
66	Spur Gear	89
67	Helical Gears	89
68	Bevel Gear	90
69	Gear Layout Arrangements	90
70	Forces applied in Spur gears and Helical gears	91
71	Neddle Roller bearing	91
72	Load distribution [71]	92
73	Design parameters for gears	93
74	Effect of applying a positive shifted correction	95
75	Tooth thickness tolerances according to ISO 286-2	96
76	Shaft tolerances according to ISO 286-2	97
77	Typical military aircraft top-level power generation system [48]	99
78	Typical military aircraft top-level environmental control [48]	99
79	Typical military aircraft top-level fuel system [48]	100
80	Typical civil systems interaction – heat exchange between systems [48]	100
81	Typical aircraft systems interaction [48]	101
82	Bearing chambers	102
83	Rough sizing results	105

List of Tables

1	Typical TSFC values for turbojet and turbofan engines	8
2	Types of arrangement for epicyclic gear systems	17
3	Order of magnitude for some turboprop engines	21
4	Order of magnitude for some Geared Turbofans	21
5	Evolution of the T56 Gearbox	22
6	Evolution of the PT6	23
7	Evolution of the PW100	24
8	P&W geared turbofan models	29
9	Number of planets in each of the designs	35
10	Steel grades classification [46]	43
11	Standard basic rack	49
12	Proposed tolerances in DIN 3967	50
13	Lubricant 's characteristics	54
14	Turbine lubricants specifications	55
15	Properties for Mobil Jet Oil II	56
16	Classification of test results of the micropitting test from [50]	56
17	List for comparing the various FZG scuffing load tests	57
18	Input speed	58
19	Applications according to the standard	59
20	Overload factor according to DIN 3990/ISO 6336	60
21	Input speed and gear ratio	62
22	Order of magnitude of the main parameters in the rough sizing step	62
23	Effects of short or long profile modification in literature	67
24	General information about the gears	69
25	Weight of the gears	69
26	Reference profile of the final tooth form	70
27	Tooth geometry - TP	70
28	Tooth geometry - GTF1	70
29	Tooth geometry - GTF2	70
30	Gears characteristics	71
31	Power density for the different gears	71
32	Gear pairs information	72
33	General influence factors	72
34	Service factors	73
35	Safety against micropitting	73
36	Safety against micropitting	73
37	Surface hardness	74

References

- [1] AEROSPACE PROPULSION, *Dries Verstraete*, School of aerospace, Mechanical and Mechatronic Engineering, University of Sydney, 2012.
- [2] POPULAR MECHANICS - WHY THE CONCORDE IS SUCH A BADASS PLANE, 2019 www.popularmechanics.com.
- [3] INNOVATIONS, TECHNOLOGY AND EFFICIENCY SHAPING THE AEROSPACE ENVIRONMENT, *Maria Mrazova*, Faculty of Aeronautics, Slovak Republic, 2013.
- [4] MECHANICS AND THERMODYNAMICS OF PROPULSION, *Philip Hill & Carl Peterson*, Second Edition, 2010.
- [5] NATIONAL AERONAUTICS AND SPACE ADMINISTRATION, IDEAL BRYTON CYCLE, <https://www.grc.nasa.gov>.
- [6] AIRCRAFT PROPELLERS, AN OUTDATED INNOVATION?, *Pedro Alves, Miguel Silvestre, Pedro Gamboa*.
- [7] TURBOPROP, <https://en.wikipedia.org/wiki/Turboprop>.
- [8] U.S DEPARTMENT OF TRANSPORTATION - FEDERAL AVIATION ADMINISTRATION, *Aviation Handbooks & Manuals*, Airplane Flying Handbook (FAA-H-8083-3B), 2006.
- [9] SCHOOL OF AEROSPACE, MECHANICAL AND MECHATRONIC ENGINEERING, *Dries Verstraete*, 2012.
- [10] AIR FREIGHT : A MARKET STUDY WITH IMPLICATIONS FOR LANDLOCKED COUNTRIES, *THE WORLD BANK GROUP*, WASHINGTON,D.C.
- [11] CHARACTERISTICS OF THE SPECIFIC FUEL CONSUMPTION FOR JET ENGINES, *Artur Bensel*.
- [12] THE GEARED TURBOFAN MAY BE A REVOLUTIONARY JET ENGINE, BUT IT'S JUST THE LATEST DEVICE TO EMPLOY PRECISION GEARING, *Lee S. Langston*.
- [13] FUNDAMENTALS OF TURBOMACHINES, *Eric Dick*.
- [14] NASA, <https://ntrs.nasa.gov>.
- [15] THEORY OF AEROSPACE PROPULSION, *Pasquale M. Sforza*.
- [16] DEVELOPMENT IN GEARED TURBOFAN AEROENGINE, *A. L. Mohd Tobi1, A. E. Ismail1*.
- [17] TURBINE TECHNOLOGY: INNOVATIONS IN TURBINE ENGINES, *Charles Chandler*, www.aviationpros.com.
- [18] ACCESORY DRIVE, https://en.wikipedia.org/wiki/Accessory_drive.
- [19] REDUCTION GEARS, UNDERSTANDING GEARS Valeri G. Nesterenko, www.thomasnet.com.
- [20] GEAR SYSTEMS, <https://khkgears.net>.
- [21] MACHINE DESIGN - THE WORLD OF PLANETARY GEARS, *Charles S. Kaim*.
- [22] WINDAGE, CHURNING AND POCKETING POWER LOSSES OF GEARS: DIFFERENT MODELING APPROACHES FOR DIFFERENT GOALS, *Franco Concli & Carlo Gorla*.
- [23] THERMAL TO MECHANICAL ENERGY CONVERSION: ENGINES AND REQUIREMENTS - VOL. III, *Valeri G. Nesterenko*.
- [24] AERO-ENGINE FAN GEARBOX DESIGN, *Cransfield University*.
- [25] EVALUATION OF SINGLE AND COUNTER ROTATION GEARBOXES FOR PROPULSION SYSTEMS *J.Godston, F.J.Mike*.
- [26] FATIGUE LIFE ANALYSIS OF A TURBOPROP REDUCTION GEARBOX, NASA Technical Memorandum, *David G. Lewicki, Joseph D. Black, Michael Savage & John J. Coy*.

- [27] NEXT GENERATION OF TURBOPROP GEARBOXES, *W. L. McIntire & D. A. Wagner*.
- [28] THE PT6 ENGINE: 30 YEARS OF GAS TURBINE TECHNOLOGY EVOLUTION, *M. Badger, A. Julien A.D. LeBlanc, S.H. Moustapha, A. Prabhu & A.A. Smailys*.
- [29] PT6A SMALL SERIES HEAVY MAINTENANCE COURSE, *Aviation maintenance training, Jaars*.
- [30] PRATT&WHITNEY, *www.pwc.ca*.
- [31] THE PW100 ENGINE: 20 YEARS OF GAS TURBINE TECHNOLOGY EVOLUTION, *E. Hosking, D. P. Kenny, R. I. McCormick S. H. Moustapha, P. Sampath & A. A. Smailys*.
- [32] KUZNETSOV NK-12, WIKIPEDIA, <https://en.wikipedia.org/wiki/KuznetsovNK-12>.
- [33] FUNDAMENTALS OF TURBOMACHINES, *Eric Dick*.
- [34] GARRETT TFE731, <https://en.wikipedia.org/wiki/GarrettTFE731>.
- [35] ROLLS-ROYCE TYNE, <https://en.wikipedia.org/wiki/Rolls-RoyceTyne>.
- [36] THE PW1000G FAMILY, <https://en.wikipedia.org/wiki/Pratt%26WhitneyPW1000GSpecifications>.
- [37] P&W GTF <https://pwgtf.com/>.
- [38] GEARED TURBOFAN ENGINE: DRIVEN BY INNOVATION, *William Sherida, Michael McCune, and Michael Winter*.
- [39] ROLLS-ROYCE SETS RECORD FOR MOST POWERFUL TURBOFAN GEARBOX IN THE WORLD, *www.popularmechanics.com/*.
- [40] CHEMISTRY AND TECHNOLOGY OF LUBRICANTS, *Roy M. Mortier, Malcolm F. Fox, Stefan T. Orszulik*.
- [41] GAS TURBINE ENGINEERING HANDBOOK, *Meherwan P.Boyce*.
- [42] UNDERSTAND THE CHOICE OF PRESSURE ANGLE IN THE DESIGN OF SPUR OR HELICAL GEARING, *Brian Bengel*.
- [43] EFFECTS OF CONTACT RATIOS ON MESH STIFFNESS OF HELICAL GEARS FOR LOWER NOISE DESIGN, *Lan Liu, Yunfei Ding, Liyan Wu and Geng Liu*.
- [44] HEAT TREATMENT OF GEARS - A PRACTICAL GUIDE FOR ENGINEERS, *A.K. Rakhit*.
- [45] GEARS –AND HOW THEIR WORLD IS CHANGING, *Neville W. Sachs, P.E.*
- [46] GRADING THE STRENGTH OF STEEL, *Gregory Vartanov*.
- [47] FUNDAMENTAL RATING FACTORS AND CALCULATION METHODS FOR INVOLUTE SPUR AND HELICAL GEAR TEETH, *AMERICAN NATIONAL STANDARD, ANSI/AGMA 2001-D04*.
- [48] AIRCRAFT SYSTEMS MECHANICAL, ELECTRICAL, AND AVIONICS SUBSYSTEMS INTEGRATION, *Ian Moir, Allan Seabridge*.
- [49] NEW DEMANDS NEW OIL 387, *www.airinternational.com*.
- [50] FORM AND POSITION MEASUREMENT ADVANCEMENT, *Gear Solutions - Your Resource for Machines, Services, and Tooling for the Gear Industry, Michael Hockmann*.
- [51] USEFUL INFORMATION ON SCUFFING LOAD TESTS, *www.klueber.com*.
- [52] SCORING TESTS OF AIRCRAFT TRANSMISSION LUBRICANTS AT HIGH SPEEDS AND HIGH TEMPERATURES, *H. Winter and K. Michaelis*.
- [53] A COMPARISON OF CURRENT AGMA, ISO AND API GEAR RATING METHODS, *John M. Rinaldo*.

- [54] COMPARING STANDARDS, DON MCVITTIE.
- [55] EFFECTS OF PROFILE CORRECTIONS ON PEAK-TO-PEAK TRANSMISSION ERROR, *Dr. Ing. Ulrich Kissling, Dipl. Ing. Hanspeter Dinner.*
- [56] PREDICTION OF DYNAMIC FACTORS FOR HELICAL GEARS IN A HIGH-SPEED MULTIBODY GEARBOX SYSTEM, *Niranjan Raghuraman, Dr. Sharad Jain and Chad Glinsky.*
- [57] THE ENGINEERING TOOL BOX, <https://www.engineeringtoolbox.com/factors-safety-fos-d1624.html>.
- [58] TOOTH FLANK CORRECTIONS OF WIDE FACE WIDTH HELICAL GEARS THAT ACCOUNT FOR SHAFT DEFLECTIONS, *Shan Chang, Dr. Donald R. Houser, Jonny Harianto.*
- [59] EFFICIENT LAYOUT PROCESS OF CYLINDRICAL GEARS WITH MANUFACTURING CONSTRAINTS, *MSc ETH I.Tsikur.*
- [60] KISSOFT MANUAL, <https://old.kisssoft.ag/Manual/en/index.htm?body=8780.htm>.
- [61] LOW-LOSS GEARS FOR PRECISION PLANETARY GEARBOXES: INFLUENCE OF THE GEAR DESIGN ON THE MESHING AND THE CHURNING POWER LOSSES, *International Conference on Gears, Concli F., Coenen J.*
- [62] AIRCRAFT TECHNOLOGY ROADMAP TO 2050, www.iata.org.
- [63] ROLLS-ROYCE AVON, https://en.wikipedia.org/wiki/Rolls-Royce_Avon.
- [64] PRATT WHITNEY J57, <https://es.wikipedia.org/wiki/Pratt26WhitneyJ57>.
- [65] PRATT WHITNEY J57 (JT3), *New England Air Museum Organization.*
- [66] T56, <https://www.rolls-royce.com>.
- [67] PW4000 DERIVATIVES CONTINUE TO DRIVE ENGINE SUCCESS STORY, *FlightGlobal.*
- [68] THE SHORT, HAPPY LIFE OF THE PROP-FAN, *Bill Sweetman-Air Space Magazine.*
- [69] DESARROLLO DE UNA HERRAMIENTA PARA EL PREDISEÑO DE COMPRESORES AXIALES, *Jacinto Luis Madrid Nebreda.*
- [70] HELICAL OR NOT HELICAL? HOW HELICAL GEARS IMPACT THE PERFORMANCE OF PLANETARY SYSTEMS, *Gerhard Antony, https://gearsolutions.com.*
- [71] HELICAL PLANETARY GEARBOXES: UNDERSTANDING THE TRADEOFFS, <https://www.designnews.com/automation-motion-control/helical-planetary-gearboxes-understanding-tradeoffs>.